Journal Pre-proof

Research progress on the structure, function, and performance evaluation of hard-target penetration fuzes

Jianzheng Xu, Rui Yu, Shengnan Fu, Lei Yang, Haijie Li, Rong Li, Zhe Chu, Xiaochao Jin

PII: S2214-9147(26)00247-3

DOI: https://doi.org/10.1016/j.dt.2026.07.019

Reference: DT 2065

To appear in: *Defence Technology*

Received Date: 18 April 2026

Revised Date: 2 July 2026

Accepted Date: 8 July 2026

Please cite this article as: Xu J, Yu R, Fu S, Yang L, Li H, Li R, Chu Z, Jin X, Research progress on the structure, function, and performance evaluation of hard-target penetration fuzes, *Defence Technology*, https://doi.org/10.1016/j.dt.2026.07.019.

Research progress on the structure, function, and performance evaluation of hard-target penetration fuzes

Jianzheng Xu[a], Rui Yu[b], Shengnan Fu[b], Lei Yang[c], Haijie Li[d], Rong Li[e], Zhe Chu[a], Xiaochao Jin[a,*]

[a] State Key Laboratory for Strength and Vibration of Mechanical Structures, School of Aerospace Engineering, Xi'an Jiaotong University, Xi'an 710049, China

[b] Xi'an Modern Control Technology Research Institute, Xi'an, 710065, China

[c] National Key Laboratory of Energetic Materials, Xi'an Modern Chemistry Research Institute, Xi'an, 710065, China

[d] Hunan Vanguard Group Co., Ltd., Changsha, 410137, China

[e] Xi'an Institute of Electromechanical Information Technology, Xi'an, 710065, China

[*] Corresponding author: jinxiaochao@xjtu.edu.cn

Research progress on the structure, function, and performance evaluation of hard-target penetration fuzes

Abstract: As the core decision-making and initiation-control unit in penetration weapons, the hard-target penetration fuze (HTPF) is critical to the terminal lethality of warheads against hard and deeply buried targets. Driven by growing operational demands and advances in key technologies, significant progress has been made in HTPF development. However, current HTPF designs and performance levels still cannot fully meet the evolving requirements of intelligent weapon systems. This article provides a comprehensive overview of the development of HTPFs, with emphasis on their technical evolution, key enabling technologies, and future trends. First, the technical evolution of HTPFs is systematically reorganized according to the trigger-information-decision chain, by which HTPFs are classified into four technical stages. This classification links triggering mechanisms, primary information sources, initiation-control modes, and representative engineering models, and is further used to compare the technological pathways of major countries. Second, following the operational sequence of digital programmable HTPFs, a system-level framework is established by coupling projectile-fuze load characteristics, dynamic response and protection, hard-target information sensing and feature extraction, precision initiation control, and performance evaluation. Within this framework, the advantages, limitations, and engineering applicability of representative technologies and methods are analyzed in detail. On this basis, the main development trends of HTPFs are identified, including high-survivability embedded electronics, multi-domain information sensing and fusion, and the stepwise use of artificial intelligence as an auxiliary recognition module while retaining deterministic safety-and-arming logic. This review provides a valuable reference for the design, evaluation, and engineering application of next-generation intelligent HTPFs.

Keywords: Hard-target penetration fuze; Load characteristic analysis; Target information sensing; Precise initiation control method; Performance evaluation

1 Introduction

The precision strike capabilities of penetration weapons have been substantially enhanced [1]. High-value strategic military targets, such as command centers and ammunition depots, have increasingly transitioned from surface installations to underground facilities [2]. Furthermore, the continuous improvement in structural strength [3, 4], combined with the widespread adoption of multi-layered protective designs, has resulted in more robust and comprehensive defense systems [5]. To effectively neutralize such high-value targets featuring multi-layered protection, the penetration weapon and the hard-target penetration fuze (HTPF) have consistently remained a primary focus in global armament development.

The fundamental operating principle of penetration weapons involves penetrating soil, granite, or reinforced concrete, followed by initiation of the warhead inside or beneath the target [6]. In the early stages of development, penetration was achieved primarily through the kinetic energy of the projectile [7]. During this period, the HTPF had relatively basic functionality, typically triggering upon target impact. To enhance lethality against hardened targets, the delay HTPF was introduced to allow the projectile to reach a predetermined depth before initiation [8, 9].

Since the integration of electronic components into a purely mechanical fuze, global research and development in penetration fuze technology has accelerated, driving these systems toward higher performance [10]. The electromechanical triggered delay penetration fuze, such as the Fuze Munition Unit (FMU)-143/B, was developed in the USA [11]. In this design, the delayed initiation function is accomplished through the use of delayed electric detonators [9]. Concurrently, to facilitate the transition toward intelligent systems, the digital programmable penetration fuze utilizing deceleration information for precise initiation control has been widely developed globally [12]. Overall, significant progress in penetration fuze technology has been made with the continuous evolution of penetration weapons.

This paper focuses on the HTPF for earth-penetration weapons, providing a comprehensive review of the state-of-the-art research. The structural framework of this study is illustrated in Fig. 1. Specifically, Section 2 explores the development of HTPFs, categorizing them into four stages based on initiation modes and triggering mechanisms. Moreover, the maturity of key technologies for intelligent fusion-recognition penetration fuzes is assessed, and the technology pathways of penetration fuze technologies among the major military powers are compared. Following the operational sequence of digital programmable penetration fuze, critical technologies including load characteristic analysis of the projectile-fuze system, hard-target information sensing, and precise initiation control are then reviewed in Sections 3, 4, and 5, respectively. Furthermore, Section 6 discusses the performance evaluation as well as safety and reliability analysis for HTPFs. Finally, future development trends are proposed in Section 7, providing a valuable reference for the design, performance evaluation, and application of intelligent HTPFs.

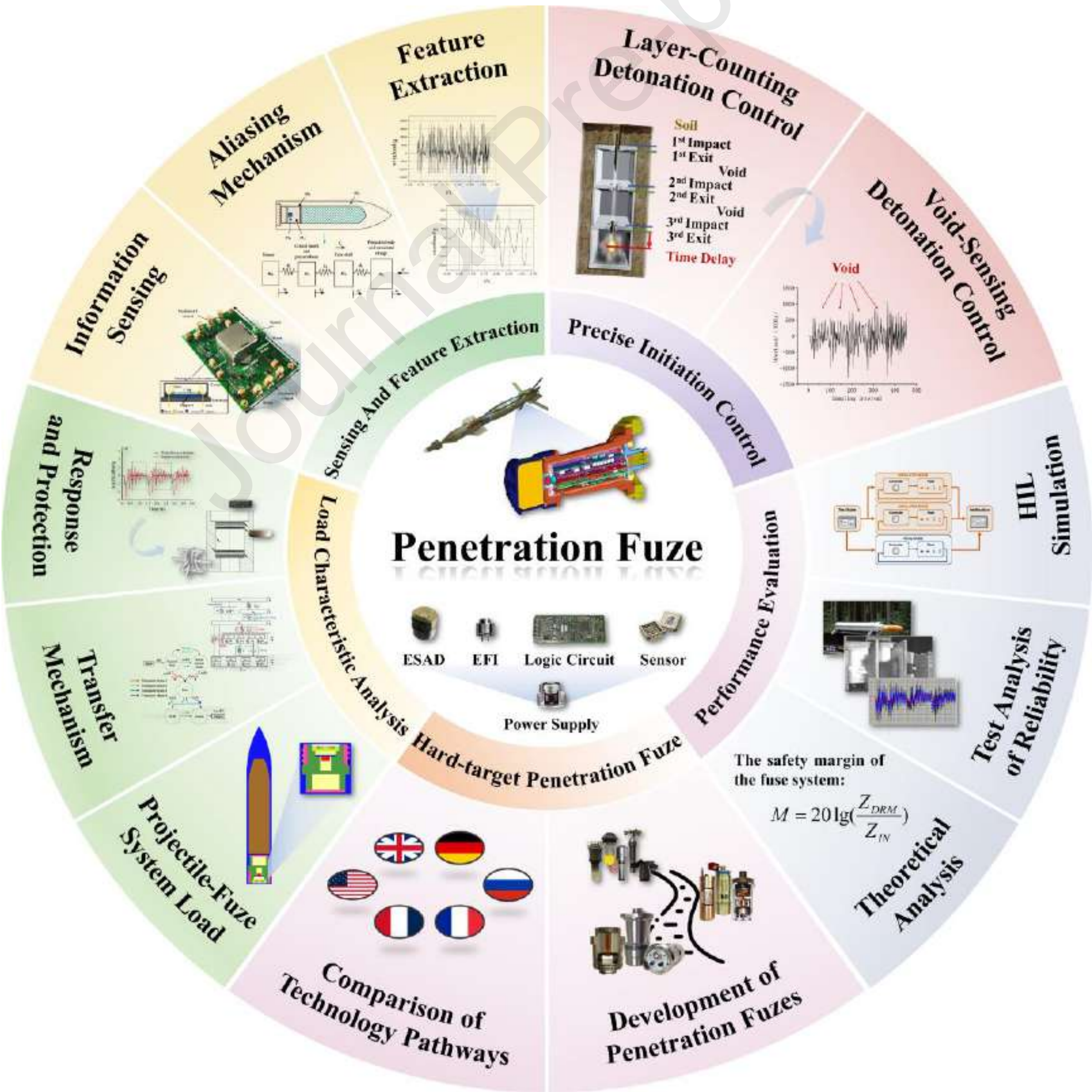

Fig. 1. The outline of this review for the development of HTPFs.

Notes: ① The outer ring of the figure is divided into five parts, starting from the "Hard-target Penetration Fuze" located at the bottom-center and arranged in a clockwise direction. Hard-target Penetration Fuze (Orange) [13–16] corresponds to Section 2; Load Characteristic Analysis (Yellow) [17–20] correspond to Section 3; Sensing and Feature Extraction (Green) [21–25] corresponds to Section 4; Precise Initiation Control (Purple) [26–30] corresponds to Section 5; Performance Evaluation (Pink) [31–36] corresponds to Section 6. ② The specific breakdown of each part generally corresponds to the content of the sections. ③ Electronic Safety and Arming Device (ESAD); Exploding Foil Initiator (EFI); Hardware-in-the-loop (HIL).

2 Hard-target penetration fuzes

The HTPF is a critical component for ensuring that penetration weapons fully achieve their terminal lethality; it is widely regarded as the brain of such weapon systems [10, 37]. The development of HTPFs has been promoted not only by the USA, but also by European countries, Russia, China, and other countries with long-term research programs in penetration weapons and fuze technologies. Publicly disclosed representative models include the FMU-143/B [16], FMU-152A/B [28, 38], Multi Application Fuze Initiation System (MAFIS) [39], AURORA [15, 40], and FMU-167/B [41], etc. The technical evolution of HTPFs since World War II is systematically organized in Fig. 2 according to the dominant trigger-information-decision chain of the HTPF. Two criteria are mainly considered: first, the triggering mechanism or primary information source used to identify penetration events; second, the initiation-control mode used to determine the initiation timing or initiation position. Based on these criteria, HTPFs are divided into four technical stages: mechanical inertial-triggered penetration fuzes, electromechanical triggered delay penetration fuzes, digital programmable penetration fuzes, and intelligent fusion-recognition penetration fuzes. In this section, the structural compositions, operating principles, and representative models of each technical stage are reviewed in the context of penetration weapon and fuze development. Moreover, the maturity of key technologies for intelligent fusion-recognition HTPFs is assessed, and the technology pathways of penetration fuze technologies among the major military powers are compared.

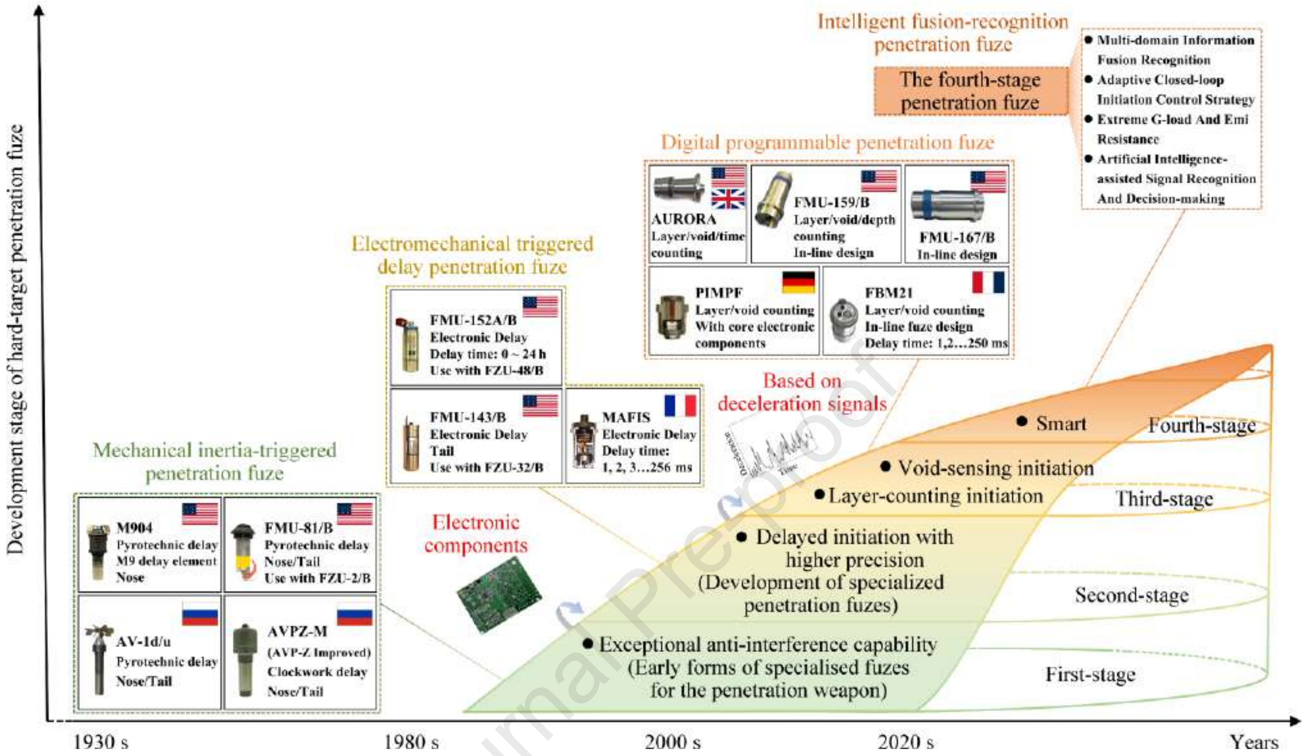

Fig. 2. Development of the HTPF technology [13, 15, 16, 36, 39, 41–49].

Notes: ① The technical evolution of HTPFs is systematically organized according to their initiation modes and triggering mechanisms. ② Regarding the fourth-stage intelligent fusion-recognition HTPF, only the key technologies potentially involved are illustrated in the figure. ③ Fuze Munition Unit (FMU); Multi-Application Fuze Detonation System (MAFIS); Programmable Intelligent Multi-Purpose Fuze (PIMPF).

2.1 Development of penetration weapons

Penetration weapons are primarily utilized for the destruction of high-value hard and deeply buried targets (HDBTs) and occupy a pivotal position within the modern armament systems [50]. Extensive research has been conducted worldwide and a comprehensive penetration weapon system spanning multiple weight classes has been gradually established [51]. The development of penetration weapons is summarized in Fig. 3. Generally, various models of penetration weapons, integrated with dedicated fuze, have been deployed or are currently being developed by nations including the USA, the UK, France, Germany, Russia, and China. In this section, the technological advancements in conventional penetration weapons among these leading military powers are reviewed to provide a reference for subsequent research.

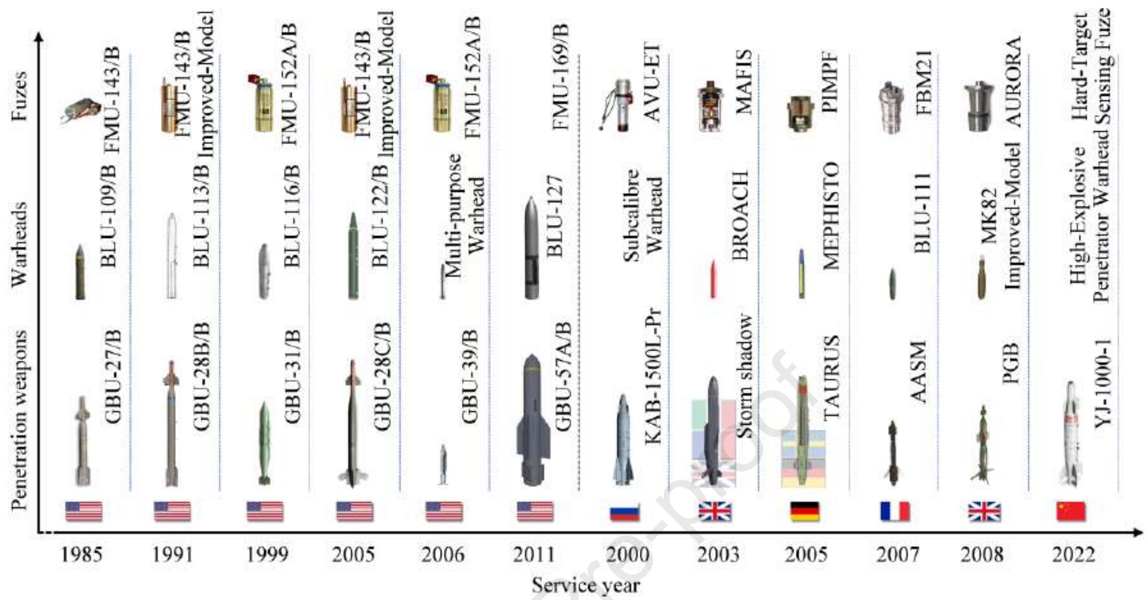

Fig. 3. Development of conventional penetration weapons [13, 15, 16, 28, 36, 39, 40, 42–49, 52–56].

Notes: ① The figure is bounded by the dark blue dashed line in the middle: the left side shows the systematic penetration weapons of the USA, and the right side shows the penetration weapons of other countries. ② The figure illustrates only typical mounting configurations for fuzes, warheads, and penetration weapons. ③ Fuzes without specific applications are omitted from this figure. ④ The FMU-152A/B is compatible with the FMU-143/B, and the BLU-116/B is compatible with the BLU-109/B. ⑤ Publicly available information indicates that the GBU-57A/B may be equipped with the FMU-169/B, the KAB-1500L-Pr may be equipped with the K047 and the AVU-ET. ⑥ Both Storm Shadow and TAURUS are products of multinational collaborative development programs. ⑦ Guided Bomb Unit (GBU); Bomb Live Unit (BLU); Fuze Munition Unit (FMU); Armement Air-Sol Modulaire (AASM); Paveway Guided Bomb (PGB); Multi-Application Fuze Detonation System (MAFIS); Programmable Intelligent Multi-Purpose Fuze (PIMPF); Bomb Royal Ordnance Augmented CHarge (BROACH).

2.1.1 Specialized penetration weapons

Penetration weapons are characterized as precision strike weapons for point targets, the operational effectiveness of which is largely determined by guidance accuracy. Consequently, the true development of penetration weapons was initiated during the Vietnam War, following the preliminary application of Precision-Guided Munitions in surface-attack roles, and entered a phase of rapid advancement after the 1980s. Building upon the foundation of the first and second stages of the Paveway series of Laser-Guided Bombs (LGB), the third-stage LGB [2, 9], represented by the Guided Bomb Unit (GBU)-24, was developed by the USA to possess precise trajectory control capabilities. The GBU-24 is characterized by its low-altitude, long-range, and all-weather operational capabilities. With a hit accuracy exceeding 1 m [57], the ground-attack efficiency of the USA has been significantly enhanced.

The GBU-27 was developed as an evolutionary improvement of the GBU-24, featuring significant enhancements in its control systems. To accommodate the internal weapons bay of the F-117A, the external dimensions of the munition were significantly reduced through the implementation of folding tail fins, a shortened nose section, and a reduction in the surface area of the forward canards. Simultaneously, to ensure the effective destruction of HDBTs, the Bomb Live Unit (BLU)-109/B was developed in 1985 [58]. Equipped with the FMU-143/B, the BLU-109/B was established as the standard warhead configuration for the GBU-27 [59]. Furthermore, because the BLU-109/B is dimensionally compatible with the MK-84 general-purpose bomb, it rapidly became the universal heavyweight penetration warhead for the USA.

2.1.2 Deep-strike penetration weapons

(1) 5000-lb class penetration weapons

The GBU-27 is a representative penetration weapon, exhibiting a penetration depth of approximately 1.8 m in reinforced concrete. Its penetration performance was significantly constrained by limited kinetic energy, a result of the terminal velocity restrictions inherent to unpowered delivery platforms [9]. To improve penetration performance, the development of the GBU-28 heavy LGB was initiated.

The GBU-28 is a representative 5000-lb class penetration weapon, utilizing the

BLU-113/B warhead. Its structural configuration was adapted from the BLU-109/B nose design, while the control algorithms of the GBU-24 guidance assembly and the delay parameters of the FMU-143 were specifically optimized. Experimental results demonstrated that the BLU-113/B achieves a penetration depth of approximately 6 m in concrete targets and approximately 30 m in soil. With a total mass of 2103 kg, the GBU-28 was initially deployable only by the F-111A [48, 49], though its carriage compatibility was subsequently extended to other aircraft, such as the F-15E.

To further enhance penetration performance, the BLU-122/B was developed through several technical refinements: the warhead geometry was optimized to enhance anti-ricochet capabilities and penetration performance [52]; the fuze mounting structure was modified to alleviate stress concentration; and the base design was reinforced to improve fuze survivability. Furthermore, the AFX-757 insensitive explosive was incorporated to comply with Insensitive Munitions (IM) standards [60].

Compared to the BLU-113/B, the penetration capability, blast damage effectiveness, and structural survivability of the BLU-122/B were increased by approximately 20%, 70%, and 30%, respectively. The GBU-28/B bombs equipped with the BLU-113/B and BLU-122/B warheads are designated as the GBU-28B/B and GBU-28C/B, respectively; both variants are fitted with the FMU-143 modified. This series of munitions is compatible with various delivery platforms, including the F-15E, F-111, and B-2, and serves as a critical asset for USA air-to-surface strikes.

To further enhance fuze protection and system survivability, the development of the BLU-138 Advanced 5000-lb Penetrator (A5K) was initiated in recent years [61]. According to the FY2026 USA ammunition procurement documentation, the BLU-138/B is the penetration warhead for the GBU-72/B. And the Bomb Stabilization Unit (BSU)-699 Kit is used to integrate the BLU-138/B with the KMU-556 Joint Direct Attack Munition (JDAM) Tail Kit Assembly to form the GBU-72/B [62]. The GBU-72 is optimized for the priority target set of tunnels and bunkers identified in the Hard Target Munitions Analysis of Alternatives. It emphasizes enhanced survivability, increased lethality, smart fuze, and the use of fielded JDAM navigation tail kits [63]. The document further states that, through significantly improved performance, the

GBU-72 reduces the number of weapons required to achieve a kill at a lower all-up-round cost, and that the GBU-72 will replace the GBU-28.

(2) Coordinate-attack penetration weapons

To mitigate the battlefield exposure risks to launch aircraft caused by the continuous target illumination required by LGBs, the USA proposed the development of air-to-surface weapons equipped with fire-and-forget capabilities in the early 1990s. Against this backdrop, the JDAM was jointly initiated by the USA Air Force and the Navy. The program was aimed at converting conventional gravity bombs into Precision-Guided Munitions (PGM) utilizing Global Positioning System (GPS)/Inertial Navigation System (INS) guidance.

The JDAM variants currently in service primarily include the 500-lb class GBU-38, the 1000-lb class GBU-32, and the 2000-lb class GBU-31, the latter of which can be configured with the BLU-109/B [58]. The JDAM series has significantly enhanced strike precision and operational flexibility while substantially reducing the dwell time of pilots and aircraft within contested environments. Consequently, these munitions have been extensively deployed in numerous regional conflicts. Regarding fuzes, the FMU-152A/B Joint Programmable Fuze (JPF) was developed by the USA for integration with the JDAM series [38]; however, its initiation control capability remains limited during HDBTs penetration.

However, several issues have been exposed during the operation of the JDAM. Significant collateral damage is prone to be caused by high-yield variants; furthermore, the carriage capacity of launch platforms is restricted by the physical dimensions and weight of these munitions, thereby constraining the strike effectiveness of individual sorties. To address these challenges, a series of development programs for small-diameter PGMs were initiated by the USA in the late 1990s, aiming to achieve reduced physical size coupled with high-performance penetration capabilities. For example, the GBU-39/B Small Diameter Bomb was developed by the USA.

The GBU-39/B was officially commissioned in 2006 and was initially deployed on multiple aircraft platforms, including the F-15E. This munition is characterized by its lightweight and compact dimensions [64], yet it is engineered to possess HDBTs penetration capabilities comparable to those of the 2000-lb class JDAM. Its compact external profile also facilitates carriage within the internal weapons bays of stealth fighters such as the F-22, thereby significantly enhancing the air-to-ground strike capabilities. Simultaneously, the damage radius is constrained to approximately 8 meters, which effectively mitigates collateral damage.

(3) 2000-lb class penetration weapons

The BLU-109/B was initially designed with the primary objective of neutralizing hardened aircraft shelters. However, combat experience during the Gulf War demonstrated that its penetration capability was limited when striking high-value HDBTs, such as deeply buried command centers. Against this backdrop, the BLU-116/B Advanced Unitary Penetrator (AUP) was developed in 1998. This warhead is highly compatible with the BLU-109/B in terms of structural dimensions and mass distribution, providing a direct form-fit replacement capability [65]. It is constructed from high-density 9430M nickel-cobalt steel alloy and features a sub-caliber penetrator design supplemented by an aluminum shroud. Consequently, a significant improvement in penetration performance is achieved, and the unit is integrated into various PGMs, including the GBU-24 and GBU-31.

The Hard Target Smart Fuze (HTSF) program, developed during the same period, was initially designated as FMU-157 and later standardized as FMU-159/B. It was intended to achieve precise sensing and initiation control regarding penetration depth, layer counts, or void numbers through the integration of high-precision accelerometers and microcontrollers. However, the program was terminated in 2003 due to significant technical implementation challenges. Consequently, development efforts by the USA were shifted toward the more technologically mature Hard Target Void Sensing Fuze (HTVSF), designated as FMU-167/B [66].

To further enhance fuze protection and system survivability, the development of the BLU-137/B was initiated. Authoritative public sources define the BLU-137/B as the Advanced 2000-lb Penetrator (A2K), a 2000-lb class penetrating warhead. The USA FY2026 ammunition procurement documentation states that it is used against bunkers, aircraft shelters, and reinforced-concrete structures, and that it is compatible with the

JDAM guidance tail kit [63]. The BLU-137/B is a newly designed 2000-lb class penetrator developed from the ground up, using AF96 high-strength steel to reduce material costs and improve performance, while also redesigning the fuzewell, aft closure plate, retaining rings, and warhead nose [67]. The AGRA approach relocates fuze-arming and power-related structures to the outside of the warhead case, thereby reducing the structural weaknesses associated with the traditional design and improving reliability and survivability. Combined with the FMU-167/B, this system is expected to gradually emerge as the new-generation core equipment for the HDBT strike capabilities of the USA.

2.1.3 Composite warhead penetration weapons

Aerial bombs released from high altitudes possess an inherent advantage in engaging HDBTs due to their high terminal velocities. In contrast, early cruise missiles were constrained by factors such as aerodynamic configuration, structural integrity, and propulsion systems, with typical speeds generally limited to approximately 0.6 Mach. Furthermore, impact velocities could not be effectively enhanced through terminal pull-up and dive maneuvers. Consequently, pronounced limitations were observed when these missiles were utilized as delivery platforms for penetration warheads.

To enhance the penetration performance of cruise missiles against HDBTs, the Bomb Royal Ordnance Augmented CHarge (BROACH) multi-stage warhead has been developed by the UK. This warhead utilizes a tandem configuration combining a precursor shaped charge with a follow-through kinetic energy penetrator. The precursor shaped charge is designed to create a pre-drilled aperture on the target surface, thereby establishing an ingress path for the subsequent kinetic penetrator [68]. Such a design not only reduces sensitivity to the impact angle and angle of attack but also significantly improves the integrated penetration depth and terminal lethality.

The precursor charge of the BROACH warhead is characterized by a diameter approximately 1.5 times that of the follow-through penetrator. This configuration is designed to facilitate the formation of a larger aperture, thereby allowing the subsequent penetrator to ingress more deeply into the target. With a total mass of approximately 450 kg, the warhead is classified within the NATO 1000-lb class. According to public data, its penetration performance is superior to the BLU-109/B. Furthermore, effective hard-target penetration is maintained even under the 59° impact angle.

The BROACH warhead has been successfully integrated into various missile systems. For instance, the Storm Shadow, jointly developed by the UK, France, and Italy, is equipped with this warhead. Having entered service in 2002, it was subsequently deployed in combat during the Libyan conflict. Additionally, the BROACH warhead is utilized in the unitary penetrator variant of the USA Joint Standoff Weapon (JSOW) /C, representing one of the few instances where European technology has been adopted within the USA military inventory.

Apart from the BROACH warhead, a similar technical approach is adopted by the Multi-Effect Penetrator, HIgh Sophisticated and Target Optimised (MEPHISTO) warhead integrated into the German TAURUS cruise missile. A larger length-to-diameter ratio is utilized in its secondary kinetic penetrator, whereby the penetration performance is further enhanced. Furthermore, multiple terminal ballistic modes and a Programmable Intelligent Multi-Purpose Fuze (PIMPF) are integrated into the missile to fully exploit the lethality potential of the warhead.

2.1.4 Massive penetration weapons

In 2002, the USA Air Force initiated the Big BLU program to develop a series of highly powerful conventional munitions [69]. Two primary weapons were associated with this concept. One was a blast variant, the GBU-43/B Massive Ordnance Air Blast (MOAB). This was a 21,700-lb conventional bomb designed for large-area destruction. The other was a penetrator variant, the GBU-57/B Massive Ordnance Penetrator (MOP). The basic technical parameters of the GBU-57A/B are summarized in Table 1.

Table 1

Basic technical parameters of the GBU-57A/B MOP [11, 47, 69, 70].

Model	Warhead	Fuze	Guidance system	Aircraft platform	Service year
GBU-57A/B	BLU-127	FMU-169/B	KMU-612/B	B-2 Spirit	~ 2011
Length	Diameter	Mass	Filling weight	Filling	Penetration depth

~ 6.25 m (~ 20.5 ft)	~ 0.8 m (~ 31.5 ft)	~ 13600 kg (~ 30000-lb)	~ 2423 kg (~ 5300-lb)	AFX-757 (~ 2082 kg) PBXN-114 (~ 341 kg)	Soil: ~ 60 m (~ 200 ft); 5000 psi Reinforced Concrete: ~ 18 m (~ 60 ft)

The GBU-57A/B is comprised of the BLU-127 bomb body integrated with a GPS/INS. Relevant information suggests that the GBU-57A/B may be equipped with the FMU-169/B [11]. To date, seven distinct variants have been developed, with the GBU-57F/B representing the state-of-the-art iteration. Due to its substantial dimensions and mass, the GBU-57/B is exclusively deployed by the B-2 Spirit stealth bomber and the B-21 Raider [70], with each platform capable of carrying two units.

The BLU-127 thermobaric warhead is integrated into the GBU-57A/B, utilizing high-temperature, high-pressure, and sustained combustion effects [2] to neutralize personnel, chemical and biological weapons, and associated facilities within enclosed environments such as underground bunkers and tunnels. The penetration performance of the GBU-57/B is significantly superior to that of earlier models, such as the GBU-28/B, demonstrating substantially enhanced deep-penetration capabilities. The GBU-57/B MOP was first employed in combat on June 22, 2025. In this operation, seven B-2 Spirit stealth bombers delivered 14 GBU-57A/B bombs against Iran's Fordow Uranium Enrichment Plant and Natanz Nuclear Facility. This operation provided the USA with critical operational data and accelerated the development of more intelligent follow-on weapons.

According to publicly available information, the USA is developing the Next Generation Penetrator as an air-to-ground prototype weapon system for HDBTs, with ARA serving as system design agent and Boeing supporting tail-kit development and all-up-round integration [71]. The weight of the NGP is required to be controlled below 22000-lb, making it lighter than the MOP. At the same time, the weapon is expected to maintain and further enhance its capability against HDBTs through the adoption of new alloy materials and an optimized penetrator nose design [72]. The USA plans to complete full-scale static testing and sub-scale dynamic testing by the end of FY 2026. The program builds on a long-standing requirement for capabilities against HDBTs.

2.1.5 Hypersonic penetration weapons

Since the development of the BLU-109/B, the USA has progressively advanced its range of penetration warheads, resulting in multiple variants tailored to diverse delivery platforms and mission requirements [73]. However, most in-service penetration weapons are subsonic, primarily launched via gravity drop from fighter aircraft or air launch. In recent years, countries around the world have continuously advanced the technological upgrading of penetration weapons. The Future Weapon Technology Blueprint issued by the USA outlined the technological framework and development roadmap for engaging HDBTs [74], emphasizing hypersonic penetration weapons as the next-generation focus direction.

(1) Hypersonic penetration weapon of USA

The development of USA hypersonic penetration weapons has generally proceeded along two technical pathways: boost-glide systems and air-breathing hypersonic cruise systems [75]. A boost-glide weapon typically uses a rocket booster to accelerate and release a hypersonic glide vehicle, after which the glide vehicle flies toward the target within the atmosphere along a non-ballistic, maneuverable trajectory. An air-breathing hypersonic cruise weapon, by contrast, is usually first accelerated by a booster into the engine's operating envelope, and then relies on a scramjet engine to sustain hypersonic flight.

Recent engineering progress shows that the USA boost-glide pathway appears comparatively farther along toward fielding. This is reflected primarily in the Army's Long-Range Hypersonic Weapon [76] and the Navy's Conventional Prompt Strike system [77, 78], which share the Common Hypersonic Glide Body and related all-up-round architecture. This arrangement is intended to reduce duplicative development across the services and improve production coordination. By contrast, the air-breathing hypersonic cruise pathway offers potential advantages in missile miniaturization, platform compatibility, and fighter-aircraft carriage. The USA Air Force's Hypersonic Attack Cruise Missile [79] is being developed in this direction, emphasizing air launch, scramjet propulsion, and fighter integration. However, this pathway remains constrained by challenges such as the organization and stabilization of supersonic combustion, thermal protection, materials, and flight-test validation. Related information indicates that its schedule and cost remain subject to uncertainty.

(2) Hypersonic penetration weapon of Russia

Russia is currently one of the most active countries in developing hypersonic strike systems, and its related weapons are increasing the threat of penetrating defenses and striking hardened and high-value targets. Among Russia's publicly disclosed systems, the 3M22 Tsirkon/Zircon, Oreshnik, and Kh-47M2 Kinzhal represent, respectively, sea-based, land-based, and air-launched hypersonic strike capabilities [80].

The Tsirkon/Zircon is generally regarded as Russia's sea-based, scramjet-powered hypersonic cruise missile. Russia claims that it can reach speeds of up to Mach 9 and has a range of approximately 1000 km [81]. The missile is assessed as being usable for both anti-ship and land-attack missions, and it has important implications for anti-access/area-denial operations. Oreshnik should be more accurately defined as a road-mobile intermediate-range ballistic missile. Through its intermediate-range reach, multiple independently targetable reentry vehicle capability, and compressed warning and response times [82], Oreshnik enhances Russia's ability to suppress theater-level targets and air- and missile-defense systems. However, there is insufficient public evidence to support the conclusion that it was specifically designed for HDBTs defeat. The Kh-47M2 Kinzhal is an important component of Russia's air-launched, long-range rapid-strike capability and is typically carried by platforms such as the MiG-31K [83]. Russia claims that the missile can reach a maximum speed of Mach 10 and has a range of roughly 1500–2000 km. It can be used against high-value ground targets and large maritime targets. Kinzhal improves Russia's ability to conduct long-range rapid strikes against high-value targets and to penetrate defenses, but its conventional penetration and destructive effects against HDBTs should still be assessed with caution [84].

(3) Hypersonic penetration weapon of European countries

As Europe's security environment deteriorates, the density of layered, in-depth air-defence systems increases, and the demand for long-range precision strike grows, European countries are accelerating the development of next-generation penetration and deep-strike capabilities. Public sources indicate that France's V-MAX hypersonic glider demonstrator programme has completed its first flight test, with a focus on validating manoeuvring during atmospheric re-entry, high-speed flight control, and related hypersonic glide technologies [85]. The programme provides a key technological foundation for future systems associated with high-speed penetration, long-range precision strike, and strategic deterrence.

In the cruise-missile domain, the Future Cruise/Anti-Ship Weapon programme (FC/ASW), subsequently named STRATUS [86, 87], is one of the core programmes underpinning Europe’s next-generation deep-strike capability. Led by MBDA, the programme aims to deliver, around 2030, a new-generation capability to replace current systems such as Storm Shadow. Its core objective is to enhance the ability to penetrate and strike land, maritime, and hardened high-value targets in highly contested environments and against dense air-defence networks [88]. The development of European hypersonic penetration weapons reflects the coordinated evolution of platform penetration capability and long-range precision strike capability.

(4) Hypersonic penetration weapon of China

Public information indicates that China has developed a hypersonic-related weapons portfolio [89] centered on boost-glide vehicles, hypersonic anti-ship ballistic missiles, and long-range conventional strike missiles. Among these systems, the DF-17 is the most representative hypersonic boost-glide system in publicly available sources; its public debut marked China’s transition in hypersonic technology from experimental validation to operational fielding [90]. In terms of mission characteristics, the primary value of China’s hypersonic weapons lies in penetrating modern air and missile defense systems, compressing an adversary’s early-warning and interception timelines, and conducting rapid precision strikes against high-value fixed or mobile targets. Centered on hypersonic boost-glide systems and high-speed maneuvering ballistic missiles, China is building a long-range penetration and precision-strike architecture for highly contested environments. Related technologies could provide higher speed, stronger penetration capability, and shorter adversary reaction time for future strikes against hardened targets; their potential capability to hold hardened targets at risk therefore has military significance.

The fuze of hypersonic penetration weapons is confronted with significant engineering challenges. During target penetration, the fuze and its embedded microsystems may experience ultra-high transient deceleration, repeated mechanical impacts within a very short time interval, strong shock-wave transmission, and severe aerothermal loading [91]. At the same time, it must retain sufficient signal processing capability to achieve precise initiation within a millisecond-scale time window. To this end, key technologies for HTPF used in hypersonic penetration weapons have been vigorously developed worldwide. Because many fuze design details and performance parameters are not publicly available, we will not make too many comments here.

Although numerous challenges are still encountered in the development of hypersonic missile technology, its developmental trajectories have become clearly defined. Novel weapons integrating hypersonic platforms with penetration warheads will leverage advantages such as rapid long-range arrival and extreme penetration depth, driving the evolution of warfare toward non-linear and multi-dimensional forms while reshaping battlefield cognition and operational paradigms.

2.2 Mechanical inertial-triggered penetration fuzes

Mechanical inertial-triggered penetration fuzes rely primarily on mechanical impact or inertial elements and fixed or selectable mechanical/pyrotechnic delay to execute the sequence of arming, trigger determination, and initiation actions. As an early configuration of dedicated fuze for penetration weapons, this type of fuze has been widely integrated into various penetration systems due to its structural simplicity, robust resistance to electromagnetic interference, and low-cost. Consequently, it is commonly referred to as the first-stage hard-target penetration fuze.

In this section, the structural composition, operating principles, and working mechanisms of this class of fuze are systematically elaborated. The technical advantages and limitations are evaluated based on the technical characteristics of representative models. Furthermore, the development trajectory of fuze technology is traced, and the primary evolutionary themes and future trends are summarized.

2.2.1 Structural composition

In the design of the mechanical inertial-triggered penetration fuze, emphasis is placed on survivability under extreme deceleration, structural redundancy, and concise, reliable triggering logic. This section presents the structural composition of the mechanical inertial-triggered penetration fuze, utilizing the typical AV-1d/u [13] as an example. The AV-1d/u HTPF is composed of several components, primarily including the Safety and Arming (S&A) device, the triggering device, the delay device, the initiation and transmission device, and the information interconnection device.

(1) Safety and arming device

The S&A device comprises several interlocks and physical stops. It is designed to facilitate the arming sequence: following launch or release, the vane at the fuze nose is driven by airflow to rotate and eventually detach, which induces shifts in the relative positions of internal arming components. Consequently, the mechanical constraint on the firing pin is removed, transitioning the device into an armed state. Furthermore, the S&A device ensures that the weapon remains in a safe condition during storage, transportation, carriage, and the initial phase of deployment. As the primary line of defense for the reliability of mechanical inertia fuze, the design of the S&A device is critically linked to both battlefield and logistics safety.

(2) Triggering device

The triggering device primarily consists of an inertial firing pin and a primer. After the fuze is armed and enters the standby state, the inertial firing pin performs the final impact upon target contact. The firing pin initiates the primer, and the flame signal is transmitted to the next stage, completing the initiation control process. In addition to the firing pin, mechanical fuze often employ impact heads or strikers in similar roles. As an energy conversion unit, the triggering device is responsible for converting the kinetic energy from mechanical impact into the energy required for the ignition and initiation of the explosive.

(3) Delay device

The delay device is primarily designed to provide time for the bomb to penetrate the target medium. This aims to achieve better damage effectiveness. To meet penetration requirements, a pyrotechnic delay element is integrated into the explosive train of the AV-1d/u. Multiple short-delay options are offered. After the primer is activated, the flame signal burns through this delay element. A brief delayed initiation is thus enabled. In addition, delay behavior is realized in some mechanical inertial-triggered penetration fuze. This is accomplished by incorporating damping, hysteresis, or mechanical delay elements.

(4) Explosive train device

The ignition chain of the AV-1d/u comprises a primary detonator, an explosive transfer structure, and a compatible interface with the main charge inside the warhead. The upstream and downstream interfaces, connected to the explosive holder and main charge, must ensure sufficient ignition energy transmission when triggering conditions are satisfied. Concurrently, stability and safety are preserved under non-detonating conditions. For mechanical hard-target penetration fuze, ignition reliability and chemical compatibility are emphasized in this component. Furthermore, structural design aims to minimize errors induced by penetration shear or thermal effects.

(5) Information cross-linking device

The fuze accomplishes information interconnection through mechanical interfaces. It is typically designed in nose, tail, or nose-tail universal configurations. This enables adaptation to various bomb wells and guidance kits. Diverse tactical installation requirements are thereby satisfied.

2.2.2 Principle and working process

The operating principles and working processes of mechanical inertial-triggered penetration fuze are fundamentally similar. In this section, the operating principle and working process of the mechanical inertial-triggered penetration fuze are introduced, utilizing the typical AV-1d/u as an example.

(1) Operating principle

During captive carry on the aircraft, the fuze remains in a safe state. After the bomb is released, airflow drives the rotation of the rotor at the head. The rotor eventually detaches, thereby driving the internal device to disengage the lock and transition the fuze into an armed state. Upon entering the standby state, its core inertial striker is kept separated from the primer solely by an extremely low-stiffness anti-float spring. This design grants the fuze exceptionally high mechanical sensitivity. Any significant shock, movement, or abrupt change in bomb attitude may generate inertial forces sufficient to overcome the weak resistance of this spring. This can cause the striker to inadvertently initiate the primer. In a normal impact initiation, impact forces from any direction can compress the anti-float spring. This drives the striker to pierce and fire the primer, achieving genuine all-ways initiation.

To meet the penetration requirements, a pyrotechnic delay element is integrated into the explosive train. After the primer is activated, the flame signal burns through this delay element. A brief delayed initiation is thereby achieved. This gains time for the bomb to penetrate target media such as concrete, soil, or building structures. Consequently, better damage effectiveness is obtained.

(2) Working process

The core working process of the AV-1d/u comprises three distinct phases:

(a) The arming phase: after the bomb is released, the rotor at the fuze head is driven by the airflow to detach. This releases the internal safety block, placing the initiation control mechanism into a ready state. A direct visual indicator of whether the fuze is armed is whether the rotor has detached.

(b) The inertial triggering phase: when the projectile impacts the target, the inertial firing pin is driven forward by inertial force. It strikes the primer, thereby generating a flame signal. Reliable and safe inertial triggering is crucial for ensuring the proper functioning of the fuze.

(c) The delay control phase: the flame first ignites the corresponding black powder delay column. After a predetermined delay time, the detonator is initiated. This achieves penetration depth control and optimizes internal damage effectiveness.

2.2.3 Representative models

The mechanical inertial-triggered penetration fuze is widely used in various penetration weapons due to its advantages of simple structure, strong resistance to electromagnetic interference, and relatively low-cost. It serves as the predecessor to dedicated HTPF. Representative models include the M904, FMU-81/B, AVP-Z series, APUV series, and AV-1 series [13], with their structures illustrated in Fig. 4. These models reflect the characteristics of early mechanical penetration fuze in terms of functional design and tactical applicability.

Fig. 4. Mechanical inertial-triggered penetration fuzes [11, 13]: (a) M904; (b) FMU-81/B; (c) AVP-Z; (d) AVPZ-M; (e) APUV-1; (f) APUVM; (g) AV-1d/u; (h) AV-1.

(1) M904

The M904 is a mechanical inertial-triggered penetration fuze designed for the MK-80 series penetrating bombs. It is installed at the nose and is typically connected to the warhead via the M148/T45 adapter, with its structure shown in Fig. 4(a). This fuze is often integrated with a booster. The overall length is approximately 235 mm, with a maximum diameter of about 69.5 mm. The integrated mass is approximately 1.0 kg. The fuze provides both instantaneous and delayed initiation modes. The operational mode is selected by interchangeable M9 series delay elements. Common delay times include multiple settings such as 0.01 s, 0.025 s, and 0.25 s. These settings are designed to meet the requirements for engaging different hardened targets and tactical missions.

This fuze incorporates a rotor-type S&A device. After release from the aircraft, the blades are driven to rotate by the airflow. Through an internal gear system, the state transition from safe, through semi-armed, to fully armed is progressively completed. The arming status can be determined via an external observation window. Upon target impact, the M9 delay element is activated by the striker. After a preset delay, the explosive train is initiated, ultimately detonating the warhead charge.

(2) FMU-81/B

The FMU-81/B is a mechanical short-delay penetration fuze, primarily employed in the nose or tail configuration of aerial bombs. It is commonly used in MK-80 series conventional bombs [11], GBU series guided bombs, and BLU-109 penetration warheads, with its structure illustrated in Fig. 4(b). In LGB systems such as Paveway II/III, this fuze serves as a standard optional component. It is designed to achieve short-delay initiation upon target impact. This allows the warhead to detonate after target entry, thereby enhancing the internal blast damage effectiveness.

This fuze employs an all-mechanical and pyrotechnic design. It is characterized by its simple structure, high reliability, and strong resistance to electromagnetic interference. It is suitable for most conventional penetration missions. However, its delay is fixed and non-adjustable. For missions requiring greater penetration depth or precise initiation control, it is often replaced by electronic programmable fuze such as the FMU-152A/B.

The FMU-81/B, as a typical short-delay mechanical fuze, holds a significant position in the development history of HTPF for penetration weapons. Its design exemplifies a reliable solution for short-delay initiation within mechanical inertial-triggered penetration fuze. The design also reflects certain functional limitations. Consequently, it has provided a technical reference and helped pave the way for the subsequent development of electronic and programmable fuze.

(3) AVP-Z and AVPZ-M

The AVP-Z is a Russian aerial bomb fuze. It is a mechanical clockwork long-delay fuze with an electronic anti-jamming device. Since the majority and core S&A devices remain purely mechanical in structure, it is classified as a mechanically triggered penetration fuze. Its structure is shown in Fig. 4(c). The structure of the AVPZ-M is shown in Fig. 4(d). The AVPZ-M is identical in appearance to the AVP-Z [11, 13]. The main difference is that the AVPZ-M is equipped with a mechanical arming device. This type is easily recognizable due to its unique dome shape. It has been equipped on FAB and OFAB type aerial bombs. It may also be equipped on ZAB type aerial bombs.

This type of electromechanical triggered delay penetration fuze can be installed at either the nose or the tail of a bomb. A mechanical clockwork structure is employed for the delay mechanism, which can be configured in 30-minute increments, allowing for a maximum initiation delay of up to six days. Prior to the installation of the fuze, the clockwork device is removed, the delay duration is set, and the battery is subsequently installed. Furthermore, an Anti-Disturbance Device (ADD) is incorporated into the design of the AVP-Z. The ADD is intended to trigger immediate initiation if any attempt is made to move the aerial bomb or remove the fuze.

(4) APUV-1 and APUVM

The APUV series represents a typical mechanical inertial-triggered delay penetration fuze. It features a precision structure and multi-mode initiation capability, primarily including models such as APUV-1 and APUVM [13]. The APUV-1 is shown in Fig. 4(e), and the APUVM is shown in Fig. 4(f). By adjusting the selection screw, the fuze can be switched among three initiation modes: instant, 0.1-second delay, and 0.3-second delay. It is suitable for FAB and BRAB series aerial bombs. A key role is played by this fuze during the penetration of armored and other hard-targets.

(5) AV-1 and AV-1d/u

The AV-1 series is a mechanically omnidirectional impact-initiated penetration fuze, including models such as the AV-1 and AV-1d/u. Its structure is shown in Figs. 4(g) and 4(h). This series of fuze is noted for its high functional complexity and high initiation reliability. It is primarily used with FAB series general-purpose aerial bombs such as the FAB-50 and FAB-1000 [13]. Its core design objective is to ensure reliable initiation upon target impact, regardless of the bomb's attitude. Regarding performance parameters, the AV-1d/u fuze features two adjustable delay settings: 22.5–31.5 seconds or 11–16 seconds. In contrast, the AV-1 and its improved variants have a fixed delay of 22–35 seconds. Arming in this series is achieved through the detachment of vane components. A self-destruct capability is not incorporated into the design.

Although these HTPF possessed significant operational value during their period of deployment, their inherent limitations remained pronounced: (a) Functional modes are restricted, with support typically limited to instantaneous, unspecified-delay, or fixed-delay initiation; (b) Adaptability to complex penetration missions is constrained by the limited capacity for sensitivity regulation; (c) When subjected to non-target physical interference such as rain, and fog, the anti-interference performance is found to be insufficient, whereby the weapon is rendered susceptible to false triggering.

2.3 Electromechanical triggered delay penetration fuzes

Due to issues such as insufficient delay initiation precision, a limited sensitivity adjustment range, and susceptibility to false triggering, the mechanical inertial-triggered penetration fuze struggles to meet modern combat requirements. To address these limitations, second-stage electromechanical triggered delay penetration fuze technology, which integrates both electromechanical triggering and delay initiation functions, has been developed. Electromechanical triggered delay penetration fuzes introduce electromechanical S&A devices, electrical triggering, and electric delay detonators, but the initiation decision remains mainly a preset delay after impact. In this section, the structural composition, operating principles, and working mechanisms of this category of fuze are systematically expounded. Technical advantages and limitations are evaluated based on the technical characteristics of representative models; furthermore, the developmental trajectory of fuze technology is traced, and the primary evolutionary paths are summarized.

2.3.1 Structural composition

For the electromechanical triggered delay penetration fuze, S&A is primarily realized through electromechanical devices, while the delayed initiation function is achieved via delay electric detonators. The FMU-143/B [16] serves as a representative model in the technological evolution of penetration weapon fuze from pure mechanical inertial-triggered penetration fuze toward electromechanical integration. In this section, the structural composition of the electromechanical triggered delay penetration fuze is introduced, with the FMU-143/B utilized as a typical example.

The FMU-143/B is designed with a modular architecture. Overall, it is divided into five major modules: the S&A device, the initiation control device, the power supply and energy management device, the electronic delay device, and the information interconnection device. Connection to the bomb body is achieved via rear threading or a mounting base. An electrical interface is also established with the external weapon control device. This interface is used for power activation and signal setting.

(1) Safety and arming device

The S&A device of the FMU-143/B [2] utilizes a dual-path, sequential safety architecture, comprising three primary modules: mechanical safety elements, a centrifugal unlocking assembly, and electrical logic safety components. Physical obstructions and centrifugal unlocking mechanisms are employed to ensure that the explosive train rotor remains in the misaligned position prior to deployment. Furthermore, redundant protection is facilitated by the electronic subsystem through the integration of external weapon bus signals and internal electrical safety circuitry.

(2) Detonation control device

The initiation process is primarily accomplished through deceleration information, a trigger switch, a delay detonator, and a booster explosive. When the fuze experiences an deceleration no less than 160 g for a duration exceeding 6.5 ms, the trigger switch is closed. The capacitor then discharges to the delay detonator. After a preset delay, the main charge is ultimately initiated. The identification of fuze control is initially performed by the FMU-143/B [16] through the utilization of deceleration information.

(3) Electronic delay device

The electronic delay device is primarily composed of delay electric detonators. Upon closure of the trigger switch, the capacitor is discharged to the delay detonator. After a preset delay, the warhead is ultimately initiated. Through continuous iteration, the delay initiation time of the FMU-143 has been made settable to 30 s, 60 s, and 120 s.

(4) Power and energy management device

The power supply is dependent on an external starter. Through the action of the starter, high-speed airflow is utilized to drive a turbine generator, which provides power to the fuze. This, in turn, drives the micro-action switch, electronic timer, and delay electric detonator to initiate operation. Additionally, capacitor charging and discharging are achieved, triggering is completed, and precise energy management is realized.

(5) Information cross-linking device

The fuze is equipped with standardized electrical and threaded interfaces. Fuze parameters are generated by the mission planning device and loaded into the carrier aircraft via a data card. They are then transmitted to the guidance unit via a bus and finally delivered to the fuze microcontroller through the electrical interface, enabling precise control over arming and initiation. This provides the foundation for subsequent cockpit programming using an RS-422 serial communication interface and reflects the engineering approach of standardization and commonality characteristic.

2.3.2 Principle and working process

The operating principles and working processes of electromechanical triggered delay penetration fuze are fundamentally similar. In this section, the operating principle and working process of the electromechanical triggered delay penetration fuze are introduced, with the FMU-143/B [9] employed as a representative example.

(1) Operating principle

The FMU-143/B is an electromechanical device that relies on an external starter for functional activation. Its operation is based on coordination with the FZU-32B/B initiator. The starter is mounted between the aircraft lugs on the side of the bomb body. During bomb release, a safety lanyard pulls open an easy-open cover. This allows high-speed airflow to drive a turbine generator, which outputs a 50 V DC voltage as the power supply for the fuze.

Upon bomb release, a safety steel cable is pulled out, thereby activating a mechanical timer. After one second, a microswitch closes to energize the electronic circuit. After an additional four seconds, the first mechanical safety is removed. Following the establishment of a stable power supply, an electronic timer is initiated. At a preset time, it drives a diaphragm-type pyrotechnic actuator. This rotates the interrupter rotor into the armed position. Once the rotor is in position, the power supply is automatically cut off. Firing energy is stored in a capacitor. The fuze is triggered when it experiences an deceleration of not less than 160 g for a duration exceeding 6.5 ms. Upon meeting this condition, a trigger switch closes. The capacitor then discharges into a delay detonator. After a preset delay, the warhead is finally initiated.

(2) Working process

The core working process of the FMU-143/B is divided into four stages [2, 9, 92]:

(a) During bomb release, the safe lanyard is pulled to open the flip-top cover. This allows high-speed airflow to drive the turbine generator, which outputs a 50 V DC voltage as the power supply for the fuze. This further provides the basis for subsequent electronic operations. The design ensures that the fuze does not require a built-in long-term energy storage unit. Simultaneously, the airflow start-up indirectly verifies the separation status between the aircraft and the munition.

(b) The arming process of the fuze is divided into mechanical and electronic phases. The mechanical phase begins when the arming cable is pulled free upon bomb release, starting the mechanical timer. After one second, the micro-switch activates the electronic circuit, followed by the release of the first mechanical safety after another four seconds. Upon receiving stable power supply, the electronic timer initiates and, after a preset interval, drives a bellows-type pyrotechnic actuator. This rotates the out-of-line rotor to the aligned position. Once the rotor is in place, the power supply is automatically cut off, with firing energy stored in a capacitor. The fuze then completes its arming sequence and enters a ready-to-fire state.

(c) The initiation trigger device is dependent on dynamic deceleration conditions. When the fuze is subjected to an deceleration of no less than 160 g for a duration exceeding 6.5 ms, the trigger switch is closed. This results in the capacitor discharging to the delay detonator. After a preset delay, the warhead is ultimately initiated.

(d) Electronic delay is realized through the adoption of delay electric detonators.

Iterative changes are achieved in the electromechanical triggered delay penetration fuze compared to the mechanical inertial-triggered penetration fuze through the incorporation of electronic components. Three primary innovations are identified: first, a starter is integrated to provide power for the fuze; second, an electronic arming stage is introduced during the arming process; and third, electronic delay is realized through the application of electric delay detonators. Essentially, electronic components are integrated into every operational phase, thereby establishing a foundation for the subsequent development of all-electronic HTPF.

2.3.3 Representative models

The second-stage HTPF, such as FMU-143/B [16], MAFIS [39], and FMU152A/B [38], have been developed. These fuzes feature both electromechanical triggering and electronic delay initiation functions.

(1) FMU-143/B

The FMU-143/B is a representative electromechanical point-detonating delay fuze widely utilized in USA penetration weaponry [16]. It is characterized by a robust electromechanical S&A device. The delayed initiation capability is facilitated by an electric delay detonator, with the internal configuration illustrated in Fig. 5(a) [2].

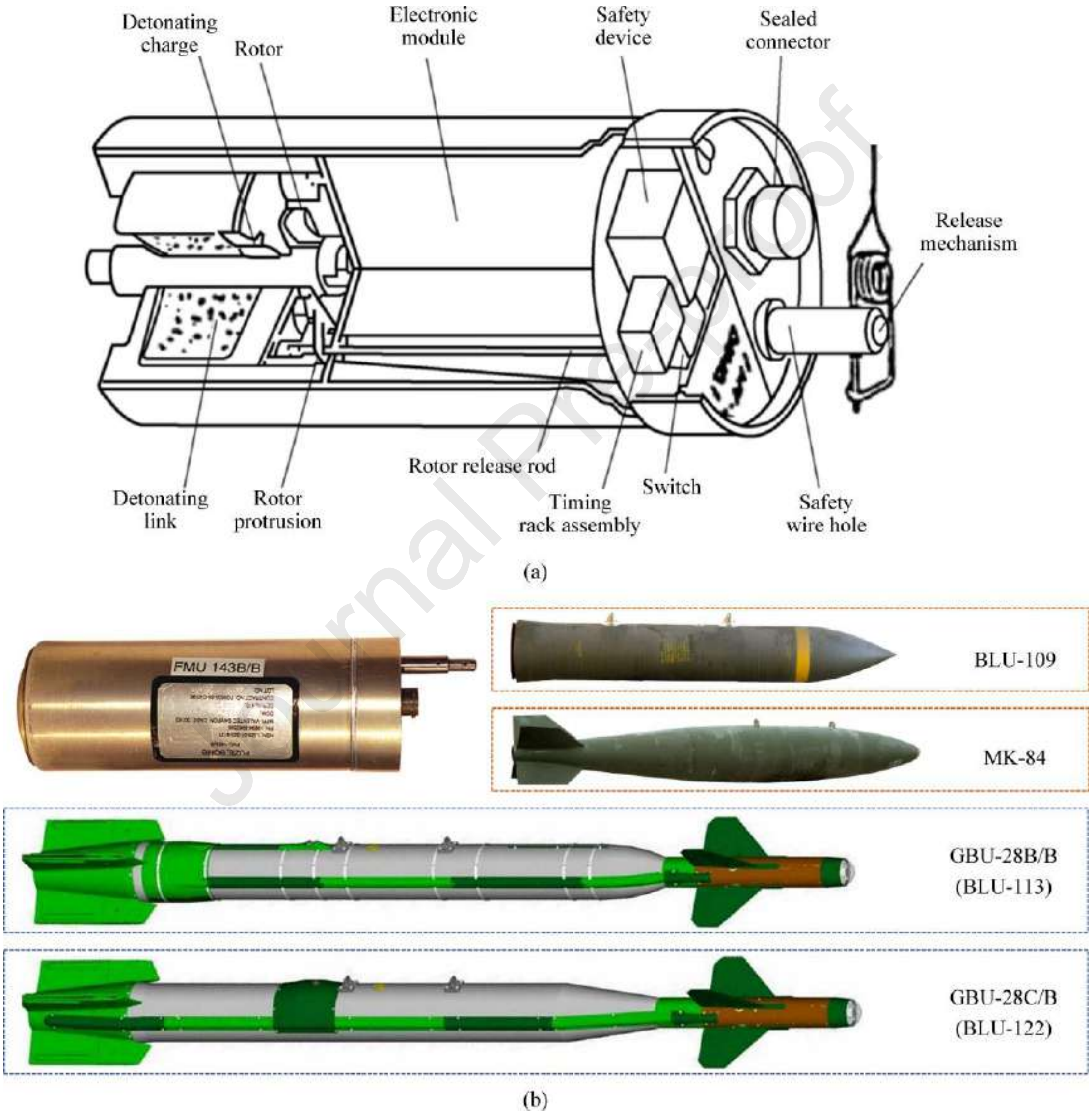

Fig. 5. FMU-143/B: (a) Schematic diagram of the fuze's internal structure [2]; (b) Schematic diagram of the fuze and partial equipped penetration weapons [13, 16, 52, 93].

The FMU-143/B was initially developed specifically for the BLU-109/B. Through long-term development and combat validation, its application has been expanded to a variety of penetration weapons, including the 2000-lb class BLU-109/B, as well as the

5000-lb class BLU-113/B and BLU-122/B. Furthermore, the FMU-143L/B variant was employed during testing of the BLU-116/B penetration warhead under the AUP program, exhibiting high versatility. The FMU-143/B [13] and its compatible weapons [52, 93] are shown in Fig. 5(b).

The FMU-143/B is required to operate in conjunction with the FZU-32B/B initiator to facilitate the arming sequence. This design configuration offers several distinct advantages: First, the necessity for an internal, long-term energy storage source within the fuze is eliminated. Second, the turbine-driven initiation device allows for the indirect verification of the weapon-platform separation status. Third, the installation position of the fuze is not constrained by the aerodynamic profile of the munition, thereby enhancing its versatility across multiple types of guided bombs. It should be noted, however, that the FZU-32B/B is designated as an early-model initiator and lacks interchangeability with later-stage fuze initiators. Subsequently, the FMU-147 was developed as a successor to the FMU-143 to enhance reliability, compatibility, and stockpile maintainability.

(2) MAFIS

The MAFIS is a multifunctional fuze developed by the French company Thales for the Storm Shadow stealth cruise missile equipped with the BROACH warhead. Based on the structural characteristics of the BROACH warhead, a trigger-delay initiator control strategy is adopted by this system [9]. The initiation control method based on penetration acceleration signals, which is selected by HTSF for penetration weapons, is not used. Its design concept originates from the fact that a larger channel can be created by the front-mounted large-caliber shaped charge armor-piercing warhead during the initial penetration phase. This significantly reduces the resistance encountered by the secondary follow-through warhead when traveling inside the target. Consequently, the influence of target impact attitude on damage effectiveness is weakened. In the context where intelligent penetration fuzes have attracted much attention, MAFIS stands out as a unique penetration fuze for penetration weapons due to its simple design and high reliability.

In technical implementation, MAFIS employs an electromechanical safety system and a reinforced electronic module. Detonation parameters are set via an RS-422 communication interface. The system has a delay setting capability within a range of 256 ms with a step of 1 ms. A manual setting function is not provided. This fuze controls the sequential initiation of the precursor shaped charge and the secondary warhead via the same activation signal. It features a compact structure and high reliability. It has passed a 50000 g deceleration test. It meets the stringent requirements of air-launched weapons for temperature characteristics and missile-level reliability.

The MAFIS [39] and its representative weapons [93] are illustrated in Fig. 6. The MAFIS architecture is integrated into stand-off weapons, including the Storm Shadow and the USA-made JSOW, and is currently deployed by the Royal Air Force and the USA Navy. Its technical significance is demonstrated by the enhanced penetration effectiveness of low-kinetic energy cruise missiles against HDBTs. Furthermore, operational adaptability is significantly improved under conditions involving complex impact angles and angles of attack.

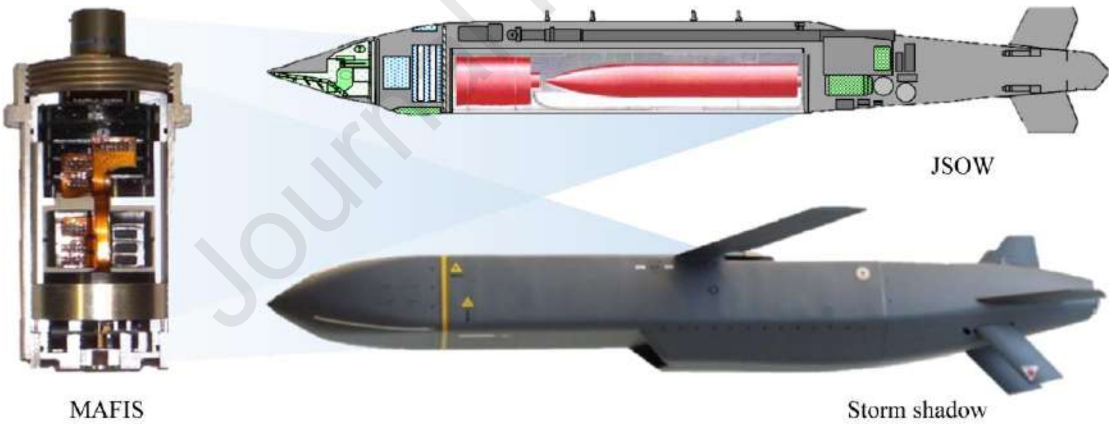

Fig. 6. MAFIS and representative equipped penetration weapons [39,93].

(3) FMU152A/B

The FMU-152 A/B is classified as an electromechanical impact fuze that supports multi-stage settings for both arming and initiation delays. To facilitate in-flight adjustments, an RS-422 serial communication interface is utilized for cockpit programming [38]. Simultaneously, the capability for manual configuration by ground personnel prior to weapon suspension is retained. This dual-mode configuration allows for the rapid setting and downloading of strike parameters during the mission cycle, thereby significantly enhancing operational flexibility. The structural assembly and an enlarged view of the programming panel for the FMU-152A/B [28, 94] are illustrated in Figs. 7(a) and 7(b), respectively. Within the JDAM operational sequence, fuze parameters are initially generated by the mission planning system and loaded onto the carrier aircraft via a data transfer cartridge. These parameters are subsequently transmitted to the JDAM guidance unit through the MIL-STD-1760 bus. Ultimately, the data is delivered to the fuze microcontroller via the RS-422 interface, enabling precise control over the arming and initiation sequences [94].

Fig. 7. FMU-152A/B: (a) Close-up view of the manual setting panel [28, 94]; (b) The fuze and components [94].

The companion FZU-55A/B initiator features a cylindrical configuration and is mounted on the sidewall of the warhead, where it is interfaced with the internal circuitry through an electrical connector. Following weapon release, the safety lanyard is pulled by the pylon, causing the protective cap to detach. The ram-air turbine generator is subsequently driven by the airflow, initiating power supply to the fuze once the airspeed exceeds 250 knots. Simultaneously with the detachment of the protective cap, a separation electrical signal is issued by the FZU-55A/B. The fuze is designed to be armed only upon the concurrent detection of both the power supply and the separation signal. By eliminating the requirement for traditional tail safety wires, this design simplifies the loading procedure and enhances the overall reliability of weapon delivery.

According to public data from the 53rd Annual NDIA Fuze Conference, the FMU-152 A/B is interchangeable with the FMU-143/B [94]. It is compatible with various

MK-80 series conventional high-explosive warheads, as well as hard-target penetration warheads such as the BLU-109 and BLU-113. The associated weapons encompass the AGM-130, GBU-10, GBU-12, GBU-15, GBU-24, GBU-27, GBU-28, and all variants of the JDAM. The arming time of this fuze can be configured within a range of 2–25 s. It features multi-stage initiation modes, ranging from instantaneous to a maximum delay of 24 h. Furthermore, proximity detection can be integrated to enable airburst functionality, thereby satisfying the diverse operational requirements for both fragmentation and penetration missions.

Although the FMU-152 A/B has been extensively utilized in operational environments, risks of failure are still encountered under high-intensity penetration conditions [2]. Current technological advancements are focused on enhancing the structural robustness of fuze against penetration impacts and replacing mechanical S&A devices with Electronic Safety and Arming Devices (ESAD). These upgrades are intended to improve penetration adaptability and satisfy the IM requirements. Overall, the FMU-152 A/B is regarded as a pivotal transitional product from electromechanical impact-initiating fuze to digital programmable fuze, signifying the evolution of penetration fuze technology toward a digitalized and programmable era.

Building upon the first stage of purely mechanical penetration fuze, electromechanical dedicated penetration fuze, represented by the FMU-143/B, MAFIS, and FMU-152 A/B, were developed by leading military powers, notably the USA. This progress led to the establishment of the second-stage penetration fuze system. Compared with the first stage, the integration of electronic components in these second-stage fuze have not only enhanced sensitivity adjustment capabilities but has also resulted in significantly higher precision regarding delay timing.

As the operational environments for weaponry become increasingly severe, new requirements are being imposed on penetration fuze, thereby driving their continuous advancement. Building upon the research and development of electromechanical delay fuze, future efforts will primarily be focused on the following three directions: (a) enhancing the high-g survivability and deceleration resistance of fuze structures; (b) improving the identification capability of fuze for cavities and layered structures; (c) developing all-electronic S&A systems to satisfy the IM requirements.

2.4 Digital programmable penetration fuzes

To address the evolution of modern combat patterns, major military powers represented by the USA, the UK, Germany, and France have further enhanced the recognition capabilities for internal voids and multi-layered media within targets. Building upon the foundation of electromechanical triggered delay penetration fuze, the resulting digital programmable penetration fuze constitute the landmark third-stage penetration fuze system. Digital programmable penetration fuzes further incorporate sensors, microcontrollers, and programmable algorithms to determine initiation timing based on penetration deceleration, layer-counting, penetration depth, or void-sensing information. In this section, the structural composition, operating principles, and working mechanisms of these fuzes are systematically expounded. Based on the technical characteristics of representative models, the technical advantages and limitations of this fuze category are reviewed. Furthermore, the developmental trajectory of fuze technology is traced, and its primary evolutionary themes and development trends are summarized.

2.4.1 Structural composition

The identification capabilities for internal voids and multi-layer media of targets are enhanced by the digital programmable penetration fuze. In this section, the structural composition of the digital programmable penetration fuze is introduced, taking the typical FMU-167/B as an example. An all-electronic, modular, and high-g-load-resistant design is adopted for the FMU-167/B [41] to withstand the extreme high-g deceleration generated when reinforced concrete several meters thick is penetrated by EPW. The fuze is primarily composed of six modules: signal sensing module, electronic control module, setting module, initiation module, power supply module, and protection module.

(1) Signal sensing module

The signal perception module primarily utilizes a high-g Micro-Electro-Mechanical Systems (MEMS) accelerometer to perceive deceleration information. It captures in real-time the minute deceleration variations during projectile penetration, enabling cavity perception. Unlike traditional fuze that rely solely on impact switches, this sensor can continuously record the acceleration variation curve throughout the projectile's flight and penetration process.

(2) Electronic control module

The electronic control module incorporates a high-performance microprocessor, high-g-resistant memory, and complex real-time signal processing algorithms. Filtering, feature extraction, and target recognition of the detection signals are performed. Arming is achieved through logical judgments based on launch deceleration and penetration pulse. Precise initiation control is subsequently accomplished.

(3) Setting module

The setting of parameters and logic control are achieved through the programming module. Parameters such as initiation delay, layer-counting strategy, and sensitivity thresholds can be set via the fire control system or wireless link prior to launch.

(4) Detonation module

The fuze contains approximately 0.1764 kg of high-explosive. This charge is responsible for amplifying the fuze signal and initiating the several tons of high-explosive in the main warhead.

(5) Power supply module

The fuze itself does not contain a long-life battery. It relies on an external nose-cone generator for power supply. It is typically used in conjunction with the FZU-60/B air-turbine initiator. According to the state-of-the-art information, the USA is testing a new FZU-65/B universal initiator. This is intended to support next-stage hypersonic and heavyweight penetration weapons.

(6) Protection module

The fuze assembly is entirely housed within a robust steel casing. Its internal circuitry is encapsulated with high-strength epoxy resin. This prevents circuit breakage or component detachment due to severe shock at the moment of impact.

2.4.2 Principle and working process

The operating principles and working processes of digital programmable penetration fuze are fundamentally similar. In this section, the operating principle and working process of the digital programmable penetration fuze are presented, with the FMU-167/B serving as a representative example.

(1) Operating principle

The FMU-167/B operates on the following principle. The dynamic response characteristics during penetration are perceived in real time by a high-g MEMS accelerometer. Filtering is applied to highlight the deceleration features. These features are then matched against preset logic or adaptive algorithms. When characteristics satisfying the initiation condition are recognized, the electronic control module of the fuze triggers the initiation chain. Consequently, the warhead is initiated at the position where damage effectiveness is maximized.

(2) Working process

The core working process of the FMU-167/B is divided into four stages:

(a) Pre-launch programming phase: mission parameters are input through the fire control system, which may include the cavity-perception number, penetration layer count, penetration depth, etc. The corresponding initiation strategy is loaded by the programmable logic unit inside the hard-target penetration fuze.

(b) Projectile flight phase: the HTPF is progressively disarmed through the S&A module in a staged manner.

(c) Target penetration phase: the information sensing module continuously acquires penetration deceleration signals and other relevant data. The acquired signals are then processed in real-time by the electronic control module to accentuate deceleration characteristics. The acceleration peaks generated upon target entry and exit are identified, enabling the accomplishment of cavity recognition or inter-layer discrimination. Based on pre-loaded initiation strategies, the fuze dynamically updates the current penetration status.

(d) Detonation decision and execution phase: when the predetermined initiation conditions are determined to be met by the electronic control system, the initiation command is issued. The initiator is then activated by the energy module, leading to the warhead initiation. If the conditions are not satisfied or system failure occurs, the self-destruction mode is entered.

Compared with the electromechanical triggered delay penetration fuze, the advantages of the digital programmable penetration fuze are demonstrated in the following aspects: first, an ESAD and an in-line initiation design are utilized to ensure stable operation under high-impact environments; second, initiation strategies can be adjusted in real-time according to various target structures, such as the number of layers and medium thickness; and third, through the application of signal recognition algorithms, layers and voids are accurately perceived, which significantly minimizes the occurrence of premature or delayed initiation.

2.4.3 Representative models

Third-stage digital programmable penetration fuze, represented by models such as the FMU-159/B [38, 54], PIMPF [36, 95], FMU-167/B [41], FBM-21 [53, 96], and AURORA [15, 40], have been developed by leading military powers including the USA, the UK, France, and Germany.

(1) FMU-159/B

The FMU-159/B was developed as a significant outcome of the HTSF program in the USA. It represents the first digital programmable fuze in which precise burst point control is achieved based on the physical characteristics of hard-target penetration. The fuze is required to be utilized in conjunction with the FZU-60/B initiator [38]; its core performance parameters are illustrated in Fig. 8(a). By leveraging accelerometers and real-time signal processing circuits, target layers and void structures are identified during the penetration process. Consequently, the penetration depth is calculated to facilitate the precise control of the initiation position.

Fig. 8. Critical performance of the FMU-159/B and FMU-167/B: (a) The FMU-159/B [2, 54]; (b) The FMU-167/B [6, 41].

An in-line architecture is utilized in this fuze to ensure high safety standards. It is designed to support 22 ground-based and 11 airborne parameter settings [54]. Three programmable initiation modes, layer-counting, void-sensing, and depth-counting are provided, alongside an integrated independent backup programmable timed initiation function (0–255 ms with a 1 ms minimum step).

High versatility is exhibited by the FMU-159/B design, which can be adapted to various penetration warheads, such as the BLU-109, BLU-113, and BLU-116, as well as guided weapon platforms including the GBU-28, AGM-130, AGM-142, JDAM, and Tomahawk cruise missiles [97]. Significant application potential in the field of hard-target defeat is demonstrated by this system. However, the FMU-159/B was ultimately not fielded. The main reasons are as follows:

(a) The FMU-159/B was required to simultaneously meet a set of demanding requirements: reliable operation after penetration, recognition of layered structures, void sensing, initiation at a preset position, and compatibility with various existing and future hard-target munitions. This combination of multi-platform compatibility, high-shock penetration environments, and intelligent sensing for initiation resulted in a program risk substantially higher than that of a conventional delay fuze. Based on the "Engineering and Manufacturing Development qualification problems" [97, 98] and the subsequent decision to switch to a mature fuze, the technical failures of the HTSF were likely concentrated in reliability, environmental adaptability, manufacturing consistency, or system integration verification.

(b) Urgent operational needs compounded the situation. Due to the contractor ATK's slow progress, insufficient program maturity, and production cost and capacity assessments that failed to meet expectations, a modified FMU-143 had to be adopted as a limited-capability replacement [38]. This indicates that the program's failure was not merely a technical problem but also a mismatch between technology maturity and the operational deployment timeline.

(c) Mature solutions such as the PIMPF became lower-risk alternatives following comparative testing, further reducing the necessity of continued investment in the original HTSF program.

The FMU-159/B HTSF was not a conceptual failure, but rather a failure at the levels of engineering, manufacturing consistency, and qualification; its required capabilities were subsequently carried forward by follow-on efforts such as the PIMPF and the FMU-167 HTVSF.

(2) PIMPF

The PIMPF, developed in Germany, is equipped on the MEPHISTO warhead of the TAURUS-KEPD350 air-launched cruise missile, jointly developed by Germany and Sweden, as well as on Norway's Naval Strike Missile. The TAURUS-KEPD350 air-launched cruise missile, fitted with the MEPHISTO warhead and the PIMPF, along with its performance parameters [95], is shown in Fig. 9. This fuze is designed to engage single-layer or multi-layer reinforced concrete targets, which may be covered with soil or gravel on the surface. Through the recognition of target structural characteristics, the fuze senses the impact and shock during penetration. Intelligent signal processing is then utilized to achieve precise initiation control. It possesses void-sensing capability and layer-counting initiation control functionality.

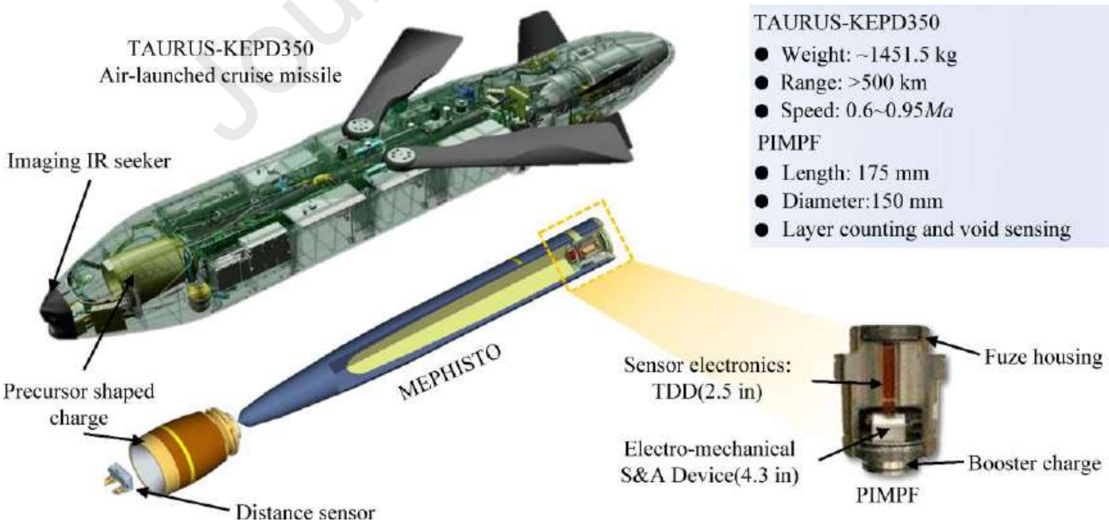

Fig. 9. The TAURUS-KEPD350 air-launched cruise missile, MEPHISTO, and PIMPF [2, 9, 36, 95].

The PIMPF has an overall dimension of φ150 mm × 175 mm. It incorporates an electromechanical S&A device [36]. The core functions of signal processing and initiation control are implemented by an electronic assembly.

The initiation control function of PIMPF is composed of a signal processing circuit, a backup power supply, a microcontroller, non-volatile memory, a firing circuit, and an electrical interface. The acceleration signal is sensed by the sensor. It is then amplified and filtered. After that, it is digitally sampled via an A/D converter. The core algorithm of PIMPF is executed in the microcontroller. This achieves cavity sensing and layer-counting initiation control. In addition, the height-determined initiation function required by the forward-shaped charge warhead is also implemented. The initiation control signal is obtained from the burst height sensor through the electrical interface. Based on this signal, the shaped charge warhead is initiated at the appropriate time.

(3) FBM21

The FBM-21 modular aerial bomb fuze, developed in France, is designed to be dimensionally compatible with the 3-inch diameter FMU-143/B and FMU-152/B series of USA-made fuze. The internal architecture of the device is illustrated in Fig. 10. Its core components consist of an electronic assembly, thermal battery, slapper detonator, booster, electrical connector, and structural housing [53,96].

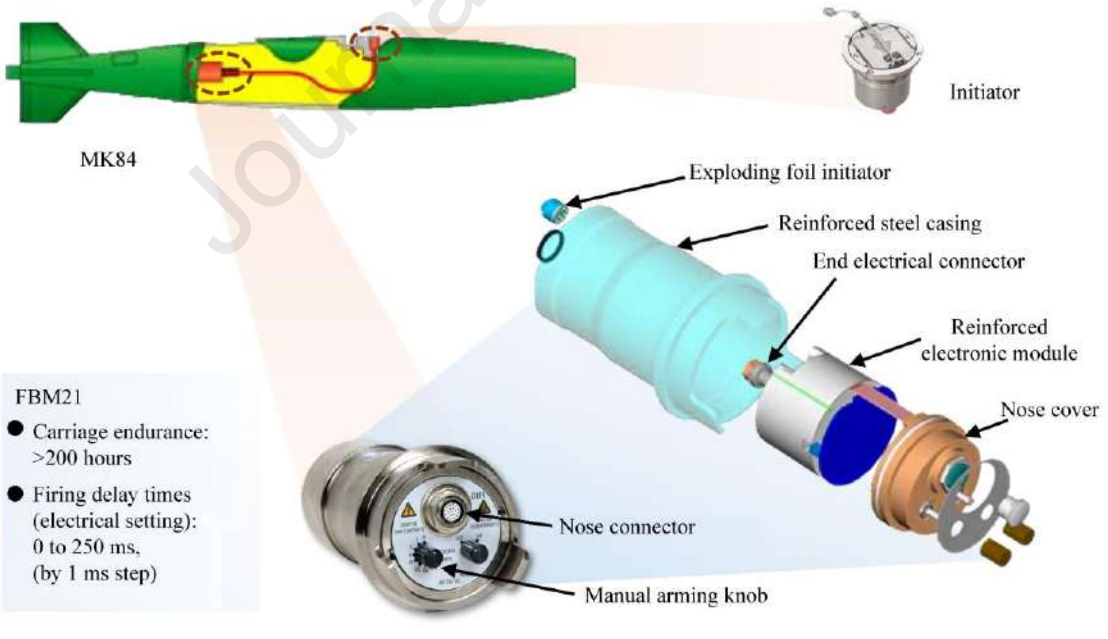

Fig. 10. Schematic diagram of FBM21's structure and equipped weapon [2, 9, 53, 96].

Diverse operational requirements, including point initiation, proximity sensing, and penetration modes, are accommodated by the FBM-21, which can be integrated with warheads such as the BLU-109. Due to the implementation of in-line fuze technology [53], the stringent IM requirements mandated for aircraft carrier-based weapons are fully satisfied by the FBM-21.

A dedicated Arming Environments Sensor (AES) is utilized by the FBM21 to perceive the first and second arming environments, thereby providing the logical and electrical conditions required for fuze arming. This AES is functionally analogous to the FZU-series initiators employed in USA aerial munitions. The first environment is supplied by the carrier aircraft, and operational parameters can be configured either manually or via a communication interface. The system is designed to receive mission data, delayed arming commands, and sterilization commands.

A trigger acceleration threshold of ±20 g is maintained, with a functioning time of less than 100 μs [2, 56]. The penetration trigger delay can be programmed within a range of 1–250 ms with a minimum step of 1 ms. Furthermore, void-sensing and layer-counting initiation capabilities are incorporated. An ESAD is adopted, and sensitive primary explosives are excluded from the design. Due to the in-line architecture of the FBM21, a detachable configuration for the booster and Exploding Foil Initiator (EFI) is featured, which facilitates the testing of the disassembled fuze. Following the completion of testing, all stored electrical energy is dissipated within five minutes of power-down, allowing the fuze to revert to a safe state, a characteristic inherent to in-line fuze systems.

(4) AURORA

AURORA, a representative model of the Multi-Event Hard Target Fuze (MEHTF), was jointly developed by the USA and the UK. It is typically integrated with warheads such as the MK-80 and BLU-109 [15]. Various initiation modes, including layer-counting, void-sensing, fixed-delay, and airburst are supported, and the fuze can be programmed during ballistic flight. An independent timed initiation circuit is embedded within the firing module to facilitate self-destruction. The operational sequence of the fuze following weapon deployment is illustrated in Fig. 11(a). Furthermore, lower costs and reduced dimensions are achieved through the adoption of standard fuze architectures, interfaces, and electronic safety systems.

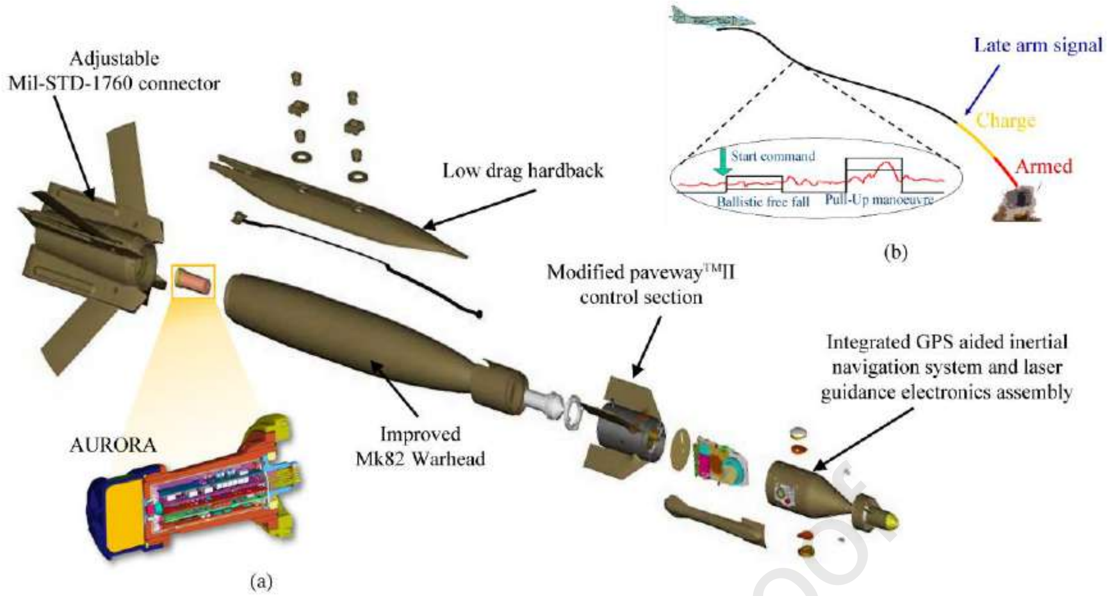

Fig. 11. AURORA: (a) Schematic of AURORA functioning process [15]; (b) Disassembly diagram of the PGB and schematic diagram of the AURORA's internal structure [40].

A secondary encapsulation method is employed to provide the core functional module with a reinforced housing, ensuring compatibility with the installation requirements of the projectile body. A waisted external profile is adopted to reserve a specific clearance between the fuze and the warhead. This design provides the fuze with a degree of protection against projectile body deformation during high-velocity impact.

The technical highlights of the AURORA can be classified into the following four aspects: (a) A highly reliable, programmable architecture is utilized for guided weapon integration; (b) An in-line S&A device is integrated, which is based on the MEHTF and power sources and firing train schemes; (c) A reinforced 3-inch fuze system is employed, whereas the core electronic assembly is miniaturized to a 2-inch diameter for optimized space efficiency; (d) A newly developed post-release safety environmental sensing scheme is adopted to ensure high levels of safety during the deployment phase.

Consistent with the HTSF, an in-line fuze architecture was selected for the MEHTF during its initial research and development phase. Its internal functional modules are comprised entirely of electronic systems [40], and all fuze operations are executed through circuit units, which ensures a high degree of safety. While no formal equipment designation was assigned to the MEHTF program within the USA Air Force weapon system, the underlying technology was successfully transitioned by Thales into the new AURORA for the Royal Air Force's PGB program [15]. An exploded view of the PGB weapon integrated with the AURORA is illustrated in Fig. 11(b).

(5) FMU-167/B

The FMU-167/B is a typical model of HTVSF. This fuze adopts an in-line configuration. To maintain compatibility with the operational use of warheads such as the BLU-109/B and BLU-113/B, this fuze continues to be installed and used on the warhead in the form of FMU plus FZU. Its initiator is the FZU-60/B, originally equipped for the FMU-159/B. Its core performance parameters [2, 6] are shown in Fig. 8(b). Its main technical features are as follows: capability to attack HDBTs, survivability against shock decelerations up to 50000 g without damage, and void-sensing or layer-counting capability in complex target environments [41].

The FMU-167/B features cockpit programmability, selectable void sensing, backup timing, and time-delay initiation functions. Public USA Air Force procurement documentation states that the FMU-167/B will be employed by the USA Air Force and USA Navy in penetration warheads for HDBTs [99].

(6) Advanced fuze associated with the GBU-72/B

The GBU-72/B equipped with the BLU-138/B is identified in recent USA Air Force procurement documentation as incorporating enhanced survivability, increased lethality, and smart fuze, and is intended to replace the GBU-28/B. The same public documentation identifies the FSU-32 and the future FZU-65/B Universal Linear Air-stream Generator within the disclosed fuze and power-supply architecture of the GBU-72/B [63]. However, detailed fuze configuration information remains limited in publicly available sources.

(7) LPSF for the GBU-57 MOP Modification program

For massive penetrators, the Large Penetrator Smart Fuze (LPSF) represents a more recent smart-fuze development associated with the GBU-57 MOP Modification program. According to the FY 2025 DOT&E annual report, the LPSF integrates advanced smart-fuze capability into the MOP warhead to increase the probability of defeating HDBTs under uncertain target-intelligence conditions. However, the available public report indicates [100] that additional test and evaluation activities are still required for eventual fielding. Therefore, the LPSF should currently be regarded as an advanced smart-fuze program undergoing continued evaluation.

The digital programmable penetration fuze has been extensively developed by leading military nations, most notably the USA, the UK, Germany, and France. These systems have reached the stage of finalized production and have been fielded within various weapon platforms across their respective armed forces. As the hallmark of third-stage penetration fuze, digital programmable variants are characterized by the following features: (a) Accurate control of the initiation point is achieved based on hard-target penetration characteristics. Multiple programmable initiation modes, including layer counting, void sensing, and penetration depth counting, are provided. Consequently, initiation strategies can be adjusted in real-time to match specific target structures, ensuring high adaptability; (b) ESAD and in-line initiation designs are utilized in the vast majority of these systems. This ensures stable operation under high-impact environments and ensures that IM requirements are strictly met; (c) Through the application of advanced signal recognition algorithms, layers and voids are accurately perceived. By utilizing these data, the occurrence of premature or delayed detonations is significantly reduced, resulting in superior terminal effectiveness.

From the perspective of European contributions, FBM21 and PIMPF are two representative engineering examples of programmable penetration fuze. PIMPF, developed for the German TAURUS/MEPHISTO warhead system, represents a typical European programmable intelligent multi-purpose fuze. These demonstrate that the development of digital programmable HTPFs is not limited to the USA FMU-series, but has also been actively promoted by European missile and warhead programs.

Overall, an evolutionary trajectory from mechanization to electronification, and subsequently to digitalization and intelligence, is followed in the field of penetration fuze technology. In earlier iterations, precise delay control was prioritized as the core technical focus. This has since been evolved into target identification based on penetration deceleration characteristics, where acceleration signals serve as the fundamental basis for target perception. Regarding control logic, a significant transition from fixed presets to programmable configurations has been achieved, whereby mission adaptability and versatility are substantially enhanced. Currently, a shift toward the stage of intelligent fusion recognition is being undertaken, with the objective of achieving precise target identification and adaptive initiation control during the penetration process via multi-domain fusion signals. Although variations in sensing mechanisms, control algorithms, and system architectures are maintained across different nations, the global developmental trend remains focused on complex target recognition, intelligent initiation control, and the enhancement of high-g impact resistance, presenting a clear and unified technological roadmap.

2.5 Intelligent fusion-recognition penetration fuzes

Intelligent fusion-recognition penetration fuzes represent an emerging direction. Compared with digital programmable fuzes, this concept emphasizes multi-domain sensing, adaptive recognition of target structures, dynamic optimization of initiation logic, and reliable decision-making under high-dynamic penetration environments and complex target conditions. However, based on currently available open-source information, no operational HTPF can be confirmed to integrate multi-domain information fusion, adaptive closed-loop initiation control, extreme-mechanics protection, and high-dynamic fault-tolerant recognition. Therefore, this section only discusses the key technologies that may be involved in the intelligent fusion-recognition penetration fuze and their maturity.

2.5.1 Technical characteristics

To adapt to the demands of new-quality warfare, higher requirements are imposed on the intelligence and adaptive capabilities of fuze for next-stage penetration weapons. This also marks a fundamental leap in the penetration fuze towards intelligence [101]. As a next-stage intelligently fuzed recognition penetration fuze, it should possess the following core characteristics:

(1) Multi-domain information fusion and intelligent recognition algorithm: By fusing signals from multiple types of sensors, such as acceleration, magnetic field, and acoustics, a multi-domain information fusion recognition algorithm is constructed to enhance the robustness of perception in complex penetration environments. Combined

with deep learning and real-time signal processing, dynamic identification of medium layer characteristic changes during penetration and accurate perception of hard-target information are achieved.

(2) Adaptive closed-loop initiation control: Based on Artificial Intelligence (AI)-assisted decision-making, an adaptive control architecture with online learning capability is constructed. It can dynamically adjust initiation parameters according to the target structure. Autonomous determination and closed-loop control of the optimal initiation point are achieved under unknown target conditions. Real-time reconstruction of initiation logic is also supported.

(3) Protection of devices under extreme mechanical environments: Efforts are focused on developing high-g-resistant miniaturized devices and protection solutions. The structural integrity and anti-interference capability of the fuze and its internal electronic modules under extreme shock and deceleration conditions are enhanced.

(4) Signal reliability and algorithmic fault-tolerance under high-dynamic conditions: For the hypersonic penetration environment, the signal chain design and fault-tolerance mechanisms are optimized. Reliability of signal acquisition and processing under extreme mechanical loads is ensured.

2.5.2 Technical maturity

Currently, the next-stage intelligently fuzed recognition penetration fuze has not yet matured into a fielded model, with most still in the stages of pre-research, demonstration, or verification. Among these, the FMU-167/B represents the highest current technical level for penetration fuze. It is equipped with a high-precision accelerometer [102], which significantly enhances the recognition capability for multi-layer media and cavity structures encountered during penetration. Based on preset strategies, it can adaptively select the initiation position, thereby achieving precise initiation control in multi-layer cavity environments. From the perspective of technological generational evolution, the FMU-167/B exhibits typical transitional characteristics from an improved third-stage to a fourth-stage fuze. The core technology maturity of current fourth-stage HTPFs is assessed in Table 2.

Table 2

The maturity of core technologies for intelligent fusion-recognition penetration fuze.

Technologies	TRL	State of research
Multi-domain information fusion and intelligent recognition technology	5–6	◆ The mainstream accelerometers in service remain single-axis or three-axis high-g devices [103, 104]. ◆ The incorporation of sensors such as magnetic and acoustic detectors is a defining feature of fourth-stage fuzes [1, 6]. ◆ To resolve issues of integral drift and signal overlapping and aliasing in single acceleration signals [105].
Adaptive closed-loop initiation control technology	4–5	◆ Most fuze in service are based on the threshold-based decision or the window-counting method [106]. ◆ If AI with online learning and parameter reconstruction capabilities were to be embedded in the microprocessor of a missile, it would face challenges in computational power and power consumption [107, 108]. ◆ The current adaptive approach primarily refers to the dynamic tuning of parameters [109].
Extreme mechanics protection technology	8–9	◆ Potting technology [110], MEMS solid-state devices [111], and deceleration-resistant structural design [3, 112] have reached a high level of maturity. ◆ The fuze capable of withstanding decelerations of 20,000 g to 100,000 g has been deployed, such as the FMU-167/B [41].
High-dynamic environment adaptation technology	7–8	◆ Signal processing and fault-tolerance mechanisms [113, 114] have entered the engineering application phase. ◆ Focus on ensuring signal integrity under Doppler effects, blackout communication scenarios, and transient impacts [115].

The development of intelligent fusion-recognition HTPFs is characterized by uneven disclosure levels among different countries. The USA has disclosed relatively more information on programmable and void-sensing fuzes, such as the FMU-159/B and FMU-167/B, which provide important references for layer-counting, void-sensing, and programmable initiation control. However, even these systems should be regarded primarily as advanced digital programmable fuzes or transitional systems rather than intelligent fusion-recognition fuzes.

European countries have also made important contributions. The MAFIS and PIMPF demonstrate mature engineering applications of programmable fuze in stand-off penetration weapons. In particular, the PIMPF used in the TAURUS/MEPHISTO system is publicly described as enabling initiation at pre-selected floors through layer-counting and void-sensing technologies [39]. These systems provide valuable examples of European progress in programmable penetration fuze, although they still do not fully represent adaptive closed-loop intelligent fusion-recognition fuzes.

For Russia, open information mainly concerns penetration weapons, hypersonic strike systems, and earlier mechanical or electromechanical fuze technologies [116]. Although Russian penetration weapons impose strong demands on fuze survivability under high overload, high thermal load, and high-speed impact conditions, no publicly available source has been found that verifies a Russian operational HTPF with full multi-domain fusion recognition and adaptive closed-loop initiation control.

In China, publicly available studies mainly focus on key enabling technologies rather than disclosed operational fuze models. These studies include high-g MEMS accelerometers [117, 118], penetration overload signal acquisition and processing, geomagnetic layer-counting, acceleration-sensor/MEMS-switch fusion, multi-source information fusion, and intelligent recognition algorithms. Such research provides an important technical foundation for intelligent fusion-recognition HTPFs.

Based on available information, no operational HTPF can be confirmed to fully integrate multi-domain information fusion, adaptive closed-loop initiation control, extreme-mechanics protection, and high-dynamic signal fault tolerance simultaneously. Therefore, the intelligent fusion-recognition category is regarded as an emerging technological direction or next-stage intelligent HTPFs. Existing advanced fuzes, represented by the FMU-167/B, exhibit partial characteristics of this trend, such as programmable logic, improved high-g survivability, and enhanced void/layer sensing capability, but they should not be considered complete fourth-stage representatives.

2.6 The HTPF technology development strategy

This section compares the HTPF technological pathways of major military powers in the first. Based on the open-access sources from the 59th to 65th Annual NDIA Fuze Conference [45, 46, 98, 119–137], the technological development strategies and research trends of HTPF were reviewed for military powers. Furthermore, the challenges facing the development of penetration fuze technology were analyzed.

2.6.1 Comparison of HTPF technology pathways

The strategic cores, technical architectures, advantages, and limitations of the three major technical systems are compared in Table 3. The USA takes the defeat of HDBTs as its absolute core, building a fuze system that covers a full spectrum of penetration weapons ranging from 500-lb to 30000-lb to support global rapid strike and strategic deterrence. Europe focuses on cruise missiles and stand-off strike weapons, prioritizing the development of fuzes compatible with composite warheads and emphasizing multi-mission commonality and NATO equipment interoperability. Russia takes hypersonic weapons as its core breakthrough direction, emphasizing survivability and reliability in extreme environments to serve an asymmetric deterrence strategy. Because detailed fuze architectures and performance parameters are often not publicly disclosed, this comparison is based primarily on open-access government budget documents, NDIA fuze conference proceedings, and studies on enabling technologies.

Table 3

Comparison of the USA, Europe, and Russian HTPF technical pathways [102, 138–144].

Dimension	USA	Europe	Russia
Strategic Core	Tri-service joint development centered on HDBT defeat; prioritize intelligence, extreme environment adaptability, and model-driven design	Focus on multi-mission versatility, composite warhead-fuze synergy, and industrial standardization	Emphasize extreme environment reliability, anti-electromagnetic interference, and low-cost mass production
Technical Architecture	All-electronic in-line design; distributed fuze system; Fuze-on-a-Chip roadmap	Modular universal design; cross-platform compatibility; electromechanical-electronic hybrid transition	Predominantly electromechanical design; robust mechanical backup; minimal reliance on complex electronics
Key Technological Advantages	1. Leading in digital programmable and void-sensing technology 2. Mature MEMS high-g sensor and ESAD technology 3. Complete HIL and	1. World-leading tandem composite warhead fuze control technology 2. Excellent multi-mission adaptability 3. Strict IM compliance	1. Exceptional high-g and thermal protection capability 2. Superior anti-plasma blackout communication technology 3. Ultra-long storage

Dimension	USA	Europe	Russia
	ground test system		reliability
Key Technological Limitations	1. Extremely high unit cost 2. Over-reliance on GPS and electronic systems 3. Complex supply chain and long production cycle	1. Lag in intelligent fusion recognition technology 2. Slow progress in hypersonic penetration fuze development 3. Fragmented national R&D systems	1. Significant gap in digitalization and intelligence 2. Limited multi-layer target recognition capability 3. Outdated manufacturing processes

The USA maintains comprehensive technological leadership with a complete system, extensive engineering expertise, and abundant combat experience, serving as the absolute benchmark for global penetration fuze technology. Its advantages lie in solid fundamental research, a mature industrial chain, and highly efficient tri-service coordination. It will continue to lead the development toward intelligent and system-of-systems approaches [139]. Its disadvantages include the excessive complexity of certain technologies and high costs.

Europe possesses unique strengths in fuzes for composite warheads, modular design, and NATO interoperability [140]. It follows a pragmatic technical route and emphasizes the spin-in of commercial technologies [39]. Its disadvantages are a lack of demand for heavy penetration weapon development, an incomplete fuze product spectrum, and reliance on the USA for some core sensors.

Russia features distinct capabilities in extreme environmental protection, hypersonic fuzes, and anti-jamming technologies. Its technical route is simple, reliable, and low-cost [143]. Its disadvantages include a weak electronics industrial base and a relatively low level of fuze intelligence.

2.6.2 Strategic direction of USA

Since 2016, the defeat of HDBTs has been established as the core of the fuze technology strategy by the three branches of the USA Armed Forces.

Strategic priority is accorded by the Army to IM safety and programmable delayed initiation during penetration, with system-level solutions, specifically the miniaturization of ESAD [145, 146] and embedded ignition systems [147–151], being actively pursued. Simultaneously, the functional reliability of fuze within complex media is underscored by the Navy, with emphasis placed on the integration of high-shock resistant MEMS S&A devices [152–154] and micro-initiation sequences [155]. The development of algorithms for intelligent multi-layer target recognition [156] and optimal burst point control is spearheaded by the Air Force, alongside the deployment of fuze technologies for extreme environments [125, 157] such as hypersonic platforms. Furthermore, the USA treats low-cost as important conditions for engineering transition and large-scale procurement [97, 98].

Technical integration and investment synergy are realized across various military services through the Joint Fuze Technology Program [124, 158], which serves to collectively drive the leapfrog development of penetration fuze capabilities.

2.6.3 Technological evolution trends of USA

(1) Intelligent perception and decision-making algorithms

The smartening of fuze represents the most distinctive feature in the evolution of USA key technologies. The technical focus has evolved from single deceleration information perception to real-time decision-making based on multi-modal information fusion, such as acceleration, radar, and magnetic sensing [133, 159]. This enables precise recognition of internal structures, including concrete layers and cavities.

Continuously upgraded intelligent algorithms, including dynamic triggering, layer-counting, and closed-loop initiation control, form the core of realizing the closed-loop perception-decision-initiation capability [155]. These algorithms aim to dynamically optimize the initiation timing based on target characteristics, so as to achieve precise initiation after penetration.

(2) Extreme environment adaptability and survivability

To address the extremely high impacts generated during penetration, the technical protection levels and design philosophies have been continuously elevated. The design objectives have evolved from the 10000 g magnitude to impact protection in the range of 50000 g to 100000 g [160]. Additive manufacturing [132] has become a key technology. It is utilized to fabricate impact-resistant MEMS structures, fuze components with complex topologies, and to achieve the integrated assembly of explosive components and electronic circuits [161, 162]. MEMS-based g-switches, sensors, and micro-actuators have become mainstream [136, 163]. Their functional integrity under extreme impact is ensured through embedded packaging technology.

(3) Distributed and miniaturized system architectures

To address the stringent spatial constraints inside penetration weapons and enhance reliability, the architecture of fuze systems has undergone profound transformations [164, 165]. In the distributed fuze architecture, the arming control unit serves as the master S&A device that validates physical arming parameters and translates them into robust Virtual Environment (VE) signals [166, 167]. These signals are then transmitted to multiple remote firing modules that control the power application to safety-critical features and execute the firing sequence upon successful VE validation. This significantly reduces the risk of single-point failure.

Furthermore, the technical roadmap points toward the integration of ESAD, sensing, and setting functions into a single chip, realizing Fuze-on-a-Chip [168]. The widespread adoption of micro-scale firing trains and in-line EFI [25, 137, 169] has provided key support for system miniaturization and insensitivity.

(4) Innovations in model-driven development and testing & verification

Model-based systems engineering has fundamentally transformed the design and verification processes for penetration fuzes. Explicit dynamics simulations and multiphysics coupling analyses enable the precise prediction of structural responses and fuze behaviors during penetration [170, 171]. This capability serves as a prerequisite for design and significantly reduces reliance on live-fire testing during development. Embedded data recorders have replaced traditional telemetry [172, 173]. They allow for the acquisition of authentic data throughout the entire penetration process. The establishment of closed-loop hardware-in-the-loop testing and a dedicated ground test system for penetration fuze provides an efficient platform [174]. This platform is used for evaluating the dynamic decision-making logic and reliability of fuze.

2.6.4 Challenges and prospects

While significant progress has been achieved in HTPF technologies, the field still confronts several critical challenges. This section focuses on the key challenges associated with ESAD, cost constraints, and the application of AI in HTPF development.

(1) Electronic safety and arming device

Although ESADs have improved the safety, arming reliability, and functional integration of HTPFs, their application in hard-target penetration environments still faces several challenges. First, penetration fuzes are subjected to extremely severe mechanical environments. These loads may induce structural deformation, solder-joint failure, connector loosening, circuit-board cracking, or transient malfunction of electronic components. Therefore, the survivability of ESADs under impact remains a primary limitation. Second, the internal space of penetration fuzes is highly constrained, whereas ESADs must integrate S&A logic, energy management, environmental sensing, and communication interfaces. This creates a trade-off among miniaturization, functional integration, safety margin, and reliability. Third, ESADs are more sensitive than purely mechanical S&A mechanisms to electromagnetic interference, electrostatic discharge, power-supply fluctuation, and long-term storage degradation.

In addition, the current ESADs used in penetration fuzes are still limited in terms of adaptive safety management and health monitoring. In many existing designs, the S&A function and the initiation-control function are relatively independent [145]. As a result, the ESAD mainly ensures safe arming before or during impact, whereas its interaction with target information sensing, penetration-state recognition, and intelligent initiation decision-making remains insufficient. Future ESAD development for penetration fuzes should therefore focus on high-survivability electronic packaging, robust interconnection and buffer-protection design, low-power and high-reliability energy management, electromagnetic protection, and redundant safety logic.

The development trend is expected to shift from electronic S&A devices toward highly integrated safety-control modules. Such modules should not only complete safe arming under severe penetration loads, but also provide health monitoring, fault diagnosis, environmental adaptability, and coordinated control with sensing and initiation-decision units. In particular, high-g-resistant microelectronic integration, redundant and fault-tolerant arming logic, electromagnetic protection, and long-term storage reliability will become key research directions. The close integration of ESADs with target-information sensing and intelligent initiation-control algorithms may further improve the safety, adaptability, and reliability of next-generation HTPFs.

(2) Low-cost design

Low-cost design is an important development requirement for penetration fuzes. For penetration fuzes operating under high-g impact, strong vibration, severe shock, and complex penetration environments, low-cost should be regarded as a system-level design objective that balances cost, reliability, manufacturability, survivability, testability, and functional performance.

From the perspective of system architecture, low-cost design can be achieved through standardization, modularization, and platform-based development [175]. A common fuze architecture can be used to support different penetration scenarios by changing software parameters, sensing modules, or control logic, thereby reducing repeated development and qualification costs. In addition, programmable electronic fuzes can reduce the number of fuze variants required for different missions, which is beneficial for production, inventory management, and lifecycle cost control. Another important route for cost reduction is the use of solid-state and integrated electronic design [176, 177]. Compared with mechanical or electromechanical structures, solid-state electronics can reduce the number of moving parts, improve consistency, and facilitate digital control. Such designs are beneficial not only for improving functional reliability but also for reducing assembly complexity and lifecycle maintenance cost.

The low-cost development of penetration fuzes should follow the principle of cost reduction without reliability degradation. Future research should focus on modular and standardized architectures, solid-state integrated electronics, lightweight embedded algorithms, design-for-manufacturing, and simulation-assisted verification. These approaches can reduce development and lifecycle costs while maintaining the safety, survivability, and initiation-control accuracy required by penetration fuze systems.

(3) Artificial intelligence application

Although AI provide promising directions for the development of modern HTPFs, their practical application still faces several technical bottlenecks, as shown in Table 4. First, the penetration process is highly transient, nonlinear, and destructive, making it difficult to obtain large-scale, high-quality, and well-labeled datasets under real penetration conditions. The lack of representative datasets restricts the training, validation, and generalization of data-driven models [178]. Second, penetration fuzes operate under severe mechanical environments, including high-g impact, strong shock, and intense vibration [179]. These conditions impose strict constraints on the survivability of sensors, processors, interconnections, power supplies, and ESADs. Third, intelligent algorithms must satisfy strict requirements for real-time response, low power consumption, limited onboard computing resources, and high reliability [44]. Large black-box models are therefore difficult to directly deploy in penetration fuzes [180]. In addition, the interpretability, fault tolerance, electromagnetic compatibility, and safety certification of AI-based decision-making remain critical challenges [181, 182], especially because erroneous arming or initiation decisions may seriously affect both mission effectiveness and safety.

Table 4

Technical bottlenecks and verifiable implementation paths of AI in HTPFs [44, 149, 178, 179, 181–184].

Technical aspects	Main bottlenecks	Verifiable implementation paths	Possible verification methods
Penetration data acquisition	Real penetration tests are costly, destructive, and difficult to repeat; labeled datasets are limited	Build multi-source datasets by combining numerical simulation, ground impact tests, controlled penetration tests, and hardware-in-the-loop simulation	Dataset consistency evaluation, repeatability tests, comparison between simulated and experimental signals
Penetration-state recognition	Penetration signals are transient, nonlinear, and strongly coupled with target structure and impact condition	Use acceleration, vibration, pressure, magnetic, acoustic, and timing signals for feature extraction and lightweight classification	Offline dataset testing, confusion-matrix analysis, robustness testing under noise and signal loss

AI algorithm deployment	Onboard computing resources, power supply, and response time are limited	Prioritize lightweight, interpretable, and embedded models rather than large black-box models	Real-time execution test, power-consumption test, embedded processor-in-the-loop verification
Reliability under severe environment	High-g impact, shock, vibration, and temperature variation may damage sensors and circuits	Use reinforced packaging, robust interconnection, redundant sensing, and fault-tolerant logic	High-g impact test, vibration test, shock test, thermal cycling test
S&A coordination	AI decision-making cannot replace deterministic S&A logic at the current stage	Use AI as an auxiliary recognition module and retain deterministic ESAD and safety logic as the final safety boundary	Safety logic verification, fault-injection test, fail-safe response test
Intelligent initiation control	Adaptive decision-making requires reliable coupling between target recognition and initiation timing	Combine programmable delay control with penetration-state recognition and target-layer identification	Hardware-in-the-loop simulation, controlled penetration experiment, initiation-control response verification

Therefore, the application of AI in penetration fuzes should follow a verifiable and stepwise implementation path. At the data level, multi-source penetration information, such as acceleration, magnetic, acoustic, and timing signals, can be obtained through numerical simulation, ground impact tests, penetration experiments, and hardware-in-the-loop simulation to establish standardized datasets [183]. At the algorithm level, lightweight and interpretable models should be prioritized for penetration-state recognition, target-layer identification, fuze health monitoring, and adaptive delay-time correction. Instead of completely replacing deterministic S&A logic, AI modules should initially serve as auxiliary recognition and decision-support units [184]. At the system level, the intelligent module should be integrated with programmable initiation-control circuits and ESADs under redundant safety constraints. Its performance should be verified through offline dataset testing, semi-physical simulation, high-g impact tests, electromagnetic compatibility tests, and controlled penetration experiments.

AI is more suitable for penetration-state recognition, multi-source information fusion, health monitoring, and adaptive parameter correction. The S&A function and final initiation-control authority should still rely on deterministic and verifiable logic. With the accumulation of penetration datasets, improvement of lightweight embedded algorithms, and maturation of high-survivability electronic packaging, AI-assisted penetration fuzes may gradually evolve toward adaptive and intelligent initiation-control systems with higher target adaptability and operational reliability.

3 Load characteristic and dynamic response analysis

During the hard-target penetration process, the fuze is subjected to extreme environments characterized by high deceleration, intense vibration, and multiphysics coupling [185]. Its load characteristics and dynamic response under high-deceleration shock conditions directly determine structural safety and affect the reliability of hard-target penetration weapons. The structural layout of a typical penetration warhead and fuze is illustrated in Fig. 12. This section will systematically review from four aspects. These aspects are the load characteristics of the projectile-fuze connection structure, the transmission mechanism of penetration deceleration, the dynamic response of the HTPF, and buffer protection technologies [186]. The review covers the deceleration characteristics of the HTPF during penetration, including the dynamic response induced by complex load excitation and the buffer protection performance.

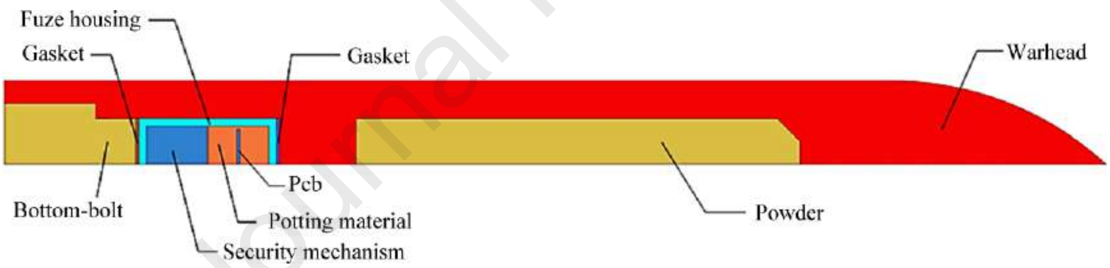

Fig. 12. Typical structural layout of penetration warhead and fuze. (Adapted from [187])

3.1 Projectile-fuze system load characteristic

The projectile-fuze connection structure serves as the critical path for transmitting impact loads from the projectile body to the fuze. Its dynamic characteristics directly affect the motion of the fuze's inertial components, the signal acquisition accuracy of sensors, and even the reliability of the entire system [188]. Common projectile-fuze connection structures are divided into the body threaded connection structure shown in Fig. 13(a) and the pressure screw connection structure shown in Fig. 13(b). A local enlarged view of the threaded connection interface is shown in Fig. 13(c). In traditional analysis, the projectile-fuze connection interface is often simplified as an ideal connection. Factors such as fitting clearance, material nonlinearity, and structural impedance mismatch are ignored. These factors may distort stress-wave propagation and cause acceleration amplification at the fuze location. The acceleration-time curves for the projectile and fuze with a body threaded connection structure are shown in Fig. 13(d), while those with a pressure screw connection structure are shown in Fig. 13(e). Both sets of curves demonstrate that the actual deceleration at the fuze location is significantly higher than that on the projectile body, which may lead to structural failure. Therefore, it is essential to conduct an in-depth investigation into the dynamic load characteristics of the projectile-fuze connection structure.

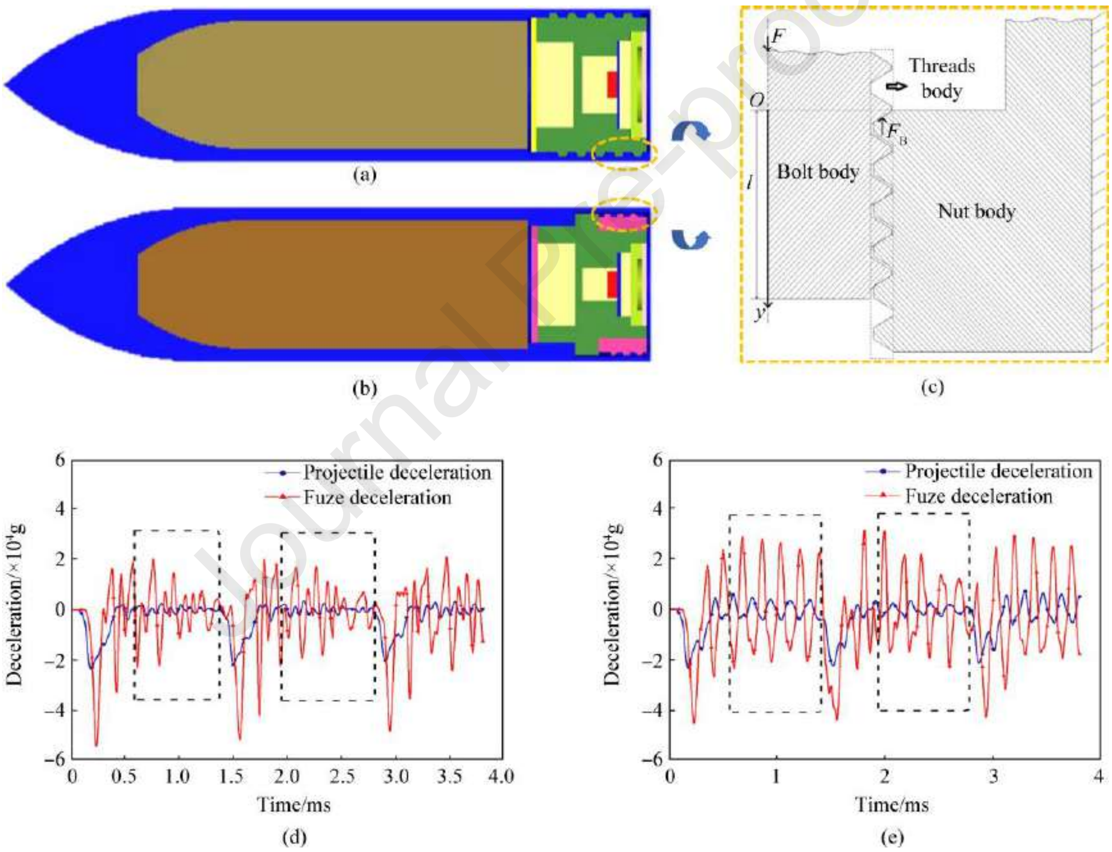

Fig. 13. Projectile-fuze connection structures: (a) Body threaded connection structure; (b) Pressure screw connection structure; (c) Partial enlarged view of the threaded connection interface; (d) Acceleration-time curve for body threaded connection structure; (e) Acceleration-time curve for pressure screw connection structure [17, 19, 179].

3.1.1 Load amplification and waveform distortion

The body threaded connection structure possesses mating clearances. During high-speed penetration, these clearances can easily induce interfacial collisions. This leads to complex dynamic responses in the projectile-fuze system. Early research demonstrated that interfacial collisions cause the deceleration peak at the fuze location to be significantly higher than that at the projectile body location. Furthermore, the dominant frequency components of its deceleration response are closely related to the collision frequency of the threaded connection structure. Consequently, simplifying the projectile-fuze connection as a rigid bond is evidently inadequate.

To thoroughly investigate the load characteristics of body threaded connection structures, a collision dynamics model for the threaded connection between a projectile body and a fuze was developed [179, 189, 190]. The stiffness, natural frequency, impact force, and other key parameters of the threaded connection structure under high impact loads were systematically analyzed. Meanwhile, it was discovered through numerical simulation that the body threaded connection structure possesses certain vibration damping capacity, effectively suppressing high-frequency oscillation components [17]. On this basis, a complete finite element model of the projectile-fuze system was developed [191]. This model incorporates multiple components and connection methods. It was clearly pointed out that rigid connections amplify the interface collision effect, exacerbating the impact load on internal components.

The essential problem of projectile-fuze connection analysis is therefore not only to calculate the peak acceleration, but also to reveal how the connection interface modulates the penetration load. Existing studies indicate that interface separation [17], repeated collisions [192], thread-tooth deformation [23], and stiffness discontinuity [191] can jointly generate waveform distortion, high-frequency oscillation, and peak amplification. For body threaded connections, the relatively low connection stiffness and unavoidable mating clearance make the interface prone to separation-impact behavior under high-g penetration loads. This leads to strong nonlinear response and a significant amplification of fuze deceleration. In contrast, pressure screw connections introduce axial clamping force through pre-tightening components, which increases connection stiffness, suppresses thread collision, and improves the fidelity of the transmitted low-frequency deceleration trend.

3.1.2 Characteristics of typical connection structures

Different connection forms exhibit significant differences in stiffness, response mode, and amplitude, which directly affect the dynamic environmental perception accuracy of the fuze. The conventional connection structures between the projectile body and the fuze, along with their characteristics, are summarized in Table 5. The body threaded connection structure is simple in form, but exhibits low connection stiffness and strong nonlinearity. Under impact, it is prone to interface separation and collision, generating complex high-frequency oscillations. This leads to an amplification effect where the deceleration peak at the fuze location is significantly higher than that on the projectile body. To improve performance, the pressure screw connection structure applies an axial clamping force through pre-tightening elements. This effectively increases stiffness and suppresses interface separation. Its response waveform can better reproduce the low-frequency trend of the projectile body's deceleration, and the deceleration amplification effect is weaker. For the most demanding applications, the bolted flange connection structure can achieve extremely high and controllable stiffness through precisely controlled bolt preload. Its dynamic response transmission path is clear. However, attention must be paid to waveform distortion possibly caused by asymmetric tensile-compressive stiffness.

Table 5

Characteristics of common projectile-fuze connection structures [17, 24, 193–198].

Projectile-fuze connection structures	Stiffness characteristics	Response form	Response amplitude
Body threaded connection structure	Low stiffness, exhibiting non-linear behaviour	Complex response, with severe waveform distortion	Significant deceleration amplification effect
Pressure screw connection structure	Significantly higher rigidity than body threads	Signal oscillates moderately, high signal fidelity	Weak deceleration amplification effect
Bolted flange connection structure	High rigidity and excellent controllability	Clear transmission path, but interface non-linearity exists	Amplitude transfer is frequency-dependent

From the viewpoint of structural progression, typical projectile-fuze connection forms can be arranged in the order of body threaded connection, pressure screw connection, and bolted flange connection. The body threaded connection is simple and compact, but its nonlinear interface response is the most pronounced. The pressure screw connection improves stiffness and reduces signal oscillation through axial preload [19]. The bolted flange connection can provide higher and more controllable stiffness through precisely controlled bolt preload, although its dynamic behavior may still be affected by asymmetric tensile-compressive stiffness and frequency-dependent amplitude transmission. Thus, the development trend of connection structures is not a simple replacement of one form by another, but a trade-off among structural simplicity, connection stiffness, response fidelity, manufacturability, and fuze survivability.

From traditional threaded connections to pressure screw connections and then to bolted flange connections, the structural complexity and cost progressively increase. However, improvements are achieved sequentially in connection stiffness, response fidelity, and deceleration control capability. The selection should be balanced according to the fuze accuracy requirements and the specific application scenarios.

3.1.3 Evolution of connection structure modeling

The modeling methods for projectile-fuze connection structures have also evolved from idealized simplifications to refined nonlinear interface descriptions [199]. Early models generally treated the connection as a rigid or linear elastic constraint, which was insufficient for describing contact separation, thread collision, and local stress redistribution. Later studies introduced collision dynamics models to quantify the mechanical behavior of threaded connections under high-impact loads [200]. In these models, the stiffness of engaged threads, collision force, collision duration, and thread-tooth bending deformation were considered, thereby providing a more physical description of the local load-transfer process. In addition, refined finite-element models and thin-layer element methods have been adopted to represent the nonlinear mechanical behavior of threaded interfaces [201], as shown in Fig. 14. Compared with linear elastic solid elements, thin-layer element strategies can better describe the coexistence of elastic thread force and impact force, and can therefore provide deeper insight into the mechanism of fuze dynamic-response amplification.

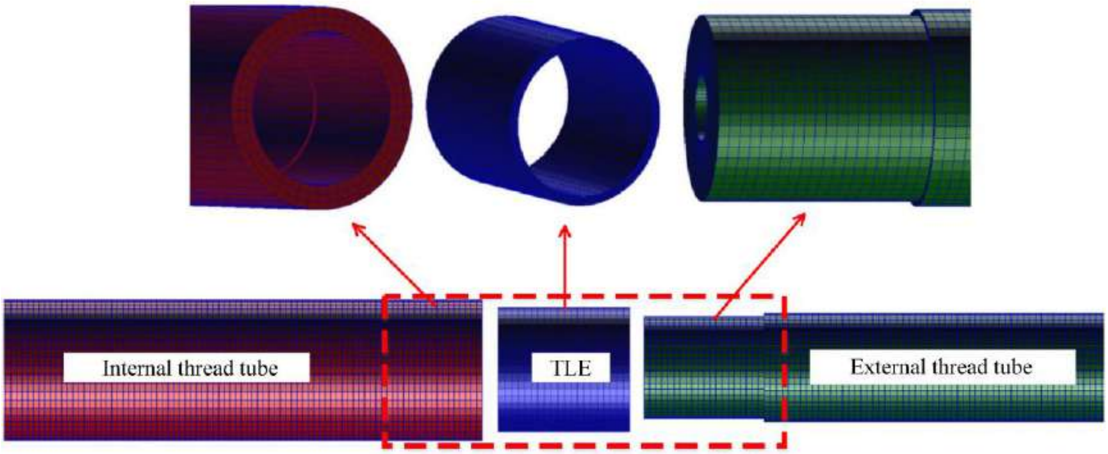

Fig. 14. A threaded characterisation strategy integrating elastic models and thin-layer elements [201].

For next-generation hypersonic penetration weapons, refined modeling should be further extended from nonlinear elastic contact to fully coupled thermo-elastoplastic contact. The constitutive model should reflect strain-rate hardening, thermal softening, damage accumulation, and possible adiabatic shear localization [202]. At the thread interface, the contact algorithm should consider frictional heat generation, transient contact separation, local slip, wear, and galling-induced stiffness degradation [85]. In addition, the material parameters used in the model should be calibrated through high-strain-rate compression, torsion, friction-wear, and thermal-mechanical tests. Without such extensions, conventional elastic threaded-connection models can only explain the qualitative load-amplification mechanism and cannot reliably predict connection failure or fuze dynamic response under Mach > 5.

3.1.4 Design implications for load amplification

The dynamic load characteristics of the projectile-fuze connection structure during penetration are notably nonlinear and complex [203]. Due to fitting clearances, impact excitation at the interfaces generates multidimensional stress wave propagation. This leads to a significantly higher deceleration at the fuze location compared with the projectile body. The above studies lead to several engineering implications. First, the fuze dynamic environment should be evaluated at the fuze installation location rather than inferred only from projectile-body deceleration. Second, improving connection stiffness and reducing assembly clearance can effectively suppress interface separation and collision. Third, preload design is a key parameter for pressure screw and flange-type connections, but excessive preload may introduce manufacturing difficulty, stress concentration, or unfavorable frequency-response characteristics. Fourth, connection-structure design should consider frequency decoupling: the dominant frequency of the projectile-fuze connection should be adjusted away from the first-order axial response frequency of the projectile to reduce resonance-induced acceleration amplification. Finally, refined nonlinear modeling and experimental calibration should be combined to improve the prediction accuracy of fuze loads. These insights provide the basis for the subsequent analysis of load-transfer mechanisms and fuze dynamic response.

The research on projectile-fuze connection structures has evolved from the observation of load amplification to the explanation of nonlinear interface mechanisms, and further to refined modeling and design-oriented suppression strategies. The progressive insight is that the connection interface should not be regarded as a passive mechanical joint. Instead, it acts as a dynamic load modulator that can amplify, filter, or distort penetration deceleration signals. Therefore, future studies should move beyond repeated comparison of acceleration curves and focus on establishing validated interface models, preload optimization methods, and connection-structure design criteria for high-fidelity fuze load transmission.

3.2 Projectile-fuze system load transfer mechanism

In the study of penetration weapons, the dynamic deceleration transfer mechanism of the connection structure between the projectile body and the fuze is a crucial yet not fully clarified scientific issue. Typically, the projectile body deceleration is directly equated with the fuze deceleration [188]. However, due to the complexity of the deceleration transfer path between the projectile and the fuze, as well as the coupling between the internal fuze sensor and the fuze itself, extensive experiments have shown that the deceleration actually measured by the fuze acceleration sensor is often significantly higher than the projectile body deceleration [204]. To reveal the complex mechanism of deceleration transfer in the projectile-fuze system, in-depth research has been primarily conducted by scholars from two perspectives: the local load transfer of the projectile-fuze connection structure and the global dynamic modeling of the system.

3.2.1 Local load transfer of projectile-fuze system

The local load transfer characteristics of the threaded connection structure are the core link in analyzing the deceleration transfer mechanism of the projectile-fuze system during penetration [205, 206]. It is pointed out by existing studies that under impact loading, the stress distribution between the threads of the connection structure exhibits significant non-uniformity along the axial direction. Thus, the one-dimensional stress wave theory is difficult to describe its dynamic propagation mechanism.

To address the above problems, systematic theoretical modeling and mechanism research were conducted [189, 191]. A collision dynamics model was established to describe the threaded connection between the HTPF and the projectile body under high-impact loads. The core of this model lies in quantifying the dynamic mechanical behavior of the structure under extreme loads. It is noteworthy that an axial deformation coefficient caused by the bending deformation of the thread teeth was introduced into the collision force model. This effectively enhanced the accuracy of the theoretical predictions. It should be emphasized that this work presents a simplified model for describing the local load-transfer mechanism of threaded projectile-fuze connections. The model assumes elastic deformation of the engaged threads, simplified contact stiffness, and idealized impact behavior. Therefore, it is mainly applicable to preliminary mechanism analysis, stiffness comparison, and qualitative prediction of acceleration amplification characteristics under conventional high-impact penetration conditions. The model does not explicitly account for elastoplastic deformation, frictional wear, thermal softening, adiabatic shear, or temperature-dependent material degradation. Under hypersonic penetration conditions, the projectile-fuze connection may experience severe thermo-mechanical coupling [91]. For such conditions, a high-fidelity model should incorporate strain-rate-dependent elastoplastic constitutive relations, temperature-dependent material properties, nonlinear frictional contact, thread damage evolution, and thermal-mechanical coupling.

This study established a theoretical model for the impact dynamics of threaded connection structures. It revealed the load transfer law of impact loads within local connection structures of the projectile-fuze system. This work provides an important theoretical foundation for the accurate prediction of fuze deceleration and for structural design under high-impact environments. In addition, simulations were conducted to investigate the effect of cushioning materials on the transmission of overloads [207]. Most existing projectile-fuze threaded-connection models have been evaluated through theoretical derivation, numerical simulation, component-level impact analysis, or comparison with limited laboratory data. Although scaled penetration tests and transfer-function-based equivalence methods have been used to reproduce HTPF deceleration environments, their validation targets are generally peak deceleration, pulse width, or overall response equivalence rather than the detailed stress, plastic strain, thermal response, and galling behavior of threaded interfaces. Therefore, the current models should only be regarded as mechanism-oriented and engineering-preliminary models.

3.2.2 Overall dynamics modeling of projectile-fuze system

In the developmental trajectory of research on projectile-fuze system dynamics modeling, a shift has been made from analyzing local load transfer laws to constructing overall dynamics models capable of fully describing system responses. In recent years, the penetration warhead-fuze system is equivalent to a multi-degree-of-freedom spring-mass-damper system [208–210]. This was achieved by equivalently representing the threaded connection structure as a linear spring with damping characteristics. The model successfully predicted the dynamic response of the system under high-impact loading. This helped reveal the mechanism of load transmission. A key advantage of this method is its clear physical significance. Using modal analysis techniques, the response of the projectile body was expressed in modal space. The fuze response was characterized as the acceleration relative to the projectile base. This approach clearly separated the excitation source from the response system. It provided an intuitive and powerful theoretical tool for gaining a deeper understanding of the load transmission path within the projectile-fuze system.

Based on the aforementioned research, addressing the challenges of the substantial computational cost of fully coupled finite element simulations and their limited engineering applications, a cascaded transmission model based on the multibody dynamics transfer matrix method was further proposed [18, 211, 212]. In this study, the complex projectile-fuze system was simplified into a cascaded transmission chain. This chain contains key components such as threaded connections, buffer media, and circuit boards, as shown in Fig. 15(a). Subsequently, a sixth-order nonlinear dynamic transmission model was constructed. This model describes the process from projectile body impact input to fuze sensor acceleration output, as shown in Fig. 15(b).

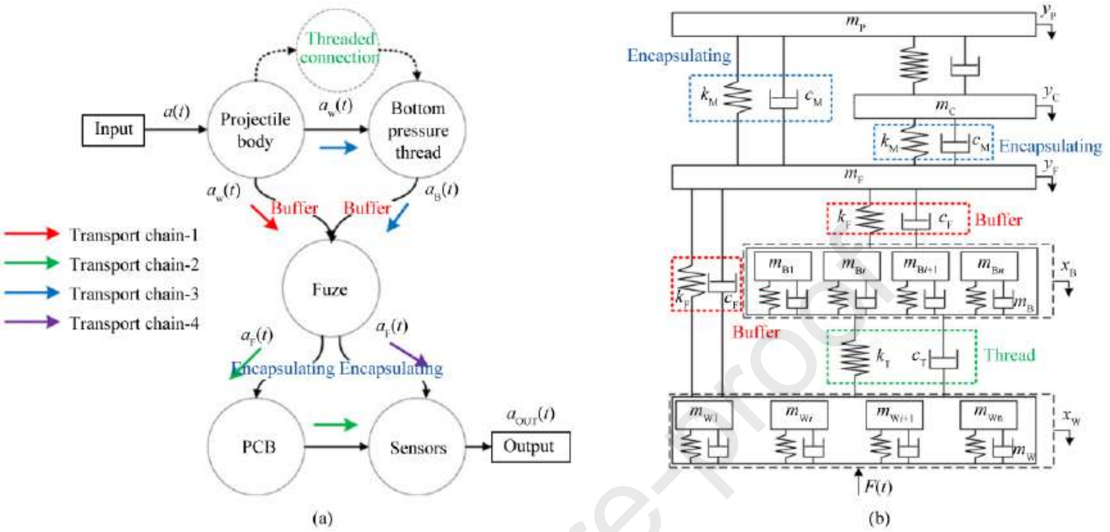

Fig. 15. Dynamics transmission of the projectile-fuze system: (a) Dynamics transmission chains of the projectile-fuze system; (b) Dynamics transmission model of the projectile-fuze system [18,212].

This model significantly reduces the time cost of dynamic simulation. Compared to the fuzzy penetration calculation method, the prediction accuracy is improved by 8.3%. A balance between model complexity and computational efficiency is effectively achieved. Consequently, a more efficient and reliable engineering tool system is provided for the dynamic response analysis of the projectile-fuze system.

During the penetration process, the projectile-fuze connection structure exhibits complex dynamic load transfer characteristics. Influenced by the fitting clearance, intermittent collisions occur at the connection interface [213]. This leads to a significant non-one-dimensional feature in stress wave propagation. Moreover, the measured deceleration at the fuze location is noticeably higher than that at the projectile body. Currently, research on the deceleration transfer mechanism of projectile-fuze systems in penetration weapons under high-velocity impact conditions remains relatively limited. Existing achievements have not yet formed a systematic and in-depth theoretical framework. To systematically reveal the deceleration transfer laws of projectile-fuze systems during penetration, future research could focus on developing high-fidelity numerical simulation methods. These methods would more accurately describe the contact nonlinear behavior at the interfaces of connection structures. The establishment and refinement of such methods are of significant theoretical importance and engineering application value. They are essential for deeply explaining the dynamic transfer mechanism of penetration deceleration within projectile-fuze systems and for achieving high-precision prediction of the fuze system's dynamic response.

3.3 Penetration fuze dynamic response

The HTPF serves as the core component for controlling projectile initiation. Its load characteristics and dynamic responses during high-speed penetration are directly related to the safety and reliability of the entire projectile [214]. While early research was primarily focused on the penetration deceleration characteristics of the overall projectile body, insufficient attention was paid to the response of the fuze, a critical component, within high-deceleration environments. Based on limit density theory, cavity expansion theory, and stress wave theory, a dynamic model for projectiles penetrating multi-layer concrete targets was established [203], providing a foundational theoretical framework for subsequent studies. However, due to multiphysics factors such as the complexity of the projectile-fuze system, stress wave propagation, and coupled vibrations of internal components, it is observed that the actual deceleration at the HTPF location is often higher than that of the projectile body itself [215]. Consequently, a systematic investigation into the deceleration characteristics at the fuze position during the penetration process is of vital significance for the design, protection, and optimization of initiation control algorithms.

3.3.1 Set-forward overload characteristic of penetration fuzes

Set-forward overload is a key ballistic parameter in HTPF design. Early research primarily relied on numerical simulation methods, and gradually established empirical models suitable for specific conditions. A calculation method for the set-forward overload coefficient, was proposed [216, 217]. The influence of various factors on the set-forward overload coefficient during the penetration process of a 30 mm small-caliber armor-piercing high-explosive projectile was systematically analyzed using numerical simulation. The factors investigated included impact velocity, impact angle, target thickness, and target strength. The results indicated that the set-forward overload coefficient is positively correlated with impact velocity, target thickness, and target strength. A negative correlation was observed between impact angle and the set-forward overload coefficient. Structural damage to the projectile body is easily induced by targets with large impact angles or large thicknesses. On this basis, the research was extended to the case of normal penetration of a 125 mm caliber projectile into concrete targets [218, 219]. Through numerical simulation, the empirical formula for the maximum set-forward load coefficient, and the empirical formula for the acceleration pulse width during penetration, were respectively established. The fitting errors were both controlled within 5%. This improved the applicability of the engineering calculation for the set-forward overload of the fuze. However, this model is only applicable to normal penetration. The laws for oblique penetration remain unclear.

Furthermore, the process of normal penetration of a projectile into three-layer concrete targets was simulated [220]. It was pointed out that a blunter nose leads to a higher penetration velocity and a greater set-forward overload. To address the limitations of the normal penetration model, Shi et al. systematically analyzed the influence of the projectile’s attack angle variation on the set-forward overload characteristics under oblique penetration conditions through numerical simulation, building upon existing research on normal penetration [221]. It was indicated that a larger attack angle increases the contact area between the projectile and the target, resulting in greater resistance and consequently a higher impact load transmitted to the fuze. Dai further pointed out that oblique penetration reduces the amplitude of the fuze’s set-forward overload while increasing its pulse width [222]. This is achieved by altering the force decomposition, increasing the actual penetration path, and causing asymmetric damage. Thus, the understanding of the set-forward overload characteristics of the fuze under oblique penetration conditions was further refined.

3.3.2 Overload characteristic considering projectile-target interaction

The overload characteristics of the fuze are significantly influenced by factors such as the projectile body structure, target configuration, and fuze layout. It was demonstrated that when a composite heterogeneous projectile body with a tungsten alloy warhead penetrates a concrete target normally, not only is the penetration capability enhanced, but its structure also provides a cushioning effect on the fuze [223, 224]. Notably, after the complete penetration of the composite heterogeneous projectile body with a tungsten alloy warhead, a distinct secondary overload peak appears at the fuze location. The reason lies in the following: during the high-speed penetration process of the composite heterogeneous projectile body, the tungsten alloy warhead and other components undergo erosion and spalling due to intense impact. As the projectile materials gradually degrade, the original overload cushioning effect of the composite structure weakens or even disappears, leading to an abrupt change in the interaction state between the projectile body and the target [225]. Simultaneously, the propagation path and characteristics of stress waves between the projectile body and the fuze components are altered [226]. The filtering effect of the composite structure on the overload ceases, resulting in the occurrence of a secondary peak in the overload signal at the fuze location. This manifests as a signal that first decreases and then rises, exhibiting a clear double-peak characteristic. This phenomenon becomes more pronounced under higher initial velocity conditions: the higher the initial velocity, the faster the erosion process of the projectile body, the more abrupt the change in interaction state, and the more prominent the secondary peak becomes.

Furthermore, the differences between warhead penetration into multi-layer spaced targets and single-layer thick targets were compared [227] through refined finite element modeling. In multi-layer targets, high-frequency oscillations were exhibited in the fuze overload. The peak values were distributed in specific stages of each layer's penetration. In thick targets, the peak value occurred at the moment of projectile tail entry into the target. Moreover, when penetrating targets with complex internal structures, overlapping and aliasing phenomena were observed in the fuze overload. It was further indicated [228]. that during warhead penetration into multi-layer targets containing beams, the peak overload of the first layer was increased by 63.67% due to the beam. The duration was prolonged by 34.95%. The overlapping degree was increased by 43.18%.

The layout of the fuze within the projectile body is also a critical factor [226]. The axial overload during penetration of reinforced concrete targets for forward and rear placements of the fuze was compared [229]. It was found that the forward-placed fuze requires at least twice the overload resistance capability of the rear-placed one. This provides engineering reference for the application of forward fuze placement structures in penetration warheads. Therefore, rear placement of the fuze is generally adopted in penetration warheads.

It should be noted that the load characteristics of the projectile-fuze system are closely related to the projectile-target interaction process. The impact resistance provided by the target is the physical source of the penetration load, while the projectile structure and fuze installation configuration determine how this load is transmitted to the fuze. Therefore, fuze load characteristics are affected not only by the structural parameters of the projectile-fuze system, but also by target material properties, target thickness, layered interfaces, cavity structures, penetration velocity, and impact attitude. In practical hard-target penetration scenarios, these factors are coupled with each other and jointly determine the peak value, pulse width, frequency content, and multi-pulse characteristics of the fuze load.

The target properties have a significant influence on the load characteristics of HTPFs. A higher target strength generally leads to a higher peak deceleration and a shorter load duration, whereas a more crushable or fragmented target may result in a more complicated multi-peak load history [230]. For layered targets, the projectile experiences repeated impact, unloading, and reloading processes when crossing different material interfaces [231]. As a result, the fuze may be subjected to multiple shock pulses with different amplitudes and frequency components. For cavity-containing or multi-layer hard-targets, the sudden change in penetration resistance at interfaces or voids can also induce transient acceleration fluctuations, which are closely related to layer-counting, void recognition, and precise initiation control.

In addition to target properties, impact conditions also affect the projectile-target-fuze coupling response. The penetration velocity [232], impact angle [233], yaw angle [234], and projectile attitude [235] determine the distribution of contact force and bending moment during penetration. Under oblique or yawed impact conditions, the projectile may experience asymmetric deformation and lateral vibration, which can introduce transverse loads and bending-induced acceleration components into the fuze. These coupled loads may be more complex than the axial set-forward overload commonly considered in simplified fuze dynamic analysis.

For this reason, the load input used in fuze dynamic response analysis should be derived from the projectile-target interaction process as much as possible, rather than being represented only by an idealized acceleration pulse. A more reliable evaluation method is to combine penetration tests, onboard acceleration measurements, recovered projectile damage analysis, and numerical simulations of projectile-target interaction [236]. In particular, finite element models considering target damage, projectile deformation, contact/interface behavior, and local fuze installation details can provide effective support for identifying the load generation mechanism, load transfer path, and dynamic response characteristics of the fuze. Consequently, coupling analysis between the projectile and target is necessary for accurately evaluating the survivability and functional reliability of penetration fuzes.

3.3.3 Dynamic response mechanisms of penetration fuzes

The dynamic response and failure mechanism of the HTPF in complex projectile-target impact environments are key scientific issues in this field. Axial sinusoidal excitation was applied to the fuze model [237, 238]. The booster installation area was identified as a weak region. This explained the phenomenon of fuze tail breakage in tests. Structural weak points were identified based on frequency response analysis.

Based on this, research has gradually focused on the intrinsic relationship between projectile-target interaction and fuze dynamic response. The cavity expansion theory and the one-dimensional viscoelastic wave equation were integrated [239]. The matching mechanism between the projectile-target interaction force and the frequency response characteristics of the projectile-fuze system was systematically revealed. It was confirmed that resonance is triggered when an axial natural frequency of the projectile-fuze system approaches an integer multiple of the fundamental frequency of the projectile-target interaction force. This leads to a significant concentration of the fuze load at the corresponding frequency. The research was further extended [240] to more practical working conditions. These conditions include broadband excitation and transient impact. The results indicate that during the penetration process, the fuze overload is drastically amplified at the first or multiple axial natural frequencies of the warhead. The maximum amplification can reach 9 times. Moreover, under multi-layer target penetration conditions, this amplification effect is more pronounced. Thus, the physical mechanism behind how different projectile-target parameters affect the fuze response is elucidated.

The typical dynamic response of HTPFs is illustrated in Figs. 16(a)–16(d). It is characterized by the complex overload environment and structural vibration during high-speed penetration. A core feature is that the actual overload at the fuze location is significantly higher than that experienced by the projectile body. This is due to the projectile-fuze threaded connection, stress wave transmission, and coupled vibration of internal components [241], shown in Fig. 16(b). It has been demonstrated that the fuze overload is markedly influenced by the penetration state, projectile-target characteristics, and the fuze's own layout. Furthermore, a dynamic amplification effect by several times can occur due to resonance at the warhead's axial natural frequency. This effect is directly related to the strength and reliability of the fuze structure. Based on the identification of structural weak points in the fuze, the projectile-target-fuze coupled resonance mechanism was revealed. The load amplification law under broad-frequency transient shock was quantified. This work provides important theoretical support for the anti-high overload design and reliability assessment of the HTPF.

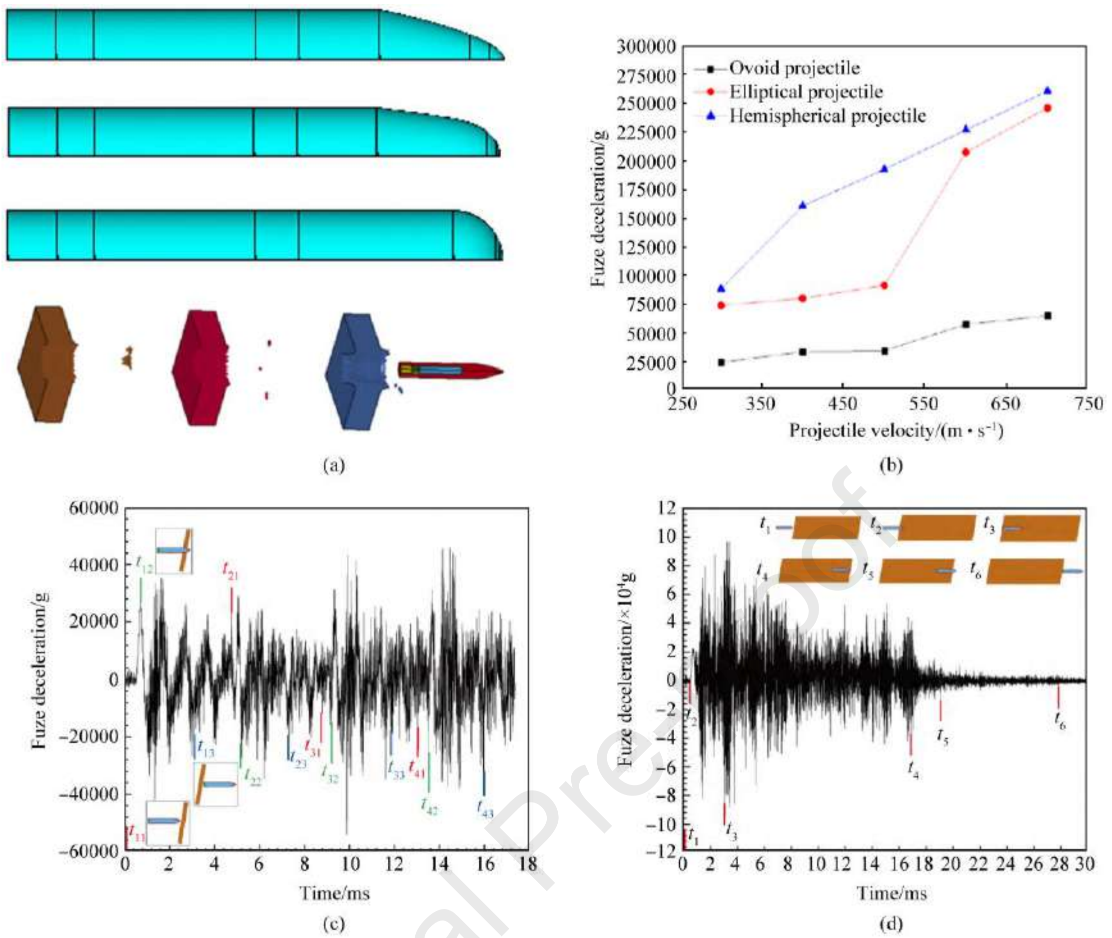

Fig. 16. Dynamic response of the HTPF: (a) Schematic diagram of projectile bodies with different nose shapes and penetration through multi-layer targets [242]; (b) Maximum deceleration curves of the fuze for projectile bodies with different nose shapes at various penetration velocities [241]; (c) Deceleration curve of the fuze during penetration of 4-layer C45 concrete targets; (d) Deceleration curve of the fuze during penetration of a 9 m C45 concrete target [227].

The simulation curves of the rigid body overload of a penetration warhead and the fuze response overload during penetration of a single-layer reinforced concrete thick target and 10-layer reinforced concrete targets at a speed of 2.5 Mach are shown in Figs. 17(a)–17(d). It can be clearly observed that the peak penetration overload at the fuze location is several times that on the warhead shell. An oscillatory signal state is exhibited by the fuze response overload, which is superimposed on the envelope of the rigid body overload signal. For multi-layer target penetration, this phenomenon is particularly evident. Clear characteristics of multiple targets are displayed by the rigid body overload signal of the warhead [243]. In contrast, the penetration overload signal at the fuze location not only has an amplified peak by several times, but high-frequency oscillatory signals are also superimposed between the overload pulses of targets. Severe signal overlapping and aliasing is present. The target characteristics are submerged by the high-frequency oscillatory signals, making them difficult to recognize.

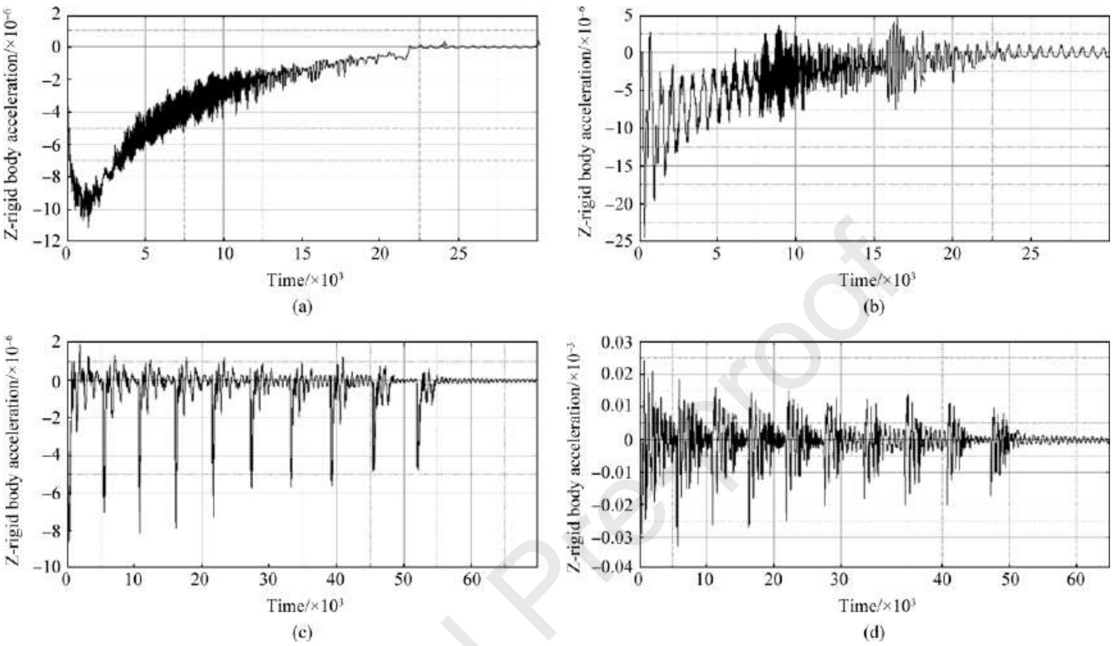

Fig. 17. Dynamic response of the warhead and fuze: (a) Deceleration curve of the warhead during penetration of a thick reinforced concrete target; (b) Deceleration curve of the fuze during penetration of a thick reinforced concrete target; (c) Deceleration curve of the warhead during penetration of 10-layer reinforced concrete targets; (d) Deceleration curve of the fuze during penetration of 10-layer reinforced concrete targets (Adapted from [6]).

The aforementioned study systematically revealed the dynamic response and load characteristics of the fuze during hard-target penetration. However, existing empirical models are mostly limited to specific working conditions. Their general applicability to penetration into complex targets is insufficient. Moreover, full validation by experimental data is lacking. Future research may focus on the following aspects. High-fidelity coupled simulation methods integrating multiple physical fields should be developed. A general overload prediction model applicable to heterogeneous targets with large oblique angles and varying thicknesses needs to be established. Real-time identification and intelligent control algorithms for fuze overload based on physical mechanisms and AI should be explored. Furthermore, key experimental data should be obtained through advanced dynamic testing techniques. This data will be used to validate theoretical and numerical models. The ultimate goal is to achieve accurate and reliable control of the penetration fuze under extreme environments.

3.4 Penetration fuze buffer protection technology

With the development of hypersonic weapons, the impact deceleration experienced by a penetrating projectile body upon hitting a target increases sharply. This induces intense elastoplastic stress waves within the projectile body, leading to instantaneous mutations in structural internal displacement, velocity, stress, and acceleration. These mutations can easily cause damage to internal electronic components of the fuze, such as solder joint detachment and ceramic capacitor fracture [244]. This seriously affects the safety and reliability of fuze functioning.

To enhance the survivability of the HTPF under extreme impact environments, cushioning and protection technologies have become a key research direction. Current protection strategies mainly cover three aspects [245]. First, the stress wave is dispersed and attenuated through optimized cushioning structure design. Second, potting materials are used to reinforce and isolate circuits and electronic components from vibration, thereby suppressing deformation. Third, a multi-layer gasket structure is arranged externally to the fuze. This utilizes plastic deformation of materials and wave impedance gradients to achieve energy absorption and deceleration attenuation.

3.4.1 Shock-absorbing structural design

To enhance the survivability of penetration fuze under high-speed impact, mechanical structure design forms the basis of their high-g resistance capability. As the primary component for structural protection, the fuze housing was addressed through the proposal of W-shaped and V-shaped rigid buffer structures [246]. The impact resistance was significantly enhanced. Among these, the W-shaped structure demonstrated better performance in most working conditions.

Based on the structural design of the fuze housing, the further introduction of an external buffer layer can effectively enhance the overall protection level. An imitation bamboo type Penetration fuze protection Microstructure (IPM) was designed [20, 247], as shown in Fig. 18(a), based on bionic principles. This structure is suitable for buffering and energy dissipation under high-impact conditions. Simulation results indicate that the structure exhibits a significant negative Poisson's ratio effect and overall coordinated deformation capability. Stress concentration can be effectively alleviated. The average peak deceleration attenuation reaches 131%, and the total energy absorption is increased by 72%. Its performance is significantly better than that of traditional structures. In addition, an elliptic sandwich curved beam structure (ESCBS) was proposed [112], as shown in Fig. 18(b), based on the bistable symmetric curved beam structure (BCBS). By utilizing the stiffness complementarity mechanism between the elliptic ring and the curved beam, efficient energy absorption and structural recoverability are achieved under impact conditions as high as 25000 g. The impact peak is reduced by more than 50%, and structural integrity is maintained above 90%. This demonstrates good potential for engineering applications.

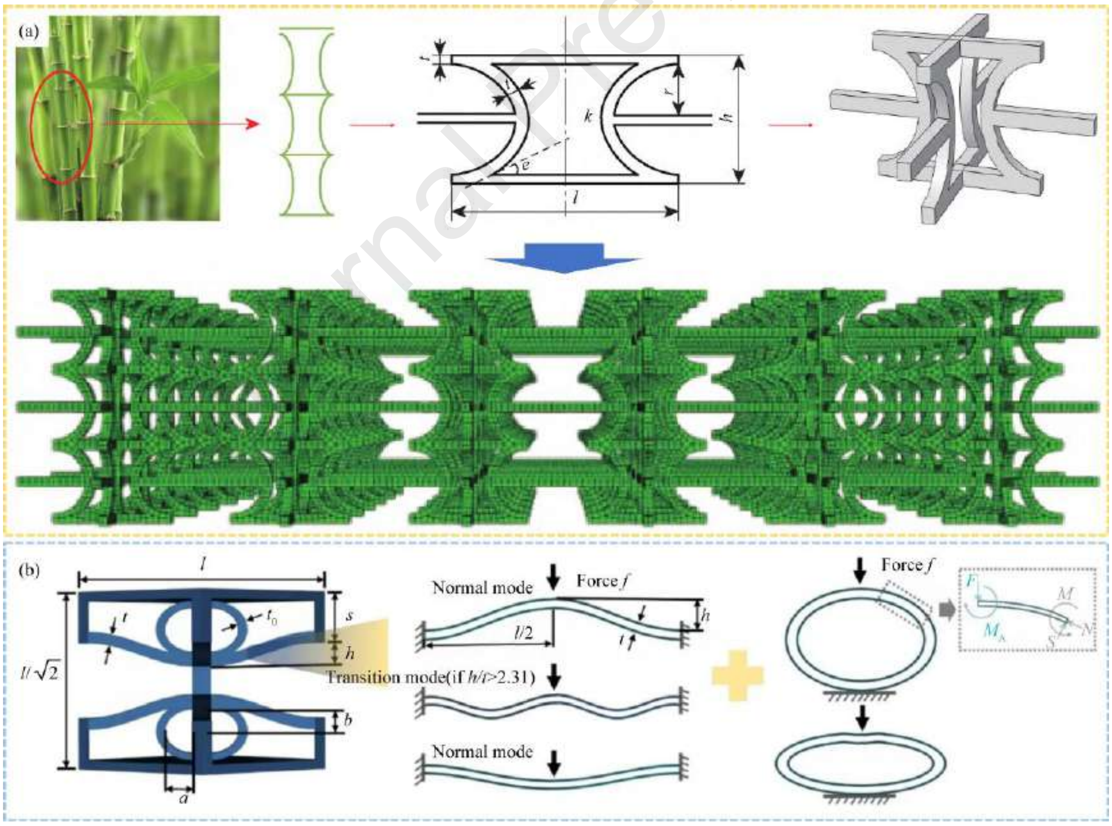

Fig. 18. Externally buffered microstructures for the penetration fuze: (a) IPM; (b) ESCBS [20, 112].

While structural optimization design is carried out, system-level anti-high deceleration strategies can be implemented synergistically from both internal and external aspects. Internally, the potting process is adopted to enhance the structural stability of electronic components and to disperse energy. Externally, buffer isolation gaskets are arranged to attenuate shock transmission. This comprehensively improves the reliability of the penetration fuze under extreme shock environments.

3.4.2 Potting protection scheme design

In the protection of internal electronic components within a penetration fuze, the most fundamental and commonly used anti-deceleration approach involves potting to reinforce and isolate the electronic components, preventing deformation of the components and circuit boards. Potting materials should possess high adhesion, low coefficient of thermal expansion, certain resistance to heat and low temperatures, low hygroscopicity and corrosiveness, as well as good fatigue resistance. Foamed aluminum, polyurethane, nylon, and phenolic resin were compared [246], and it was found that foamed aluminum provides the best cushioning effect for the fuze circuit module, with an impact overload attenuation rate of 87.93%. To further investigate the influence of material parameters, it was discovered through finite element simulation that the viscosity of the potting material has a significant independent effect on the protective performance, while density and elastic modulus play weaker roles [248, 249]. Moreover, based on the ZWT nonlinear viscoelastic constitutive model, a systematic analysis was conducted on the influence of various parameters of epoxy resin potting material on the dynamic response of printed circuit boards and components [250]. Research indicated that reducing the nonlinear elastic modulus, low-frequency elastic constant, and relaxation time can effectively enhance buffering performance. The influence of material density showed a non-monotonic characteristic, while the high-frequency elastic constant had minimal effect. This study provided a theoretical basis for the design of potting materials oriented toward different engineering objectives, but further expansion is still needed in combination with changes in fuze structural dimensions.

The selection of potting materials is critical in the high-deceleration protection of penetration fuze. According to publicly available research data, epoxy resin, silicone rubber, and polyurethane are the most commonly used potting materials. The performance comparison of the above three potting materials is shown in Table 6.

Table 6

Characteristics of common potting materials [251–255].

Materials	Characteristics	Protective mechanism	Limitations
Epoxy resin	High strength, high hardness, strong adhesion, chemical corrosion resistance	Utilising its own high-strength structure to withstand impact	Highly brittle, lacking in toughness, with limited impact resistance
Silicone rubber	Highly elastic, excellent cushioning properties, strong resistance to thermal cycling	Utilising its own deformation to absorb impact energy	Low hardness, poor adhesive properties
Polyurethane	Lies between epoxy resin and silicone rubber	Balancing structural support with energy absorption	Poor temperature resistance, relatively weak chemical corrosion resistance

Single materials often struggle to meet all requirements simultaneously. The composite potting method shown in Fig. 19 has become a current research hotspot. This method is based on the stress wave propagation theory. By layering materials with different moduli, stress waves are reflected and attenuated at multiple interfaces. Thus, core electronic components are more effectively protected. Based on this principle, a three-layer composite potting method using silicone rubber-epoxy resin-electronic potting compound was proposed [256]. Impact energy is weakened through the reflection and absorption mechanisms at multi-material interfaces. Tests show that this method can attenuate the deceleration peak by more than 70%. It also possesses multiple high-impact load-bearing capabilities.

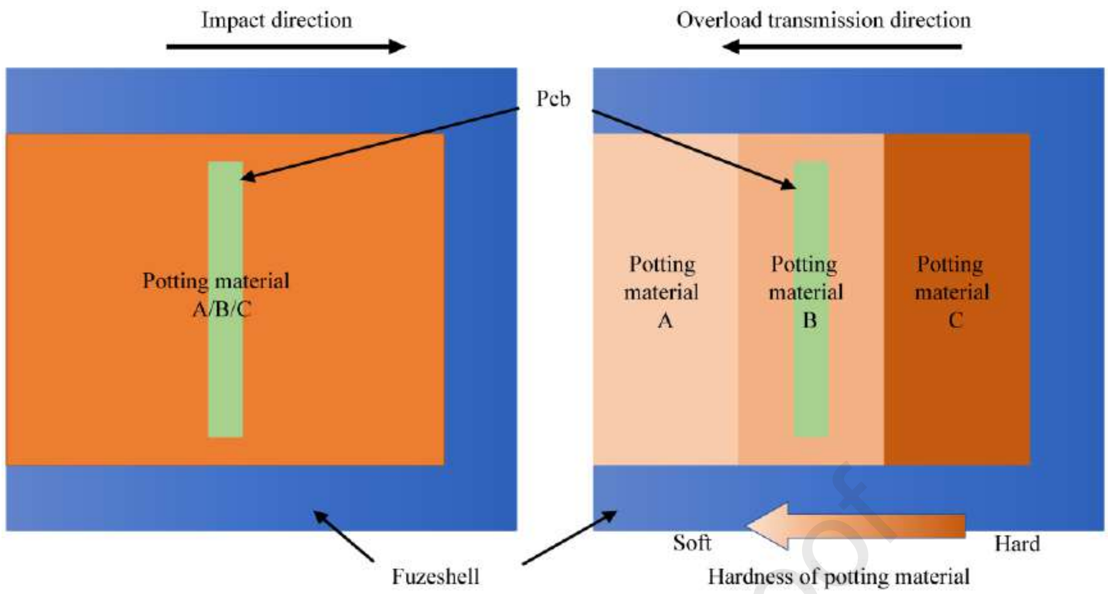

Fig. 19. Single-layer or multi-layer composite potting method (Adapted from [256]).

In practical applications, the selection of potting materials and the design of protection schemes must also comprehensively consider the layout and orientation of electronic components, as well as the potting process. The orientation of the circuit board within the housing significantly influences the propagation path of stress waves and the stress concentration. Simultaneously, the potting process scheme needs to be well matched with the structural design of the product. An improper potting process may lead to defects, affecting the protection effectiveness.

A scheme combining foam cushioning and polymer material potting was employed. After optimizing the structural parameters, the stress on the circuit module was reduced by 65.1%. For deceleration testing devices, an integral potting scheme using multi-layer cushioning materials was adopted [257]. Combined with a secondary power supply design, the testing device was enabled to operate stably in a 20000 g deceleration environment. A cushioning scheme using polytetrafluoroethylene and silicone rubber as intervals and polyurethane as filler was further designed [258]. In penetration tests, an deceleration signal as high as 192,435 g was successfully recorded, validating the effectiveness of the potting structure under extreme impact.

The potting protection of penetration fuze is a systematic issue. Epoxy resin, silicone rubber, and polyurethane are the three fundamental materials. The adoption of composite potting schemes is an effective approach to enhance performance. The design of potting materials and schemes must comprehensively consider material dynamic characteristics, stress wave propagation mechanisms, and system integration methods [259]. This is to enhance the survivability of penetration fuze and its internal electronic components during the penetration process. Future research will focus more on refined numerical simulation and multi-objective optimization. These efforts aim to customize the optimal potting solutions for specific application scenarios.

3.4.3 Isolation gasket protective design

In the impact protection design of penetration fuze, the external buffer-isolation gasket is one of the key measures against high deceleration. The typical installation position of the isolation gasket in penetration weapons is shown in Fig. 20(a). The buffer-isolation gasket primarily prolongs the impact duration through material deformation and utilizes stress wave reflection attenuation caused by impedance mismatch to isolate and weaken the shock energy transmitted to the fuze electronic system. The high-deceleration resistance, resilience, and stability of its material directly affect the survivability of the electronic system under extreme impact. Commonly used gasket materials include aluminum foam, polytetrafluoroethylene, and rubber, as shown in Figs. 20(b)–20(d), whose performance is compared in Table 7. This section reviews the research progress in buffer-isolation gasket design from the perspectives of single-layer gaskets and multi-layer composite gaskets. Schematic diagrams of the protection structures for single-layer gaskets and multi-layer composite gaskets are shown in Fig. 21(a).

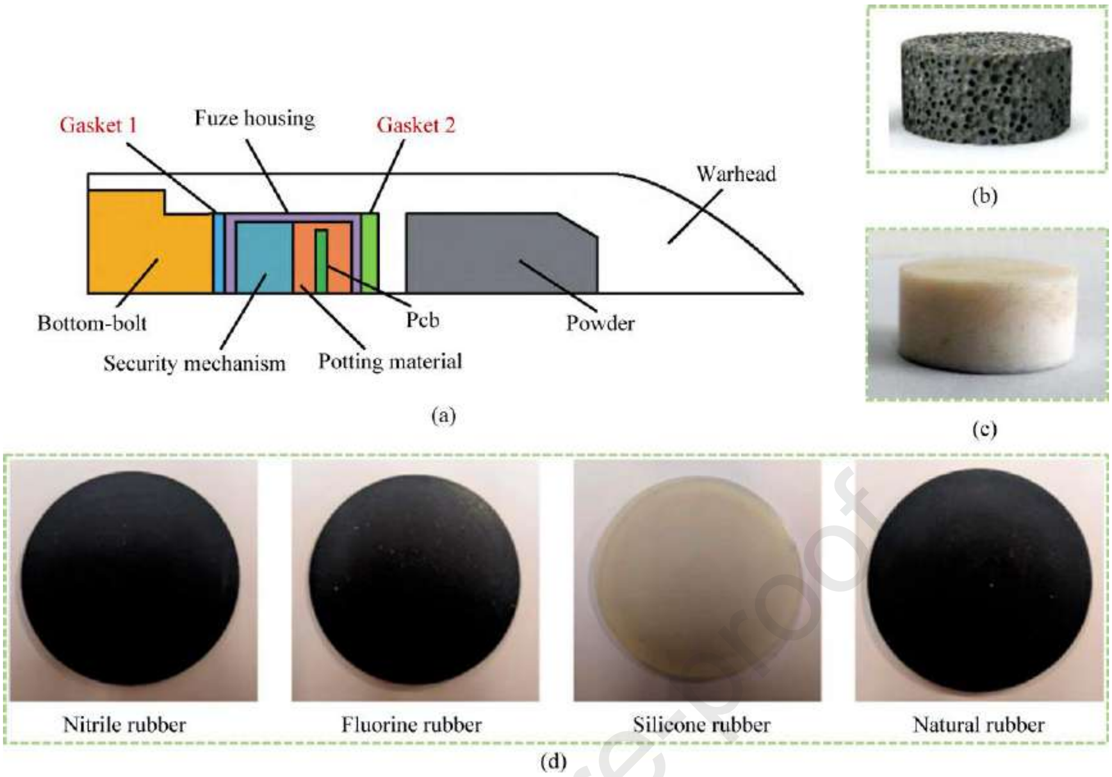

Fig. 20. Single-layer gaskets: (a) Schematic diagram of the gasket installation position in penetration warhead; (b) Foam aluminum gasket; (c) Polytetrafluoroethylene gasket; (d) Different types of rubber gasket [260, 261 – 263].

Table 7

Characteristics of common gasket materials [253, 254, 260, 264 – 270].

Materials	Characteristics	Limitations
Foam aluminium	Lightweight yet highly rigid, with strong energy-absorption capabilities, resistance to both high and low temperatures	Prone to compaction under high deceleration; plastic deformation
Polytetrafluoroethylene	Extreme temperature stability, excellent lubricity, outstanding chemical resistance	Lower energy absorption efficiency and weaker wear resistance
Rubber	High elasticity, relatively low-cost	Low strength, prone to ageing
Polyurethane	Wide range of adjustable mechanical properties, excellent overall mechanical performance	Relatively low strength and rigidity, unsuitable for extreme deceleration conditions
Artificial cartilage biomimetic material	Exceptionally high impact protection efficiency, capable of withstanding multiple impacts	Emerging materials, with cost and application maturity yet to be enhanced

Porous elastic composite material	Combining energy-absorbing properties with resilience, capable of withstanding multiple impacts	Complex structure, demanding preparation process, performance highly dependent on design

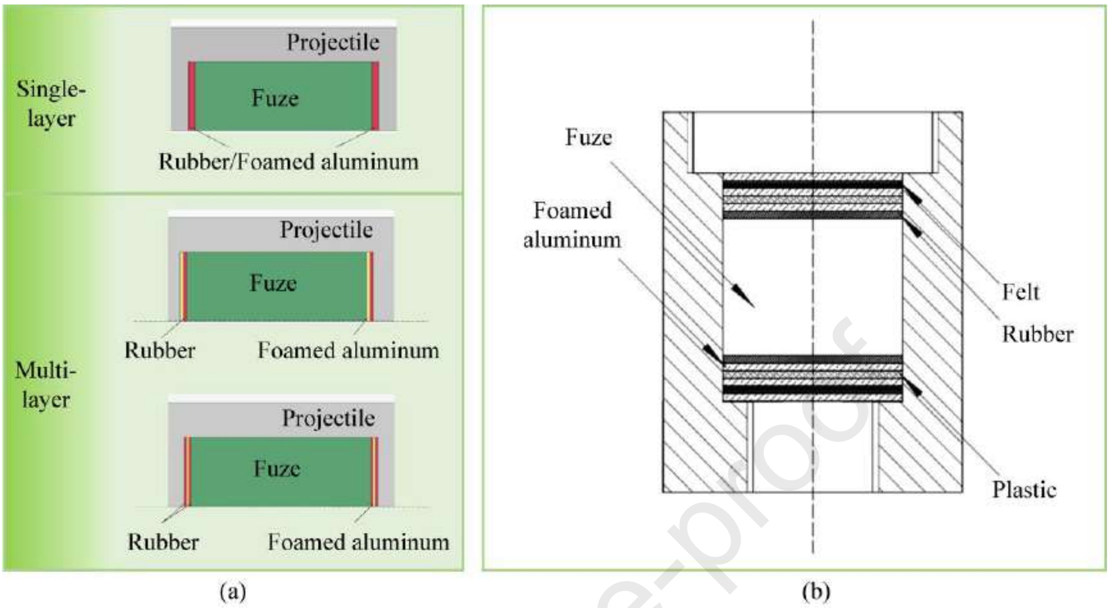

Fig. 21. Multi-layer composite gaskets: (a) Schematic diagram of protective structures for single-layer gasket and multi-layer composite gaskets; (b) A protective scheme for specific multi-layer composite gaskets [271–273].

In studies on single-layer gaskets, scholars have predominantly employed numerical simulations combined with marchet hammer impact tests to analyze their protective performance under penetration conditions. It was found by that the cushioning effect of polytetrafluoroethylene and foam aluminum gaskets was insensitive to thickness variation. Based on stress wave theory, a mathematical model was established [274]. It was proposed that the reflection and transmission behavior of stress waves could be optimized by adjusting the gasket thickness and gradient structure design, thereby enhancing the protective effectiveness. The effects of porosity and thickness of foam aluminum on its cushioning performance were systematically investigated [275]. It was indicated that an optimal parameter combination exists to achieve the best protective efficiency. The performance of foam aluminum and rubber gaskets was compared [276, 277]. It was observed that foam aluminum performed better in vibration suppression and deceleration filtering. However, rubber demonstrated higher reliability under multiple impacts due to its strong elastic recovery capability.

Furthermore, an investigation into the application of artificial cartilage biomimetic material in fuze buffering and protection was conducted [269]. Through Machete hammer tests, it was demonstrated that under an acceleration deceleration with an amplitude of approximately 40000 g and a duration of about 100 μs, the buffering performance of bionic artificial cartilage materials surpasses that of traditional buffering materials. A porous elastic composite material by blending porous media with elastic polymers was developed [270]. This material features a spatial skeleton of elastic polymer fibers enveloping porous media particles. During repeated Machete hammer impacts, its performance was found to be superior to that of conventional buffering materials.

In the field of multi-layer composite gaskets, the synergistic protection mechanisms of different material combinations and arrangement methods have been explored. The attenuation performance of aluminum and polytetrafluoroethylene composite gaskets on the peak deceleration at the fuze was investigated [278, 279]. A steel plate-foam aluminum sandwich structure was proposed [275]. This structure utilizes impedance mismatch and stiffness enhancement to suppress the compaction effect. Additionally, a multi-layer gasket with alternating high and low impedance was designed [280]. Its applicability under various penetration velocities and target types was expanded. The rubber and foam aluminum composite structure was further analyzed [271]. It was found that specific stacking sequences can significantly reduce the impact peak and extend the load duration. Based on stress wave theory, verification was conducted [281]. Gradient foam aluminum gaskets arranged in decreasing density have optimal wave impedance matching performance. These gaskets can significantly reduce axial deceleration and possess good angle adaptability.

Currently, aluminum foam and polytetrafluoroethylene are commonly used cushioning materials. New materials such as artificial cartilage biomimetic materials and porous elastic composites demonstrate better application prospects. Meanwhile, a multi-layer composite anti-impact protection system was constructed [282], as shown in Fig. 21(b). This provides a theoretical basis and structural optimization path for the cushioning protection design of the penetration fuze under various high-deceleration conditions. Although extensive research has confirmed that the multi-layer gasket structure effectively protects the internal electronic components of the fuze during penetration, in practical applications, cases still exist where gasket damage leads to a decrease in protection performance. Therefore, the design of the cushioning protection system requires further systematic research on its dynamic response and durability under high-speed penetration conditions. This is to ensure the functional integrity of the fuze.

The dynamic response analysis of penetration fuzes involves several closely related research aspects, including connection structure response, load transmission, overload characteristics, stress-wave propagation, and buffer protection. These aspects are different in research scale and technical focus. Since penetration fuzes usually work under extremely high overload, strong impact, short-duration pulse, and complex projectile-target interaction conditions, a single research method is usually insufficient. Therefore, different modeling and test methods should be selected according to the research objective, and applicable scale.

As shown in Table 8, methods for load and dynamic response analysis of penetration fuzes are systematically compared. For mechanism analysis, theoretical and semi-analytical models are useful. For structural design and local failure analysis, explicit finite element simulation is more suitable. For system-level response estimation, calibrated dynamic transfer models can reduce computational cost while maintaining acceptable accuracy within their applicable configuration range. For engineering verification, full-scale tests remain indispensable, but they should be combined with component-level tests, material-level dynamic tests, and simulation-based analysis to reduce cost and improve repeatability. Therefore, the load and dynamic response analysis of penetration fuzes should follow a multi-scale and multi-method framework, including material-level characterization, component-level impact evaluation, projectile-fuze system modeling, and full-system experimental verification.

Table 8

Comparison of methods for load and dynamic response analysis of HTPFs [18, 20, 178, 246, 260, 282–284].

Research aspect	Typical modeling methods	Typical test methods	Applicable scale	Main input parameters	Main output parameters	Advantages	Limitations
Connection-structure response	Finite element model; multibody dynamic model; simplified spring-damping model	Projectile-fuze assembly impact test; vibration/shock test; recovered-structure inspection	Projectile-fuze assembly; fuze housing; sensor mounting structure; circuit-board support	Connection type, thread/preload condition, material properties, impact velocity, target condition, boundary constraints	Acceleration response, connection stress, deformation, local failure mode, frequency response	Can evaluate the influence of structural connection on fuze response and sensor signal characteristics	Sensitive to contact, preload, damping, and boundary assumptions; experimental validation is required
Load-transmission mechanism	Stress-wave propagation model; impedance-matching model; finite element simulation; nonlinear dynamic transfer model	Hopkinson bar test; impact table test; projectile penetration test; sensor-based overload measurement	From projectile body to fuze location; from fuze housing to internal components	Projectile geometry, material impedance, target resistance, impact velocity, interface stiffness, damping parameters	Load path, stress-wave arrival time, transmitted acceleration, load attenuation ratio	Helps reveal how external impact load is transferred to internal fuze components	Simplified models may not capture complex three-dimensional contact and nonlinear material behavior
Penetration overload response	Cavity-expansion model; empirical/semi-empirical penetration model; explicit finite element simulation; rigid-body dynamic model	Full-scale or scaled penetration test; onboard data recorder; high-g acceleration measurement	Whole projectile; fuze installation position; sensor location	Target material, target thickness, projectile mass, projectile velocity, nose shape, impact angle	Rigid-body deceleration, structural vibration response, overload peak, pulse width, penetration depth	Directly related to fuze survivability and signal acquisition	Full-scale tests are costly and destructive; measured signals may include rigid-body motion, structural vibration, and sensor noise

Dynamic transfer from projectile to fuze	Multibody dynamic transfer model; transfer-matrix method; calibrated reduced-order model	Calibration test; projectile-target penetration test; sensor comparison at different locations	Projectile-fuze coupled system; multiple measurement points	System mass/stiffness/damping parameters, connection parameters, external impact load, calibration data	Fuze-location acceleration, sensor overload signal, dynamic amplification factor	More efficient than full finite element simulation after calibration; suitable for system-level response estimation	Accuracy depends on calibration quality and applicability to similar projectile-fuze configurations
Local stress and strain response	Local finite element model; sub-modeling method; stress concentration model; dynamic stress concentration analysis	Strain-gauge test; high-speed impact test; recovered-component inspection	Fuze shell, potting material, circuit board, solder joint, local support structure	Local geometry, material parameters, loading pulse, interface condition, defect or cavity parameters	Local stress, strain, stress concentration factor, damage risk region	Useful for identifying vulnerable parts and local failure mechanisms	Difficult to obtain accurate material parameters and interface conditions under high-g impact
Buffer-protection performance	Explicit finite element simulation; porous-material constitutive model; sandwich-structure model; energy-absorption model	Drop-weight test; impact table test; penetration test with buffer layer; recovered-state inspection	Buffer material; buffer layer; fuze module; fuze-warhead assembly	Buffer material density, porosity, thickness, layer configuration, impact velocity, loading direction	Overload attenuation ratio, energy absorption, deformation mode, residual deformation, protected-component response	Can guide selection of protective materials and structural forms	Buffer may become compacted under severe loading; excessive deformation may affect available installation space
Material-level impact behavior	Constitutive modeling; strain-rate-dependent material model; porous-material model	Split Hopkinson pressure bar; quasi-static compression; dynamic compression; material recovery analysis	Material coupon; foam metal; polymer; composite or potting material	Strain rate, material density, porosity, temperature, loading mode	Stress-strain curve, plateau stress, densification strain, energy absorption capacity	Provides fundamental data for simulation and protection design	Material-level behavior may differ from system-level response due to boundary and assembly effects

System-level verification	Coupled simulation; hardware-in-the-loop test; full-system penetration test	Integrated projectile-fuze test; ground impact test; full-scale penetration test	Complete fuze or projectile-fuze-target system	Complete structural configuration, mission condition, sensor layout, target condition, impact velocity	Functional survivability, overload history, signal integrity, structural damage, initiation-control-related response	Provides the highest level of engineering credibility	High-cost, poor repeatability, limited number of measurable internal states

3.5 Summary and assessment

The dynamic environment experienced by a penetration fuze is governed by a cascade of mechanical interactions, beginning at the projectile-target interface and propagating through the projectile body, the projectile-fuze connection, and the internal potting, buffering, sensing, and electronic structures. Although considerable progress has been made in analytical modeling and finite element simulation, a clear gap remains between mechanism-oriented academic models and engineering-level predictive tools. In particular, many existing models are still based on elastic thread deformation, simplified contact stiffness, or weakly nonlinear impact assumptions. These treatments are useful for explaining load amplification, stress-wave distortion, and interface-induced high-frequency interference under conventional penetration conditions, but they are insufficient for hypersonic penetration environments, where elastoplastic deformation, frictional heating, local failure, and thermo-mechanical coupling may significantly alter contact stiffness and load transmission.

For projectile-fuze connection structures, pressure-threaded connections can reduce acceleration amplification and signal disturbance relative to body-threaded connections under multi-layer hard-target penetration conditions. Therefore, they may represent a favorable engineering compromise between load-transfer performance, structural stiffness, and manufacturability in many penetrator configurations. However, this conclusion should not be generalized without qualification, because connection performance is strongly dependent on projectile geometry, thread parameters, preload, material properties, penetration velocity, target configuration, and thermal environment. Bolted flange-type connections may offer better assembly controllability and load-path definition, but their volume and mass penalties limit their applicability in compact fuze layouts and make them more suitable for large penetrators.

Future studies on HTPFs should move from isolated component analysis toward integrated projectile-target-fuze coupling models. Such models should simultaneously account for penetration mechanics, target damage evolution, projectile structural dynamics, interface load transfer, and the refined dynamic response of fuze components. By doing so, a more reliable mapping can be established among target characteristics, projectile penetration behavior, fuze load input, and fuze functional reliability.

Future research should also place greater emphasis on the long-term reliability of internal protective structures. Multi-layer potting systems, compliant buffering layers, and bio-inspired gasket designs can improve shock attenuation and local stress redistribution in laboratory tests, but their reliability under storage aging, thermal cycling, humidity exposure, cure shrinkage, and long-duration micro-vibration remains insufficiently quantified. An engineering direction is to replace purely deterministic finite element evaluations with probabilistic structural reliability frameworks. Such frameworks should incorporate thread-gap tolerances, preload scatter, material-property dispersion, cure-induced residual stress, potting shrinkage, and interface degradation. This would allow more realistic margin assessment and reduce dependence on overly conservative safety factors that may unnecessarily penalize fuze sensitivity, structural compactness, and system performance.

Ultimately, future fuze design should embrace system-level co-design rather than treating the fuze body as a rigid casing that must be passively protected. A more advanced design philosophy is to regard the connection, casing, potting, buffering layer, sensor package, and signal-processing circuit as an integrated dynamic system. In this framework, the projectile-fuze connection and internal support structures may be intentionally designed as mechanical filters that attenuate specific resonant frequency bands before the signal reaches sensitive electronic components. Realizing this concept requires early-stage collaboration among penetration mechanics researchers, structural dynamicists, material engineers, reliability analysts, and fuze circuit designers. Such interdisciplinary co-design is likely to be essential for improving the survivability, signal fidelity, and functional reliability of future hard-target penetration fuzes.

4 Target information sensing and feature extraction

To achieve precise lethality against underground multi-layer hardened protective targets, information such as penetration depth, medium type, and the number of layers must be accurately identified by HTPF to ensure initiation at the optimal position [285, 286]. Target information sensing and feature extraction are established as the prerequisites for achieving such precise lethality [185]. In this section, research progress in target information sensing and feature extraction technologies for HTPs is reviewed. The discussion is organized around three primary aspects: target information sensing, signal overlapping and aliasing mechanisms, and feature extraction.

4.1 Hard-target information sensing

Hard-target information sensing is the prerequisite for accurate initiation control of HTPF. During penetration, the projectile body is subjected to deceleration that can reach tens of thousands to hundreds of thousands of g. Hence, the development of deceleration signal sensing technology capable of reliable operation in such extreme environments becomes the core of the HTPF system.

Penetration fuze commonly employ acceleration sensors [287–289] and threshold switches [290–292] to obtain deceleration information during penetration. Since threshold switches can only provide switch signals that indicate whether the penetration deceleration reaches or exceeds one or multiple threshold levels, precise control of the initiation point is difficult to achieve. Therefore, acceleration sensors are more frequently used in HTPF to acquire complete deceleration profiles during penetration. The experimental layout for high-speed normal penetration of a warhead into four layers of reinforced concrete thick targets is shown in Fig. 22(a), along with the penetration acceleration curve measured by an acceleration sensor [293, 294]. The projectile body is approximately 1.4 m in length. The first target is 0.3 m, while the remaining three targets are each 0.18 m. The spacing between targets is 2.5 m. From the moment the projectile nose contacts the first target to the moment the tail exits the last target, the actual total displacement of the penetration process is about 9.755 m. The initial impact velocity, determined by high-speed camera recording, is 345 m/s. The velocity after penetrating the four layers is 270 m/s. The deceleration at the fuze, sensed by the acceleration sensor during a range test where a projectile undergoes high-speed penetration of 10-layer thin concrete targets is illustrated in Fig. 22(b). The deceleration at the fuze detected by the acceleration sensor when the warhead penetrates 7-layer of reinforced concrete targets at 2.5 Mach is presented in Fig. 22(c).

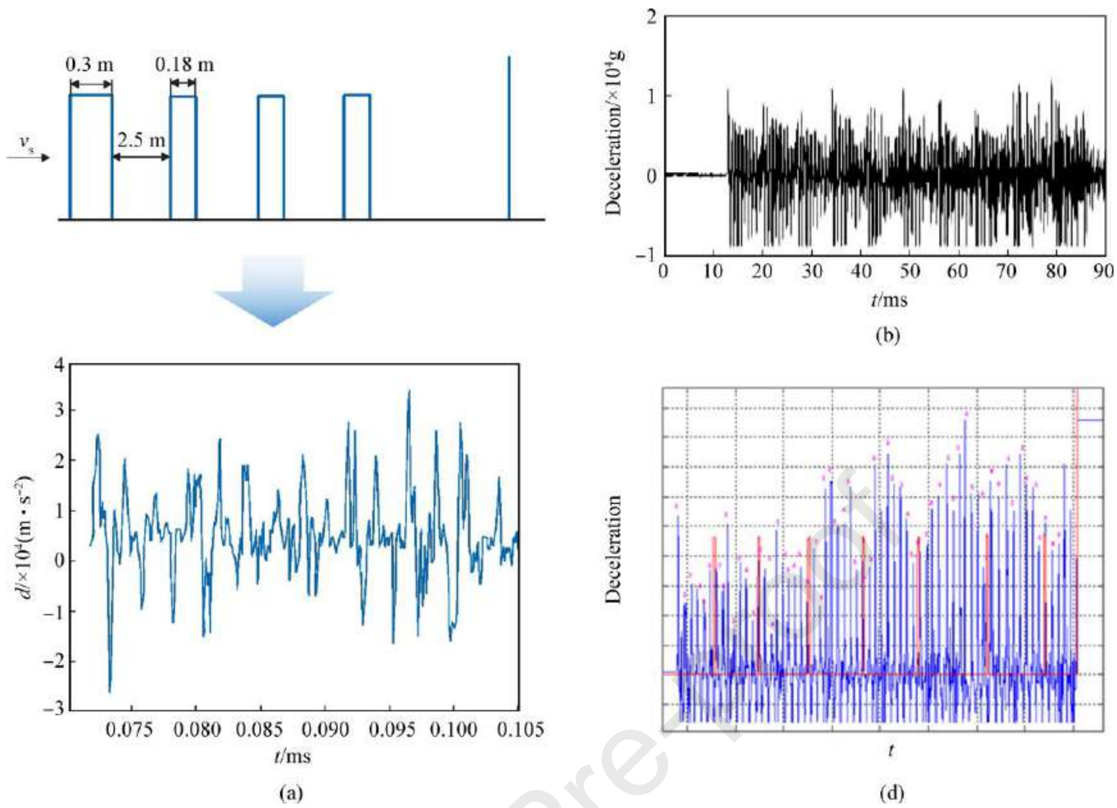

Fig. 22. Measured deceleration curves during penetration of multi-layer targets: (a) Test layout and the measured deceleration curve of the fuze during penetration of 4-layer enhanced thick concrete targets [293, 294]; (b) Measured deceleration curve of the fuze during penetration of 10-layer thin concrete targets [295, 296]; (c) Measured deceleration curve of the fuze during penetration of 7-layer reinforced concrete targets at 2.5 Mach [297–299].

Common acceleration sensors include piezoresistive [56, 111, 288, 300, 301], capacitive [302, 303], and piezoelectric [304, 305] acceleration sensors. Piezoelectric acceleration sensors are characterized by a wide response bandwidth, high sensitivity, high signal-to-noise ratio, and simple structure. Before MEMS piezoresistive acceleration sensor technology matured, they were the primary sensors used in penetration fuzes [306]. However, after being subjected to prolonged high-deceleration shocks, piezoelectric acceleration sensors exhibit a phenomenon where the output signal cannot return to the measurement baseline. This limitation restricts their application in penetration fuze. At the 63rd Annual NDIA Fuze Conference, it was pointed out by Adriane [307] that the piezoresistive acceleration sensor has been established as the preferred type in the fuze field by the USA.

Based on the sensing principles, this paper categorizes the mainstream technological approaches in recent years into piezoresistive acceleration sensors, capacitive acceleration sensors, and novel sensors. Their developmental trajectories and current research status are systematically reviewed.

4.1.1 Piezoresistive acceleration sensor

Piezoresistive acceleration sensors utilize the piezoresistive effect, where the resistivity of a material changes under mechanical stress, to measure acceleration. Compared to other types of acceleration sensors, piezoresistive acceleration sensors offer high frequency response, small size, high accuracy, and high reliability. Consequently, piezoresistive sensors are widely used in HTPFs. Publicly available parameters of typical high-g accelerometers are summarized in Table 9.

Table 9

Publicly available specification-level parameters of typical high-g accelerometers for HTPFs [2, 6, 9, 10, 232, 308–313].

Model	Country	Technology	Range/g	Shock Limit/g	Sensitivity /(μV·g^{-1})	Frequency Response/Hz	Resonant Frequency/kHz	Damping	Time Constant/s	Zero Shift/mV	Non-Linearity	Transverse Sensitivity	Excitation Voltage	Operating Temperature
Endevco 7270A-200K	USA	Piezoresistive (MEMS)	±200000	200000	~ 1.0	0–150000 (±5%)	~ 1200	Undamped		< 0.5	< 2% FSO	< 5%	DC Coupled	−55 °C–+121 °C
Kulite GD-4500-100K	USA	Piezoresistive (SOI)	±100000	120000	~ 1.0–1.5	0–30000 (±5%)	> 300	Undamped		< 1.5	±1% FSO	< 3%	DC Coupled	−55 °C–+235 °C
AS-100K	China	Piezoresistive (MEMS)	±100000	150000	~ 1.5	0–40000 (±1 dB)	> 600	Undamped		< 1.0	< 1.5% FSO	< 3%	DC Coupled	−40 °C–+100 °C
Kyowa BKF-A-100K	Japan	Piezoresistive (MEMS)	±100000	120000	~ 1.5	0–40000 (±1 dB)	> 500	Undamped		< 2.3	< 1% FSO	< 3%	DC Coupled	−40 °C–+120 °C
AYZ-4-100K	China	Piezoresistive (MEMS)	±100000	120000	~ 1.5	0–40000 (±1 dB)	> 600	Undamped		< 2.3	< 2% FSO	< 5%	DC Coupled	−40 °C–+85 °C
Endevco 7280A-60K	USA	Piezoresistive (MEMS)	±60000	240000	~ 5.0	0–20000 (±1 dB)	~ 130	Gas Damped		< 0.2	< 2% FSO	< 3%	DC Coupled	−55 °C–+121 °C
PCB 3501A-60K	USA	Piezoresistive (MEMS)	±60000	100000	~ 3.0	0–20000 (±1 dB)	> 120	Gas Damped		< 1.5	< 1% FSO	< 3%	DC Coupled	−54 °C–+121 °C
PCB 3991-60K	USA	Piezoresistive (MEMS)	±60000	100000	~ 3.5	0–20000 (±1 dB)	> 125	Gas Damped		< 1.5	< 2% FSO	< 3%	DC Coupled	−54 °C–+121 °C
Dytran 3200B-70K	USA	Piezoelectric (IEPE)	±70000	100000	~ 50.0	0.35–10000 (±10%)	> 90		~ 1.0–1.5	< 250	±1% FSO	< 5%	AC Coupled	−51 °C–+121 °C
Kistler 8742A-100K	Switzerland	Piezoelectric (IEPE)	±100000	120000	~ 50.0	1–30000 (±5%)	> 100		> 0.5	~ 50–250	±1% FSO	< 3%	AC Coupled	−54 °C–+120 °C

Note: ① The parameters listed in this table are publicly available specification-level or literature-reported values. ② The performance parameters of the piezoresistive accelerometer are typical values at 10 V DC. ③ They are useful for preliminary comparison of sensor range, bandwidth, sensitivity, and environmental adaptability. But, quantitative survivability comparison requires controlled penetration tests under identical projectile, target, impact velocity, mounting, packaging, and data-acquisition conditions.

Taking the AS-100K and Endevco 7270A-200K as examples, their publicly available specifications indicate different performance envelopes. The Endevco 7270A-200K provides a wider measurement range of ±200000 g, a shock limit of 200000 g, a frequency response of 0–150000 Hz, and a resonant frequency of approximately 1200 kHz [308]. In comparison, the AS-100K provides a measurement range of ±100000 g, a shock limit of 150000 g, a frequency response of 0–40000 Hz, and a resonant frequency above 600 kHz [309]. These data suggest that the Endevco 7270A-200K has advantages in range margin, high-frequency response, and resonant-frequency margin, which are important for capturing short-duration high-g pulses and avoiding structural resonance during severe penetration events. The AS-100K, however, exhibits comparable nominal sensitivity and nonlinearity within its rated range, indicating that it may still be suitable for conventional high-g penetration measurements when the expected deceleration and frequency content remain within its operating envelope.

Nevertheless, such specification-level comparison cannot be directly translated into real-world survivability under multi-layer penetration. Sensor survival is affected by the entire measurement chain, including chip structure, wafer-level packaging, die attachment, potting protection, mounting stiffness, cable and connector integrity, signal-conditioning circuits, power supply stability, and data-storage reliability. Therefore, the survivability gap between each high-g accelerometers cannot be quantitatively determined from its specification-level parameters.

(1) Single-axis high-g accelerometer

With the maturation and application of MEMS technology, significant progress has been made in the miniaturization, integration, and cost reduction of single-axis high-g accelerometers. To effectively alleviate the inherent contradiction between high range and high sensitivity in such sensors, research has been systematically focused on the beam-island and its derived composite structures [285, 287, 306, 314–316]. Through refined mechanical design, these structures achieve efficient stress concentration and distribution between the pressure-bearing area and the supporting boundaries. This enables the synergistic optimization of sensor performance.

The USA Endevco developed the 7270A-200K high-g accelerometer, with a range of up to 200000 g [317]. The accelerometer uses wafer-level packaging to form a glass-silicon chip-glass sandwich structure to provide airtight packaging for the sensitive components in the middle layer. To further improve reliability, the chips use through-hole interconnects, reducing the number of wire-bonded interconnects.

Through the application of microstructural geometric optimization represented by the beam-island structure, rational configuration of island mass, and advanced microfabrication processes such as SOI, a technological breakthrough has been achieved. This breakthrough significantly enhances deceleration capacity while maintaining high sensitivity. Additionally, key indicators like linearity and natural frequency have been improved. The anti-deceleration capability of single-axis high-g MEMS accelerometers has reached and exceeded 10^5 g [104, 111]. These sensors can maintain structural integrity and achieve effective measurement under extreme impacts. A solid technical foundation has thus been laid for applications such as penetration, collision, and explosion impacts.

(2) Three-axis high-g accelerometer

With the maturation of single-axis high-g accelerometer technology, to meet the demands of complex functions such as layer-counting and attitude recognition in penetration environments, the research focus has gradually shifted to the development of three-axis high-g accelerometers. A monolithically integrated piezoresistive three-axis high-g accelerometer was developed [318]. Its range reached 10^5 g, and its sensitivity, resonant frequency, and nonlinearity were systematically tested. A single-chip three-dimensional MEMS piezoresistive accelerometer based on an E-type diaphragm structure was proposed [319]. Simulation results indicated that this structure could withstand transient impacts of 2×10^5 g. A monolithically integrated three-axis high-range MEMS accelerometer was reported [315, 320]. The sensitivity of each axis was better than 0.1 μV/g, and the inter-axis transverse sensitivity ratio was less than 10%. The three-axis sensitive chip was optimized through theoretical analysis and simulation [321]. This further improved key performance indicators such as sensitivity, natural frequency, and nonlinearity.

The practicality of acceleration sensors is inseparable from system integration and precise calibration. Early on, dynamic impact calibration was conducted [322], using a Hopkinson bar on a triaxial acceleration sensor with a range of up to 50000 g. It was verified that good linear response characteristics were exhibited under extreme impact conditions. This laid the foundation for high-impact testing. Subsequently, a projectile-borne high-impact three-dimensional acceleration storage was developed [323, 324]. Experimental results demonstrated that stable operation was maintained in a high-deceleration environment of 48000 g. This marked an important breakthrough in system integration and engineering applicability for this category of sensors.

With the advancement of research, the refinement of calibration models has become crucial. The calibration model considering the transverse sensitivity effect was further developed [325, 326]. They also proposed a corresponding relative transverse sensitivity calculation method, significantly advancing the calibration theory for high-impact acceleration testing. In recent years, studies have increasingly focused on improving calibration accuracy. A multi-component high-impact calibration test system was developed [327]. This system achieved high-precision calibration with axial impact sensitivity errors below 10%. It provides critical support for the precise evaluation and reliability design of penetration fuze.

4.1.2 Novel acceleration sensor

To overcome the limitations of acceleration sensors, scholars have begun exploring novel acceleration sensors based on new principles [103]. Among these, an inertial switch as the detection device was employed [328–330]. The deceleration curve at the fuze position was successfully obtained when a 125 mm projectile penetrated a 3 m C30 concrete target at 761 m/s. The inertial switch operates by utilizing the inertial response of a mass-spring system to achieve circuit on-off switching, thereby outputting purely digital signals. This design provides strong anti-interference capability. However, a drawback is that minor manufacturing deviations may lead to inconsistent responses, which can affect sensing accuracy.

Moreover, a composite sensor integrating capacitive plates and PVDF piezoelectric film was designed [331]. A method based on capacitive-piezoelectric composite detection for acquiring fuze target information was proposed. This approach combines the complementary advantages of different sensing mechanisms. A capacitive sensor for penetration fuze was designed [332]. Through optimization of the signal processing circuit, interference from the severe structural response of the projectile body and complex noise during penetration was effectively suppressed. Signal quality was significantly improved. Addressing the challenge of signal overlap between layers caused by structural vibration of traditional accelerometers during high-speed penetration of multi-layer hard-targets, a layer-counting sensor sensitive only to rigid-body deceleration was proposed and developed [333]. This sensor is based on the low-frequency inertia principle. A capacitive structure with a natural frequency much lower than the vibration frequency of the projectile body is employed. Through parameter optimization, high-frequency interference is effectively filtered out. Simulations and experiments demonstrate that each impact can be clearly distinguished by this sensor under multi-layer target penetration conditions. The time recognition error is less than 10%. Performance is significantly superior to that of traditional accelerometers.

Significant progress has been achieved in the field of acceleration sensors for HTPF, both domestically and internationally. Currently, research abroad is more systematic. Sensor designs are highly aligned with target characteristics, and rigid-body deceleration features are prominently exhibited in test signals. Compared with the most mature foreign high-g accelerometers, some domestic devices still show limitations in publicly available specification margins, high-frequency response, environmental adaptability, and suppression of oscillation-induced signal aliasing. However, due to the lack of publicly available, side-by-side penetration tests, this gap should be interpreted mainly as a specification-level and application-adaptability gap.

Future research should focus on enhancing the accurate sensing capability of sensors under complex conditions such as high-speed penetration, short spacing, and large length-to-diameter ratios. Efforts should also be made to promote their continuous development toward intelligence, high reliability, and strong adaptability. For future applications, high-g accelerometers still face several technical challenges. First, the reliability of signal transmission, material stability, and temperature compensation capability of sensors need to be enhanced under extreme environments such as high temperature, high impact, and strong magnetic fields. Second, new communication protocols and technologies with strong anti-interference capability and complete, accurate data transmission should be developed. Third, efficient coordination and intelligent fusion between acceleration sensing units and multi systems such as attitude sensing and fuze control must be achieved.

4.2 Mechanisms and cause of signal overlapping and aliasing

The process of projectile penetration into a target is considered highly complex. Since the projectile body is not a rigid entity, the acceleration signals detected by internal sensors during the penetration and subsequent free-flight stages are not characterized as ideal pulse signals. Due to the abundance of vibrational signals within the projectile, phenomena such as signal overlapping and aliasing are frequently observed in the acceleration curves sensed by the penetration fuze. The deceleration test curve for a specific penetration warhead striking multi-layer targets at high velocity is presented in Fig. 22(c) [299]. It can be observed that the penetration signals are severely aliased, with the deceleration for each layer being composed of several small oscillatory envelopes. The accuracy of layer-penetration identification is severely compromised by this signal overlapping and aliasing. Consequently, the extraction of accurate and effective layer-penetration information from these aliased signals has become a critical technical challenge that must be overcome for HTPFs.

Analyzing the causes of overlapping and aliasing in multi-layer penetration deceleration signals and revealing the overlapping and aliasing mechanism of through-layer signals are prerequisites for solving the problems of signal overlapping and aliasing. At the 52nd Annual NDIA Fuze Conference, it was pointed out by Lundgren in the analysis of penetration fuze that the characteristics of fuze deceleration signals are complex, mainly containing signals in multiple frequency bands from kHz to MHz. Currently, regarding the problems of overlapping and aliasing in deceleration signals during actual measurement, in-depth research has been conducted by scholars at home and abroad from multiple dimensions. The focus is on projectile body vibration response and projectile-fuze system resonance, among others. Additionally, it is believed by a few scholars that the installation position and arrangement form of sensors can also lead to overlapping and aliasing in deceleration signals. In this section, the effects of projectile body vibration response and projectile-fuze system resonance on deceleration signals will be discussed.

4.2.1 Projectile body vibration response

Projectile body vibration is one of the main causes of inter-layer overlapping and aliasing in the deceleration signal of penetration fuze. Projectile body vibration mainly includes projectile body structural vibration, threaded connection vibration, and internal component vibration of the fuze. It primarily generates vibration response in the kHz frequency band. Regarding the causes and internal mechanisms of signal overlapping caused by projectile body vibration, in-depth research has been conducted.

Early studies provided a systematic description of the signal overlapping phenomenon. The measurement signal from the accelerometer was defined as the result of overlapping in the time domain between the rigid-body deceleration due to the overall deceleration of the projectile body and the local vibration response of the projectile body. It was characterized by high-frequency oscillatory signals superimposed on the deceleration envelope. Through experiments, it was found that overlapping is closely related to the penetration velocity. When the penetration velocity was not higher than 500 m/s, the signal overlapping phenomenon was not significant. When the velocity exceeded 600 m/s, a large number of high-frequency oscillatory signals were superimposed on the deceleration envelope, and the envelope could even be submerged by the oscillations, resulting in signal overlapping. Based on the different modes of superposition, it was classified into two types: time-series overlapping and time-parallel overlapping. This work laid the foundation for subsequent research.

Subsequently, scholars began to explore the underlying mechanisms of the overlapping phenomenon from different perspectives. It was pointed out [290] that overlapping occurs because the stress wave effect induced by the impact on the upper layer has not fully attenuated when the projectile penetrates the next layer. It was confirmed [334] through interference source identification that projectile body vibration caused by stress wave transmission is the main source of interference signals. It was further noted [299] that the intrinsic mechanism of interlayer signal overlapping during high-speed penetration of multi-layer targets is as follows: the high-strain-rate stress waves excited by high-speed impact propagate, reflect, and superimpose along the projectile axis, forming oscillatory signals related to the projectile length. Projectile body vibration can be regarded as the steady-state result formed after multiple reflections and superposition of stress waves within a finite bounded structure.

4.2.2 Projectile-fuze system resonance

The aforementioned research only considered the influence of projectile body vibration on the overlapping and aliasing of deceleration signals, while neglecting the influence of the projectile-fuze system response on deceleration signals. Based on the clarification that the overlapping and aliasing of deceleration signals are closely related to projectile body vibration, further studies were conducted on the influence of the dynamic response of the projectile-fuze system on penetration deceleration signals.

Early studies have pointed out that the resonance of the ejection system is the cause of the oscillation of the overload signal. Since then, the essence of overload signal adhesion is the resonance effect caused by the coupling between the penetration resistance excitation frequency and the natural frequency of the elastic connection system was clearly pointed out [335]. The adhesion is divided into time domain adhesion and time-frequency domain adhesion according to the severity.

The resonance effect depends not only on external excitation, but also on the inherent frequency of the system itself. A study revealed how threaded connection parameters such as material elastic modulus, engagement length, and pitch significantly influence the natural frequency of the projectile-fuze connection structure by altering the connection stiffness [189, 190]. It was also pointed out that when this natural frequency couples with the rich vibration frequencies during penetration, it leads to abnormal amplification of the vibration signals measured by sensors.

Based on this, further research has been conducted by scholars on how to achieve quantitative optimization of signal overlapping through the regulation of key parameters. Pitch is the key factor affecting signal overlapping among various thread parameters was pointed out [336]. The core mechanism was revealed: connection stiffness is increased by reducing pitch, which exacerbates overlapping and aliasing of deceleration signals. Therefore, by appropriately increasing pitch while ensuring strength, thread connection stiffness can be reduced. This accelerates signal attenuation and significantly improves signal recognition reliability. At the same time, preload was proposed [337] as a key control parameter for pressure screw connections. It was indicated that insufficient preload leads to dynamic gaps at the interface and triggers high-frequency collisions. Parasitic oscillations are introduced by the nonlinear effects caused by high-frequency collisions. This exacerbates overlapping. The application of sufficient minimum preload to suppress gaps is key to optimizing signal quality.

Existing research has indicated that the dynamic response of the projectile-fuze system is one of the causes of deceleration signal overlapping and aliasing, revealing the resonant nature of this phenomenon in the projectile-fuze system. The conclusions demonstrate that by optimizing key mechanical connection design parameters, such as pitch and preload, the dynamic response of the projectile-fuze system can be actively regulated. This provides an effective approach to suppress deceleration signal overlapping from the structural design source and enhance fuze reliability.

4.2.3 Other cause

Most studies have considered the effects of projectile body vibration or stress wave reflection and superposition at the projectile-fuze connection on the overlapping and aliasing of deceleration signals. It is believed that projectile body structural vibration and projectile-fuze system resonance are the main causes of signal overlapping and aliasing. Based on this, the effects of key factors such as sensor installation position, projectile body shape, and penetration initial velocity on penetration deceleration signals have been investigated by some scholars.

In penetration deceleration measurement, the mounting method of sensors and the structural characteristics of the projectile body significantly affect signal quality. Scholars pointed out that if the main resonant frequency of the projectile body overlaps with the dominant frequency of the shock load due to improper sensor design or installation, or due to insufficient stiffness or large dimensions of the projectile body, it becomes difficult to effectively extract the rigid-body acceleration from the measured data. Stress wave propagation inside the projectile body leads to inconsistent acceleration responses at different locations was found [192]. It was further emphasized that the sensor installation method has a significant impact on the signal. The use of rigid connections and increased installation stiffness were recommended to improve measurement accuracy.

Moreover, the shape of the projectile body and the penetration attitude can also cause overlapping of the deceleration signal [338–340]. The overlapping characteristics of the signal are closely related to multiple physical factors was clearly pointed out. These factors include the instantaneous strain rate of the projectile body, the shape of the projectile body, the initial penetration velocity, and the free flight time between adjacent targets [341]. A qualitative mechanistic analysis was conducted on this. However, quantitative experimental or simulation verification of the influence degree of each factor was not provided by this study. In addition, an in-depth and systematic discussion on the inter-layer overlapping characteristics was lacking. Building on this, an important deepening and development in this field is represented [339, 340]. This research shifts from qualitative analysis to quantitative and parametric research. Through systematic numerical simulation, they focused on four core controllable variables: penetration velocity, incidence angle, attack angle, and the length-to-diameter ratio of the projectile body. Specific parameter levels were set. The influence of these variables on the overlapping characteristics of the deceleration signal was systematically investigated. The deceleration signal was measured by the tail sensor under the specific condition of penetrating 5-layer C40 concrete targets. This work not only transformed the theoretical qualitative correlations proposed by previous scholars into quantifiable parameter influence laws, but more precise data support was also provided for understanding and predicting the signal overlapping behavior under complex penetration conditions. This was achieved through simulations of multi-variable combinations.

A unified understanding has gradually been reached that the adhesion and aliasing of overload signals can be attributed to the combined effects of multiple factors, including projectile-target interactions, structural dynamics, and measurement limitations. Specifically, the pulse response duration is prolonged by the slow attenuation characteristics of the projectile's elastic vibrations. Waveform distortion is caused by the superposition of multiple stress wave reflections within the projectile and the mutual interference between incident and reflected stress waves. Additional interference is introduced by the sustained impact of penetration-induced fragments on the projectile body within interlayer spaces. The time-domain response of a single impact event is further broadened by the global vibration and spallation effects. Furthermore, the original impact signal is subjected to distortion by measurement system factors, such as the limited frequency response of the sensor and resonance induced by the mounting structure. As a consequence of the synergistic action of the aforementioned mechanisms, the originally discrete overload signals corresponding to individual layers are deprived of clear temporal demarcation, resulting in adhesion and aliasing phenomena that are not readily amenable to direct analytical interpretation.

The mechanism of deceleration signal overlapping and aliasing is essentially a dynamic process. In this process, multi-physical field stress pulses generated during penetration superimpose and interfere with each other in both time and space. During the penetration of multi-layer targets, the instantaneous stress wave excited by the projectile body impacting a single-layer target is transmitted along the projectile body. This transmission induces sustained elastic vibration of its overall structure, forming the high-frequency components in the deceleration signal. When the projectile body passes through a layer and enters the inter-layer gap, the vibration of the projectile body and the impact response from high-speed fragments, both initiated by the previous impact, do not dissipate immediately. Consequently, a continuous noise response is formed in the sensor signal. As the projectile body impacts the next layer and generates a new stress wave, this signal superimposes with the still-unattenuated existing vibration wave and the interaction response from the inter-layer medium. These signals become intertwined in the time domain and coupled in the frequency domain. Ultimately, the signal collected by the acceleration sensor presents as a continuous, complex waveform that is characterized by blurred boundaries and connected pulses.

Moreover, to address the lack of quantitative evaluation criteria for the degree of interference superposition in acceleration signals of penetration fuze, two sets of indicators were proposed [22]: the layer coefficient and the inter-layer coefficient. The layer coefficient reflects the oscillation degree of the signal within each layer. The inter-layer coefficient reflects the distinguishability between signals of adjacent layers. These indicators are used to quantitatively measure the interference degree on target characteristics of acceleration signals during multi-layer penetration. A larger value for either indicator indicates more severe interference superposition. This study provides an objective quantitative basis for the layer-counting control algorithm of HTPF.

Scholars have developed a research trajectory regarding the issue of overlapping and aliasing in deceleration signals, progressing from phenomenological understanding, causal analysis, and mechanistic explanation to parametric control. The vibration of the projectile body and the reflection and superposition of stress waves within it are identified as the primary causes of overlapping and aliasing in deceleration signals. Recent studies have placed greater emphasis on revealing the influence patterns of specific structural parameters on signal quality through multi-parameter simulations and experiments. This shift demonstrates an evolution in research thinking from mechanistic explanation toward active control. Some studies have demonstrated the feasibility of suppressing signal overlapping at its structural-dynamic source by controlling key design variables such as thread parameters and preload force. This body of research not only systematically elucidates the mechanisms and multi-factor coupled causes of deceleration signal overlapping and aliasing, but also provides a foundation for suppressing signal overlapping at the source through structural optimization.

4.3 Signal processing and feature extraction

For HTPFs, detection and identification are two closely related but different technical issues. Detection mainly refers to the acquisition of penetration-related physical signals, such as acceleration, vibration, pressure, magnetic, acoustic, and timing signals. Identification further extracts target-related information from these signals, including medium type, layer number, void or interface characteristics, penetration state, and structural discontinuities. Therefore, the review of penetration fuze technology should not be limited to sensing or detection methods alone, but should also include the identification of complex media and complex structures.

The identification of complex media and structures is particularly important for HTPFs. In practical penetration processes, the target may contain multi-layer concrete [342], reinforced concrete [343], soil [247], rock [344, 345], steel plates [346], and cavities [347]. The penetration response is highly transient, nonlinear, and strongly coupled with the projectile-target interaction. As a result, the measured signals often contain impact peaks, high-frequency oscillations, structural vibration components, and overlapping features between adjacent layers. This is especially severe during high-speed penetration by projectiles with high length-to-diameter ratios, where signal overlapping and aliasing phenomena are prominent. These issues make initiation control for HTPF particularly challenging. In response, researchers both domestically and internationally have developed various signal filtering and feature extraction methods, as shown in Table 10. These methods aim to extract effective layer-penetration information from aliased signals.

Table 10

Comparison of signal-processing methods for HTPF signals [187, 247, 342, 343, 345, 346, 348 – 360].

Method category	Typical methods	Noise resistance	Signal aliasing suppression	Real-time performance	Computational resource consumption	Interpretability	Small-sample applicability	Applicability to penetration fuze signals
Linear filtering	Low-pass filtering, band-pass filtering, adaptive filtering	Effective for known-frequency noise	Useful features and noise may overlap in frequency band	Excellent; suitable for embedded real-time processing	Low	High; filter parameters have clear physical meaning	Good; does not require training data	Suitable for preliminary denoising and signal conditioning, but insufficient for complex feature separation
Time-frequency analysis	STFT, wavelet transform, Wigner-Ville distribution	Depends on window, basis, or kernel selection	Can reveal transient energy changes and layer-transition features	Medium; some methods can be simplified for online use	Medium to high	Medium; time-frequency features can be physically interpreted	Good to medium; mainly feature-based and does not necessarily require large datasets	Suitable for non-stationary penetration-signal analysis and transient feature extraction
Modal decomposition	EMD, EEMD, CEEMDAN, VMD	Can separate modal components and suppress noise	Useful for separating vibration, trend, and high-frequency components	Medium to poor; depends on decomposition complexity	Medium to high	Modal components may correspond to physical components	Good to medium; does not require large training datasets but parameter tuning may be needed	Suitable for nonlinear and non-stationary signals, but endpoint effects, mode mixing, and computational cost should be considered
Machine learning with handcrafted features	SVM, decision tree, random forest, shallow neural network	Depends on feature quality	Relies on manually designed features	Lightweight models can be deployed online	Low to medium	Medium to high; especially for tree-based or feature-based models	Medium; more suitable than deep learning for limited samples	Suitable for recognition tasks when reliable physical features are available
Deep learning	CNN, LSTM, TCN, Transformer-based models	High under representative training data	Can learn nonlinear and high-dimensional features	Limited; inference latency and model size must be evaluated	Depends on model structure and hardware	Low to medium; black-box characteristics are obvious	Poor to medium; usually requires large and representative datasets	Suitable for complex recognition and multi-source fusion, but real-time deployment, and interpretability are major limitations

Hybrid method	Filtering + time-frequency analysis + lightweight learning model	Combines denoising and feature learning	Complementary processing improves robustness	Medium; depends on model simplification	Medium	Medium; physical features improve explainability	Medium; can reduce data requirement through prior features	Recommended for engineering applications; balances accuracy, real-time performance, and interpretability

Different signal-processing methods show different adaptability to penetration fuze signals. Penetration signals are usually transient, nonlinear, non-stationary, and strongly coupled with projectile-target interaction, structural vibration, sensor noise, and shock-induced interference [18]. Therefore, the selection of signal-processing methods should consider not only denoising accuracy, but also signal aliasing suppression, real-time performance, computational resource consumption, interpretability, and applicability under small-sample conditions.

Overall, traditional filtering methods are more suitable for real-time preliminary denoising; time-frequency analysis and modal decomposition are more suitable for feature extraction and mechanism interpretation [361]; deep learning methods are more suitable for complex nonlinear recognition when sufficient data and computing resources are available [187]. For engineering applications of penetration fuzes, a practical solution is to combine lightweight preprocessing, physically interpretable feature extraction, and compact learning models, so as to balance recognition accuracy, real-time performance, resource consumption, and reliability.

It should be emphasized that deep learning methods have obvious real-time deployment limitations in penetration fuzes. Penetration fuze signal processing must be completed within a very short time window under high-g impact and strong vibration conditions. Deep neural networks usually require large memory, floating-point computation, and relatively long inference time, especially for recurrent networks and transformer-based models [348, 349]. Moreover, HTPFs are constrained by limited power supply, small volume, restricted processor capability, and strict reliability requirements. Therefore, before deep learning methods are applied to onboard systems, their inference latency, memory footprint, power consumption, robustness, and fail-safe behavior must be verified. A more feasible approach is to use offline training and online lightweight inference, combined with model pruning, quantization, compact network design, and physically interpretable preprocessing features.

4.3.1 Linear filtering and transform method

(1) Low-pass filtering methods

The low-pass filtering approach represents one of the earliest and most straightforward methods. It is based on the separability in the frequency domain between low-frequency penetration signals and high-frequency vibration signals. By setting a cutoff frequency, high-frequency vibration components are attenuated, while low-frequency rigid-body deceleration is preserved. The frequency response of the low-pass filter is calculated to determine the attenuation characteristics of the deceleration at different frequencies. Figs. 23(a) and 23(b) illustrate the experimental deceleration curves and the low-pass filtered deceleration curves at the fuze position during the penetration of 7-layer C40 concrete targets by a 500 kg warhead at a velocity of 850 m/s. Similarly, Figs. 23(c) and 23(d) present the deceleration curves and filtered results for a 500 kg warhead penetrating a 6 m C40 concrete target at 750 m/s. It can be observed that the deceleration curves processed by the low-pass filtering algorithm exhibit distinct penetration characteristics.

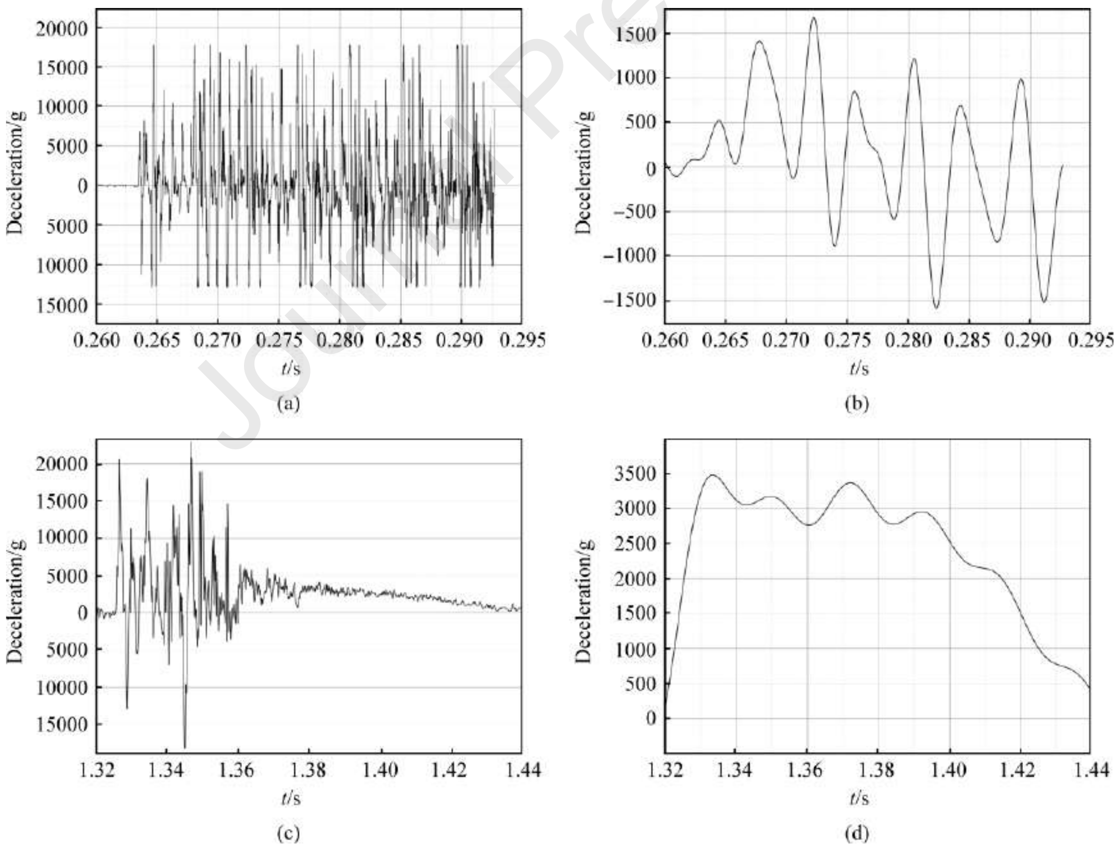

Fig. 23. Measured and low-pass filtered deceleration curves for hard-target penetration: (a) Measured deceleration curve for penetration of 7-layer C40 concrete targets; (b) Low-pass filtered deceleration curve for penetration of 7-layer C40 concrete targets; (c) Measured deceleration curve for penetration of a 6 m C40 concrete target; (d) Low-pass filtered deceleration curve for penetration

of a 6 m C40 concrete target (Adapted from [6]).

The low-pass filtering method is suitable for projectiles with short bodies and low impact velocities, where the shock and vibration frequencies differ significantly. To optimize the low-pass filtering approach, a low-pass filtering method based on pseudo-autocorrelation was proposed [362]. Local mean decomposition and a matched correlation algorithm to enhance the extraction of penetration layer features were introduced [363, 364]. The optimal transmission characteristics of the matched filter were also provided. When the projectile length exceeds 1.5 m, the vibration frequency of the projectile body can drop to approximately 1.7 kHz was pointed out [286, 365], which is comparable to the shock frequency. In such cases, low-pass filtering becomes ineffective for signal separation.

To enhance the adaptability of low-pass filtering methods under complex working conditions, the edge detection concept from digital image processing was introduced into signal preprocessing [366]. They proposed a layer-counting signal processing method based on box-difference filtering to address the interlayer overlapping problem during high-speed penetration. Subsequently, a filter passband algorithm based on numerical integration was presented and a low-pass analog filter was designed that meets real-time requirements [367, 368]. This algorithm enables accurate calculation of the cutoff frequency, resulting in clear layered features in the filtered signal. Combined with backend threshold and time-window judgment, it effectively supports the recognition of penetration-through-target signals.

(2) Wavelet transform method

Wavelet transform is extensively utilized for the processing of non-stationary penetration deceleration signals owing to its superior time-frequency localization characteristics. The associated application methodologies have been continuously refined and evolved in alignment with the progression of specialized research.

Building upon early explorations, a signal preprocessing method combining lifting wavelet with median filtering was proposed [363]. This approach effectively enhanced the signal-to-noise ratio and laid a solid foundation for subsequent feature extraction. Subsequently, researchers began to focus on the selection of core parameters in wavelet analysis. Two quantitative evaluation criteria were introduced [296]. The reconstruction capability of a wavelet basis was measured by the root mean square error between the reconstructed signal and the original signal. Its ability to extract key penetration-layer motion features was assessed by the root mean square error of the velocity change. A systematic comparison was conducted on the performance of different wavelet bases in signal reconstruction and key penetration-layer feature extraction. This provided a theoretical basis for the optimal selection of wavelet bases.

In recent years, the application of wavelet analysis was deepened [369]. By applying wavelet analysis to the shock excitation signal, a mathematical model between the penetration shock vibration and the circuit noise response was successfully established. Furthermore, a new targeted noise processing method based on wavelet analysis was proposed. This further expanded the application depth and breadth of wavelet analysis in solving practical engineering problems of penetration fuze.

(3) Short-time Fourier transform

The Short-Time Fourier Transform (STFT) is a technique that processes a signal by dividing it into windows. In the time domain, a window function is used to select segments of the signal. The Fourier transform is then performed on the signal within each window. By repeatedly applying the Fourier transform to consecutive windows, a collection of transforms is obtained. STFT to process overload signals was applied [370], but the results obtained were unsatisfactory in terms of time and frequency resolution.

4.3.2 Adaptive mode decomposition methods

To overcome the limitations inherent in low-pass filtering and wavelet analysis when processing non-linear and non-stationary signals, adaptive decomposition methods based on intrinsic signal characteristics have been introduced to the field of penetration deceleration signal analysis. Consequently, the capabilities for noise suppression and feature extraction within this domain have been continuously enhanced.

A signal reconstruction method for penetration deceleration based on singular value decomposition was proposed [371, 372]. A joint filtering scheme was constructed by combining Ensemble Empirical Mode Decomposition (EEMD) and wavelet transform (WT). This effectively improved the denoising performance of signals under strong noise backgrounds. On this basis, blind source separation technology was further introduced [373]. A blind source separation method for penetration deceleration signals with source number estimation capability was proposed. This method reduced the dependence on the number of sensors. It enhanced applicability in actual complex penetration environments. In recent years, variational mode decomposition (VMD) for signal feature extraction was adopted [374, 375]. Research has shown that, compared with Empirical Mode Decomposition (EMD), VMD performs better in terms of feature extraction effect, signal-to-noise ratio, and integration accuracy of the reconstructed signal. It can more accurately invert the penetration depth of the projectile body. This demonstrates good potential for engineering application.

4.3.3 Cohen class bilinear time-frequency distribution

By mapping one-dimensional time-domain signals onto a two-dimensional time-frequency plane, the distribution laws of signal energy over time are revealed through time-frequency analysis methods. This approach provides a novel perspective for the identification of layer-penetration timing during the penetration process, thereby facilitating a paradigm shift from traditional amplitude threshold comparison to time-frequency feature extraction.

In early exploration, a penetration layer-counting recognition method based on Choi-Williams distribution was proposed [376]. This method utilizes the excellent energy concentration characteristics of the Choi-Williams distribution in the time-frequency plane. Cross-term interference is effectively suppressed. By setting an energy threshold for comparison, effective recognition of penetration layers is achieved. It was experimentally demonstrated that the recognition performance of this method is superior to that of the traditional low-pass filtering method. However, its computational load may pose a challenge to the real-time performance of the system.

In recent years, research on performance comparison and optimization of different time-frequency analysis methods continue. A systematic comparison of the short-time Fourier transform, wavelet transform, and Wigner-Ville distribution in layer recognition was conducted [377]. The study found that the Wigner-Ville distribution demonstrated the highest recognition rate in this research. However, despite its superior performance, the computational complexity resulting from the high-dimensional information it generates remains a critical bottleneck restricting its widespread application in practical engineering. Further optimization is urgently needed to enhance its practicality. A feature extraction method based on an effective short-time energy spectrum was proposed [378]. In this method, oscillation interference is suppressed by calculating the effective value of acceleration. Combining windowing and framing reduces spectral leakage and ringing effects. The short-time energy spectrum and the maximum value envelope are utilized to effectively extract penetration-layer features. This approach shows good accuracy and adaptability in both simulations and experiments, providing a new pathway for the application of penetration fuze in high-speed multi-layer targets.

4.3.4 Deep learning-based data-driven methods

With the continuous integration of AI technology, deep learning models are gradually being introduced into the processing of penetration deceleration signals, opening up new approaches for real-time prediction and feature extraction [379, 380]. A PF-Informer model based on an improved Transformer architecture and proposed a real-time penetration deceleration prediction method using deep neural networks was developed [381]. Time-frequency images of signals were extracted using the STFT was conducted. A Denoising Convolutional Neural Network (DnCNN) was employed [360] to learn the mapping from noisy time-frequency images to those containing only rigid-body overload, followed by an inverse transform back to the time domain. Based on 5-fold cross-validation, an average absolute error (MAE) of 0.968% and a Pearson correlation coefficient of 90.35% were achieved. The denoising capability of this method was found to be significantly superior to low-pass filtering, EEMD, and wavelet transform, with the average MAE reduced by 1.82%, 1.00%, and 0.75%, respectively. These models can efficiently predict future deceleration curves based on historical data. It assists the fuze in target recognition and projectile body attitude estimation, demonstrating good adaptability and application potential in complex penetration environments. This provides new intelligent insights for research in this field.

The technologies for signal processing and feature extraction in penetration fuze have undergone an evolutionary progression, advancing from traditional low-pass filtering to adaptive time-frequency analysis and modal decomposition, and further toward the deep integration of physical mechanisms with intelligent algorithms. Although various methodologies have demonstrated effectiveness under specific conditions, several common challenges persist: (a) The parameters and thresholds of most algorithms remain heavily dependent on specific operating conditions; consequently, their adaptability, real-time performance, and robustness necessitate further enhancement when subjected to diverse penetration conditions, target types, and warhead structures. (b) While noise is being filtered, the deceleration magnitudes may be inadvertently altered and signal delays may be introduced by signal processing techniques, thereby compromising the accuracy and real-time capability of layer-counting identification.

Future efforts should be directed toward developing adaptive signal processing frameworks with enhanced generalization, achieved through a deeper integration of physical models and data-driven approaches. Simultaneously, hardware-software co-design must be investigated to address the challenges of real-time massive data processing under high-speed penetration conditions. Such advancements are expected to drive the evolution of penetration fuze toward superior precision and intelligence.

4.4 Summary and assessment

Publicly reported studies indicate that acceleration signals remain one of the primary information sources for penetration state recognition and layer-counting tasks. However, during high-speed penetration into multi-layer hard-targets, the measured acceleration response is often affected by transient impact pulses, structural vibration, stress-wave propagation, and sensor-mounting dynamics. These factors may cause oscillation superposition, feature adhesion, and ambiguous peak structures, thereby increasing the risk of missed or false layer-counting. Therefore, acceleration-based recognition should not be regarded as a simple peak-detection problem, but rather as a transient, nonlinear, and nonstationary signal interpretation problem.

To improve the extraction of penetration-related features, time-frequency analysis has been increasingly introduced into the processing of penetration signals. Compared with conventional low-pass filtering, methods such as the short-time Fourier transform, wavelet transform, Choi-Williams distribution, and adaptive decomposition techniques can provide joint temporal and spectral descriptions of transient energy evolution. Such representations are useful for locating short-duration impact events, separating slowly varying rigid-body deceleration from higher-frequency structural vibration, and revealing changes in signal energy near material interfaces. Nevertheless, the advantages of time-frequency methods are conditional rather than universal. Their performance depends on window length, basis or kernel selection, mode-separation assumptions, noise level, and the degree of spectral overlap between physical components. Consequently, these methods should be evaluated not only by denoising quality but also by recognition robustness, computational resource consumption, and sensitivity to target and impact-condition variations.

Multi-source information fusion represents a further direction for improving recognition robustness in complex media and multi-layer structures. Acceleration signals are highly sensitive to impact and structural vibration, whereas magnetic, magnetoelectric, pressure, acoustic, vibration, and timing-related information may provide complementary observations of material discontinuities, structural interfaces, or penetration progression. By fusing heterogeneous sensing channels at the data, feature, or decision level, the HTPF can reduce dependence on a single signal mechanism and improve tolerance to signal distortion, missing features, and strong shock-induced interference. However, the effectiveness of fusion depends on the physical independence, synchronization accuracy, survivability, and calibration consistency of the sensing channels. Fusion methods should therefore be designed as physically constrained recognition frameworks.

A critical assessment of recent signal-processing methods reveals a trade-off between recognition performance and engineering practicability. Advanced decomposition and learning-based denoising methods, such as variational mode decomposition and deep convolutional denoisers, can show strong performance in offline signal enhancement or feature extraction. However, their direct use in embedded penetration sensing is constrained by parameter dependence, training-data requirements, memory footprint, inference latency, and verification difficulty under high-g shock and vibration environments. In particular, methods validated on simulated or limited laboratory data may not generalize to variations in target material, layer thickness, impact velocity, obliquity, projectile structure, sensor location, and signal transmission path. Thus, algorithmic accuracy alone is insufficient for field-oriented evaluation; real-time reliability, interpretability, resource consumption, and hardware survivability must be considered simultaneously.

Future research should therefore move from isolated algorithm optimization toward hardware-software co-design and standardized validation. At the sensing front end, protective packaging, and physically informed filtering can improve signal fidelity before digital processing. At the algorithmic level, robust feature extraction, lightweight interpretable classifiers, uncertainty estimation, and multi-sensor fusion should be prioritized over overly complex post-processing models that are difficult to verify in embedded systems. At the validation level, progress requires standardized and security-compliant benchmark datasets, numerical simulation, ground testing, and hardware-in-the-loop evaluation. Such a framework would enable reproducible comparison of recognition methods while accounting for the severe environmental, computational, and data-scarcity constraints inherent to penetration sensing.

5 Precision initiation control methods

Precision initiation control of penetration weapons is a pivotal component for achieving the high-efficiency destruction of hard targets [382]. A representative operational workflow for HTPF initiation control is illustrated in Fig. 24. Its performance directly dictates the matching accuracy between the initiation point and the vulnerable internal structures of the target. Detonation control algorithms and strategies are fundamental to the precision initiation of HTPFs [383]. Currently, HTPF initiation control methodologies are primarily classified into the following five types: fixed-delay initiation, depth-integration initiation, layer-counting initiation, void-sensing initiation, and multi-feature logic initiation. And their comparison is shown in Table 11. In recent years, research efforts in this field have been predominantly focused on layer-counting and void-sensing technologies, whereas comparatively less attention has been devoted to fixed-delay and depth-integration methods. This section systematically reviews the research progress of HTPF initiation control, focusing primarily on layer-counting and void-sensing methodologies, while delineating the trajectory of their technical evolution.

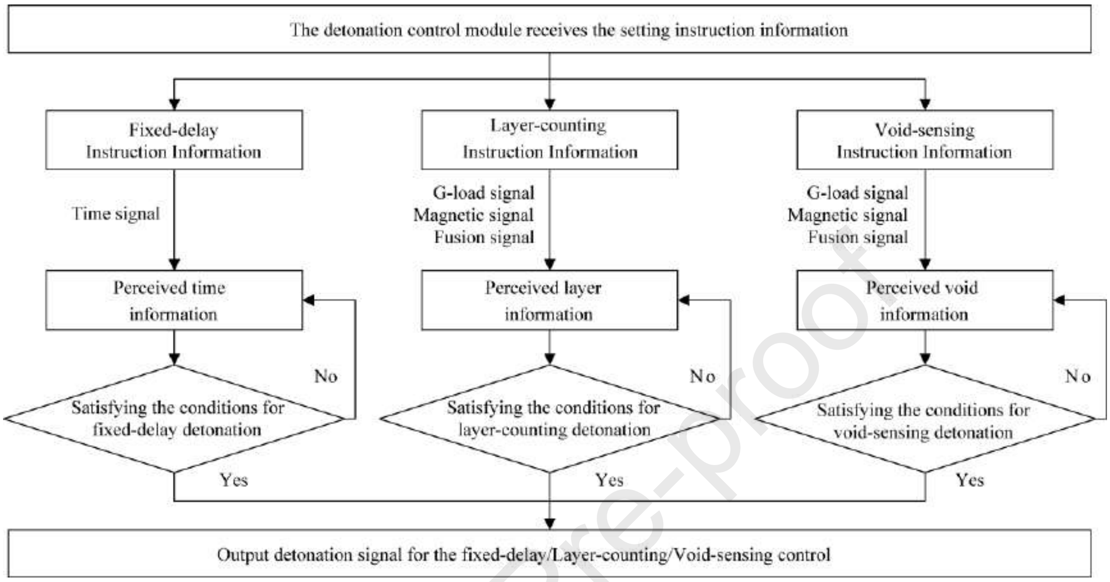

Fig. 24. Workflow of typical initiation control methods (Adapted from [6]).

Table 11

Multi-dimensional comparison of precise initiation control methods [2, 6, 187, 384–389].

Methods	Principles	Advantages	Limitations	Technical Approaches	Applicable Scenarios
Fixed-delay initiation control	Trigger the timer upon impact, and detonate upon reaching the preset duration.	① Simple in design ② Low-cost ③ High resistance to load	① Unable to gauge actual penetration depth ② Highly susceptible to target material properties	① Chemical delay ② Mechanical delay ③ Digital oscillator delay	Single-material targets, Shallow targets, etc.
Depth-integration initiation control	Measure deceleration in real time, dynamically calculating depth through secondary integration.	Detonation at a relatively accurate penetration depth	Integral drift	① Mechanical double integration ② Integration in analogue circuits ③ MEMS + MCU/DSP	Homogeneous-deep targets, HDBTs, etc.
Layer-counting initiation control	Identify peaks and troughs in the deceleration curve and calculate the number of layers.	Detonation at the specific layer	Poor adaptability to non-standard structures such as sandwich panels	① Simulated hardware threshold comparison ② Digital morphological analysis	Command centers, Multi-layer buildings, etc.
Void-sensing initiation control	Detect abrupt step-like reductions in deceleration and detonate within this low-resistance zone.	Detonation at a cavity for max damage effectiveness	Susceptible to internal cracks, pockets of soft soil or small voids	① Single-axis acceleration drop detection ② Multi-axis vibration energy drop detection	Warehouses, Command centers, Hangars, etc.

Multi-feature logic initiation control	Integrating multiple features including time, depth, and cavities, using complex logical algorithms for assessment.	Exceptional resistance to interference and adaptability to the environment	① Complex algorithm ② The computational load is very high.	① Multi-source heterogeneous sensor fusion ② Edge AI and machine learning inference	High-value targets, etc.

It should be noted many reported layer-counting and void-sensing methods are verified mainly through numerical simulations, reconstructed penetration signals, Hardware-in-the-loop (HIL) tests, or laboratory multi-impact experiments. These approaches are useful for algorithm design and repeatable comparison, but they cannot fully reproduce the coupled effects of projectile-target interaction, structural deformation, sensor saturation, shock-induced circuit failure, temperature variation, electromagnetic interference, and stochastic impact conditions.

5.1 Layer-counting initiation control methods

In the layer-counting initiation control method, the deceleration characteristics and time history during the impact, penetration, and perforation of a target by a penetration warhead are sensed in real-time by the HTPF. Through this process, the entry into and exit from layers are identified, and the cumulative number of penetrated layers is recorded. Subsequently, an initiation signal is issued at a designated layer. The workflow of the layer-counting initiation control method is illustrated in Fig. 25. The primary advantage of this method lies in its capability to enable the warhead to penetrate deep into multi-story structures and detonate at a predetermined layer, thereby achieving high-efficiency lethality against targets at specific locations. This initiation control method is particularly suitable for engaging targets such as ground-based buildings and multi-story command centers. A schematic representation of a projectile penetrating multi-layer targets is shown in Fig. 26(a).

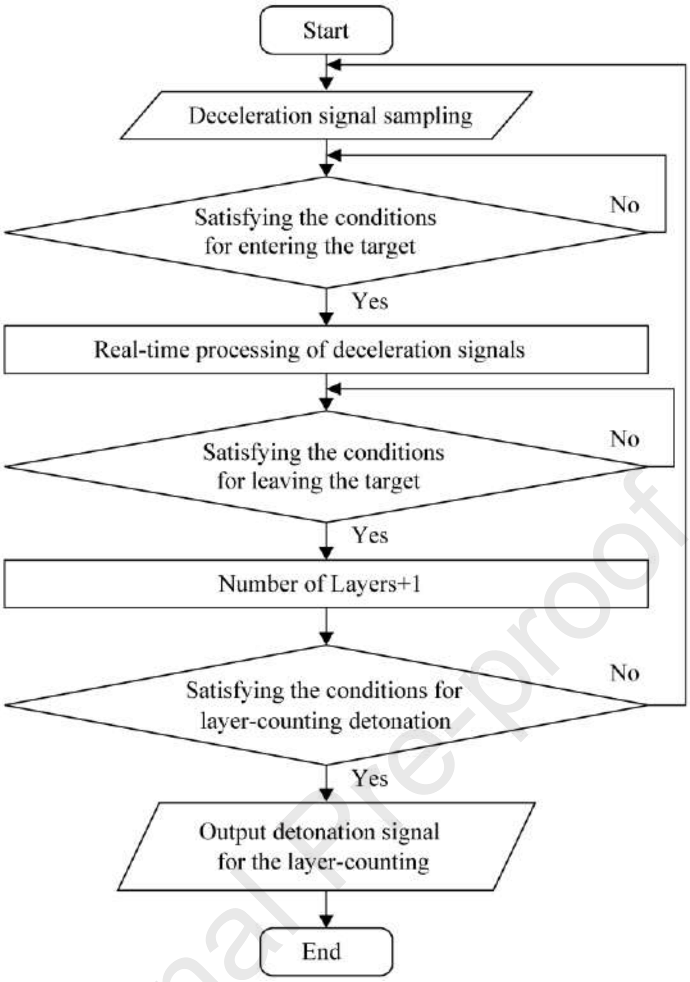

Fig. 25. Workflow of layer-counting initiation based on time information (Adapted from [6, 333]).

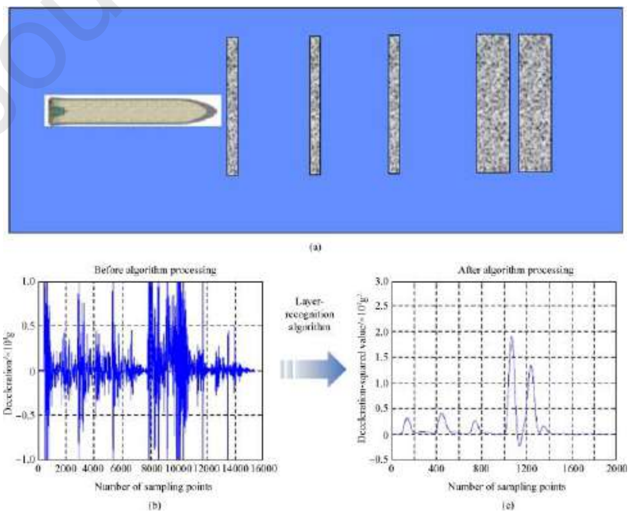

Fig. 26. Layer-counting initiation control method: (a) Schematic diagram of projectile penetrating multi-layer targets [390]; (b) Comparison of data before and after processing by layer-recognition algorithm [382].

The layer-counting initiation control method is a core technology based on real-time signal processing during the penetration process. Its primary mechanism lies in the dynamic identification and accumulation of the number of layers penetrated by the projectile. The penetration deceleration data, before and after real-time processing by the layer identification algorithm, is presented in Fig. 26(b). Traditionally, a fixed-threshold determination method is employed for each layer, where thresholds are preset according to specific experimental targets to ensure reliable fuze initiation across various operating conditions. However, in practical applications, significant variations in target types and penetration velocities result in substantial differences in acceleration signal characteristics, thereby limiting the adaptability of the fixed-threshold approach. Layer-counting initiation control methods have gradually evolved from single time-domain feature analysis toward multi-dimensional sensing modalities, such as magnetic detection and multi-domain information fusion. This section provides a systematic review of the technical advancements subsequent to the fixed-threshold method.

5.1.1 Layer-counting based on time-domain information

Time-domain information specifically refers to the correlation between deceleration and time, which constitutes the primary basis for this category of layer-counting methods in this section. Relevant research has been primarily conducted from two perspectives: first, layer-counting methods utilizing time information as characteristic parameters were derived based on the fixed threshold method; subsequently, methods employing deceleration information as characteristic parameters were further developed. A comprehensive review of layer-counting methods based on time-domain information is presented from the two aforementioned aspects.

To address the issues of peak dependency, poor robustness, and high false detection rates in wave peak detection using the fixed-threshold method, a full-temporal relative wave peak detection method was proposed [391]. In this approach, time-domain information such as the polarity of differences before and after peaks, pulse width, and peak intervals is employed for layer-counting. Pulse width and peak-to-peak intervals serve as the core basis for layer-counting, while amplitude is only used to handle baseline jitter and minor oscillations. Consequently, the robustness problem caused by threshold uncertainty is resolved. Subsequently, a layer-counting method based on dynamic time shielding was introduced [392]. The decay of projectile velocity after penetrating each layer is considered, and the shielding duration is dynamically adjusted. This associates the shielding time with velocity decay, thereby avoiding the drawbacks of traditional fixed time windows. Such fixed windows lead to miscounting if too short and missing counts if too long. The deviation between simulation and experimental results is less than 5%.

A detection algorithm was also proposed by Sandy J Risha [156]. Multi-layer acceleration thresholds are employed to distinguish the number of layers and cavity locations. Whether the projectile has penetrated multi-layer targets or reached the predetermined initiation position is identified. This recognition is based on analyzing deceleration switch signals from multiple thresholds. In addition, a detection algorithm was proposed [156] that utilises multi-layer acceleration thresholds to determine the number of targets and the position of the cavity; by analysing the overload switch signals at multiple thresholds, the algorithm identifies whether the projectile has penetrated multiple layers of medium or reached the predetermined initiation position.

The aforementioned studies focus on layer-counting methods developed from the fixed-threshold method. Time-domain information is used as the core basis in these methods. Meanwhile, layer-counting methods primarily relying on deceleration information as the key reference have also been investigated by researchers.

To address the poor robustness of the fixed-threshold method and the high error rate in layer-counting, a dynamic threshold layer-counting method based on envelope prediction was proposed [393]. Its principle is shown in Fig. 27(a). The exponential decay characteristic of the penetration deceleration signal is utilized. In this method, the signal envelope is fitted and a relative threshold is applied. Consequently, the layer-counting threshold is dynamically adjusted. The problem of miscounting layers is effectively resolved. This problem occurs when the signal has not fully decayed in traditional fixed-threshold and time-window methods. The simulation results are presented in Fig. 27(b). However, the determination of the first layer still requires a fixed threshold to be manually input in this method. Based on this foundation, an adaptive-threshold layer target recognition algorithm was introduced [394]. Its operational principle is illustrated in Fig. 28(a). The dynamic threshold for identifying the next layer is calculated in real time using measured sensor signals, eliminating the need for prior data. Adaptation to varying targets, velocities, and other conditions is thus achieved. HIL simulation verifies that accurate layer-counting is achieved under four different test conditions. The identified layer positions show high consistency with high-speed camera recordings. Partial simulation results are presented in Fig. 28(b). This method can be integrated with other signal processing algorithms, such as low-pass filtering and wavelet decomposition. Consequently, the applicable scenarios of the layer-counting algorithm are further expanded. A universal and adaptive layer-counting solution is provided for the HTPF. In addition, an accurate layer recognition method based on data augmentation and fully connected neural networks was proposed [395]. Simulations and experiments demonstrate that this method does not rely on prior parameters and exhibits good robustness for complex adhesive signals. Accurate layer recognition can also be achieved under different working conditions, such as various targets and warheads, with a recognition error of less than 1.6%. Meanwhile, real-time requirements are met, with a single prediction taking approximately 2.1 ms. By introducing data augmentation and neural networks into the field of layer recognition for penetration fuze, this research enables the neural network to autonomously learn the characteristics of penetration signals. Manual parameter setting—such as thresholds and pulse widths—is no longer needed, thereby completely eliminating dependence on working conditions. The issue of small-sample training is also addressed. As a result, the generalization capability of the layer-counting method is enhanced.

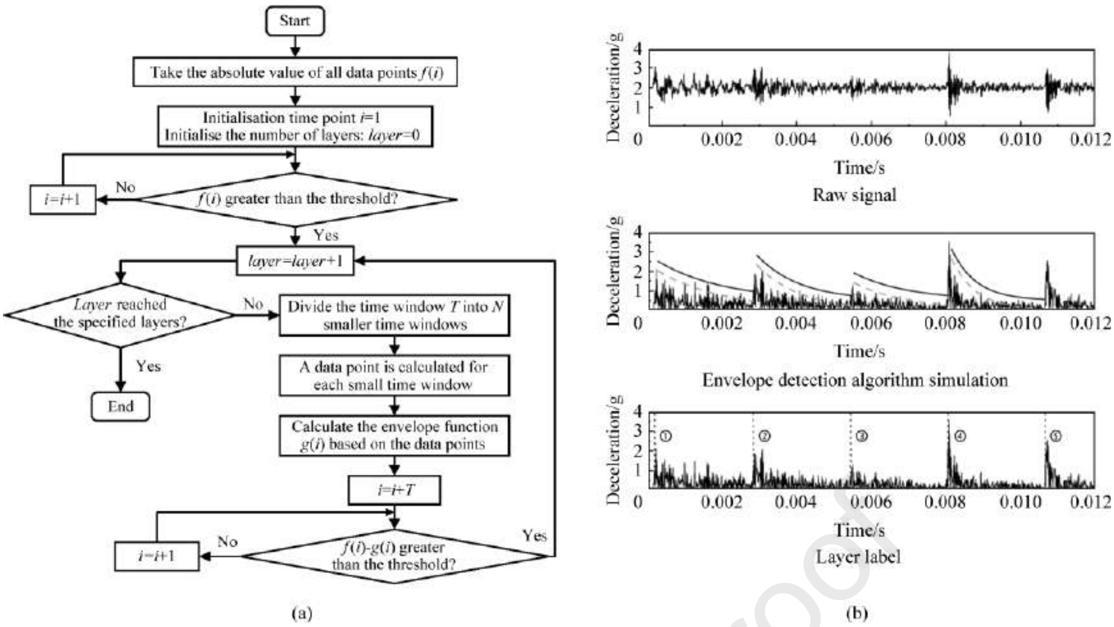

Fig. 27. Dynamic threshold layer-counting method based on envelope prediction: (a) Principle block diagram of the dynamic-threshold algorithm; (b) Simulation results of the dynamic-threshold algorithm [393].

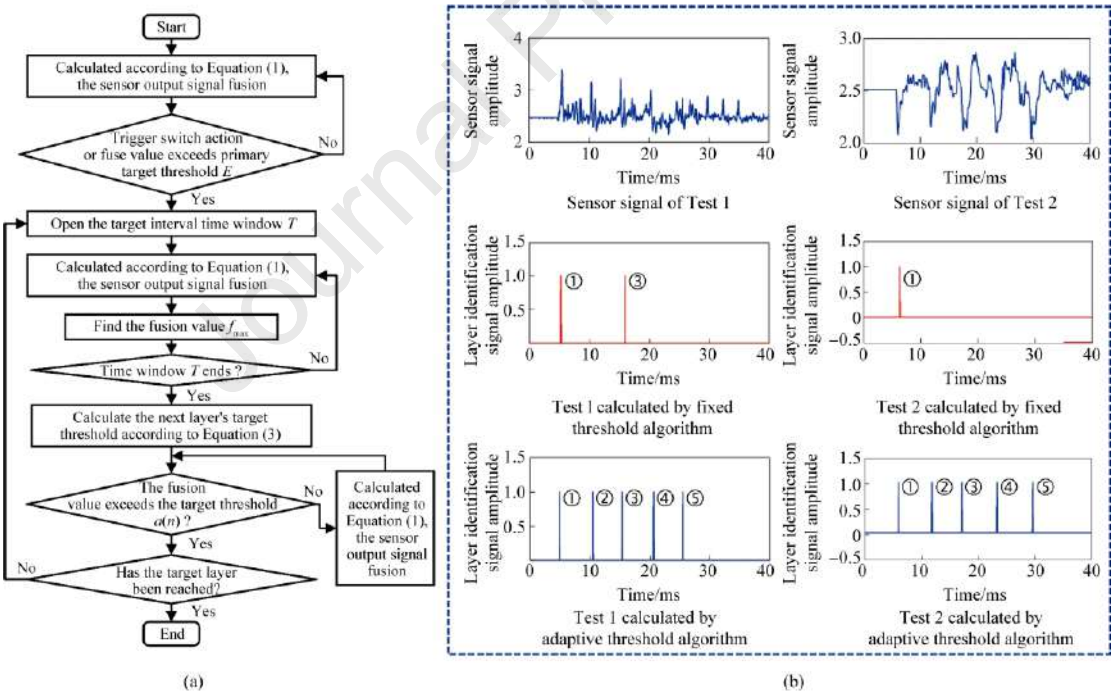

Fig. 28. Self-adaptive threshold layer-recognition algorithm: (a) Principle block diagram of the self-adaptive threshold algorithm; (b) HIL simulation results [394].

It should be noted that the dynamic-threshold method is adaptive in the sense that the detection threshold is updated according to the measured penetration signal envelope. However, it does not constitute a closed-loop control system. No feedback from the achieved damage effect, actual burst location, or post-penetration telemetry is used to correct the initiation decision during the same penetration event.

5.1.2 Layer-counting based on magnetic detection information

Layer-counting methods based on magnetic detection information primarily utilize magnetic principles to achieve layer-penetration identification [396]. Currently, two main technical approaches are employed: active magnetic detection and passive magnetic detection. Active magnetic detection relies on an internal magnetic excitation source within the penetration fuze and is classified as active magnetic sensitive detection. In contrast, passive magnetic detection is based on the recognition of geomagnetic field disturbances and is classified as passive Magnetic Anomaly Detection (MAD). In this section, layer-counting methods based on magnetic detection information are reviewed from these two perspectives.

A novel magnetic-sensitive layer-counting technique was proposed [397]. In this method, a magnet and a magnetic sensor are installed inside the penetration fuze. The variation in magnetic field intensity within the fuze is utilized during the penetration of reinforced concrete targets. This enables layer-counting to be achieved. Simulation and experimental results show that the method is unaffected by velocity or vibration. Accurate layer-counting is allowed for large aspect-ratio warheads during high-speed penetration of multi-layer reinforced concrete targets. Thus, magnetic detection technology is introduced into the layer-counting field of penetration fuze. Dependence on deceleration signals is eliminated. Interference from vibration is also avoided. However, the reliability of the magnetic-sensitive layer-counting method can be further improved. Optimization of the magnet's dimensions, shape, and arrangement inside the fuze can be conducted. Based on this foundation, to address the issues of large volume, poor installation consistency, and susceptibility to stress wave interference associated with dual magnetic blocks, an active magnetic detection method using a single magnetic block to generate a magnetic field was proposed [398, 399] for penetration process recognition. The optimal distance between the magnetic block and the magnetic sensor was determined as 155 mm through COMSOL simulation. This balances signal strength and stability. The magnetic response characteristics were systematically studied under different conditions. These included projectile penetration into a three-layer target, a 1 m target, and oblique penetration. It was found that oblique penetration causes a signal lag. However, it does not affect the recognition of penetration features. Thus, the applicability of the method to different working conditions was verified. The main reason for the signal lag is attributed to the longer actual penetration path through the target compared to vertical penetration. This occurs when the projectile engages the target with an angle of attack [400]. Additionally, changes in the relative position between the sensor and the reinforcing mesh lead to a delay in the action time. Important optimizations in structural design and signal stability were achieved in this study. As a result, the engineering applicability and anti-interference capability of the active magnetic detection method were enhanced. A further systematic analysis of the magnetic response characteristics during projectile penetration under complex conditions was conducted [401]. Ferromagnetic interference and beam-structured targets were included. A triaxial magnetic signal fusion processing algorithm is proposed to enhance recognition robustness. Measured triaxial magnetic signals are acquired by constructing a three-layer reinforced mesh free-fall experimental platform. The reliability and engineering feasibility of active magnetic detection in complex environments were verified. As a result, the active magnetic detection method was extended from ideal conditions to simulated real scenarios.

The active magnetic detection layer-counting method relies on internal magnetic excitation and is classified as a form of active magnetic sensitivity detection. The relationship between magnetic induction and distance during the active magnetic detection process is illustrated in Fig. 29(a), where an upward peak is observed. This method requires the pre-installation of permanent magnets, which increases the complexity of structural and anti-deceleration designs. Concurrently, research has been conducted by various scholars on passive MAD layer-counting methods based on geomagnetic field disturbances. The variation in magnetic field intensity throughout the penetration process is depicted in Fig. 29(b), characterized by a downward peak. At the same time, the correspondence between magnetic signals and deceleration signals during the penetration process is shown in Fig. 29(c).

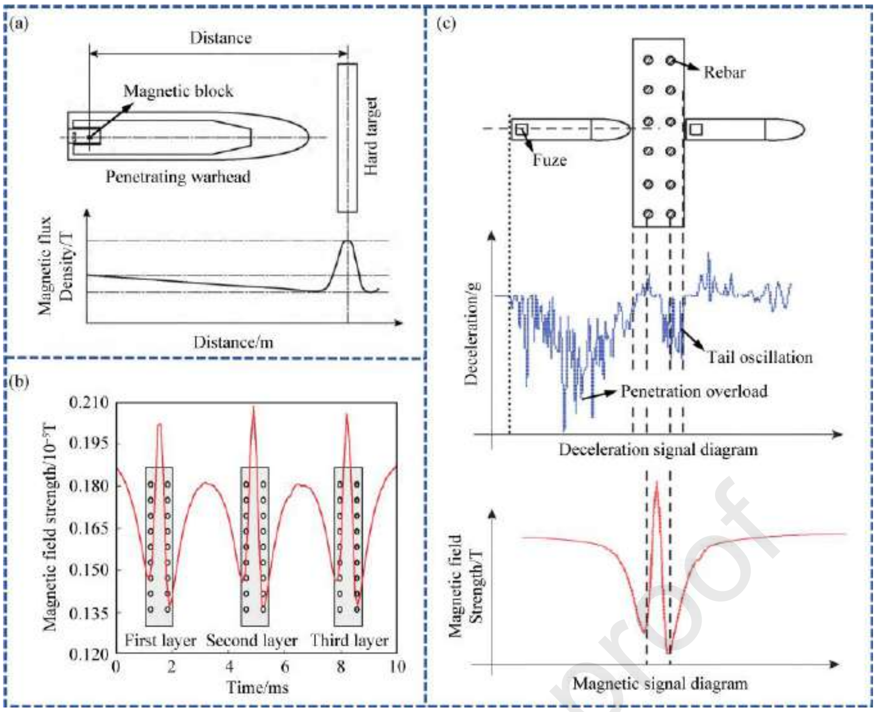

Fig. 29. Layer-counting method based on magnetic detection information: (a) Variation of magnetic flux density with the distance between the projectile and the target (active magnetic detection); (b) Variation of magnetic field strength with the penetration process (passive magnetic detection); (c) Correspondence between magnetic signals and deceleration signals during the penetration process [343, 397].

A novel layer-counting method based on geomagnetic anomaly signal detection was proposed [390] to address the inaccurate layer-counting caused by acceleration signal overlapping and aliasing during the penetration of multi-layer reinforced concrete targets. The influence of the additional magnetic field on the detection signals of projectile-borne magnetic sensors was analyzed through simulation. A layer-counting strategy based on pulse features such as amplitude and gradient variation was also proposed. In this research, MAD technology was introduced into the field of HTPF layer-counting. A theoretical foundation and simulation methodology were provided for subsequent studies. However, experimental validation has not been conducted.

Subsequently, more comprehensive simulations were conducted [187, 343] to analyze the influence of factors such as oblique penetration, reinforcement density, and penetrator material on magnetic signals. It was indicated that a lower magnetic permeability of the penetrator and a higher density of reinforcement lead to more distinct magnetic signals. Furthermore, a theoretical cylindrical coordinate model for the magnetic shielding of the penetrator was established. The Shielding Effectiveness was quantified through simulation, yielding a value of approximately 18.82. Drag experiments verified that the magnetic signals vary significantly as the penetrator passes through different layers. Based on these findings, a composite layer-counting strategy incorporating time windows was proposed. This study promoted the development of layer-counting technology for penetration fuze based on MAD from theoretical research toward engineering application.

Currently, magnetic detection-based layer-counting methods remain at the laboratory proof-of-concept stage. To facilitate the transition toward practical engineering applications, the following core challenges must be overcome: Sensor reliability and signal stability must be ensured within high-deceleration environments; Robust detection and amplification techniques must be developed for extremely weak signals at the nano-Tesla (nT) level; Comprehensive validation must be conducted under conditions that more closely approximate actual operational environments, such as high-velocity gas gun experiments.

5.1.3 Layer-counting based on multi-domain fusion information

For the issue where single-sensor signals are prone to stress wave oscillations or ferromagnetic interference, leading to inaccurate layer-counting, as well as poor adaptability to unknown targets and complex working conditions, a layer-counting algorithm was proposed [290]. based on the fusion of acceleration sensor signals and MEMS switch signals. In this method, the two types of signals are separately convolved and weighted with different window functions in the time domain. A composite signal is then formed to determine the penetration characteristics of the projectile through layers. The feasibility of the method was verified through simulation.

This algorithm can be applied when the projectile velocity is relatively high, or when the spacing between multi-layer targets is relatively small, resulting in some overlapping in the sensitive signals. However, the weighting coefficients α and β, as well as the entry threshold and exit threshold used in this method, must be determined according to specific projectile shapes and penetration conditions. For a fixed projectile shape and determined penetration conditions, these values are obtained based on extensive prior data. When the projectile shape or penetration conditions change, the numerical values of the entry threshold and exit threshold will also change accordingly. They then need to be re-determined based on a large amount of prior data under the corresponding conditions.

The above studies remain reliant on prior data and lack adaptability to diverse targets. To address this, a layer-counting method for hypersonic penetration fuze was proposed as shown in Fig. 30(a) [402]. This method integrates deceleration information and induced electric-field information. The electromagnetic effect of a projectile with high permeability and high conductivity during hypersonic penetration is utilized. Induced electric-field information and deceleration information are employed as complementary sources. Nonlinear dimensionality reduction and fusion are achieved through Kernel Principal Component Analysis. Subsequently, composite information is constructed. Among them, the deceleration acceleration curve is shown in Fig. 30(b), and the multi-sensor composite signal curve is shown in Fig. 30(c). An adaptive layer-counting strategy is designed based on the first-order difference and the extreme-value difference of the fuzed information. This strategy can accurately determine the moments of target entry and target exit without preset thresholds. Simulation results demonstrate that the penetration time is accurately recognized by this method for a 600 kg large warhead penetrating four layers of targets at 1700 m/s. The recognition time error is maintained within 10%. The method can be applied to different penetration conditions and it compensates for the condition-dependence defect of traditional methods. It also significantly enhances the autonomous layer-counting capability of hypersonic penetration fuze in complex environments.

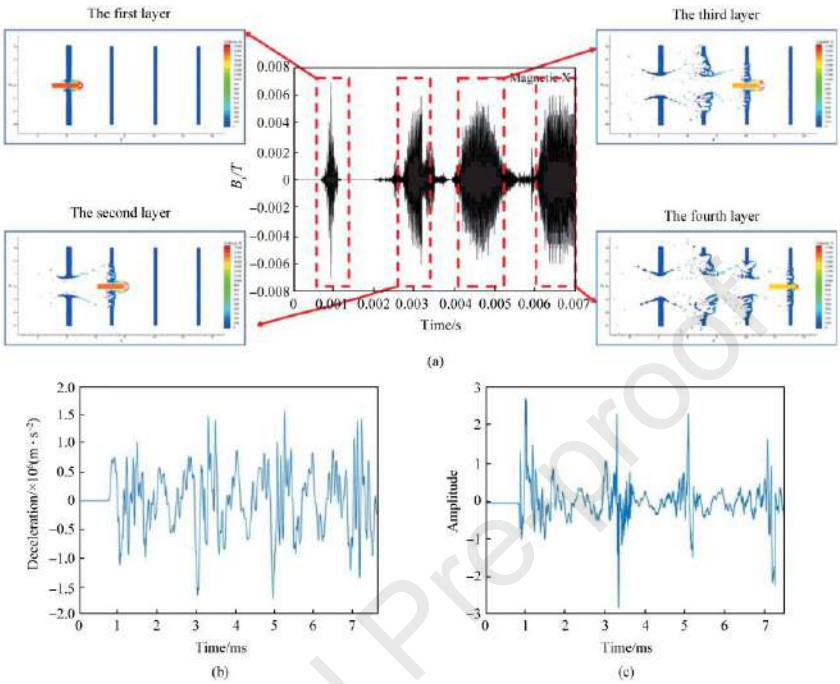

Fig. 30. A layer-counting method based on the fusion of deceleration information and induced electric field information: (a) The relationship between electromagnetic field signal characteristics and the penetration process [402]; (b) Deceleration acceleration curve; (c) Multi-sensor composite signal curve [356].

Additionally, a multi-domain information fusion layer-counting method based on TCN-LSTM was introduced [187], as shown in Fig. 31. In this method, deceleration information and triaxial magnetic anomaly information were fused, and the layer-recognition problem was transformed into a regression prediction problem for the distance between the penetration fuze and the target. Simulation results showed that the recognition error of the fusion method was reduced by 60% compared with the single-deceleration method and by 50% compared with the single-magnetic-information method. It should be noted, however, that this improvement was obtained under simulation conditions and has not been confirmed by publicly available full-scale live-fire tests. Moreover, the adaptability of the method to realistic reinforced-concrete targets with nonuniform rebar distribution, aggregates, cracks, voids, and large inter-layer spacing variations remains to be further validated. High computational demand also remains a challenge for projectile-borne processors.

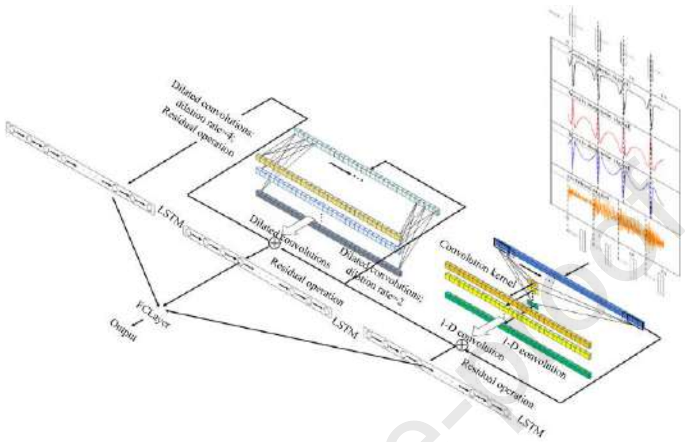

Fig. 31. A multi-domain information fusion layer-counting method based on the TCN-LSTM network architecture [187].

Although the TCN-LSTM-based multi-source fusion method demonstrates improved layer-counting accuracy at the algorithmic level, its onboard real-time deployability remains insufficiently verified. The published study does not report inference latency, memory footprint, or power consumption on representative embedded hardware such as ARM Cortex-M processors, FPGA platforms, or dedicated edge-AI accelerators. In particular, direct implementation of an uncompressed TCN-LSTM on a conventional projectile-borne microcontroller is likely to be constrained by recurrent computation, memory access, and power budget. FPGA- or micro-NPU-based implementation may potentially meet the real-time requirement only after lightweight redesign, fixed-point quantization, pruning, pipelined inference, and hardware-in-the-loop validation. Consequently, embedded inference latency, energy consumption, and high-g survivability should be considered key evaluation indicators for future intelligent layer-counting fuze algorithms.

Taking advantage of the fact that accelerometers have a faster response time than magnetic sensors, a method for processing penetration layers that combines accelerometers with magnetic sensors was proposed [403]. Furthermore, a layered technique for the fusion of cross-origin analysis for intrusion fuses based on the Fuzzy Weighting Algorithm and Backpropagation Neural Networks was proposed [384]. In recent years, a Target Scene Generator has been developed [98, 124]. This system is based on multiple sensors and complex signal-processing algorithms. When coupled with high-precision height-of-burst sensors, it has significantly enhanced the damage effectiveness of hard-target penetration weapons against HDBTs.

Significant evolution has been observed in layer-counting initiation control algorithms. The field has transitioned from single-signal processing to multi-domain information fusion, and from fixed-threshold methods which rely on manual parameterization and a priori data to intelligent approaches integrating deep learning and time-series modeling. Adaptive capabilities and robust generalization have been progressively achieved in machine learning-based control methods, resulting in substantial enhancements in recognition accuracy. However, adaptability toward complex targets characterized by significant variations in interlayer spacing remains to be further optimized. Furthermore, to meet the stringent demands of real-time data processing, the performance of on-board processors must be further enhanced.

Multi-domain information fusion is a promising route for improving the robustness of layer-counting initiation control. By combining deceleration, magnetic, acoustic, induced-electric-field, or other physical-domain signals, the fuze may obtain complementary information about projectile-target interaction. However, most currently reported fusion-based layer-counting methods are supported by numerical simulation, reconstructed signals, HIL platforms, or simplified laboratory experiments. No full-scale live-fire result has been found that quantitatively demonstrates the improvement of acceleration-magnetic-acoustic fusion over an accelerometer-only baseline under identical realistic reinforced-concrete penetration conditions.

In realistic reinforced-concrete targets, magnetic and acoustic signatures are highly non-stationary and target-dependent. Rebar meshes may introduce strong local magnetic disturbances, and their signal characteristics vary with reinforcement spacing, bar diameter, projectile attitude, sensor-target distance, and the relative position between the projectile and the rebar mesh. Aggregates, cracks, interfaces, and voids may further change the local penetration resistance and induce nonuniform stress-wave propagation. For acoustic sensing, wave scattering, attenuation, mode conversion, reflection from interfaces, and coupling with projectile structural vibration can obscure layer-boundary features. Therefore, the addition of magnetic or acoustic channels does not automatically guarantee higher layer-counting accuracy. Its effectiveness depends on sensor survivability, bandwidth, mounting position, signal synchronization, feature stability, and the robustness of the fusion algorithm under strong target heterogeneity.

Although high layer-counting accuracy has been reported in several studies, most of these results were obtained under numerical simulation, reconstructed signal, HIL, or laboratory multi-impact conditions. Such results demonstrate the feasibility of the corresponding recognition logic, but they should not be directly interpreted as live-fire validated accuracy. In actual penetration scenarios, layer-counting performance may be degraded by target heterogeneity, oblique impact, projectile attitude variation, structural vibration, sensor saturation, signal aliasing, electronic survivability, and the limited time window available for real-time decision-making. Where no live-fire validation was available, the engineering validity remains to be confirmed by scaled penetration tests and full-scale range tests.

5.2 Void-sensing initiation control methods

Void-sensing initiation control is essential for achieving warhead initiation after penetrating thick targets. Its workflow is shown in Fig. 32. This approach relies on void-sensing algorithms. These algorithms typically use deceleration information from the entire projectile penetration process to recognize the target and determine the initiation point. In terms of information usage, void-sensing initiation control is similar to layer-counting initiation control. Essentially, it can be regarded as a form of layer-counting initiation control in which the layer number is set to one. The void-sensing initiation control method is suitable for attacking single-layer thick targets or complex thick structures. Examples include hangars, tunnel warehouses, and bridges. Following this introduction, a systematic review will be provided on studies related to the void-sensing initiation control method.

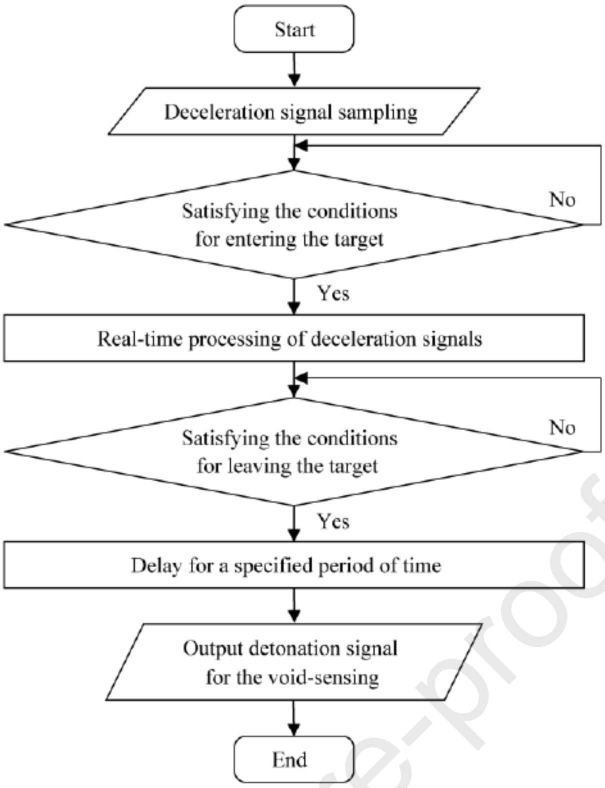

Fig. 32. Workflow of void-sensing initiation based on time information (Adapted from [6, 385]).

A timer-based void-sensing initiation control method was proposed [385]. The cavity was identified using the amplitude and temporal features of the acceleration signal. A timer was introduced to distinguish interference from pseudo-cavity and double-cavity conditions. Based on this method, a dedicated hardware circuit system was designed to implement the algorithm. Results show that the system offers strong real-time performance and high resistance to deceleration. Subsequently, a void-sensing algorithm based on pseudo-autocorrelation was introduced [293]. Frequency-modulated pulse compression was realized by means of signal self-multiplication. Afterwards, a low-pass filter was employed to extract the envelope of the penetration signal. Simulations and measured data were used for validation. The results showed that the proposed algorithm could accurately identify the number of penetrated media layers. The relative error between the displacement obtained from double integration of shock acceleration and the actual projectile displacement was about 3%. Integration of the pseudo-autocorrelation algorithm with the depth calculation algorithm enhanced the precision of the initiation control algorithm. Additionally, to address the difficulty in achieving precise cavity initiation control when a penetrator strikes a concrete target of unknown thickness, an adaptive delayed initiation method based on the penetration response characteristics of concrete was proposed [386]. This method uses a threshold approach to identify the target entry moment and the target exit moment. The delay time is dynamically adjusted by incorporating projectile velocity information. This enables accurate initiation against targets with different thicknesses. Live-fire tests were conducted to verify the effectiveness of the algorithm. Under conditions involving a 6 m target and an initial velocity of 670 m/s, the initiation delay error was only 0.45 meters. By integrating initial velocity information with penetration response characteristics, adaptive initiation control for targets of unknown thickness was achieved. The research significantly improves initiation accuracy during the penetration of a single-layer thick target. Meanwhile, a precise initiation control method after target penetration was proposed [404]. This method is based on stress wave compensation. It enables accurate recognition of the target impact moment. The residual velocity after target penetration can also be calculated in real time. As a result, precise initiation at a specific distance behind the target is achieved. Verification tests showed that this algorithm reduces initiation control errors to about 2%. This was demonstrated under penetration conditions at velocities of 600 m/s and 800 m/s. The damage effectiveness of penetration warheads is significantly improved as a consequence.

In addition, common fuze often employs open-loop control. This approach exhibits poor adaptability and low accuracy, and it cannot cope with complex modern battlefield environments such as multi-physical-field interference, time-varying targets, and high-speed engagements [405]. To address these issues, the Three-element Cascade Control Architecture was proposed [178, 406, 407]. Its schematic diagram is shown in Fig. 33. This architecture achieves precise initiation decisions through a three-stage series configuration, which consists of an environment-adaptive detection controller, a self-triggered delay-compensation state controller, and a virtual closed-loop initiation controller. The virtual closed-loop refers to an internal computational loop among sensing, state estimation, and initiation decision modules. It uses real-time penetration signals to update the internal fuze state before initiation.

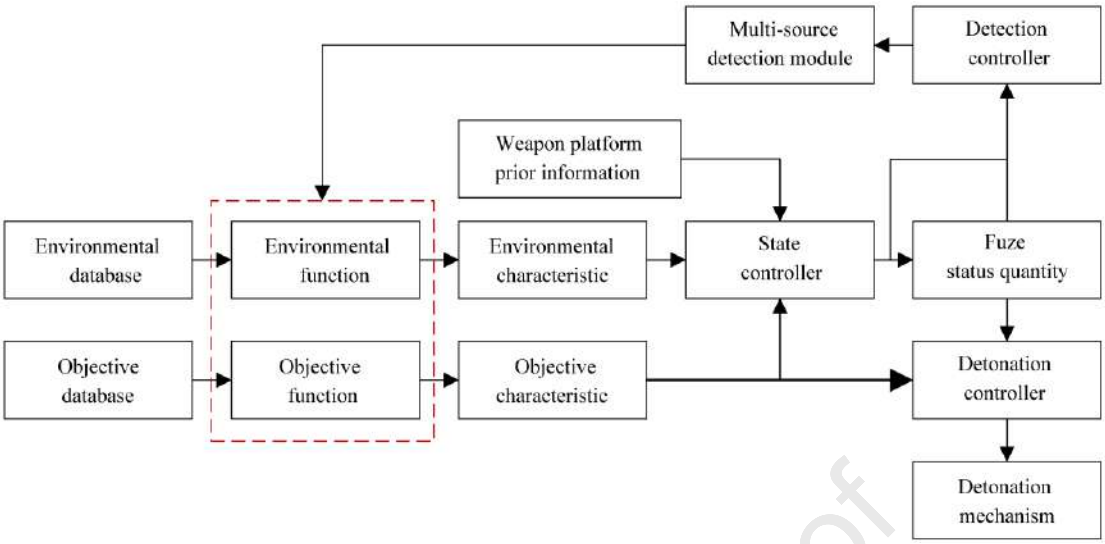

Fig. 33. Schematic diagram of the Three-element Cascade Control Architecture [178, 406].

For the multi-layer hard-target penetration fuze, online Squeeze-Net deep learning combined with offline lightweight execution was utilized. Under high-speed and multi-overlapping conditions, the layer recognition rate was improved from the conventional 69.7% to 97.34%. The system can complete multi-dimensional spatio-temporal information fusion, state updates, and initiation decisions within microseconds. Consequently, the damage effectiveness in complex battlefield environments is significantly enhanced. This work provides an engineering implementation foundation for the development of intelligent penetration fuze.

5.3 Summary and assessment

The development trajectory summarized in Table 11 indicates a clear shift in hard-target penetration fuze technology from fixed-delay initiation toward target-feature-based and logic-assisted initiation. The central challenge, however, is no longer limited to sensing target features during penetration, but lies in converting incomplete, noisy, and highly transient sensing information into reliable, explainable, and certifiable initiation-control decisions. Existing layer-counting, and void-sensing approaches have demonstrated engineering value under controlled conditions, particularly for regularly spaced reinforced-concrete or multi-layer test targets. Nevertheless, many of these methods still depend on deterministic signal features, preset thresholds, or target-specific decision rules. Their robustness can degrade when target structures contain irregular cavities, nonuniform partitions, heterogeneous reinforcement layouts, soil-rock overburdens, or strongly coupled projectile-target dynamic responses.

By combining acceleration, magnetic, acoustic, and other physical-field signals, fusion-based methods can reduce the ambiguity associated with any single sensing. However, the present open literature suggests that many reported improvements are still obtained from numerical simulations, hardware-in-the-loop platforms, or laboratory-scale penetration experiments. These studies are valuable for feasibility demonstration and algorithm screening, but their results should not be interpreted as direct evidence of operational layer-counting accuracy or field reliability. Therefore, future work should move from isolated algorithm comparison toward controlled, system-level benchmarking in which accelerometer-only, acceleration-magnetic, acceleration-acoustic, and acceleration-magnetic-acoustic configurations are evaluated under identical projectile, target, impact-velocity, obliquity, sensor-mounting, and data-acquisition conditions. In addition to recognition accuracy, evaluation should include false-count rate, missed-count rate, recognition latency, sensor survivability, onboard data recovery, and uncertainty calibration.

The future initiation control algorithms should gradually depart from deterministic threshold-based decision rules and incorporate probabilistic inference frameworks. Bayesian inference is particularly attractive because it enables the HTPF to continuously update its cognitive state regarding possible target geometries, material interfaces, and residual penetration states under uncertainty. Rather than triggering initiation once a fixed set of criteria is satisfied, the fuze could evaluate multiple possible target-state hypotheses and select the initiation point that maximizes expected damage effectiveness or mission utility under constrained safety requirements. Such a framework would allow HTPFs to operate more robustly in complex, partially unknown, or structurally irregular targets.

At the same time, the introduction of Edge AI into fuze systems must be governed by explainability, verifiability, and safety. Pure black-box neural networks are difficult to reconcile with the stringent safety-certification requirements of fuze systems. Therefore, future research should prioritize physics-informed neural networks, neurosymbolic models, or other hybrid intelligent frameworks that embed penetration mechanics, impact dynamics, and sensor-response characteristics into the learning process. Such models can provide a traceable relationship between sensor inputs, intermediate recognition results, and final initiation commands, which is essential for qualification testing, fault diagnosis, and engineering acceptance.

From an engineering perspective, advanced initiation-control algorithms must be developed through system-level co-design. Algorithmic performance cannot be separated from high-g-resistant sensors, shock-protected electronics, embedded processors, power-management units, S&A mechanisms, and explosive-train interfaces. In addition to recognition accuracy, engineering indicators such as false-trigger probability, missed-recognition probability, decision latency, computational burden, electromagnetic compatibility, environmental adaptability, and post-impact survivability must be assessed under statistically meaningful impact conditions. These factors determine whether an advanced recognition algorithm can be transferred from laboratory validation to engineering-grade applications.

Accordingly, future validation should follow a hierarchical and progressive framework. Early-stage studies may begin with numerical simulation and reconstructed-signal verification, followed by hardware-in-the-loop testing, laboratory multi-impact experiments, scaled penetration trials, and finally instrumented full-scale live-fire testing. Each validation level should address different technical risks: algorithm correctness, sensor robustness, data-recovery reliability, embedded real-time feasibility, system survivability, and operational reliability. Only through such stepwise validation can advanced initiation-control algorithms be credibly assessed and eventually integrated into qualified HTPFs.

6 Performance evaluation and reliability analysis

HTPFs are required to accurately sense targets, reliably release safety mechanisms, and achieve precise initiation under extreme conditions [408, 409], including high-impact decelerations of tens of thousands of g and complex stress wave environments. Simultaneously, absolute safety must be guaranteed throughout the entire lifecycle, encompassing production, assembly, storage, transportation, and launch. Consequently, the development process of penetration fuze relies on extensive mechanical environment simulations and dynamic tests. Reliability and safety margin analyses are conducted during the production, acceptance, and storage phases to achieve closed-loop management across the full life cycle [410]. A comparative analysis of common performance evaluation and assessment methods for the HTPF is presented in Table 12. This section provides a systematic review of the research progress in the performance evaluation and reliability analysis of HTPF from three perspectives: HIL simulation experiments, performance assessment and reliability testing, and theoretical analysis.

Table 12

Methods for HTPF performance assessment and evaluation [2, 367, 411–414].

Methods	Objectives	Advantages	Challenges	Validation level
HIL simulation test	Verify real-time performance and correctness of control algorithms through a closed-loop system combining models and physical components	High flexibility; strong reproducibility; low-cost	Results depend on model fidelity; difficult to reproduce structural deformation and real projectile-target coupling	Low-to-medium; suitable for early-stage algorithm and hardware-software verification
Multi-impact simulation test	Replicate short-interval continuous impacts during multi-layer penetration	Controllable impact number and intervals; cost-effective	Cannot fully reproduce real penetration stress waves and environmental coupling	Medium; suitable for laboratory robustness assessment
Penetration fuze scaled test	Use small-calibre projectiles to approximate full-calibre penetration process	Lower cost; closer to real physical processes	Scale effects may introduce data bias; similarity laws are difficult for complex targets	Medium-to-high; suitable for engineering pre-validation
Full-scale live-fire test	Evaluate fuze performance through full-scale range trials	Highest authenticity; system-level verification	Extremely costly; long cycle; low sensor survival rate; limited repeatability	Highest; necessary for fielded-system validation

6.1 Hardware-in-the-loop simulation experiment analysis

HIL simulation is conducted within a laboratory environment. By constructing a simulation loop, the hardware system is integrated into a virtual penetration environment, simulated via mathematical models and simulation equipment, to test the operational status of the fuze. The schematic block diagram of a typical HIL simulation system for HTPFs is illustrated in Fig. 34. As a critical component in evaluating penetration fuze performance, HIL simulation is primarily employed to assess environmental adaptability, autonomous recognition capability, and initiation control accuracy during simulated real-world penetration processes. Through this approach, unqualified products are screened out, thereby enhancing fuze reliability and the success rate of prototype trials. Additionally, statistical analysis of test results for defective products is performed to localize software and hardware issues, providing essential technical support for both engineering prototypes and finalized products.

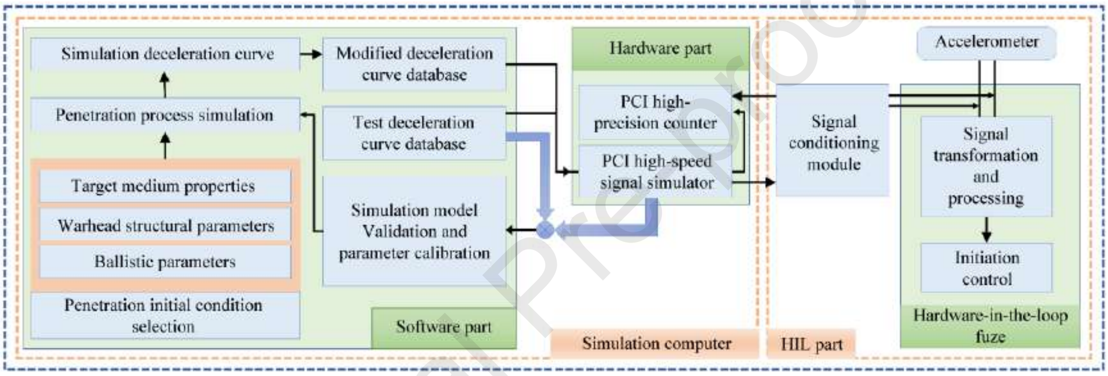

Fig. 34. Principle diagram of a typical HIL simulation system for HTPF (Adapted from [415]).

As an effective alternative to field range tests, HIL simulation is widely utilized in the development of autonomous recognition and initiation control algorithms, as well as the comprehensive performance evaluation of penetration fuze. A schematic diagram of a typical HIL simulation system for HTPFs is illustrated in Fig. 35. Early research focused on constructing the framework of HIL simulation systems. The HIL simulation technology for HTPFs was systematically studied. A complete system was established. It included target characteristic analysis, deceleration numerical simulation, hardware interfaces, and signal processing methods. A deceleration database was also constructed. Based on this, the research was advanced from three modules: hardware design [416], driver development [417], and signal reconstruction [418]. The hardware design of the signal simulator was focused on by Fu, including the PCI interface and FPGA logic control. The driver was optimized based on the WDM model by Zhang, enhancing real-time performance and stability. More accurate signal reconstruction and noise reduction were achieved through wavelet analysis by Feng. In addition, signal analysis and high-speed data transmission interfaces were studied [419]. Electromagnetic compatibility (EMC) design was emphasized.

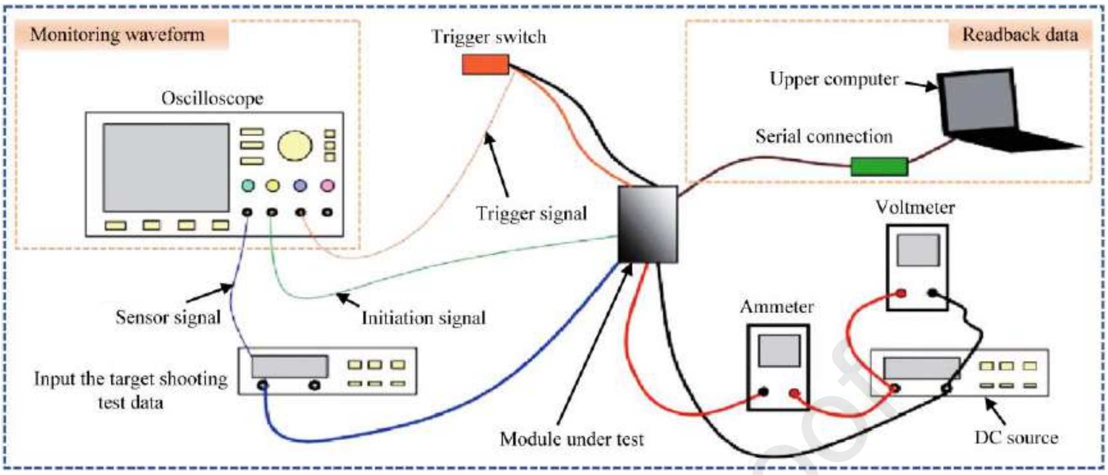

Fig. 35. Schematic diagram of a HIL simulation system for HTPF (Adapted from [394, 412]).

Subsequently, research on HIL simulation systems has focused more on system integration and engineering applications. Based on the C8051F021 microcontroller, a simulation system was constructed [420], while a modular design was adopted [421] to build another simulation system. Both works emphasized practicality and operability, though there remained room for improvement in accuracy. Further verification of the consistency between simulation data and measured data was conducted [422]. On this basis, a layer-counting initiation simulation method was proposed [328], extending the validation dimensions of HIL simulation. Further development was made [335], who designed a HIL simulation system with an error controlled within 5%. This system supports the evaluation of multiple performances, including initiation control and firing reliability. In recent years, the magnetic perception and measurement technology of penetration angle was verified through HIL simulation experiments. Similarly, the layer-counting method for penetration was verified through HIL simulation experiments [394, 423－425].

Overall, research concerning HIL simulation experiments has evolved through a developmental trajectory, ranging from framework construction and key technical breakthroughs to system integration and engineering applications, while simulation accuracy and functional integrity have been continuously enhanced. Modern HIL simulation for HTPF is dedicated to the establishment of high-fidelity integrated testing environments. Through the utilization of advanced physical models and simulation equipment, the critical mechanical environments and boundary conditions encountered by fuze during the penetration process are accurately replicated. This enables researchers to evaluate fuze response characteristics, verify initiation-control logic, and investigate potential failure modes under controlled and repeatable conditions, thereby reducing the cost and risk associated with direct live-fire testing.

Nevertheless, HIL simulation should not be regarded as a substitute for live-fire validation. Its credibility is fundamentally constrained by the fidelity of the penetration dynamic model, the accuracy of reconstructed acceleration signals, and the representativeness of the hardware boundary conditions. In particular, HIL platforms generally cannot fully reproduce target heterogeneity, projectile attitude variation, transient structural deformation, sensor mounting errors, thermal-mechanical coupling, and shock-induced electronic failure. Therefore, HIL results are most suitable for early-stage functional verification, algorithm debugging, and comparative evaluation, whereas final engineering validation still requires scaled penetration tests and full-scale live-fire tests.

6.2 Test analysis of performance evaluation and reliability

Generally, the development and production of fuze are accompanied by extensive experimental testing. Due to the extremely harsh terminal ballistic environments encountered by penetration fuze, various tests conducted throughout the research, production, and service phases are of critical importance [426]. The objectives of these test assessments across different stages of the fuze's full life cycle are summarized in Table 13. In addition to conventional service, environmental, and EMC tests, various targeted dynamic tests must be performed to evaluate the survivability and dynamic performance of the fuze under high-impact conditions.

Table 13

Objectives of the full life cycle testing and evaluation for the HTPF [2, 6, 426].

Testing phases	Objectives
Design phase	Validate system functionality, identify design flaws, and refine design concepts.

Finalisation phase	To assess whether the newly designed fuze meets the tactical and technical specifications.
Production phase	Monitor batch production quality, identify issues within batches, and refine production processes.
Operational phase	Examine performance changes following transportation and storage to identify potential hazards.

Dynamic testing of penetration weapon fuze is conducted to establish excitation conditions comparable to those encountered during the actual penetration process, thereby providing the necessary environment for the verification and evaluation of fuze performance. At present, universal and standardized testing standards have not yet been established globally in the field of penetration weapon dynamic testing; however, several commonly used testing and evaluation methods have gradually matured through practical application.

6.2.1 Multi impact simulation test analysis

To ensure the reliable performance of penetration fuze, functional verification of the initiation control strategy, particularly the layer-counting initiation strategy, must be conducted. While range testing is associated with high operational costs, dynamic simulation testing allows for the adjustment of the amplitude and pulse width of acceleration signals, thereby effectively reducing expenses. The ranges of acceleration amplitude and pulse width for commonly used dynamic testing techniques were summarized [411] as shown in Fig. 36. In these dynamic simulation tests, actual mechanical environments are simulated using impact equipment such as Martingale hammers, drop tables, air guns, and Hopkinson bars [427]. This approach is conducive to the identification of potential design flaws and the validation of functional requirements; it has been increasingly prioritized within the engineering field.

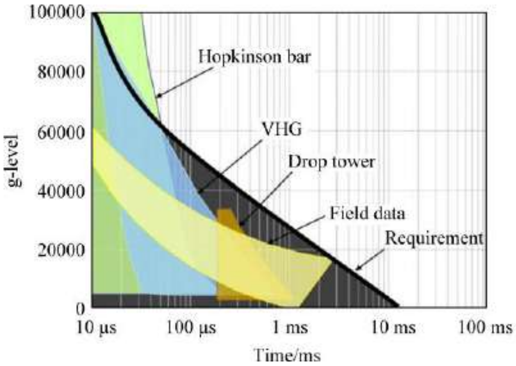

Fig. 36. Deceleration amplitude and pulse range for typical dynamic testing techniques [427].

To address the challenges of high costs and long cycles associated with range testing, as well as the difficulty of laboratory equipment in simulating short-interval high-g shocks, researchers have developed multiple high-impact testing devices. A rotational short-interval multi-impact scheme was proposed [330, 428], achieving continuous shocks with intervals ≤10 ms and amplitudes ≥5000 g. By establishing a model of kinematic pairs with clearance, contact stability was optimized, providing a fundamental means for laboratory testing of penetration fuze. However, the impact interval remained relatively large. Building on this, the impact head structure and employed motor vector control to regulate rotational speed was improved [429], reducing the impact interval to ≤3 ms, which better approximates actual inter-layer penetration intervals. A quantitative model linking impact parameters to acceleration signals was established, significantly enhancing signal authenticity and consistency, thereby advancing testing from functional verification to performance evaluation. Furthermore, Li addressed the issue that pure shock simulations neglect stress wave-vibration coupling by proposing a coupled loading technique combining active excitation and self-excited vibration [411, 430]. This achieved millisecond-level short-interval, high-amplitude multiple impacts while simultaneously resolving the challenge of matching amplitude and frequency. Additionally, the introduction of fractal contact theory refined the contact model, improving simulation accuracy under conformal contact conditions. A platform for conducting multiple high-impact tests at short intervals was further developed, as shown in Figs. 37(a)–37(c). Subsequently, a short-interval multi-impact high-shock testing device to simulate multiple high-shock environments within millisecond-level intervals in the laboratory was utilized [367], validating the layer-counting initiation control strategy of HTPF under multi-layer target strikes.

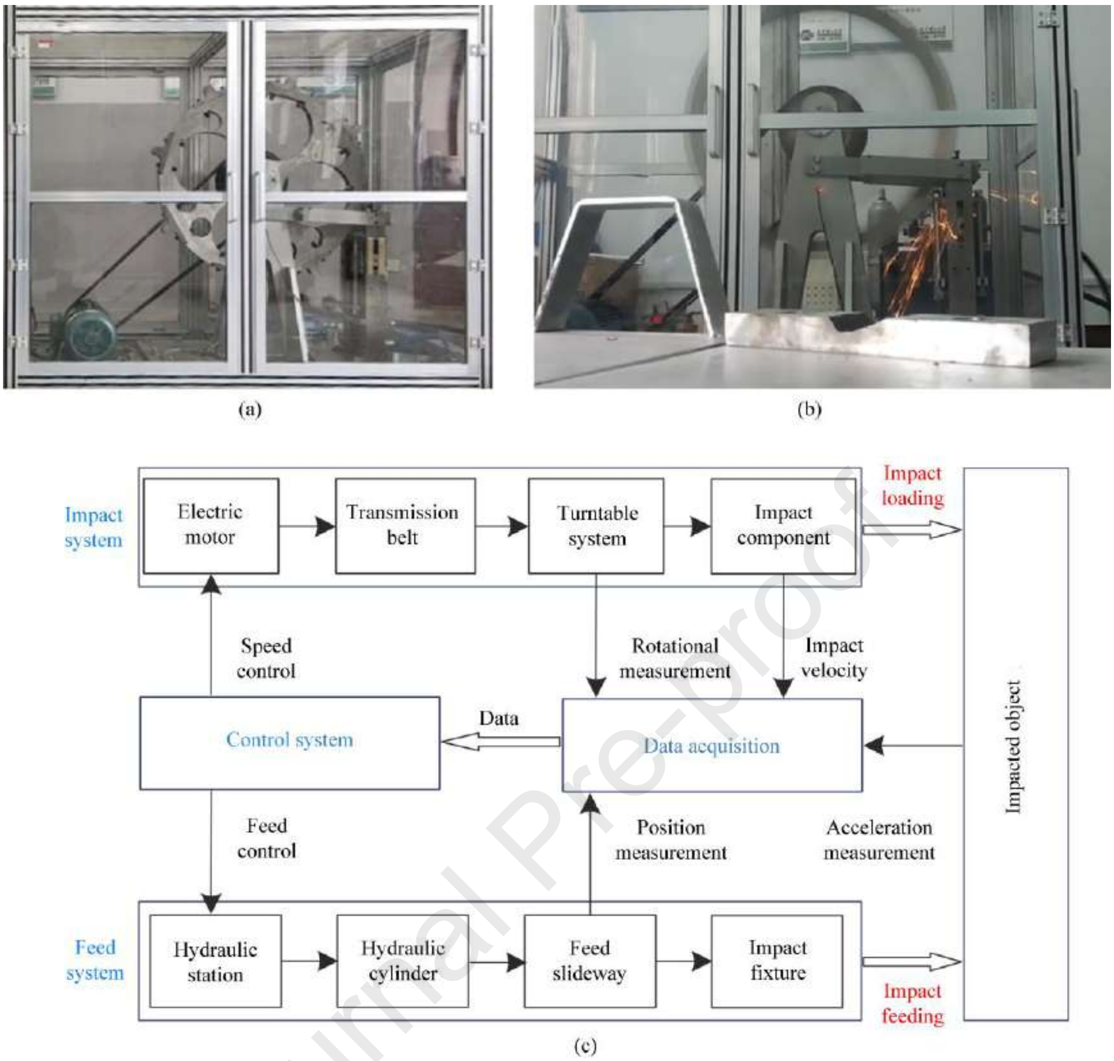

Fig. 37. Short-interval multiple high-impact testing platform [411, 430]: (a) Multiple-impact on the equipment prototype; (b) Multiple-impact test; (c) Principle diagram of multiple-impact equipment.

Currently, the full spectrum of conditions, ranging from low to high strain rates and low to high g-levels, has been successfully covered by single impact experiments, resulting in a well-established technical framework. In contrast, research on multi-impact tests remains constrained by the fact that simulated peak impact values are frequently lower than those encountered in actual penetration environments. Due to the unresolved trade-off between impact amplitude and frequency, the development of theoretical systems and experimental methodologies has lagged. Consequently, overcoming the technical bottleneck of short-interval, high-g impact simulation is considered critical for enhancing both simulation accuracy and practical utility.

6.2.2 Range test analysis of penetration fuze

During the development phase of HTPF, performance evaluation has traditionally relied on live-fire range tests. Field test assessments for HTPFs are classified into full-scale live-fire tests and sub-scale tests, encompassing methods such as gun-firing tests, Davis gun tests, and rocket sled tests.

Full-scale testing of HTPF is considered a critical stage for verifying the reliability and effectiveness of fuze under authentic battlefield conditions [431]. Given that the penetration process is characterized by high-impact decelerations reaching tens of thousands of g and complex multi-layer target penetration effects, the mechanical environments and timing control challenges faced by fuze in practical applications can be most accurately reproduced through full-scale testing. A shock-hardened penetration data recorder, specifically designed to support the research and development of HTPF, was developed [432, 433] at Sandia National Laboratories. This technology serves as a pivotal support during the research and development, testing, and validation phases of HTPF, facilitating the acquisition of data within high-deceleration environments during high-speed penetration events. Additionally, a ground testing system for HTPFs was established [434, 435]. to mitigate the risks associated with live-fire trials.

While full-scale testing provides a realistic representation of penetration fuze performance, it is inherently limited in capturing information that requires a large volume of experimental data, such as environmental uncertainties and the stochastic nature of projectile-target impacts. Furthermore, it fails to provide critical data regarding algorithmic robustness, component operational status, thermal expansion of potting compounds, and dynamic shock responses. Given the high costs and lengthy development cycles involved, full-scale testing is more appropriate for product qualification and delivery acceptance rather than serving as the optimal approach for evaluating comprehensive fuze performance during the research and development phase [436]. In this context, low-cost scaled-down testing is employed to analyze the deceleration characteristics and mechanical environment of the penetration fuze during penetration. Key dynamic parameters are obtained through this approach, making it an important supplement to field tests. The adoption of low-cost penetration fuze scaled-down testing effectively reduces development costs and shortens the cycle, demonstrating high engineering application value.

Research on scaled penetration test methods for warheads has formed a relatively mature theoretical system. It mainly focuses on the equivalent simulation of indicators such as penetration capability and depth. In terms of fuze assessment, the HTPF dynamic scaled test system was constructed [437]. Based on cavity expansion theory and simulation design, a fin-stabilized test projectile with good deceleration consistency was achieved. To address the distortion problems of acceleration, time, and depth, the scale-invariant criterion with projectile diameter squared/(mass × target correlation coefficient) as the core was further proposed [438]. By reducing the hardness of the target, the authenticity of the acceleration curve was significantly improved. However, the relationship between the target correlation coefficient and the target hardness was not clarified. Only the peak deceleration could be equivalent. To simultaneously achieve the equivalence of peak and pulse width, the non-proportional scaled test method was proposed [439]. Through dimensional analysis and derivation from the Forrestal model, high-precision simulation of deceleration peak and pulse width was achieved under the condition of consistent head coefficient and penetration velocity. The error was less than 10%. The three-characteristic equivalence principle of peak deceleration-pulse width-overlapping was introduced [440] based on this. The scaled projectile and the prototype projectile are equivalent in three characteristic quantities: peak deceleration, duration, and overlapping. By adjusting the ratio of projectile length to target spacing, the deceleration overlapping phenomenon between multi-layer targets was effectively reproduced.

Recently, regarding the size-effect mechanism of projectile penetration into rock media, a series of penetration tests using geometrically similar steel projectiles with diameters of 10 mm and 20 mm against high-strength granite were conducted [413]. It was found that the scaling factor for normalized penetration depth between model and prototype projectiles depends not only on the scaling ratio α, but also on the prototype projectile diameter and target material parameters such as dynamic shear strength and fracture toughness. The scaling factor increases with larger prototype diameter and decreases with a larger scaling ratio. Consequently, a penetration depth calculation model was established, with the projectile shape coefficient and diameter coefficient as control variables. Theoretically, it was clarified that the size effect mainly originates from the strain-rate hardening effect and the differences in meso-fracture characteristics of the target material. This study effectively addresses the significant deviation encountered when extrapolating traditional scaling test results to prototypes, providing a theoretical basis and methodological support for scale-effect correction in penetration fuze design. Breaking through the geometric scaling framework, an equivalent method based on the transfer function of the projectile-fuze system was proposed [441]. An analytical expression of the transfer function was derived using a multi-degree-of-freedom vibration model. Structural responses such as stress wave propagation and coupled vibration were incorporated into the scaling design parameters. This method reduces the peak deceleration error and pulse width error to less than 6%, is not limited by scaled projectile design, and offers low-cost and wide applicability. Taking the peak deceleration and the inter-layer oscillation amplitude of the deceleration signal as equivalence criteria, a variable-mass scaling design method for HTPF based on energy equivalence was proposed [442]. Simulation results under two conditions showed that the peak deceleration of the scaled fuze increased by 22.9% and 22.7% respectively compared to the full-scale fuze. This meets the equivalence criterion that the peak deceleration should increase by 0–30%. Furthermore, the inter-layer oscillation amplitude of the deceleration signal remained comparable before and after scaling.

Although the above scaling laws provide useful criteria for reproducing penetration depth, peak deceleration, pulse width, and, to some extent, inter-layer oscillation amplitude, they should not be regarded as complete equivalence criteria for penetration fuze evaluation. For modern HTPFs, the initiation decision is not governed only by the peak value of the deceleration pulse, but also by the time-frequency characteristics of the measured signal [357]. Signal adhesion and aliasing may be induced by stress-wave propagation, projectile-body vibration, projectile-fuze coupled resonance, mounting-interface nonlinearity, and the dynamic response of potted electronic modules. Therefore, a scaled test that matches only the acceleration peak or pulse width may still fail to reproduce the frequency-domain characteristics that affect layer-counting, void-sensing, and adaptive initiation decision-making.

To preserve the decision-relevant signal characteristics, a hybrid response-spectrum and transfer-function-based scaling protocol is recommended [443]. First, conventional penetration similarity should be maintained as far as possible, including impact velocity, nose-shape coefficient, penetration depth, peak deceleration, impulse, and pulse width. Second, the transfer function from the projectile body to the fuze sensor and electronic module should be identified and used as an additional scaling constraint. The dominant natural frequencies, damping ratios, shock response spectrum, and frequency-band energy distribution of the scaled projectile-fuze system should be matched within the passband of the fuze sensing and signal-processing chain. Third, the internal fuze assembly should be represented by the real electronic module or by a dynamically equivalent surrogate with matched mass, stiffness, damping, mounting stiffness, and potting-compound viscoelastic properties. It should also be emphasized that strain-rate-dependent material behavior must be considered when scaled-test results are extrapolated to full-scale penetration conditions. The dynamic shear strength, fracture toughness, strain-rate hardening, and meso-fracture characteristics of the target material can change the stress-wave excitation and the frequency content of the measured deceleration signal. Therefore, target-material selection and constitutive calibration are necessary components of a reliable scaling protocol for HTPF evaluation.

A critical limitation of current scaled testing is that most similarity criteria remain dominated by macroscopic mechanical quantities, such as penetration depth, peak deceleration, and pulse width. These quantities are necessary but not sufficient for evaluating HTPFs. For initiation algorithms based on layer counting or void sensing, the decisive information is often embedded in the time-frequency structure of the deceleration signal. In particular, signal adhesion caused by stress-wave reflection, projectile-fuze coupled resonance, and electronic-module vibration may lead to false layer identification or missed void detection, even when the peak deceleration is correctly reproduced.

Moreover, the hard-target penetration deceleration was simulated [432] through ballistic water impact tests. This enabled the performance assessment of the HTPF under coupled high deceleration and strong shock. To address the challenge of assessing initiation reliability for extremely weak targets such as 1 mm steel plates, a test fuze was designed [444]. The 155 mm smoothbore gun and other loading equipment were employed. Muzzle safety technology and low-cost delay charging technology were combined. The initiation performance of fuzes in the terminal trajectory was assessed.

Current research has established a complementary and verifiable framework comprising HIL simulations, laboratory simulation tests, scale-model tests, and full-scale live-fire tests. This system has revealed the extreme deceleration environments encountered by HTPF and the complex internal load characteristics of the system, while also validating the effectiveness of laboratory and range test simulation evaluation methods. However, further in-depth exploration is required regarding the structural response and equivalence characteristics of fuze under stress wave effects. There is an urgent need to establish more systematic projectile-target relationship models and dynamic response similarity criteria to provide technical support for the dynamic range testing and evaluation of HTPF.

6.3 Theoretical analysis of reliability and safety margins

The HTPF represent a specialized category of fuze; however, the analysis of their reliability and safety margins remains within the established framework of fuze engineering. Conducting reliability and safety margin analyses based on HIL simulation and dynamic testing is an essential approach for assessing operational reliability. This section not only quantifies fuze reliability within complex penetration environments and identifies potential failure modes but also facilitates the assessment of safety margins [445], thereby providing closed-loop data support for life-cycle health management. Consequently, systematic reliability and safety margin analysis is of paramount importance for enhancing the battlefield adaptability and operational safety.

6.3.1 Security theoretical analysis

From the 1990s to the early 21st century, the Markov process model was introduced into fuze safety system analysis [446–448]. The system logic structure and state transition behavior were characterized, enabling the modeling and assessment of system failure probability. This provided theoretical support and qualitative analysis tools for fuze safety. In 2011, a reliability prediction method for fuze circuits based on the component count method and stress analysis method was proposed. Failure rate modeling was performed using reliability block diagrams and series system models. This work drove a significant transition in fuze design from experience-dependent to reliability-driven. With increasing system integration and complexity, the research scale was expanded from components to the entire machine system. To address the issues of insufficient reliability and high misjudgment rates in penetration fuze test systems, software fault tree analysis, hardware failure mode and effects analysis, and dynamics simulation were integrated [449]. A system-level reliability engineering method was developed, achieving a key leap from local circuit analysis to comprehensive evaluation of the entire system. With regard to penetration fuses, methods for reliability assessment under conditions of small sample sizes were investigated [60], supporting system-level reliability modelling of the fuze-initiation sequence in penetration warheads.

In recent years, electromagnetic environmental adaptability and safety throughout the full life cycle have emerged as research frontiers. The impact of electrical and electromagnetic environments on the all-electronic safety system was investigated [450]. EMC analysis was introduced during the design phase. This enhanced the reliability design capability of fuze under complex electromagnetic interference. Building on this, a systematic assessment framework for the electromagnetic environmental safety margin of fuze was proposed [451]. A margin quantification model covering multiple dimensions such as voltage, current, and energy was established. Corresponding test standards and procedures were also developed. This provided key technical support for the forward design of fuze. Meanwhile, from a systems engineering perspective, safety evaluation system throughout the full life cycle for fuze was constructed [452]. This system integrates safety design logic, failure mode analysis, and safety margin assessment. The research covers three critical stages: pre-isolation removal, post-isolation removal, and unexploded ordnance handling. Potential path analysis approaches and safety margin quantification verification directions were proposed. A complete theoretical framework and method system was established for the systematic safety assessment of electromechanical fuze.

Currently, electromagnetic safety margin assessments predominantly remain at static or quasi-static levels, making it difficult to accurately characterize the transient impacts and potential latch-up risks imposed on fuze circuits by time-varying and frequency-varying electromagnetic fields in actual combat environments. Furthermore, a gap exists in data-driven intelligent prediction for reliability and safety margin analysis. Existing methodologies fail to effectively integrate Built-In Test data with digital twin technology for real-time condition monitoring and Remaining Useful Life assessment. Consequently, reliability evaluations continue to rely over-heavily on design expectations and phase-based testing, lacking comprehensive life-cycle closed-loop management capabilities.

6.3.2 Case analysis of fuze failure

In addition to theoretical reliability modeling and safety-margin assessment, documented failure cases and program-level setbacks provide valuable evidence for understanding the engineering limitations of HTPFs. Unlike conventional electronic devices, the reliability of HTPFs is not determined only by component failure rates. It is a system-level mission reliability problem involving impact survivability, target-information sensing, real-time decision-making, power supply continuity, S&A logic, explosive-train integrity, and compatibility with weapon-platform interfaces [453]. Therefore, failure-oriented analysis is necessary for bridging the gap between reliability theory and operational fuze performance. Publicly available information on HTPF failures is limited because detailed range-test data, combat-damage assessment, and fuze malfunction records are often classified. Nevertheless, several documented program-level cases reveal important reliability lessons.

(1) Hard Target Smart Fuze program

The HTSF, designated as FMU-159/B, was intended to achieve precise initiation control according to penetration depth, layer count, or void count through high-precision accelerometers and microcontrollers. This concept represented an important transition from fixed-delay or programmable-delay fuze toward target-structure-aware initiation control. However, the program was terminated in 2003 due to significant technical implementation challenges [97].

This case indicates that successful algorithmic concepts and promising laboratory demonstrations do not necessarily lead to fielded fuzes. For HTPFs, the recognition algorithm must be co-designed with survivable sensors, shock-protected electronics, reliable power supplies, S&A devices, and explosive-train interfaces. Otherwise, sensing or decision functions may fail to survive the real penetration environment or may not satisfy weapon-system qualification requirements.

This termination should not be interpreted merely as a program-management outcome; rather, it reflects the difficulty of converting layer-counting and void-counting concepts into a survivable, qualifiable, and operationally reliable fuze [98]. In particular, the fuze must maintain sensor integrity, electronic functionality, power continuity, and initiation-train safety under high-g shock, severe vibration, and uncertain projectile-target interaction.

(2) Joint Programmable Fuze program

The FMU-152A/B significantly improved mission flexibility by allowing fuze parameters to be generated by the mission planning system, transmitted through the MIL-STD-1760 bus, and delivered to the fuze microcontroller via the RS-422 interface. However, the improvement in programmability does not eliminate the inherent limitations of time-delay-based initiation control during HDBT penetration. When the internal structure, layer thickness, void distribution, or penetration resistance of the target deviates from the pre-strike estimate, the FMU-152A/B may still detonate before or after the optimal damage location [94]. Publicly available HTVSF-related materials indicate that low fuze reliability at long time delays and insufficient void-detection capability were among the motivations for developing more survivable void-sensing fuzes [141]. Therefore, the JPF experience illustrates the distinction between platform-level programmable fuze and truly target-structure-aware hard-target fuze.

(3) Large Penetrator Smart Fuze program

The LPSF program provides a representative case of qualification and integration difficulty in modern intelligent penetration fuze. DOT&E reported that the LPSF was intended to improve the probability of kill against HDBTs by mitigating target-intelligence uncertainty, but fielding of the LPSF-enabled MOP was delayed multiple times because planned subscale tests and final full-scale qualification events could not be completed on schedule [100]. Later DOT&E and DoD budget documents further showed that target-construction delays, DTRA resource constraints, efforts to restore MOP accuracy, reduced subscale testing, and B-2 integration issues affected the test program [63]. Iranian claimed in 2026 that unexploded USA bunker-buster munitions, allegedly including GBU-57/MOP weapons, had been found and neutralized.

These facts indicate that the reliability of a modern penetration fuze cannot be assessed only at the component level. Smart fuzes for deep penetrators face not only high-g survivability and initiation-timing challenges, but also system-level reliability risks associated with platform integration, test representativeness, underground target modeling, and limited full-scale validation. Future reliability research should combine failure-mode analysis, HIL testing, multi-impact tests, scaled penetration tests, full-scale live-fire tests, and post-test forensic analysis.

6.4 Summary and assessment

The multi-tiered evaluation framework, including numerical simulation, hardware-in-the-loop simulation, multi-impact laboratory testing, scaled penetration experiments, and full-scale live-fire trials, constitutes an essential foundation for the qualification of modern HTPFs. However, its effectiveness is increasingly challenged by the discrepancy between controllable test conditions and complex operational environments. HIL simulation plays an indispensable role in algorithm debugging, real-time logic verification, and hardware-software interaction assessment, but its credibility depends heavily on the fidelity of the underlying penetration dynamics model and the reconstructed mechanical inputs. Reduced-order or simplified models may have difficulty fully capturing the coupled effects of stress-wave propagation, localized plastic deformation, structural damage evolution, and thermo-mechanical response during high-velocity penetration. As a result, fuze algorithms or hardware modules that perform reliably under laboratory or HIL conditions may still exhibit unexpected behavior when exposed to the highly uncertain boundary conditions of actual penetration events.

Full-scale live-fire testing remains the highest-confidence validation method for penetration fuze performance, but it also faces inherent practical constraints. The high-cost, complex organization, and safety requirements of such tests often limit the number of available samples, making statistically robust reliability evaluation difficult. In addition, the harsh penetration environment may damage onboard instrumentation, which restricts the acquisition of authentic in-situ mechanical, electrical, and failure-process data. Scaled penetration testing provides a more economical and repeatable intermediate approach and can partially reproduce projectile-target coupling characteristics. Nevertheless, its validity depends on the rationality of similarity criteria. In particular, it remains difficult to simultaneously preserve all relevant dynamic response characteristics, such as peak overload, pulse duration, frequency-domain features, structural response, and sensor-output characteristics.

Future scaled testing should therefore shift from single-parameter mechanical equivalence to multi-level signal equivalence. A more reliable evaluation framework should combine projectile-target similarity, projectile-fuze transfer-function similarity, shock-response-spectrum similarity, and algorithm-in-the-loop decision consistency. The scaled test should be regarded as valid only when the reproduced signal not only matches the full-scale acceleration peak and pulse width, but also preserves the dominant frequency bands, damping characteristics, inter-layer oscillation amplitude, signal-adhesion duration, and decision outputs of the fuze algorithm. This framework provides a more appropriate basis for evaluating next-generation intelligent penetration fuzes than traditional peak-deceleration-based scaling alone.

Therefore, the transition from academic algorithms to fielded HTPFs requires a clearly defined hierarchical validation route. Numerical simulation should mainly be used for mechanism analysis, parameter sensitivity studies, and preliminary design optimization. HIL simulation is suitable for verifying real-time decision logic, signal-processing algorithms, and hardware-software coordination. Multi-impact laboratory tests can further evaluate repeated-shock survivability, circuit robustness, and decision stability under controlled impact conditions. Scaled penetration experiments provide a closer representation of projectile-target interaction while maintaining relatively manageable cost and risk. Finally, full-scale live-fire tests remain indispensable for final engineering qualification and operational confidence.

The cases of HTPF programs indicate that reliability evaluation for HTPFs must go beyond theoretical reliability prediction and isolated component tests. A fuze may satisfy basic electronic reliability requirements but still fail to achieve mission reliability if its sensing logic, delay setting, survivability, or explosive-train response is not matched to the actual penetration environment. Therefore, future reliability evaluation should incorporate failure-oriented evidence, including failed or delayed programs, range-test anomalies, dud events, false triggering, missed void detection, and post-impact damage analysis. Such evidence is essential for identifying weak links in the complete fuze chain and for preventing an overestimation of the maturity of intelligent initiation-control technologies.

Looking forward, digital twin technology offers a promising direction by combining multiphysics penetration models with sparse but high-value experimental and live-fire data to construct an evolving virtual representation of fuze response and degradation. Such a framework may support not only post-test analysis but also reliability prediction, failure-mode tracing, and functional-margin assessment throughout the development process. Meanwhile, embedded self-diagnostic and data-recording capabilities should be strengthened to capture key response features and failure signatures during penetration, even when complete data recovery is not possible. These capabilities can help close the loop between design assumptions, test observations, and field performance. The reliability of modern penetration fuzes should be supported by a progressively validated, quantitatively assessed, and continuously updated evidence chain.

7 Summary and prospects

7.1 Summary

Focusing on the advancement of HTPFs, this paper outlines the trajectory of their technological evolution. Based on this comprehensive overview of penetration fuze technology, the primary conclusions are summarized as follows:

(1) The development of penetration fuze technology is characterized by a clear

evolutionary trajectory, progressing from mechanization and electronization to digitalization and, ultimately, intelligence. Although divergent research methodologies are observed globally, particularly concerning target sensing mechanisms, control strategies, and system architectures, the overarching developmental direction remains consistent. Collective focus is directed toward key objectives, including the enhancement of high-g load resistance, the achievement of accurate target sensing, and the realization of intelligent initiation control.

(2) Regarding penetration deceleration characteristics, existing research has been primarily focused on the mechanical analysis of the projectile body, with preliminary progress being achieved in theoretical modeling and numerical simulation. However, research concerning the dynamic response of the projectile-fuze system and the high-g load transfer mechanisms between components remains insufficient. In particular, systematic investigations into the projectile-fuze connection structures are still lacking.

(3) The overlapping and aliasing of deceleration signals constitute critical challenges affecting the initiation recognition accuracy of HTPF. Currently, these issues are primarily suppressed through material optimization, filtering algorithms, and mechanical filtering techniques. With the advent of emerging combat modalities, such as hypersonic strikes, deceleration signals are expected to become increasingly complex. Consequently, the development of signal acquisition and processing technologies tailored for extreme velocity conditions is urgently required.

(4) Initiation control strategies are governed by multiple constraints, including penetration conditions, target characteristics, and projectile structure, etc. Current research on initiation control methods is primarily conducted based on time-domain and magnetic information, with preliminary progress being achieved in multi-domain information fusion. While deep learning has been introduced to this field in recent years, its application remains in the nascent stages. In the future, model-driven initiation control strategies based on deep learning could be further explored. Such advancements will facilitate the evolution of initiation control toward greater intelligence, systematization, and robust generalization capabilities.

(5) More stringent requirements are imposed on fuze reliability by the modalities

of modern warfare. Although Markov models have been introduced to the analysis of fuze safety systems in some studies, related explorations remain relatively limited. In recent years, safety margin analysis has increasingly been prioritized by researchers; however, reliability research specifically concerning HTPFs remains scarce, and a specialized, systematic analytical methodology has yet to be fully established.

7.2 Prospects

In response to the evolving trends of system-of-systems warfare and the shift toward informationized and intelligentized operations, increasingly rigorous requirements are being imposed on HTPFs by emerging operational patterns, combat environments, and advanced weaponry. The projected future developmental trajectories for HTPFs are summarized in Fig. 38 and are detailed as follows.

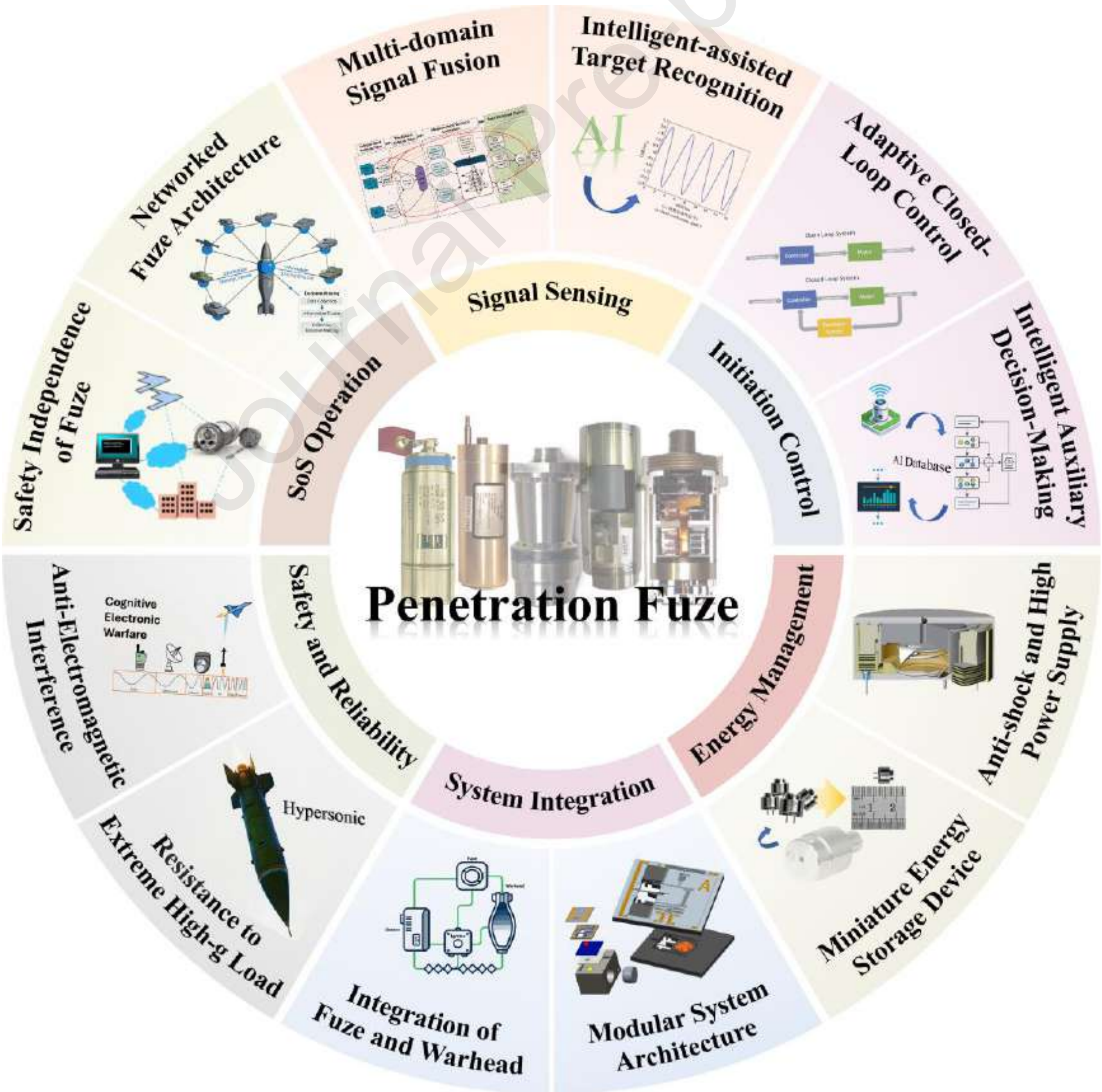

Fig. 38. Prospects for the development of penetration fuze technology.

(1) Multi-domain information fusion recognition

Accurate target perception remains the basis of precise initiation. However, acceleration signals are easily affected by projectile vibration, fuze-structure resonance, signal overlapping, and target heterogeneity. Introducing additional sensing channels may improve recognition, but it may also increase signal inconsistency, synchronization difficulty, and system complexity. Future work should start from acceleration-based recognition and gradually incorporate complementary magnetic, acoustic, and timing information. The priority is to identify robust feature combinations for typical layered targets, construct standardized penetration-feature datasets, and develop lightweight fusion models that can improve layer-counting, void-sensing, and penetration-state identification without exceeding embedded computing and safety constraints.

(2) AI-assisted decision-making and initiation control

The main difficulty of adaptive initiation control is transforming uncertain, noisy, and incomplete sensing information into a reliable initiation decision under extremely short time windows. Existing methods are still mainly based on fixed delay. Future development should progress from preset initiation parameters to feature-assisted correction and then to internal pre-initiation computational feedback. The penetration fuze should continuously update penetration state, layer information, and functional health before initiation. AI can support recognition and parameter correction, but deterministic S&A logic should remain the final safety boundary.

(3) High-reliability power supply and energy management

Intelligent sensing, embedded processing, data storage, and adaptive initiation control all require stable energy support, but the power system must survive high-g impact, vibration, temperature variation, and long-term storage. Insufficient or unstable energy may directly affect recognition, timing, and initiation reliability. Future research should treat power supply as a system-level design constraint rather than an isolated component. Power-source selection, energy activation, voltage regulation, low-power acquisition, algorithm complexity, and initiation-control timing should be co-designed. The route should emphasize high-reliability activation, energy prioritization during the penetration window, and coordinated energy management among sensors, processors, storage units, and execution modules.

(4) Modular integration and functional unification

HTPFs must integrate sensing, signal conditioning, embedded processing, power management, safety logic, and initiation execution within a constrained volume while maintaining high-g survivability, interface compatibility, storage reliability, and testability in the future. Excessive functional stacking may increase structural coupling, failure modes, and verification cost. Future design should shift from component-level optimization to modular system architecture. Sensing, computation, energy, and execution modules should be functionally coordinated, while safety-critical logic should remain independently constrained. Standardized interfaces, robust packaging, redundant key links, and design-for-testability should be introduced early. The goal is a compact, maintainable, and verifiable sensing-decision-execution unit.

(5) Interference resistance under extreme environment

Future HTPFs will face stronger mechanical, thermal, electrical, and electromagnetic disturbances, especially under high-speed or complex penetration conditions. Fuze failure may arise from circuit damage, interconnection failure, data loss, electromagnetic interference, or algorithmic misjudgment. Future research should expand anti-interference design from signal filtering to mechanical-electrical-information reliability. The route should combine high-shock-resistant sensors, reinforced packaging, robust interconnections, shock-isolation structures, redundant sensing, fault-tolerant logic, and electromagnetic compatibility design. Anti-interference capability should be embedded into the whole fuze architecture, so that sensing, computation, energy supply, and initiation-control modules maintain coordinated reliability under extreme environments.

(6) Systematic networked collaboration and information sharing

In system-of-systems warfare, HTPFs may evolve from isolated initiation devices to information-aware nodes within the weapon system. However, information sharing must not weaken fuze safety independence or introduce uncontrolled external interference during penetration. Future networked development should proceed cautiously from secure mission-parameter loading, platform-fuze matching, and status monitoring to survivable data recording and post-test data recovery. In the near term, networked collaboration should mainly support pre-launch configuration, in-flight status confirmation, and test-evaluation feedback, rather than unrestricted real-time external control. Cybersecurity protection, electromagnetic compatibility, and lifecycle reliability should be integrated into the system architecture.

Driven by continuous advancements in military technology, HTPFs are progressively transitioning from traditional functional components toward intelligent sensing-decision-execution systems. Future studies should pay more attention to the transition from algorithm-oriented research to system-oriented validation. It should be emphasized that these intelligent functions, especially multi-domain fusion recognition and adaptive closed-loop initiation control, remain at different stages of maturity across countries. In open literature, most reported studies are concentrated on enabling technologies such as sensing, signal processing, feature extraction, and information fusion, whereas publicly verifiable fielded models remain unavailable. Therefore, future reviews should continue to distinguish between operational fuzes, engineering demonstrations, and academic research progress.

Declaration of competing interest

The authors declare that they have no known competing financial interests or personal relationships that could have appeared to influence the work reported in this paper.

Acknowledgements

This work was supported by the National Natural Science Foundation of China (Grant No. 12102320); and the National Science and Technology Major Project (Grant No. J2019-IV-0003-0070).

References

[1] Mou WM, Wu MX, Ju YB, others. Introduction to weapon science and technology. Beijing: National Defense Industry Press; 2025.

[2] Wang DW, Li XF, Wang YB. Theory and technology for hard target smart fuze. Beijing: Beijing Institute of Technology Press; 2021.

[3] Oliphant A. Defining structural dynamic environments for penetrator fuzes. 61st Annual NDIA Fuze

Conference. San Diego, USA; 2018
[4] Zhang H, Dai KR. Development and prospect of advanced fuze technology. Chin Sci Bull 2023;68(25):3293 – 310.
[5] Jiang CL, Wang ZC, Mao L, et al. Ammunition theory. Beijing: National Defense Industry Press; 2022.
[6] Shi KL, Gui YN, Niu LJ, others. Fuze technology. Beijing: National Defense Industry Press; 2025.
[7] Li HS, Zhang XQ, Gao JC. A cloud model target damage effectiveness assessment algorithm based on spatio-temporal sequence finite multilayer fragments dispersion. Def Technol 2024;40:48 – 64.
[8] Jiang H, Sun FY, Gao Y. Weapon technology fundamentals. Beijing: National Defense Industry Press; 2025.
[9] Li XF, Wang YB, Wu B. Fuze of penetration ammunition. Beijing: National Defense Industry Press; 2016.
[10] Cai Y, Cheng HC, Zhou DF. Weapon core component technology. Beijing: National Defense Industry Press; 2025.
[11] Parsch A. FEU to FZU - Equipment Listing, https://www.designation-systems.net/usmilav/asetds/u-f.html; 2025 [2025-10-15].
[12] Xue H, Zhou Q, Xiao C, Huang GY. Perspectives on additive manufacturing for warhead applications. Def Technol 2025;43:225 – 51.
[13] Hinge L. CAT-UXO Fuzes, https://cat-uxo.com/explosive-hazards/fuzes; 2026 [2026-4-14].
[14] NDIA. NDIA Conference Proceedings, https://ndia.dtic.mil/; 2026 [2026-4-14].
[15] Clutterbuck R. AURORA Fuze for PGB PWIV. The 50th Annual NDIA Fuze Conference. Norfolk, USA; 2006.
[16] Kaman DI. Evolution of the fmu-143 fuze family. Proceedings of the 48th Annual NDIA Fuze Conference. Charlotte, USA; 2004.
[17] Song YY. Research on Dynamic Characteristics of Projectile-fuze System in Concrete Penetration [D]. Beijing: Beijing Institute of Technology; 2017. (in Chinese)
[18] Yu D, Yang BQ, Yan K, Li CS, Ma X, Han XY, et al. Dynamic transfer model and applications of a penetrating projectile-fuze multibody system. Int Journal Mech Sys Dyn 2023;3(4):360 – 72.
[19] Zhang JM, Zhang H, Yu D, Yang BQ, Chen ZP. Research on dynamic characteristics of missile-fuze system with different connection structures during penetrating multi-layer hard target. Journal of Ordnance Equipment Engineering 2022; 43(9): 186 – 92. (in Chinese)
[20] Zhang A, Liu P, Zhang H. Analysis and experiment of stress concentration in penetration fuze buffer materials under stress wave incursion. Front Phys 2024;12:1401538.
[21] Liu YT, Yan XP, Liu Q, An T, Dai J. Automatic modulation recognition of radio fuzes using a DR2D-based adaptive denoising method and textural feature extraction. Def Technol 2024;34:328 – 38.
[22] Ma MX, Li R, Niu LJ. Evaluation Index of Disturbance Superposition Degree in Multi-layer Penetration Acceleration Signal. Acta Armamentarii 2022; 43(1): 20 – 8. (in Chinese)
[23] Liu J, Cheng XL. A study on the overload transmission characteristics of penetrating fuze threaded connection structures. The 21st Fuze Academic Annual Conference of the China Ordnance Society. 2019:457 – 62.
[24] Liu P, Li J, Li CS, Li HJ, Zhang JM, Zhang H. Analysis of the influence of different initial velocities on dynamic performance of multi-layer hard target penetration process. Front Phys 2023;11:1241762.
[25] Nance C. LEEFI detonator characterization in high temperature applications. 65th Annual NDIA

Fuze Conference. Renton, USA; 2022.

[26] Wang YL, Li CS, Zhang H, Wang XF. Research on a rapid prediction method for magnetic anomaly responses in the penetration process based on an improved proper orthogonal decomposition (POD)-radial basis function (RBF) neural network. Measurement 2025;256:118266.

[27] Campbell J. Mechanical survivability of embedded fireset in quasi-static and dynamic high-pressure environment. 59th Annual NDIA Fuze Conference. Charleston, USA; 2016.

[28] Wiese J. Joint programmable fuze emulation. Proceedings of the 53rd Annual NDIA Fuze Conference. Lake Buena Vista, USA; 2009.

[29] Oliphant A. Tail Kit Impact Environment Analysis and Ground Test Design. The *62nd Annual NDIA Fuze Conference*. Buffalo, USA; 2019.

[30] Peairs D, Millard N, Dao T, Worthington M, Doolittle C. Test method to evaluate high-G component susceptibility. 61st Annual NDIA Fuze Conference. San Diego, USA; 2018: 1 – 12.

[31] Morales E. Hard Target Detonator Pyroshock Testing and Test Results. The *65th Annual NDIA Fuze Conference*. Renton, USA; 2022.

[32] Cochran K. Survivable fuzing for high-speed engagements of maritime targets. 65th Annual NDIA Fuze Conference. Renton, USA; 2022.

[33] White C, Curtis S. Effects of orientation & boundary condition on encapsulated electronics. Proposed for Presentation at the NDIA 64th Annual Fuze Conference. Online; 2021.

[34] Dosch J. Calibration and Acceptance Tests for Accelerometers Used in Severe Shock Applications. The *62nd Annual NDIA Fuze Conference*. Buffalo, USA; 2019.

[35] Atwell AR, Okojie RS, Kornegay KT, Roberson SL, Beliveau A. Simulation, fabrication and testing of bulk micromachined 6H-SiC high-g piezoresistive accelerometers. Sens Actuators A Phys 2003;104(1):11 – 8.

[36] Euba C. Testing capabilities and instrumentation strategies. 58th Annual NDIA Fuze Conference. Baltimore, USA; 2015.

[37] Yao W, Pan X, Qian J, others. Intelligent ammunition system engineering and related technologies. Beijing: Beijing Institute of Technology Press; 2021.

[38] Siefke W. Air force fuze overview. Proceedings of the 47th Annual NDIA Fuze Conference. New Orleans, USA; 2003.

[39] Turner L. Hard target reliability for MAFIS. 50th Annual NDIA Fuze Conference. Norfolk, USA; 2006.

[40] Turner LJ. AURORA – Next Generation Fuzing System. The *53rd Annual NDIA Fuze Conference*. Lake Buena Vista, USA; 2009.

[41] Tobik T. United states air force fuze science technology. 56th Annual NDIA Fuze Conference. Baltimore, USA; 2012.

[42] Curtis S. Advanced fuzing technology. 63rd Annual NDIA Fuze Conference. Online; 2020.

[43] Smith-Roberts B. Fuze Incident, Shoalwater Bay, Australia, 2014. The *63rd Annual NDIA Fuze Conference*. Online; 2020.

[44] Schumacher L. Test observed considerations for embedded smart fuzing of penetrating munitions. 62nd Annual NDIA Fuze Conference. Buffalo, USA; 2019.

[45] Connolly M. Hardened selectable multipoint fuzing. Proceedings of the 60th Annual NDIA Fuze Conference. Cincinnati, USA; 2017.

[46] Walker L. Test and model observed needs for natural media test design supporting embedded smart fuzing. 65th Annual NDIA Fuze Conference.Renton, USA; 2022.

[47] Wikipedia. GBU-57A/B_MOP, https://en.wikipedia.org/wiki/GBU-57A/B_MOP; 2026 [2026-4-14].

[48] Wikipedia. GBU-28B/B, https://en.wikipedia.org/wiki/GBU-28B/B; 2026 [2026-4-14].

[49] Wikipedia. GBU-28C/B, https://en.wikipedia.org/wiki/GBU-28C/B; 2026 [2026-4-14].

[50] Wang HF, Yu QB, Ge C. Physics of reactive filling enhanced penetrating warheads. Beijing: Beijing Institute of Technology Press; 2020.

[51] Moxnes JF, Frøyland Ø, Skriudalen S, Prytz AK, Teland JA, Friis E, et al. On the study of ricochet and penetration in sand, water and gelatin by spheres, 7.62 mm APM2, and 25 mm projectiles. Def Technol 2016;12(2):159 – 70.

[52] Lauden M. BLU-122 Warhead Program Precision Strike Technology Symposium. The *49th Annual NDIA Fuze Conference*. Seattle, USA; 2005.

[53] Perrin M. European LEEFI based fireset and ESAD. 59th Annual NDIA Fuze Conference. Charleston, USA; 2016.

[54] Hendershot J. Weapon fuzing/safety & arming programs overview. Proceedings of the 47th Annual NDIA Fuze Conference. New Orleans, USA; 2003.

[55] Kopp C. Soviet/Russian guided bombs: APA-TR-2009-0806[R]. AusAirPower; 2009

[56] Deagel. YJ-1000, https://www.deagel.com/Weapons/YJ-1000-1/a004286; 2023 [2026-6-10].

[57] Wikipedia. GBU-24 Paveway III, https://en.wikipedia.org/wiki/GBU-24_Paveway_III; 2026 [2026-4-15].

[58] Wikipedia. BLU-109 bomb, https://en.wikipedia.org/wiki/BLU-109_bomb; 2026 [2026-4-15].

[59] Wikipedia. GBU-27 Paveway III, https://en.wikipedia.org/wiki/GBU-27_Paveway_III; 2026 [2026-4-15].

[60] Lotz AD, Hicks M. Binary Trial and Statistical Analysis Methods for Electro-Explosive Device Characterization. The *64th Annual NDIA Fuze Conference*. Online, 2021.

[61] SAM. BLU-138 Warhead, https://sam.gov/opp/1dee4cc1d6934bf691c541cebe72d701/view; 2026 [2026-6-10].

[62] Jr. King S. Eglin AFB test squadron releases GBU-72 for first time, https://www.af.mil/News/Article-Display/Article/2808949/eglin-afb-test-squadron-releases-gbu-72-for-first-time/; 2021 [2026-6-10].

[63] U.S. Department of Defense. Fiscal Year (FY) 2026 Budget Estimates, https://www.saffm.hq.af.mil/Portals/84/documents/FY26/FY26%20Air%20Force%20Ammunition%20Procurement.xml; 2025 [2026-6-3].

[64] Shen RQ, Ye YH. *Special Effects and Applications of Energetic Materials*. Beijing: National Defense Industry Press; 2020.

[65] Wikipedia. BLU-116, https://en.wikipedia.org/wiki/BLU-116; 2026 [2026-4-15].

[66] Wang ZC, Li M, Jiang CL, others. Introduction to ammunition. Beijing: Beijing Institute of Technology Press; 2024.

[67] AFRL. Partnership Rapidly Transitions Advanced Penetrating Weapon | Air Force Research Laboratory, https://afresearchlab.com/partnership-rapidly-transitions-advanced-penetrating-weapon-2/; 2026 [2026-6-3].

[68] Qian LF, Zhang L, Chen GS. Long range artillery and rocket technology. Beijing: National Defense Industry Press; 2025.

[69] Miller EA. Global strike capabilities: the ballistic missile option. Astropolitics 2004;2(1):1 – 31.

[70] Parsch A. Boeing GBU-57/B MOP, https://www.designation-systems.net/dusrm/app5/mop.html;

2026 [2026-6-2].

[71] ARA. ARA Awarded Next Generation Penetrator Contract, https://www.ara.com/news/ara-awarded-next-generation-penetrator-contract/; 2025 [2026-6-2].

[72] USA Spending. Contract to Applied Research Associates, inc., https://usaspending.gov/award/CONT_AWD_FA868125FB063_9700_FA865621DA007_9700; 2026 [2026-6-2].

[73] Zhang YM, Wang NF, Ma WH, Wang R, Bai L, Wu Y. Investigations of the mechanical response of dummy HTPB propellant grain under ultrahigh acceleration overload conditions using onboard flight-test measurements. Def Technol 2024;32:473 – 84.

[74] Zhang H, Li ZS, Zhou XD. Theory and technology of information interaction between fuze and weapon system. Beijing: Beijing Institute of Technology Press; 2021.

[75] Urzay J. Supersonic combustion in air-breathing propulsion systems for hypersonic flight. Annu Rev Fluid Mech 2018;50:593 – 627.

[76] News U. Report to Congress on U.S. Army's Dark Eagle Hypersonic Weapon, https://news.usni.org/2026/04/09/report-to-congress-on-u-s-armys-dark-eagle-hypersonic-weapon; 2026 [2026-6-3].

[77] Navy. Contracts for March 31, 2026, https://www.war.gov/News/Contracts/Contract/Article/4448853/contracts-for-march-31-2026/; 2026 [2026-6-3].

[78] Mallory S. Navy Wants to Start Conventional Prompt Strike Tests Aboard USS Zumwalt in 2027, https://news.usni.org/2024/11/14/navy-wants-to-start-conventional-prompt-strike-tests-aboard-uss-zumwalt-in-2027; 2024 [2026-4-14].

[79] Air Force. Air Force announces hypersonic missile contract award, https://www.af.mil/News/Article-Display/Article/3167976/air-force-announces-hypersonic-missile-contract-award/; 2022 [2026-4-14].

[80] Sayler KM. Hypersonic Weapons: Background and Issues for Congress, https://s3.documentcloud.org/documents/26049568/hypersonic-weapons.pdf; 2025 [2026-6-3].

[81] Faulconbridge G. Putin deploys new Zircon hypersonic cruise missiles to Atlantic, https://www.reuters.com/world/europe/putin-sends-off-frigate-armed-with-new-hypersonic-cruise-missile-2023-01-04/; 2023 [2026-4-14].

[82] Threat M. Oreshnik, https://missilethreat.csis.org/missile/oreshnik/; 2026 [2026-4-14].

[83] Threat M. Kh-47M2 Kinzhal, https://missilethreat.csis.org/missile/kinzhal/; 2024 [2026-4-14].

[84] Montgomery AH, Nelson AJ. Ukraine and the Kinzhal: Don't believe the hypersonic hype | Brookings, https://www.brookings.edu/articles/ukraine-and-the-kinzhal-dont-believe-the-hypersonic-hype/; 2023 [2026-4-14].

[85] Arianegroup. Hypersonic systems, https://www.ariane.group/en/defence-systems/hypersonic-systems/; 2026 [2026-6-3].

[86] MBDA. MBDA unveils STRATUS for future cruise and anti-ship capabilities, https://www.mbda-systems.com/mbda-unveils-stratus-future-cruise-and-anti-ship-capabilities; 2025 [2026-6-3].

[87] MBDA. MBDA welcomes Italy's intent to join the FC/ASW programme, https://www.mbda-systems.com/mbda-welcomes-italys-intent-join-fcasw-programme; 2023 [2026-6-3].

[88] Defence MO, Mp HB. UK and France strengthen defence cooperation with new weapon system agreement, https://www.gov.uk/government/news/uk-and-france-strengthen-defence-cooperation-with-new-weapon-system-agreement; 2017 [2026-4-14].

[89] U.S. Department of Defense. 2025 Annual Report to Congress: Military and Security Developments Involving the People's Republic of China, https://media.defense.gov/2025/Dec/23/2003849070/-1/-1/1/ANNUAL-REPORT-TO-CONGRESS-MILITARY-AND-SECURITY-DEVELOPMENTS-INVOLVING-THE-PEOPLES-REPUBLIC-OF-CHINA-2025.PDF; 2025 [2026-6-3].

[90] Boyd H, Barrie D. Chinese triad: a nuclear family affair, https://www.iiss.org/online-analysis/military-balance/2025/09/chinese-triad-a-nuclear-family-affair/; 2025 [2026-6-3].

[91] Peters AB, Zhang DJ, Chen S, Ott C, Oses C, Curtarolo S, et al. Materials design for hypersonics. Nat Commun 2024;15:3328.

[92] Zhang H, Li HJ. The fuze mechanism. Beijing: Beijing Institute of Technology Press; 2014.

[93] Hinge L. CAT-UXO Warheads, https://cat-uxo.com/explosive-hazards/warheads; 2026 [2026-4-14].

[94] Willis M. Joint programmable fuze. 53rd Annual NDIA Fuze Conference. Lake Buena Vista, USA; 2009.

[95] Muthig H. Penetrating Effector Systems from EADS / TDW. The *Precision Strike Technology Symposium (PSTS – 05)*. Laurel, USA; 2005.

[96] Perrin M. Hard Target Fuzing Solutions. The *52nd Annual NDIA Fuze Conference*. Sparks, USA; 2008.

[97] Agency DTR. Fiscal Year (FY) 2008/2009 budget estimates: Procurement, defense-wide. USA: Department of Defense; 2007.

[98] Malinoski N. Army Fuze S&T Overview. The *63rd Annual NDIA Fuze Conference*. Online; 2020.

[99] Air Force. Department of War Fiscal Year (FY) 2027 Budget Estimates, https://www.af.mil/Portals/1/documents/Secretariat%20of%20the%20AF/SAF-FM/Budget%20-%202027/Budget%20docs/FY27%20Air%20Force%20Aircraft%20%20Ammunition%20Procurement.pdf; 2026 [2026-4-14].

[100] DOT&E. DOT&E FY2025 Annual Report - Air Force - Massive Ordnance Penetrator (MOP) Modification, https://www.dote.osd.mil/Portals/97/pub/reports/FY2025/af/2025mop.pdf; 2025 [2026-6-3].

[101] Wang ZX, Zheng HL, Wang MY, Li XT, Li XC, Luo CW, et al. Data-driven lightweighting and terminal lethality enhancement of PELE projectiles: a comparative machine learning and multi-objective optimization framework. Def Technol 2026. https://doi.org/10.1016/j.dt.2026.03.007

[102] Li M, Hu TJ. Research status and development trend of MEMS S&A devices: a review. Def Technol 2021;17(2):450–6.

[103] Li Y, Pan ZW, Shang F. High-impact overload penetration attitude measurement using accelerometer array. 2025 5th International Conference on Sensors and Information Technology. Nanjing, China. IEEE, 2025:80–5.

[104] Shi YB, Li Y, Zhang JJ, Zhao R, Wang YT, Cao HL, et al. Design and experiment of a hybrid-integrated ultrahigh-g accelerometer with variable-section beam. IEEE Trans Instrum Meas 2023;72:2003811.

[105] Zu J, Ma X, Zhang Y, Yu D, Dai KR. Adaptive end-side intelligent feature recognition system for acceleration measurement signals with strong adhesion interference under continuous multi-impact. Def Technol 2026. https://doi.org/10.1016/j.dt.2025.12.018

[106] Xia M, He LL, Gu Y, Liu XJ, Murengami BG, Janneh LL, et al. Tassel counting of individual ridge from UAV RGB imagery based on YOLOv8m with deep SORT and double-step Otsu thresholding algorithm by filtering abnormal IDs for maize breeding. Comput Electron Agric 2025;239:111041.

[107] Han W, Li CJ, Su XC, Zhang Y, Guo F, Yu TT, et al. Real-time decision support for bolter recovery safety: long short-term memory network-driven aircraft sequencing. Def Technol 2026;56:184 – 205.

[108] Senjaya D, Limantoro SE. Enhancing reconstruction capability of wavelet transform amorphous radial distribution function *via* machine learning assisted parameter tuning. J Non Cryst Solids 2026;681:124062.

[109] Ning Z, Li A, Zhai Z, Cheng ZY, Zhao SM, Wang M, et al. Design and characterization of multi-point exploding foil initiator system for directional warheads. Energ Mater Front 2026. https://doi.org/10.1016/j.dt.2025.12.018

[110] Haynes A. Optimized Potting Solutions for High G Electronics: Optimization Methodology. The *61st Annual NDIA Fuze Conference*. San Diego, USA; 2018.

[111] Choi Y, Seok M, Yoon SH, Uhm WY, Jang J, Cho Y, et al. High-G MEMS accelerometer with cross-symmetric structures. IEEE Sens J 2024;24(2):1275 – 86.

[112] Zhang KJ, Yang BQ, Zhu ZS, Fu JT, Han XY, Zhang WL, et al. Structural optimized mechanical metamaterial for multi transient high-g impact suppression and self-monitoring. Mater Des 2025;253:113884.

[113] Kim S, Lee S, Lee J, Kim M, Yoon H, Youn BD. Multi-scale signal transformer with signal processing-based attention interpretation for fault diagnosis of rotating machinery under variable speed conditions. Reliab Eng Syst Saf 2026;271:112243.

[114] Lv Y, Liu HY, Yuan R, Dong X, Wang YF, Wu H, et al. Advances and prospects of phase space reconstruction-based high-dimensional signal processing for fault diagnosis: a systematic review. Mech Syst Signal Process 2026;246:113919.

[115] Wu SM, Guan YJ, Tian Y, Yang ZB, Cao JH, Tian SH, et al. Blade micro-Doppler measurement: a novel non-contact rotor blade vibration measurement method compliant with the Nyquist – Shannon sampling theorem. Mech Syst Signal Process 2025;238:113197.

[116] Schmidt A. Hypersonic Capabilities: A Journey from Almighty Threat to Intelligible Risk, https://www.armyupress.army.mil/Journals/Military-Review/English-Edition-Archives/March-2024/Hypersonic-Capabilities/; 2024 [2026-4-14].

[117] Shi YB, Qu YT, Zhao R, Wang YT, Guo C, Cao HL, et al. Integrated package and calibration of high-g MEMS ASIC acceleration sensor. Measurement 2025;240:115510.

[118] Guo HN, Shi YB, Zhao R, Chen YN, Zhang P, Chen L, et al. Impact attenuation mechanism of single/double-layer potting structures of MEMS devices under continuous double-pulse impact. Def Technol 2025;48:104 – 14.

[119] Krafick J. MEMSAD - Maturing the Technology, Part II. The *65th Annual NDIA Fuze Conference*. Renton, USA; 2022.

[120] Cao C. High Shock Modeling of Fuze Components. The *65th Annual NDIA Fuze Conference*. Renton, USA; 2022.

[121] Neff C. Next generation additively manufactured survivable 3D conformal fuze radome antenna. 65th Annual NDIA Fuze Conference. Renton, USA; 2022.

[122] Cao C. High voltage fireset component behavior at elevated temperatures. 64th Annual NDIA Fuze Conference. Online; 2021.

[123] Pray D. Exploding foil initiator development. Proceedings of the 64th Annual NDIA Fuze Conference. Online; 2021.

[124] Jolly G. Air force S&T strategy. 63rd Annual NDIA Fuze Conference. Online; 2020.

[125] Leibovich T. Proximity sensors for hypersonic applications. 62nd Annual NDIA Fuze Conference. Buffalo, USA; 2019.

[126] Joshi V. Small-Scale Testing of Electronic Components in Shock Loading. The *62nd Annual NDIA Fuze Conference*. Buffalo, USA; 2019.

[127] May C. Survivability and Reliability of Silicon MEMS Components. The *62nd Annual NDIA Fuze Conference*. Buffalo, USA; 2019.

[128] Hatcher T. Evaluation of embedded fuze components in explosives. 62nd Annual NDIA Fuze Conference. Buffalo, USA; 2019.

[129] Gun JD. Hardened command armed MEMS fuze. 61st Annual NDIA Fuze Conference. San Diego, USA; 2018.

[130] Connolly M. Hardened selectable multipoint fuzzing (HSMF). 61st Annual NDIA Fuze Conference. San Diego, USA; 2018.

[131] Etheridge M. Design Guidelines for Implementing a Low Voltage Distributed Fuzing System. The *61st Annual NDIA Fuze Conference*. San Diego, USA; 2018.

[132] Chen E. Using Modeled Impact Response of 3-D Printed Materials for High-G Survivability. The *60th Annual NDIA Fuze Conference*. Cincinnati, USA; 2017.

[133] Schrand A. Shock Testing of 3D Printed Multi-material Circuits. The *60th Annual NDIA Fuze Conference*. Cincinnati, USA; 2017.

[134] Tesla M. Modeling and simulation of a high fidelity electronics assembly responding to drop test. Proceedings of the 60th Annual NDIA Fuze Conference. Cincinnati, USA; 2017.

[135] Connolly M. Hardened Selectable Multipoint Fuze (HSMF) - JFT Project. The *59th Annual NDIA Fuze Conference*. Charleston, USA; 2016.

[136] Hill J. Using multiple G-switches for target detection. 59th Annual NDIA Fuze Conference. Charleston, USA; 2016.

[137] Euba C. Advantages of an EFI multi-point initiation system to direct the warhead performance. The *59th Annual NDIA Fuze Conference*. Charleston, USA; 2016.

[138] Northrop Grumman. FMU-167/B Hard Target Void Sensing Fuze Datasheet, https://cdn.northropgrumman.com/-/media/Project/Northrop-Grumman/ngc/what-we-do/missile-products/FMU-167B-Datasheet.pdf; 2025 [2026-6-9].

[139] U.S. Air Force. FY2026 Air Force Ammunition Procurement Justification Book, https://www.saffm.hq.af.mil/Portals/84/documents/FY26/FY26%20Air%20Force%20Ammunition%20Procurement.pdf; 2025 [2026-6-9].

[140] MBDA. TAURUS KEPD 350 Product Sheet, https://www.mbda-deutschland.de/wp-content/uploads/2018/03/Taurus-e-18.pdf; 2018 [2026-4-14].

[141] U.S. Department of Defense. Acquisition of the Air Force Hard Target Void Sensing Fuze Program, https://media.defense.gov/2013/Aug/21/2001713296/-1/-1/1/DODIG-2013-118.pdf; 2013 [2026-6-9].

[142] Yu MZ, Wu XY, Zhao LB, Jia C, Xia Y, Han XG, et al. Monolithically integrated triaxial high-performance high-g accelerometer for high shock vibration signal measurements. Microsyst Nanoeng 2025;11:206.

[143] ODNI. Annual Threat Assessment of the U.S. Intelligence Community, https://www.dni.gov/files/ODNI/documents/assessments/ATA-2025-Unclassified-Report.pdf; 2025 [2026-6-9].

[144] Service CR. Hypersonic Weapons: Background and Issues for Congress,

https://www.everycrsreport.com/files/2023-01-10_R45811_4ea364e6ea0537d2ad12d8b51502d41bc5e5df29.html; 2023 [2026-4-14].

[145] Adams N. Antifuse Obsolescence Mitigation in ESAD Applications: Analysis of High Shock, Acceleration and Vibration Effects on Safety Critical Logic Devices. The *62nd Annual NDIA Fuze Conference*. Buffalo, USA; 2019.

[146] Gokce C. Applied Tests Simulating the Impact Shock on an Operating ESAD inside a Missile/Smart Munition. The *61st Annual NDIA Fuze Conference*. San Diego, USA; 2018.

[147] Curtis S. Modeling and Experimentation of Embedded Fuzing Fire-Train in Harsh Dynamic Pressure Environments. The *65th Annual NDIA Fuze Conference*. Renton, USA; 2022.

[148] Mlejnek M. Embedded Fuze Forward Assembly Cannon Test. The *62nd Annual NDIA Fuze Conference*. Buffalo, USA; 2019.

[149] Marquardt P. The Influence of Explosive Fill Dynamics on Embedded Smart Fuzing for Hard Target Munitions. The *61st Annual NDIA Fuze Conference*. San Diego, USA; 2018.

[150] Lefrancois A. Influence of the Embedded Position for Damages and Reactive Threshold Induced by Concrete Penetration. The *60th Annual NDIA Fuze Conference*. Cincinnati, USA; 2017.

[151] Malechuk A. Development of Modeling Methodologies for Simulation of Fuze Firetests Embedded in Explosive Fill. The *59th Annual NDIA Fuze Conference*. Charleston, USA; 2016.

[152] Kim J. MEMS G-Switch Encapsulation for High-G Environments. The *61st Annual NDIA Fuze Conference*. San Diego, USA; 2018.

[153] O’Connor KM Jr. Developments in metal MEMS latching, setback sensing mechanism. 63rd Annual NDIA Fuze Conference. Online; 2020.

[154] Jean D. Fully resettable MEMS safe/arm with lock and slider position feedback. 63rd Annual NDIA Fuze Conference. Online; 2020.

[155] Pray D. Detonation transfer reliability-axial and angular alignment evaluations using a neyer statistical sensitivity approach. 64th Annual NDIA Fuze Conference. Online; 2021.

[156] Risha SJ. Hard target detection algorithm using multi-threshold G-switches. Proceedings of the 59th Annual NDIA Fuze Conference. Charleston, USA; 2016.

[157] Chen A. Development and simulation of high curie temperature PZT material for impact sensing in hypersonic environments. 65th Annual NDIA Fuze Conference. Renton, USA; 2022.

[158] Jolly G. Fuze S T decomposition —hard target defeat. 63rd Annual NDIA Fuze Conference. Online; 2020.

[159] Gutser R. Shock Hardened Multi-Output Fuze for TDW's Radius® Controllable Effect Technology. The *59th Annual NDIA Fuze Conference*. Charleston, USA; 2016.

[160] Tesla M. Grand Challenge Test Article 2 Modeling During Impact on Very High G Machine. The *59th Annual NDIA Fuze Conference*. Charleston, USA; 2016.

[161] Cao C. High Shock Modeling of Fuze Components. The *64th Annual NDIA Fuze Conference*. Online; 2021.

[162] Cao C. High Voltage Fireset Component Behavior at Elevated Temperatures. The *65th Annual NDIA Fuze Conference*. Renton, USA; 2022.

[163] Christenson T. Integrated Inertia Switches for Fuzing Applications. The *60th Annual NDIA Fuze Conference*. Cincinnati, USA; 2017.

[164] Cochran K. High Reliability DPICM Replacement (HRDR). The *61st Annual NDIA Fuze Conference*. San Diego, USA; 2018.

[165] Ostar-Exel L. Development and Testing of Setback Locks for High Reliability in DPICM-XL. The

62nd Annual NDIA Fuze Conference. Buffalo, USA; 2019.

[166] Mckinnon C. Smart Distributed Embedded Fuzing: Current and Future Research Directions. The *62nd Annual NDIA Fuze Conference*. Buffalo, USA; 2019.

[167] Beliveau A. Instrumentation methods for distributed embedded fuzes environment in hard target attack. 65th Annual NDIA Fuze Conference. Renton, USA; 2022.

[168] Morales E. Hard target detonator research using binderized RSI-007 and alternate microchip. 60th Annual NDIA Fuze Conference. Cincinnati, USA; 2017.

[169] Zheng L. Characterization of Materials for EFI Performance. The *65th Annual NDIA Fuze Conference*. Renton, USA; 2022.

[170] Gutsler R. Explicit dynamics based system simulation of hardened fuzing systems. Proceedings of the 60th Annual NDIA Fuze Conference. Cincinnati, USA; 2017.

[171] Joshi V. Dynamic characterization of shock mitigating materials for electronics assemblies subjected to high acceleration. 61st Annual NDIA Fuze Conference. San Diego, USA; 2018.

[172] Knobler R. OmniShock™: a high G data recorder and wireless data exfiltration system for penetration testing. 59th Annual NDIA Fuze Conference. Charleston, USA; 2016.

[173] Metria GP. New high speed, high acceleration data recorder. 59th Annual NDIA Fuze Conference. Charleston, USA; 2016.

[174] Norris J. Detonator survivability phase 1: post environmental evaluation of DHD detonator and RSI-1120 detonator. 65th Annual NDIA Fuze Conference. Renton, USA; 2022.

[175] Chang GN, Fu WX, Zhao JM, Li JP, Miao HC, Zhang XF, et al. Overview of research on intelligent swarm munitions. Def Technol 2025;54:225–44.

[176] Sui L, Niu SH, Shi GC. Fundamental of MEMS elements design for fuze. Beijing: National Defense Industry Press; 2016.

[177] Lou W, Feng Y, Niu L. High dynamic microsystems and MEMS fuze technology. Beijing: National Defense Industry Press; 2016.

[178] Liu P, Li J, Yu H, Zhang H. Innovation of control technology for smart fuzes: precise detonation and efficient damage *via* a ternary cascade controller. Front Phys 2023;11:1309373

[179] Zhang DM, Gao SQ, Niu SH, Liu HP. Study on collision of threaded connection during impact. Int J Impact Eng 2017;106:133–45.

[180] Rudin C. Stop explaining black box machine learning models for high stakes decisions and use interpretable models instead. Nat Mach Intell 2019;1(5):206–15.

[181] Rehan M, Mansoor M. Application of MEMS in safety and arming devices: an overview. Microsyst Technolog 2021;27(10):3599–610.

[182] Li BM, Others. Directed energy and electromagnetic weapon technology. Beijing: National Defense Industry Press; 2025.

[183] Zhou Y, Cao RG, Li P. A target spatial location method for fuze detonation point based on deep learning and sensor fusion. Expert Syst Appl 2024;238:122176.

[184] Seshia SA, Sadigh D, Sastry SS. Toward verified artificial intelligence. Commun ACM 2022;65(7):46–55.

[185] Chen BH, Zhao SW, Zou HH, Wang WG, Dai XH, Wang KH. Research Progress of Overload Signal Characteristics and Processing Technologies of Penetrating Projectile. *Acta Armamentarii* 2024; 45(9): 2906–28. (in Chinese)

[186] Yang SX, Zhao LY, Yan XY. Dynamic stability of spinning missiles. Beijing: National Defense Industry Press; 2014.

[187] Wang YL, Li CS, Wang XF. A multi-source information fusion layer counting method for penetration fuze based on TCN-LSTM. Def Technol 2024;33:463 – 74.

[188] Shi YH, Yang P, Deng ZF, Xie RZ, Chen JH, Guo LL, et al. Research Advance on Impact Load Transfer Characteristics and Impact Response Behavior of Bolted Connection Structures. *Packaging Engineering* 2024; 45(19): 1 – 28. (in Chinese)

[189] Zhang DM. Research on the Extreme Overload and Impact Transmission of Projectile-fuze System During High Speed Penetration [D]. Beijing: Beijing Institute of Technology; 2016. (in Chinese)

[190] Zhang DM, Gao SQ, Niu SH. Simulation analysisof stress transmission of screw joint structures during projectile penetration. Acta Armamentarii 2015;36(S1):284 – 8. (in Chinese)

[191] Zhang DM, Gao SQ, Li SZ. Study on impact transfer characteristics of projectile system during penetration. J Sichuan Ordnance 2020;41(12):27 – 34. (in Chinese)

[192] Zhao XL, Ma TH, Xu P, Fan JB. Acceleration signal test and analysis for projectile penetrating into concrete. *Explosion and Shock Waves* 2014; 34(3): 347 – 53. (in Chinese)

[193] Xu PZ, Ma GS, Wang S, Cui SK. Strength calculation and simulation study of threaded connection of penetration fuze. 2024 5th International Seminar on Artificial Intelligence, Networking and Information Technology (AINIT). Nanjing, China. IEEE, 2024:1952 – 7. (in Chinese)

[194] Jian L, Peng L, He Z. Analysis of the influence of different fixation structure missile-fuze system of hard target penntration proess. 2023 3rd International Conference on Electrical Engineering and Mechatronics Technology (ICEEMT). Nanjing, China. IEEE, 2023:469 – 73. (in Chinese)

[195] Guo YC, Wei YP, Zou JL, Huang CG, Wu XQ, Liu ZS, et al. Impact and usage of the shear thickening fluid (STF) material in damping vibration of bolted flange joints. Smart Mater Struct 2019;28(9):095005.

[196] Shi TF, Qi ZY, Liu CS, Li XY. Tension and torsion distributions in tapered threaded connections. Int J Mech Sci 2025;291 – 292:110135.

[197] Yin L, Liu K, Chen W, Ye JH, Zhang M, Fang ZY, et al. Behaviour of screwed connections in cold-formed steel sheets at elevated temperatures. Thin Walled Struct 2025;213:113317.

[198] Zhang YX, Yang Z, Li YL, Cheng XT, Huang ZW. Experimental and theoretical investigation of self-tapping bolt core tube flange column connection of prefabricated steel structure. Eng Struct 2023;278:115482.

[199] Su Y, Li Y, Liu XY, Zhou CY. Study on the Simulation Method of Impact Transmission Characteristics of Threaded Connection Interface of Fuze System. *Transactions of Beijing Institute of Technology* 2024; 44(02): 135 – 45. (in Chinese)

[200] Blackham J, Stoker C, Allen MS, Rapp B. Nonlinear model updating for dynamics of riveted joints. Mech Syst Signal Process 2025;237:113100.

[201] Yan AM, Wang XF, Yang H, Huang FL, Pi AG. Research on the shock response characteristics of a threaded connection using the thin-layer element method. Appl Sci 2021;11(12):5611.

[202] Hu F, Wang JK, Sui ZC, Lin GH, Zhao W, Jin H, et al. A review on research progress of large area thermal protection structures for hypersonic vehicles. Acta Astronaut 2025;232:541 – 56.

[203] Gao SQ, Jin L, Liu HP. Dynamic response of a projectile perforating multi-plate concrete targets. Int J Solids Struct 2004;41(18 – 19):4927 – 38.

[204] Guo YY, Chen C, Wang RZ, Tang EL. Macro meso response and stress wave propagation characteristics of MCT high-voltage switch under shock load. Def Technol 2024;32:317 – 35.

[205] Chen XW. Modelling on the perforation and penetration Ⅰ. Beijing: Science Press; 2019. (in Chinese)

[206] Chen XW. Modelling on the perforation and penetration. Beijing: Science Press; 2019. (in Chinese)
[207] Wang S, Pi AG, Wang SH, Huang H. Influence patterns of shear-thickening gel on overload transmission: a numerical simulation study. J Phys: Conf Ser 2024;2730(1):012065.
[208] Cheng XL, Liu B, Zhao H, Liu J. Dynamic Modeling and Simulation for Penetration Warhead-fuze System. *Acta Armamentarii* 2020; 41(4): 625-33. (in Chinese)
[209] Cheng XL, Zhao H, Liu B, Liu J. Load transfer characteristics of threaded connection structure for penetration fuze. DEStech Transactions on Computer Science and Engineering. 2019, DOI:10.12783/dtcse/iteee2019/28754.
[210] Cheng XL, Zhao H, Jiao M, Ye HF, Li LC. Dynamic response characteristics of the protection system for a projectile-borne recorder under high impact loading. *Explosion and Shock Waves* 2019; 39(12): 114-22. (in Chinese)
[211] Chen BY, Ma X, Yu D, others. Dynamic modeling and simulation of projectile fuze multibody system based on Hunt-Crossley contact model. J Nanjing Univ Sci Technol 2025;49(4):412–23. (in Chinese)
[212] Yu D. Study on high impact dynamic transfer of multi-body system and failure mechanism of typical energy storage devices [D]. Nanjing: Nanjing University of Science & Technology; 2022. (in Chinese)
[213] Zheng ZY, Dong H, Wu HJ, Jia TQ, Yang GX, Huang FL. Nonlinear Dynamic Model and Response Characteristics of Penetration Projectile-fuze System. *Acta Armamentarii* 2025; 46(4): 241-54. (in Chinese)
[214] Ma HL, Wang JY, Fu DX, Zhang R, Li F. Reseach on numerical simulation overload response of semiconductor bridge detonators in multi-layer steel target penetration environment. 2020 Asia-Pacific Conference on Image Processing, Electronics and Computers (IPEC). Dalian, China. IEEE, 2020: 325–329. (in Chinese)
[215] Yuan Y, Cai YQ, Guo HG, Chen PW, Liu R, Wang HF. Time-sequenced damage behavior of reactive projectile impacting double-layer plates. Def Technol 2023;27:263–72.
[216] Chen YJ, Wang YS, Wen Q. Set-forward Overload Factor Simulation of APHE Projectile Base Fuze. *Journal of Detection & Control* 2015; 37(2): 40-5, 50. (in Chinese)
[217] Chen YJ. Numerical Simulation Study of Small-Caliber Armor-Piercing Explosive Projectiles Penetrating Targets [D]. Nanjing: Nanjing University of Science & Technology; 2013. (in Chinese)
[218] Wang XP, Wang YS, Wen Q, Zhang ZB. Fuze Set-forward Overload Empirical Formula of Concrete Target Penetration of Limited Thick. *Journal of Detection & Control* 2017; 39(5): 14-9. (in Chinese)
[219] Wang XP. Research on Technologies Related to Base-Detonating Fuzes for Multi-Functional Ammunition of Large-Caliber Smoothbore Guns [D]. Nanjing: Nanjing University of Science & Technology; 2015. (in Chinese)
[220] Jia SQ, Wang FS, Yu KH, Bai ZG. Study on fuze overload characteristic of high speed rocket in penetration process. *Structure & Environment Engineering* 2016; 43(3): 23-31. (in Chinese)
[221] Shi HF, Ma SJ, Li FY, Wei J, Tang T. The influence of attack angle on projectile trajectory and fuze in oblique penetration. J Phys: Conf Ser 2021;2029(1):012023.
[222] Dai HY. Dynamic characterization of Projectile-fuze System for highspeed intrusion into concrete [D]. Taiyuan: North University of China; 2023. (in Chinese)
[223] Xiao Y, Li C, Miao C, et al. Analysis of overload response characteristics of high-speed penetration of composite heterogeneous warhead. The *Proceedings of SPIE - The International Society for*

Optical Engineering, 2023: 126451C.

[224] Xiao YK. Research on Overload Response Characteristics and Attitude Measurement Methods of Composite Heterogeneous Warhead Projectiles [D]. Nanjing: Nanjing University of Science & Technology; 2023. (in Chinese)

[225] Xu PZ, Ma GS, Zhao N, Shi KL. Research on the characteristics of projectile penetration into water based on fluid-structure Interaction. J Phys Conf Ser 2023;2599(1):012031.

[226] Hu Y, Sun H, Li ZS. Distributed Detection Overload Response of Composite Warhead Penetration Fuze. *Journal of Detection & Control* 2024; 46(1): 54-62. (in Chinese)

[227] Du CH, Li CF, He YX, Shao ZH, Zhang K, Li R. Fuze Dynamic Overload Feature of High Speed Penetration Warhead Terminal Trajectory. *Journal of Detection & Control* 2023; 45(4): 76-81. (in Chinese)

[228] Hua JQ, Li R, Gao WX, Wang ZC. Penetration Overload Characteristics of Multi-layer Crossbeam Structure Target. *Journal of Detection & Control* 2023; 45(1): 61-6. (in Chinese)

[229] Zhang DS, Lu YZ, Zhou T, Wang YS, Wen Q. The overload influence factors of front or rear end penetration fuze. J Detect Control 2016;38(6):41 – 5,50. (in Chinese)

[230] Forrestal MJ, Frew DJ, Hickerson JP, Rohwer TA. Penetration of concrete targets with deceleration-time measurements. Int J Impact Eng 2003;28(5):479 – 97.

[231] Xiao X, Feng SS, Gao YG, Zhang B. Trajectory prediction of rigid projectile for oblique penetration into multi-layer aluminum targets. Int J Impact Eng 2024;190:104967.

[232] Frew DJ, Forrestal MJ, Cargile JD. The effect of concrete target diameter on projectile deceleration and penetration depth. Int J Impact Eng 2006;32(10):1584 – 94.

[233] Liu JF, Zhong MS, Xie XB, Long Y. Dynamic response and microscopic damage mechanism of EFP oblique penetration to the finite aluminum alloy targets. Int J Str Stab Dyn 2026:2750389.

[234] Wang JR, Tang K, Wang JX, Hao XL, Gu MH. Numerical simulation and theoretical modelling of the penetration process of shape-stable rifle bullets into ballistic gelatine. Int J Impact Eng 2026;210:105594.

[235] Liang JX, Ma LY, Liu C, Shen TR, Zhai Z, Xiao C, et al. A prediction model for projectile ballistic characteristics in multi-layered spaced concrete thin targets based on CNN. *Explosion and Shock Waves* 2026; 46(05): 105-19. (in Chinese)

[236] Zhang XY, Wu HJ, Zhang S, Huang FL. Projectile penetration of reinforced concrete considering the effect of steel reinforcement: experimental study and theoretical analysis. Int J Impact Eng 2020;144:103653.

[237] Wang S, Xu PC, Huang HD. Harmonic Analysis Method of Penetration Fuze Weak Link. *Journal of Detection & Control* 2017; 39(3): 12-6. (in Chinese)

[238] Chen XW, Jiao WJ, Song WJ. Long-rod high-speed and hypervelocity penetrations: theoretical models and numerical analyses. Beijing: Science Press; 2025.

[239] Liu B, Cheng XL, Yang H, Zhao H, Wu XX, Liu T. Analysis of Load Characteristics of Fuze during Penetrating a Multi-layer Target Based on the Matching Relation of Projectile and Target. *Acta Armamentarii* 2024; 45(7): 2240-50. (in Chinese)

[240] Zhao H, Cheng XL, Liu J, Liu B, Wu XX. Analysis of loading characteristics of penetrating warhead on fuze in wide frequency domain. Acta Armamentarii 2024;45(10):3696 – 705. (in Chinese)

[241] Gao HY, Guo L, He Y, Wang G, Cai JL, Zhou J, et al. Study on penetration performance and mass abrasion characteristics of Zr-based alloy projectiles penetrating concrete target. Def Technol 2026.

https://doi.org/10.1016/j.dt.2026.01.001

[242] Ge YX, Chen PW, Wu X, Zhou Q, Fan H, Wang CG, et al. Experimental and numerical study on ballistic impact behavior of explosively-welded double-layered Weldox700E targets against ogival-nosed projectiles. Int J Impact Eng 2025;195:105134.

[243] Wang RZ, Wang ZQ, Tang EL, Li L, Yang GL, Cheng C, et al. Predicting the electromechanical properties of small caliber projectile impact igniter using PZT dynamic damage constitutive model considering crack propagation. Def Technol 2023;28:121 – 35.

[244] Wang K, Zheng J, Shi ZJ, Guo S, Ren XL, Hu HW. Anti-overload Research Status Quo of Electronic Safety and Arm Fuze. *Journal of Detection & Control* 2025; 47(1): 15-23. (in Chinese)

[245] Wang HF, Xie JW, Ge C, Guo HG, Zheng YF. Experimental investigation on enhanced damage to fuel tanks by reactive projectiles impact. Def Technol 2021;17(2):599 – 608.

[246] Lou W, Liu C, Wang Z. Protection and reinforcement technology of smart penetration fuze. J Beijing Inst Technol 2012;21(3):285 – 90.

[247] Zhang A, Li ZS, Zhang H, Ma SJ, Yang BQ. Experimental Study on IPM for Buffering and Energy Absorption. *Acta Armamentarii* 2024; 45(7): 2260-9. (in Chinese)

[248] Jiao M, Chen XW, Ruan ZY, Qu M. Numerical analysis on potting protection of electronic components in projectile. Acta Armamentarii 2014;35(S2):51 – 6. (in Chinese)

[249] Jiao M. Protection Analysis and Numerical Simulation onpotting-layer in fuze under high-impact penetration circumstances [D]. Mianyang: China Academy of Engineering Physics; 2014. (in Chinese)

[250] Xu X, Gao SQ, Niu SH, Shen L, Liu HP, Ou ZC. Dynamic Analysis of Projectile-borne Electronic Devices under Impact Loading. *Acta Armamentarii* 2017; 38(7): 1289-300. (in Chinese)

[251] Zhang HT, Zhang K, Li CY, Xu PC. Secondary Packaging Materials to Reduce the Acceleration Sensor Signal Blocking. *Journal of Ordnance Equipment Engineering* 2016; 37(7): 37-41, 73. (in Chinese)

[252] Peng W, Qian SJ, Li CY, Jiang WB, Lv JB, Xu YX. The tritium-induced radiation ageing mechanism of epoxy resin adhesives. Mater Lett 2026;409:140183.

[253] Bozkurt MO, Hooshmand-Ahoor Z, Das S, Deshpande VS. Deformation-induced domains in silicone rubber. J Mech Phys Solids 2026;212:106592.

[254] Bartczak P, Ejm W, Borysiak S. Application of plant-based by-products in the design of sustainable formed-in-place polyurethane foam gaskets. Compos Part B Eng 2026;316:113577.

[255] Xie JW, Zheng YF, Liu ZY, Liu CZ, Liu AX, Chen PW, et al. Enhanced structural damage behavior of liquid-filled tank by reactive material projectile impact. Def Technol 2024;31:211 – 29.

[256] Zhang ZY, Zhao Y, Guo ZY, Cui D, Chang YK. Anti-overload Composite Potting Method of Penetration Fuze. *Journal of Detection & Control* 2023; 45(4): 124-9. (in Chinese)

[257] Zhang MY, Wang JB, Wang D, Shi GC. Overload testing technology of penetrating multi-layer steel target plate. J Sichuan Ordnance 2016;37(10):114 – 6. (in Chinese)

[258] Zhang JM, Zhang H, Yu D. Design of ultra-high g penetration fuze data record device. 2018 IEEE 4th International Conference on Control Science and Systems Engineering (ICCSSE). Wuhan, China. IEEE, 2018:505 – 9.

[259] Guo HG, Zheng YF, He S, Yu QB, Ge C, Wang HF. Reaction characteristic of PTFE/Al/Cu/Pb composites and application in shaped charge liner. Def Technol 2022;18(9):1578 – 88.

[260] Ding LB, Zhang A, Peng JW, Li CS. The protective performance of rubber pads for penetration fuze. Front Mater 2023;10:1284738.

[261] Du H, Weng PP, Fang C, Zhang JJ, Weng GJ. Mechanical-thermal coupling of carbon fiber/aluminum/silicone foams under axial loading. Int J Mech Sci 2025;293:110201.

[262] Kim D, Park G, Baek J, Lim J, Park J, Youn J, et al. Polytetrafluoroethylene-coated carbon nanotube sheet as superhydrophobic microporous layer for polymer electrolyte membrane fuel cells. Int J Hydrogen Energy 2025;186:151708.

[263] Zhang GL, Zhang WJ, Cao WZ, Wang BD, Lai TT, Guo WS, et al. A novel test setup for determining waterproof performance of rubber gaskets used in tunnel segmental joints: development and application. Tunn Undergr Space Technol 2021;115:104079.

[264] Jiang XC, Cheng X, Zhang JM. Research on Buffer Performance of Aluminum Foam During Penetration. *Journal of Sichuan Ordnance* 2018; 39(11): 81-4. (in Chinese)

[265] Ceng F, Pan Y, Hu SS. Evaluation of Cushioning Properties and Energy-absorption Capability of Foam Aluminium. *Explosion and Shock Waves* 2002; 22(4): 358-62. (in Chinese)

[266] Chakka V, Trabia MB, O'Toole B, Sridharala S, Ladkany S, Chowdhury M. Modeling and reduction of shocks on electronic components within a projectile. Int J Impact Eng 2008;35(11):1326–38.

[267] Zhang P, Zhang H, Chen NQ, Wang NZ, Song CP, Yang RY, et al. A novel composite of Closed-Cell aluminum foam and Phase-Change material for enhanced mechanical safety in EV battery systems. Compos Struct 2025;371:119504.

[268] Li TY, Xie CY, Zhou XG, Yue F, Chen QQ, Zhu YF, et al. Upcycling discarded polytetrafluoroethylene to anode protective layer for high-performance lithium-ion batteries. Chem Eng J 2025;519:165165.

[269] Chen RF, Shi GC, Zhang L, Qiu QQ, Wei XX. Application of Artificial Cartilage Biomimetic Material in Fuze Buffer. *Journal of Detection & Control* 2020; 42(6): 8-12. (in Chinese)

[270] Zhang JM, Zhang H, Dai KR, Yu D,Yang BQ. Preparation of Elastic Porous Composite Material and Its Energy-absorption Characteristics. *Acta Armamentarii* 2022; 43(1): 159-68. (in Chinese)

[271] Chen ZP, Li HJ, Yang BQ. Study on the buffering properties of composites during high-speed penetration. J Phys Conf Ser 2021;2029(1):012057.

[272] Zhang Y, Zhang D, Ning L, others. Metal laminated protective mechanism and optimization design for penetration fuze. The 24th Fuze Academic Annual Conference of the China Ordnance Society. Jilin, China; 2025.

[273] Wang MH, Zhang HF, Cheng QL, others. Design and analysis of metal wire mesh damper for penetration fuze protection. Proceedings of the 24th Fuze Academic Annual Conference of the China Ordnance Society. Jilin, China; 2025.

[274] Cao J, Zhang H, Wang XF. Optimization of isolated protection for the hard-target penetration fuze. *Journal of Vibration and Shock* 2015(24): 192-6. (in Chinese)

[275] Yu KH, Zhang XH, Xu HY, Li R, Kang XG. Numerical Simulation of Aluminum Foam Cushion Performance Analysis on Set-forward Overload of Fuze. *Journal of System Simulation* 2017; 29(6): 1311-6. (in Chinese)

[276] Peng JW, Li CS, Zhang YZ. Influence of different protective gaskets on Fuze cushioning performance in the process of penetration. Proceedings of the International Conference on Computer, Artificial Intelligence, and Control Engineering (CAICE 2023). 2023:141–7.

[277] Peng JW. Study on the Protective Performance of Rubber Gaskets for Penetrating Fuze Cushioning [D]. Nanjing: Nanjing University of Science & Technology; 2023. (in Chinese)

[278] Xu PC, Huang HD, Zhang LS, Zhou P, Xu R. Stress Wave Reflecting Attenuation to Improve Anti-

shock Capacity by Gasket. *Journal of Detection & Control* 2012; 34(2): 1-6. (in Chinese)
[279] Xu PZ, Huang HD, Jie T, Liu P. The foamed aluminium gasket in hypersonic penetrating fuze. J Detect Control 2010;32(6):63–7. (in Chinese)
[280] Chen J, Niu SH, Tang B, Tao FG, Sun YC, Liu TG, et al. Anti-impact Performance Simulation of Fuze Multi-layer Gasket Protection Structure. *Journal of Detection & Control* 2021; 43(5): 15-21. (in Chinese)
[281] Liu X, Liang T, Cui S, Xu PZ , Chang YK. Gradient aluminum foam gasket in the penetration fuze. The *Proceedings of SPIE - The International Society for Optical Engineering*, 2023: 1263935.
[282] Zhang A, Liu P, Zhang H. Advancements in research on high-overload impact-buffering protective materials. Front Mech Eng 2024;10:1284758.
[283] Rosenberg Z, Dekel E, Vayig Y, Kositski R, Malka-Markovitz A. Penetration mechanics of rigid projectiles impacting metallic and concrete targets—a summary of our work. Int J Prot Struct 2025;16(2):566–90.
[284] Anderson CE Jr. Analytical models for penetration mechanics: a Review. Int J Impact Eng 2017;108:3–26.
[285] Hu Y, Ma T, Wang JL, Du ZB, Huang XC, Ji HN, et al. Shock wave detection and evaluation techniques for individual protection. *Explosion and Shock Waves* 2025; 45(4): 1-32. (in Chinese)
[286] Zhang MY, Shi GC, Liu Q, Zhang L, Qiu QQ. Acquisition and Processing Technology of Penetrating Signal of Penetrating Hard Target Fuze. *Guidance & Fuze* 2020; 41(3): 1-10, 24. (in Chinese)
[287] Zhang J, Shi YB, Cao HL, Zhao SH, Zhao YQ, Wang YL, et al. Design and implementation of a novel membrane-island structured MEMS accelerometer with an ultra-high range. IEEE Sens J 2022;22(21):20246–56.
[288] Yu MZ, Zhao LB, Jia C, Wang HY, Zhao YL, Jiang ZD. A high-g triaxial piezoresistive accelerometer with sensing beams in pure axial deformation. 2019 IEEE 14th International Conference on Nano/Micro Engineered and Molecular Systems (NEMS). Bangkok, Thailand. IEEE, 2019: 176–180.
[289] Han S, Ma YC, Qin L, Wang YK, Ding N. MEMS piezoresistive sensor based design of low-power consuming and high-overloaded testing system. *Explosion and Shock Waves* 2016; 36(5): 721-7. (in Chinese)
[290] Ou Y, Yang Y, Ruan C. A layer count algorithm based on fusion of acceleration sensor and MEMS impact switch signals. J Detect Control 2012;34(2):7–10. (in Chinese)
[291] Ma Y, Hu Z, Ran X, others. Design parameters study of inertial switch for penetration fuze. The 24th Fuze Academic Annual Conference of the China Ordnance Society. Jilin, China; 2025.
[292] Wang Y, Zhang Y, He L, others. Structural modeling and simulation analysis of MEMS setback switch for fuze. Proceedings of the 23rd Fuze Academic Annual Conference of the China Ordnance Society. Jilin, China; 2025.
[293] You JC, Li DJ, Ou YK, Zhao H. Precise detonating-control technique for hard-target penetration fuze. *Journal of Chinese Inertial Technology* 2016; 24(1): 114-8. (in Chinese)
[294] You JC, Li DJ, Huang SL, Zhu HZ, Yang H. Recovery of distorted shock acceleration records for investigating kinetic energy perforation of multi-layered concrete slabs. China Meas Test Technol 2016;42(10):95–9.
[295] Wang J, Shao ZH, Gao Y, Liang HH, Dai LH, Li R, et al. Design method for high overload and strong impact protection of rocket fuze: CN202410581472.4; 2024.

[296] Wang J, Li R, Huang HD. Layer Penetrating Adhesion Signal Characteristic Extractting Based on Wavelet Coefficients. *Journal of Detection & Control* 2016; 38(1): 13-7, 23. (in Chinese)

[297] Liu WJ, Li R, Shao ZH, et al. An accurate layer counting method for penetration fuzes that identify strong aliasing overload signals. China Patent CN202411200110.2; 2024.

[298] Shao Z, Li R, Liu W, others. A signal feature extraction method for identifying the warhead impact process using a penetration fuze based on multi-source information fusion: CN202411201323.7; 2024.

[299] Li R, Dai LH, Wu MZ, Shao ZH, Liang JH. Multi-level Target Adhesion Mechanism of High-speed Penetration Fuze Overload. *Journal of Detection & Control* 2020; 42(2): 1-4, 9. (in Chinese)

[300] Wang YT. Design of piezoresistive three-axis high g value acceleration sensor [D]. Taiyuan: North University of China; 2023. (in Chinese)

[301] Bae KM, Lee JM, Kwon KB, Han KH, Kwon NY, Han JS, et al. High-shock silicon accelerometer with suspended piezoresistive sensing bridges. J Mech Sci Technol 2014;28(4):1449 – 54.

[302] Sui L, Wang DW, Yu HY, He YJ, Su HW, Chen H, et al. A type of penetration-inducing capacitive sensor: CN202011467713.0; 2021.

[303] Yu HY, Sui L, Wang DW, He YJ, Chen H, Qiu HC, et al. A signal conditioning circuit for a penetration-inducing capacitive sensor: CN202111174231.0; 2023.

[304] Sui L, Wang DW, Zhang ZZ, et al. A composite sensor combining capacitance and piezoelectricity for penetrating magnetic fields. China Patent CN202211293439.9; 2025.

[305] Zhao JZ, Li HJ, Zhang CH, et al. Target Recognition Method for Underwater Complex Medium Penetration Fuze Using Acceleration-Capacitance Composite Sensor Information Fusion. The *The 24th Fuze Academic Annual Conference of The China Ordnance Society*. Jilin, China; 2025.

[306] Liu J, Cao HL, Shi YB, Tang J, Shen C. Research status of high overload micro inertial devices. Navig Control 2020;19(4/5):188 – 96.

[307] Moura A, Beliveau A, Dodson J. Shock accelerometer characterization for high-g applications. Proceedings of NDIA 63th Annual Fuze Conference. Online, 2020.

[308] Walter PL. Selecting Accelerometers for and Assessing Data from Mechanical Shock Measurements, https://www.pcb.com/contentstore/MktgContent/Linkeddocuments/Technotes/TN-24_MechShock.pdf; 2024 [2026-4-14].

[309] Li C, Zhang R, Hao L, Zhao YL. Development of a MEMS piezoresistive high-g accelerometer with a cross-center block structure and reliable electrode. Sensors 2024;24(17):5540.

[310] North Carolina I. Accelerometer, https://buy.endevco.com/accelerometer p=12; 2026 [2026-4-15].

[311] Kulite Semiconductor Products, inc. Products | Kulite | The Leader in Pressure Transducer Technology, https://kulite.com; 2026 [2026-4-15].

[312] Group K. Shock accelerometers | Kistler INT, https://www.kistler.com/INT/en/cp/shock-accelerometers-8742a/P0000556; 2026 [2026-4-15].

[313] Kjær HB. 3200B, https://www.hbkworld.com/web/dytran/global/en/products/accelerometers/iepe/uniaxial/3200b; 2026 [2026-4-15].

[314] Zhao Y, Jiang Z, Gao J, others. High g value accelerometer: CN200510042775.6; 2006.

[315] Shi YB, Zhu ZQ, Liu XP, Du K, Liu J. The design and impact analysis of high-g accelerometer. *Explosion and Shock Waves* 2010; 30(3): 329-32. (in Chinese)

[316] Wu Q, Lin J, Yang JT. Design and simulation of a MEMS high-gn acceleration sensor. *Transducer*

and Microsystem Technologies 2014; 33(9): 77-80. (in Chinese)

[317] Gmbh D. Endevco accelerometers are the industry standard for high g shock measurement, https://www.endevco.ch/content/13-weapons; 2026 [2026-4-14].

[318] Dong PT, Li XX, Zhang K, Wu XZ, Li SY, Feng SL. Design, fabrication, and characterization of a high-performance monolithic triaxial piezoresistive high-g accelerometer. J Semicond 2007; (09): 1482-7.

[319] Zhang ZH, Li KJ, Ren XR, Liu J. Design, simulation and optimization of sensing chip of high-g three-axis MEMS accelerometer. Acta Armamentarii 2008;29(6):690 – 3. (in Chinese)

[320] Shi YB, Zhao R, Tang J, Liu J, Li KJ. Testing and Analysis of a Single-Chip Triaxial High Measure Range MEMS Accelerometer. *Chinese Journal of Sensors and Actuators* 2012; 25(9):1236-41. (in Chinese)

[321] Chen JJ. Optimization Design of Triaxial High-g Accelerometer and Its Application Research in Penetration of Multi-Layer Hard Targets [D]. Nanjing: Nanjing University of Science and Technology; 2020. (in Chinese)

[322] Jing P, Ma TH, Wang Y. Shock Calibration of a Piezoresistive Three-Axis High-g Microaccelerometer. *Chinese Journal of Sensors and Actuators* 2008; 21(6): 954-8. (in Chinese)

[323] Chen HL, Ma SJ, Zhang JM. High impact three-dimensional acceleration storage tester. J Ordnance Equip Eng 2018;39(2):41 – 5. (in Chinese)

[324] Zhang L, Zhang ZH, Li KJ, Li ZQ. Onboard storage testing device based on high impact tri-axial accelerometer. J Detect Control 2016;38(2):13 – 7. (in Chinese)

[325] Zhang SX, Zhou W, Lu P, Yu HJ, Peng B. Research on the calibration method of triaxial acceleration sensor with transverse sensitivity. *Chinese Journal of Scientific Instrument* 2021; 42(4): 33-40. (in Chinese)

[326] Lin R, Zhang ZH, Li KJ, He X, Zhang L. New Calibration Technology of Relative Transverse Sensitivity of High Shock Triaxis Accelerometer. *Journal of Vibration, Measurement & Diagnosis* 2016; 36(5): 922-8. (in Chinese)

[327] Liu M, Zhang ZH, He G, Niu LJ, Tian ZW, Sun HL, et al. Multi-component High-impact Calibration Test Device. *Journal of Detection & Control* 2023; 45(3): 99-108. (in Chinese)

[328] Man XF, Zhang H, Ma SJ, Wang XF. Study of Physical Simulation Experiment of Penetration Fuze Layer-count Burst Point Control. *Acta Armamentarii* 2014; 35(10): 1556-61. (in Chinese)

[329] Man X, Zhang H, Ma S, Wang XF. Calculation of projectile penetration target impact speed based on acceleration switch. J Test Meas Technol 2014;28(5):456 – 60.

[330] Man XF. Research on key technologies of short-interval multiple high-impact test device [D]. Nanjing: Nanjing University of Science and Technology; 2017. (in Chinese)

[331] Zhang ZZ, Sui L, Yu HY, Shi GC. Target information acquisition method of penetration fuze based on composite detection. J Phys: Conf Ser 2023;2566(1):012098.

[332] Zou QP, Sui L, Zhang MY, Shi GC. Simulation and experimental study of capacitive sensors for penetration fuze. Ninth International Conference on Energy Materials and Electrical Engineering (ICEMEE 2023). 2024;12979.

[333] Sui L, Zhang ZZ, Yu HY, Zou QP, Zhang L. Optimal design and experimental study of a layer counting sensor for high-speed penetration through multilayer hard targets. IEEE Sens J 2025;25(13):23781 – 92.

[334] Man XF, Tian XY, Cheng X. Analysis of jamming signal source of a penetration fuze. 2020 3rd International Conference on Unmanned Systems (ICUS). Harbin, China. IEEE, 2020:1220 – 3.

[335] Liu ZB. Penetration detonation control technology based on dynamic characteristics of projectile priming system [D]. Beijing: Beijing Institute of Technology; 2016. (in Chinese)

[336] Zhao MX, Niu SH, Li B. Fuze Threaded Connection Influencing Factors of Overload Signals Adhesion. *Journal of Detection & Control* 2024; 46(3): 23-7, 32. (in Chinese)

[337] Qiu YX, He LL, Chen G, Wu H, Li JC. Influence of Pressed Connection on Accelerometer Signal Adhesion between Target Layers. *Chinese Journal of High Pressure Physics* 2022; 36(4): 41-52. (in Chinese)

[338] Wei XC, Ceng T, Li JL, others. Research progress on projectile penetration attitude measurement methods. Proceedings of the 24th Fuze Academic Annual Conference of the China Ordnance Society. Jilin, China; 2025.

[339] Zhang HR, Niu SH. High-speed Penetration Fuze Multi-level Target Interlayer Adhesion Characteristics of Overload. *Journal of Detection & Control* 2023; 45(5): 27-33. (in Chinese)

[340] Zhang HR, Niu SH. Analysis the influence of projectile penetration velocity and length - diameter ratio on fuze overload signal adhesion. J Phys Conf Ser 2023;2478(7):072035.

[341] Liu SH. Analysis and Modeling of Dynamic Response Characteristics of Fuze Under High Speed Penetration [D]. Beijing: Beijing Institute of Technology; 2018. (in Chinese)

[342] Tang T, Shi HF, Li FY, Ma SJ, Zhang XP. Optimizing equivalent testing for scaled projectile penetration into multilayer concrete targets with fuse overload *via* layer-by-layer chasing-catching methodology. Sci Rep 2025;15:28780.

[343] Wang YL, Li CS, Wang X, Zhang H, Wang XF. A layer counting method for penetration fuze based on magnetic anomaly detection. Acta Armamentarii 2024;45(3):695 – 704. (in Chinese)

[344] Tian FM, Chen L, Wang JF, Chen ZA, Zhang WZ, Chen XL, et al. Cratering characteristics and modified penetration depth model for large-diameter projectiles penetrating into rock-filled concrete. Int J Impact Eng 2026;215:105768.

[345] Feng L, Guo ZH, Zhang Q, Dong XW, Su JP, Fan CY. Numerical simulation and experimental study on penetration of dual cutter into coal rock containing hard nodules based on SPH method. Comput Part Mech 2026;15:384 – 405.

[346] Yao SJ, Gao YQ, Long GC, Zhang D, Sun CM, Chen FP. Penetration resistance and mechanisms of micro-steel-fiber-reinforced ultra-high-strength concrete under medium to high-velocity impact. J Build Eng 2026;127:116316.

[347] Wang LB, Chen BH, Bai Z, Qian BW, Hu YT, Yao H, et al. Prediction of penetration trajectories for repeated strikes in concrete by spherical cavity expansion model with the modified free-surface effect. Int J Impact Eng 2026;216:105767.

[348] Shan F, He XZ, Armaghani DJ, Sheng DC. Effects of data smoothing and recurrent neural network (RNN) algorithms for real-time forecasting of tunnel boring machine (TBM) performance. J Rock Mech Geotech Eng 2024;16(5):1538 – 51.

[349] Zheng WL, Yang K, Chen JD, Yang JW, Huang HS. Recognition of penetration state in CMT based on Swin Transformer using erratic arc acoustic. Results Eng 2026;30:110677.

[350] Lin GW, Yang J, Sun HR, Li HK, Liu WQ, Zhu Q. Optimization of energy management strategy with fuzzy logic control and low-pass filtering for hydrogen production system. Int J Hydrogen Energy 2025;116:473 – 85.

[351] Ren PZ, Xie XQ, Zhang K, Peng DD, Wang H. Aero-engine bearing anomaly detection framework based on adaptive wavelet transform network and neighborhood angle factor analysis. Aerosp Sci Technol 2026;171:111686.

[352] Zhang BL, Wan ST, Zhao XY, Wang CY, Zhang X, Sheng XL. Instantaneous rotational frequency estimation and fault diagnosis for rotating machinery based on multi-component short-time Fourier transform. Measurement 2025;253:117565.

[353] Hu JW, Jiang YC, Xu YX, Mai SP. A high-precision crosstalk coefficient calibration method based on modified empirical mode decomposition and phase orthogonal fringes. Measurement 2025;253:117429.

[354] Ali A, Wang XH, Razzaq I. Pipeline leak detection through implementation of empirical mode decomposition and cluster analysis. Measurement 2025;248:116873.

[355] Zhang DB, Li J, Wei XK, Feng KQ, Wang Y, Zhao JH, et al. Research on dynamic test of hyper-velocity impact penetration acceleration signal. IEEE Access 2020;8:194879 – 93.

[356] Xie YC, Fang AQ, Gao WX, others. Penetration overload signal feature extraction based on MOMEDA and mutual information. J Detect Control 2024;46(5):1 – 7. (in Chinese)

[357] Xie YC, Gao WX, Shao ZH, et al. Penetration Overload Signal Time Frequency Analysis Method Based on Adaptive OVMD. *Journal of Detection & Control* 2024; 46(4): 69-78. (in Chinese)

[358] Fan YX, Wang ZR, Wei ZQ, Hu Q. Multi-scale attention-based spectral neural network for underwater reverberation suppression. Measurement 2025;256:118484.

[359] Zhang ZC. Choi – Williams distribution in linear canonical domains and its application in noisy LFM signals detection. Commun Nonlinear Sci Numer Simul 2020;82:105025.

[360] Zheng HL, Jia SQ, Guo YP, Xue YJ, Han J, Zhao HM. Time-Frequency Denoising Method for Penetration Overload Signals Based on Denoising Convolutional Neural Network(DnCNN). *Equipment Environmental Engineering* 2024; 21(8): 17-24. (in Chinese)

[361] Shi HF, Ma SJ, Li FY, Tang T, Jia KM, Zhang H. Research on the EEMD-SE-IWTD combined noise reduction method for high-speed transient complex features in acceleration signals. Sensors 2025;25(19):5940.

[362] Guo XX, Zhang Y, Li SZ, Wang W, Li J. Penetration Data Processing Based on Pseudo Autocorrelation. *Journal of Detection & Control* 2012; 34(6): 45-8. (in Chinese)

[363] Hao HY, Li XF, Liu MJ. Fast Algorithm Research of Penetration Concrete Target Layers. *Fire Control & Command Control* 2013; 38(3): 167-70. (in Chinese)

[364] Hao HY, Li XF, Liu MJ. Study on Rigid Body Overload Feature Extraction Method in Penetrating Target Process. *Fire Control & Command Control* 2012; 37(12): 42-4, 47. (in Chinese)

[365] Sui L, Wang DW, Zou QP, et al. A method for determining the entry and exit times of a penetration-guided three-state inertial switch. China Patent CN202210728058.2; 2024.

[366] Sun QH, Sun K, Zhang HY. An Acceleration Signal Preprocessing Method Based on Difference of Boxes Filter. *Journal of Detection & Control* 2020; 42(5): 27-30. (in Chinese)

[367] Du TY. Research on Key Technologies of All-Electronic Security System for Penetration Fuze [D]. Nanjing: Nanjing University of Science and Technology; 2023. (in Chinese)

[368] Du TY, Zhang XJ, Guo JJ. Research on penetration overload characteristics and passband algorithm of electronic safety and arming device. *Journal of Ordnance Equipment Engineering* 2023; 44(3): 288-94. (in Chinese)

[369] Cui SL, Xi XR, Wang XA. Study on vibration noise processing method of penetration fuse circuit. Mech Sci Technol Aerosp Eng 2018;37(5):742 – 6.

[370] Jiao C. Research on multi-layer penetration fuze overload signal acquisition and layer identification technology [D]. Taiyuan: North University of China; 2018. (in Chinese)

[371] Zhao HF, Zhang Y, Li SZ, Guo Y. Research of the penetration overload signals de-noising method

based on singular value decomposition. J Vibr Meas Diagn 2015;35(4):770 – 6.
[372] Zhao HF, Zhang Y, Li SZ, Guo Y. Frequency characteristics analyses of penetrating missile and penetration overload signal processing. China Mech Eng 2015;26(22):3034 – 9.
[373] Zhao H, Zhang Y, Li S. Undetermined blind source separation and feature extraction of penetration overload signals. Chin J Sci Instrum 2019;40(10):208 – 18. (in Chinese)
[374] Zhang CY, Zhang Y, Li PY, Li SZ, Zhao HF. Feature Extraction of Penetration Overload Signal Based on Variational Mode Decomposition. *Journal of Detection & Control* 2021; 43(3): 16-21. (in Chinese)
[375] Zhang CY, Zhang Y, Li SZ. Blind separation of penetration overload signals based on VMD. J Vibr Shock 2022;41(5):280 – 6. (in Chinese)
[376] Wang Y, Ma TH, Xu P, Fan JB. Identification of penetration layers based on Choi-Williams distribution. *Explosion and Shock Waves* 2015; 35(5): 758-62. (in Chinese)
[377] Zheng DZ, Qiao MT, Li ZX, Hu C, Zhang CJ. Research on overload signal acquisition and layer identification algorithm based on array sensor penetration. *Chinese Journal of Scientific Instrument* 2023; 44(3): 221-33. (in Chinese)
[378] Li CF, Gao WX, Liang HH, Shao ZH, Zhang K. Penetration Acceleration Signals Drill Layer Characteristics Extracting Method Based on Effective Short-time Energy Spectrum. *Journal of Detection & Control* 2024; 46(4): 79-86. (in Chinese)
[379] Wang JR, Tang K, Wang JX, Gu MH, Li YB. Machine learning and numerical simulation based prediction of the penetration efficiency of depleted uranium long-rod projectiles: a multi-factor analysis. Int J Impact Eng 2026;209:105534.
[380] Wadagbalkar P, Liu GR. Real-time prediction of projectile penetration to laminates by training machine learning models with finite element solver as the trainer. Def Technol 2021;17(1):147 – 60.
[381] Ma HR, Sun H, Li CS. Penetration overload prediction method based on a deep neural network with multiple inputs. Appl Sci 2023;13(4):2351.
[382] Liu WZ, Li R, Niu LJ, Shi KL. Research Status and Prospect of Hard-Target Penetration Initiation Control Technology. *Acta Armamentarii* 2023; 44(6): 1602-19. (in Chinese)
[383] Lu Y, Sui L, Wang D, Shi G. Current status and trends in the study of penetration fuze initiation control methods. International Conference on Automation Control, Algorithm, and Intelligent Bionics (ACAIB 2023). 2023:127590B.
[384] Wang YL, Li CS, Zhang H, Wang XF. A multisource information fusion layering method for penetration fuzes based on fuzzy weighting algorithm and backpropagation neural network. 2nd International Conference on Electronics, Electrical and Control System (EECS 2025). 2025:1365919.
[385] Liu H, Li SZ, Li JF. The void-identify method of penetration fuze based on timing control. AMM 2013;427 – 429:1223 – 7.
[386] Sun QH, Zhuang L, Xue ZQ. A Void Identification Method Based on Concrete-penetration Response Characteristic. *Journal of Detection & Control* 2022; 44(5): 26-30. (in Chinese)
[387] Fan ZQ, Yang XP, Sun Y, Guo YJ, Cui YX. High-g acceleration measurement for layer-counting tests based on coupling piezoelectric effect of PVDF film. Measurement 2025;256:118471.
[388] Peng LZ, Yue ZW, Hu Y, Yu S, Wang X. Fracture characterization and prediction in directional blasting of layered rock using CT, fractal Analysis, and LSTM. Eng Fract Mech 2026;340:112138.
[389] Chen H, Zha BT, Zheng Z, Zhang H. Study on the optimal damage model for directional detonation

control of aimable warhead. Ain Shams Eng J 2025;16(12):103722.

[390] Jiang K, Liu Z, He Z, others. Layer counting method of hard target penetration fuze based on geomagnetic signal detection. Proceedings of the International Conference on Mechatronics Engineering and Artificial Intelligence (MEAI 2022). 2023.

[391] Jin H, Jin SY, Chen CX, Wang Y. Research of relative wave crest detection method based on all the tenses on penetration layer. J Vibr Shock 2014;33(23):150 – 4. (in Chinese)

[392] Li HJ, Hu HC. Layer counting detonating control method for fuze based on penetration overload numerical simulation. *Journal of Nanjing University of Science and Technology* 2016; 40(6): 715-9. (in Chinese)

[393] Dai ZH, Gao SQ, Li ZZ, others. Dynamic threshold layer count algorithm based on envelope prediction. J Ordnance Equip Eng 2020;41(12):53 – 6. (in Chinese)

[394] Huang SL, Zhu HZ, Cheng XL, others. Adaptive threshold setting method for layer-count in penetration fuse. Acta Armamentarii 2020;41(9):1762 – 71. (in Chinese)

[395] Fang AQ, Li R. Penetration Fuze Accurate Layer Recognition Neural Network Data Enhancement Method. *Journal of Detection & Control* 2022; 44(1): 1-6. (in Chinese)

[396] Ding LB, Zhang H. Geomagnetic detection theory and application of modern fuze. Beijing: Beijing Institute of Technology Press; 2021. (in Chinese)

[397] Zhang XX, Zou JL, Wang W, et al. Research on a Novel Magnetic Sensitive Layer-counting Method for Penetration. *Acta Armamentarii* 2019; 40(11): 2204-11. (in Chinese)

[398] Zhao J, Zs L. Identification method of projectile penetration process based on active magnetic detection. J Detect Control 2024;46(1):40 – 6. (in Chinese)

[399] Zhao J, Wang RB, Li ZS. Simulation analysis of magnetic response under complex penetration conditions based on magnetic anomaly detection. J Ordnance Equip Eng 2024;45(7):158 – 66. (in Chinese)

[400] Cheng C, Du ZH, Chen X, Xu LZ, Du CX, Han JL, et al. Damage of multi-layer spaced metallic target plates impacted by radial layered PELE. Def Technol 2020;16(1):201 – 7.

[401] Cao J, Zhao J, Ma S. Research on magnetic anomaly response characteristics of penetration fuze based on active magnetic detection. J Ordnance Equip Eng 2024;45(11):51 – 8. (in Chinese)

[402] Shao Z, Xie Y, Liang Z, others. High-speed penetration fuze layers identification method based on multi-source information fusion. J Detect Control 2023;45(5):34 – 9,48. (in Chinese)

[403] Ma H, Shi Y, Zhao R, others. Penetration meter layer method based on magnetic acceleration signal. J Detect Control 2024;46(2):80 – 7. (in Chinese)

[404] Ma M, Niu L, Li R, others. Post-penetration precision detonation control based on acceleration signal stress wave compensation. J Detect Control 2022;44(5):31 – 8. (in Chinese)

[405] Zhang H, Li ZS. The basic design theory and application of smart fuze. Beijing: Beijing Institute of Technology Press; 2019. (in Chinese)

[406] Zhang H. "Three-element" cascade control method of a smart fuze. Sci Sin-Tech 2023;53(9):1449 – 64.

[407] Zhang H, Yu H, Dai KR, Liu P; Yang YX; Ma X. Precision Detonation Control Problem of Smart Fuze in Complex Wide-Area Battlefield. *Acta Armamentarii* 2022; 43(10): 2527-33. (in Chinese)

[408] He GL, Fan NJ. Analysis and design of the fuze safe and arming. Beijing: National Defense Industry Press; 2016. (in Chinese)

[409] Zhang Y, An X. Fuze reliability technology. Beijing: National Defense Industry Press; 2016. (in Chinese)

[410] Li HS, Zhang XQ. An equivalent target plate damage probability calculation mathematics model and damage evaluation method. Def Technol 2024;41:82 – 103.

[411] Li FY. Research on the Theory and Methods of Multiple Short-Interval Impact-Vibration Coupled Mechanics Tests [D]. Nanjing: Nanjing University of Science and Technology; 2021. (in Chinese)

[412] Qiao FX, Shi JP, Qu XB, Lyu YX. Hardware-in-loop adaptive neural control for a tiltable V-tail morphing aircraft. Def Technol 2023;22:197 – 211.

[413] Gao F, Deng SX, Zhang GK, Ji YG, Liu CK, Wang MY. Experimental Study and Theoretical Analysis of the Size Effect for Scale Model Projectile Penetrating into Rock Target. *Acta Armamentarii* 2023; 44(12): 3601-12. (in Chinese)

[414] Li H, Cha B. System analysis theory and method of modern fuze. Beijing: Beijing Institute of Technology Press; 2021. (in Chinese)

[415] Zhang Z. Research on Hardware-in-the-Loop Simulation Technology for Hard Target Penetration Fuzes [D]. Nanjing: Nanjing University of Science and Technology; 2007. (in Chinese)

[416] Fu CC. Design of a signal simulator for a PCI bus-based hard target penetration fuze testing system [D]. Nanjing: Nanjing University of Science and Technology; 2008. (in Chinese)

[417] Zhang L. High-speed signal simulator driver design for hard target penetration fuze testing system [D]. Nanjing: Nanjing University of Science and Technology; 2008. (in Chinese)

[418] Feng LN. Research on Signal Reconstruction Method of Hard Target Penetration Fuze Simulation Test System [D]. Nanjing: Nanjing University of Science and Technology; 2008. (in Chinese)

[419] Li X. Penetration Fuze Simulation Test System Signal Analysis and Dedicated Data Transmission Interface Technology [D]. Nanjing: Nanjing University of Science and Technology; 2011. (in Chinese)

[420] Wang L. Research on Hardware-in-the-Loop Simulation System for Hard Target Penetration Fuze [D]. Nanjing: Nanjing University of Science and Technology; 2013. (in Chinese)

[421] Gao YJ. Design of a test system for testing the performance of hard target penetration fuzes [D]. Nanjing: Nanjing University of Science and Technology; 2013. (in Chinese)

[422] Yao FL, Gao SQ, Liu ZB, Liu HP, Shen L. Semi-physical measurement and test for hard target penetrating fuze. J Proj Rockets Missiles Guid 2013;33(3):52 – 5.

[423] Chen HB, Jing YD, Wang KN, Zhang XX, Wang W, Guo ZL, et al. A magnetic susceptor layer device for penetration fuzes: CN108507425B; 2019.

[424] Huang SL, Xie YB, Zhu HZ, others. Device and method for detecting target release time: CN201910207828.7;2022.

[425] Chen HB, Jing YD, Wang KN, others. A magnetically sensitive penetration measurement method for penetration fuzes: 201810251993.8;2019.

[426] Wang JB, Song RC, Dong HP, Wang W. Small sample reliability test and evaluation for high-value ammunition fuze. 5th ed. Beijing: National Defense Industry Press; 2016. (in Chinese)

[427] White HG, Tobik T, Mabry R, et al. High-G Testing for Fuze Research. The *Symposium on Shock and Vibration (Tth)*. San Diego, USA; 2003.

[428] Man XF, Men SY, Ma SJ, Zhang H. Using air hammer device simulate hard target penetration process. J Detect Control 2016;38(3):90 – 3. (in Chinese)

[429] Wang XD. Research on key technologies for simulating multi-layer penetration impact signals [D]. Nanjing: Nanjing University of Science and Technology; 2017. (in Chinese)

[430] Li FY, Ma SJ. Analysis and experimental study of acceleration model for short interval and multiple impact equipment. Shock Vibr 2019;2019:5139137.

[431] Catovic A, Kljuno E. A novel method for determination of lethal radius for high-explosive artillery projectiles. Def Technol 2021;17(4):1217 – 33.

[432] Wilson N, Curtis S, White C. Extreme environment testing *via* ballistically fired water impact with dialable effects. Proposed for Presentation at the 65th NDIA Fuze Conference. Renton, USA; 2022.

[433] Curtis S. Shock-hardened penetrator data recorder to support hard-target fuze development. Proceedings of the 59th Annual NDIA Fuze Conference. Charleston, USA; 2016.

[434] Amborn E. Ground testing suite to reduce risk for fuzes in hard target penetrators. Proceedings of the 62nd Annual NDIA Fuze Conference. Buffalo, USA; 2019.

[435] Amborn E. Embedded fuze environment requirements for large penetrating weapons. Proceedings of the 61st Annual NDIA Fuze Conference. San Diego, USA; 2018.

[436] Zhang J, Li YC, Huang JY, Wu JX, Liu Q, Wu SZ, et al. The effect of al particle size on thermal decomposition, mechanical strength and sensitivity of $Al/ZrH_2/PTFE$ composite. Def Technol 2021;17(3):829 – 35.

[437] Li MY. Research on Simulation Test Technology of Hard Target Penetration Fuze [D]. Xi'an: Xidian University; 2014. (in Chinese)

[438] Li MY, Jing HS, Liu Q, Wu P. Penetration fuze scaling test method of using small projectile simulating big ones. J Detect Control 2017;39(6):21 – 4. (in Chinese)

[439] Liu Y, Pi AG, Yang H, others. Study on similarity law of non-proportionally scaled penetration/perforation test. Explos Shock Waves 2020;40(3):63 – 75. (in Chinese)

[440] Li R, Shi KL, Niu LJ, Du CH; He YX; Liu WZ. Penetration Fuze Overload Feature Equivalence Evaluation Method. *Journal of Detection & Control* 2023; 45(1): 17-21. (in Chinese)

[441] Xu FK, Li LG, Li ZS. Penetration Fuze Overload Equivalent Scaled Test Method. *Journal of Detection & Control* 2024; 46(2): 74-9. (in Chinese)

[442] Wei S, Cao J, Li CS. Variable mass reduction design method for penetration fuze based on energy equivalence. J Detect Control 2025;47(4):167 – 73. (in Chinese)

[443] Peng Y, Wu H, Fang Q, Gong ZM. Geometrical scaling effect for penetration depth of hard projectiles into concrete targets. Int J Impact Eng 2018;120:46 – 59.

[444] Wei ZR, Yao BZ, Ran XL, others. Dynamic firing test method of fuze for very weak target. J Sichuan Ordnance 2020;41(7):64 – 8. (in Chinese)

[445] Xu CY, Zha BT, Bao JQ, Zhang H, Li HX. Analysis of temporal and spatial distribution characteristics of ammonium chloride smoke particles in confined spaces. Def Technol 2022;18(7):1269 – 80.

[446] He GL, Chen KS, Li SY. Interface Circuit Design of Electronic Safe and Arming Based on CPLD. *Journal of Detection & Control* 2003; 25(2): 36-8. (in Chinese)

[447] Shi KL, Tan HM. An analysis on the logical structure of fuze safety systems. Acta Armamentarii 1993(4):40 – 6. (in Chinese)

[448] Shi KL, Tan HM. The application of Markov theory in the safety analysis of fuse safety systems. J Detect Control 1991(4):9 – 20. (in Chinese)

[449] Wang ZQ. Reliability Analysis and Performance Improvement of Dedicated Testing System for Penetration Fuzes [D]. Nanjing: Nanjing University of Science and Technology; 2017. (in Chinese)

[450] Wang YL, Ma QH. The Electric and Electromagnetic Envi ronment Influence at Electronic Safety-and-arming System. *Journal of Detection & Control* 2022; 44(3): 1-10. (in Chinese)

[451] Zhang H, Yu D. Analysis and experimental methods for safety margins in fuse electromagnetic environment. J Army Eng Univ PLA 2025;4(2):9 – 14.

[452] Wang FL, Shi KL, Wang YL, Ning B. Essential Elements of Electromechanical Fuze Safety Designs Evaluation. *Journal of Detection & Control* 2025; 47(1): 33-40. (in Chinese)

[453] Sharp A, Andrade J, Ruffini N. Design for reliability for the high reliability fuze. Reliab Eng Syst Saf 2019;181:54–61.

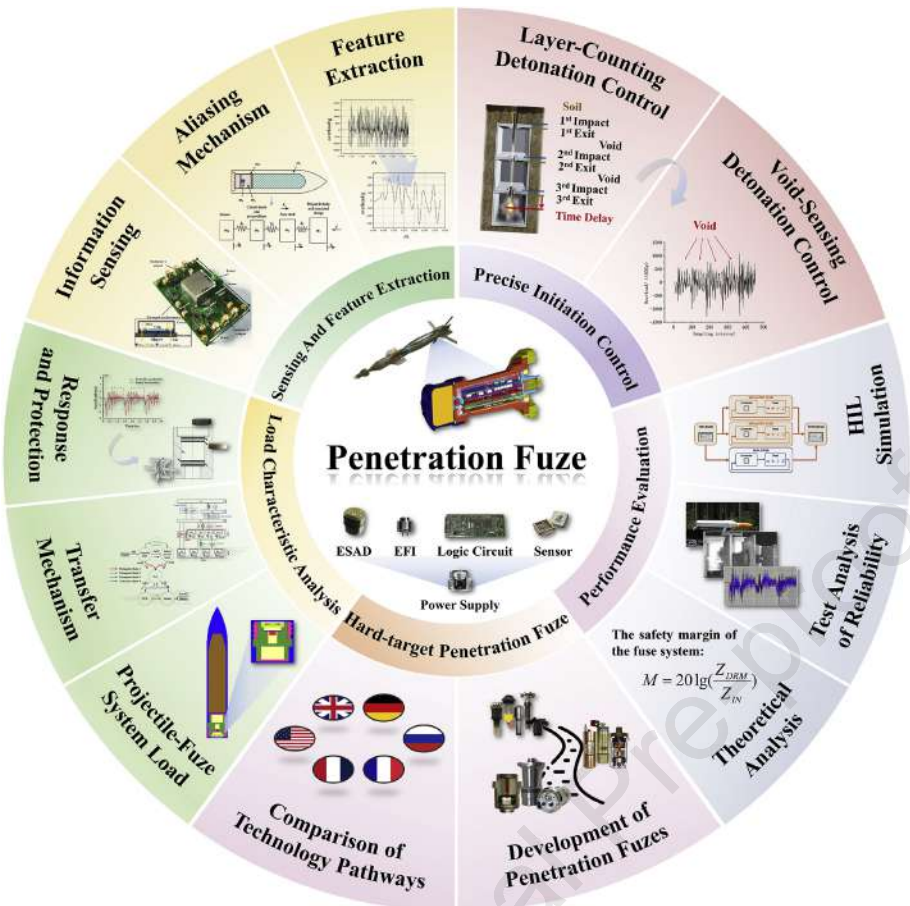

Penetration Fuze
ESAD
EFI
Logic Circuit
Sensor
Power Supply
Sensing And Feature Extraction
Precise Initiation Control
Performance Evaluation
Hard-target Penetration Fuze
Load Characteristic Analysis
Feature Extraction
Aliasing Mechanism
Information Sensing
Layer-Counting Detonation Control
Soil
1st Impact
1st Exit
Void
2nd Impact
2nd Exit
Void
3rd Impact
3rd Exit
Time Delay
Void-Sensing Detonation Control
Void
HIL Simulation
Test Analysis of Reliability
Theoretical Analysis
The safety margin of the fuse system:
$M = 20\lg(\frac{Z_{DRM}}{Z_{IN}})$
Development of Penetration Fuzes
Comparison of Technology Pathways
Projectile-Fuze System Load
Transfer Mechanism
Response and Protection

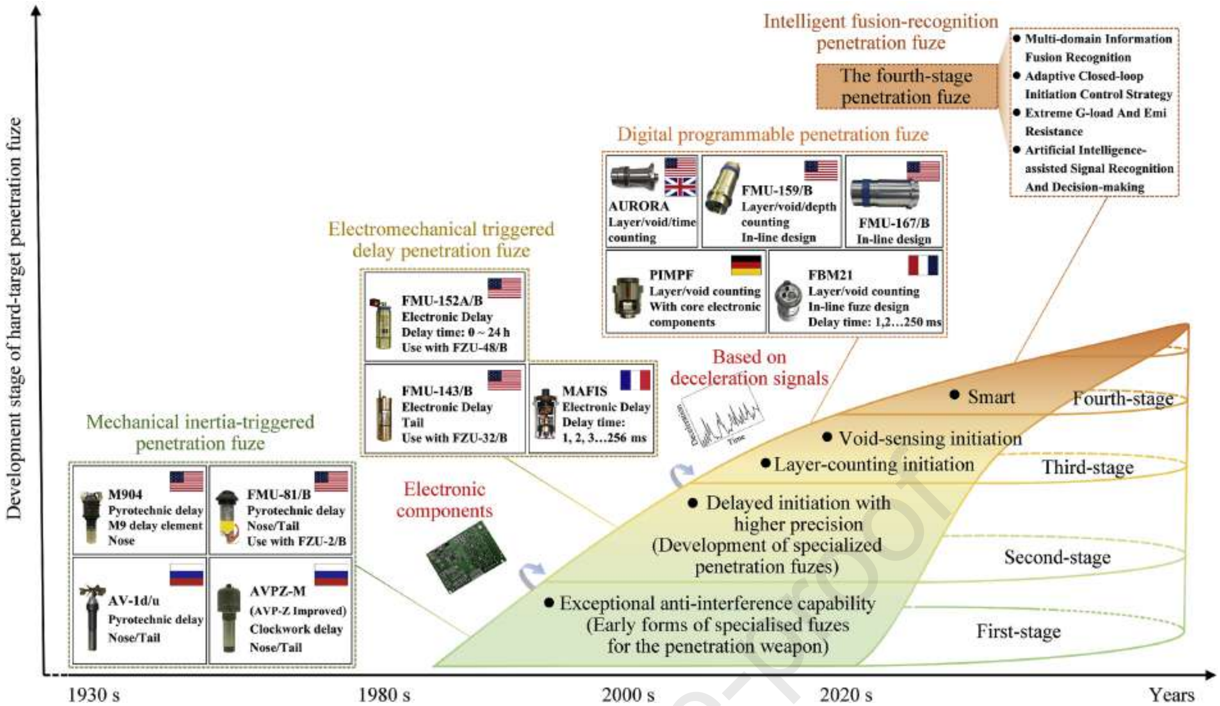

Development stage of hard-target penetration fuze
Intelligent fusion-recognition penetration fuze
The fourth-stage penetration fuze
Multi-domain Information Fusion Recognition
Adaptive Closed-loop Initiation Control Strategy
Extreme G-load And Emi Resistance
Artificial Intelligence-assisted Signal Recognition And Decision-making
Digital programmable penetration fuze
AURORA Layer/void/time counting
FMU-159/B Layer/void/depth counting In-line design
FMU-167/B In-line design
PIMPF Layer/void counting With core electronic components
FBM21 Layer/void counting In-line fuze design Delay time: 1,2…250 ms
Electromechanical triggered delay penetration fuze
FMU-152A/B Electronic Delay Delay time: 0 ~ 24 h Use with FZU-48/B
FMU-143/B Electronic Delay Tail Use with FZU-32/B
MAFIS Electronic Delay Delay time: 1, 2, 3…256 ms
Based on deceleration signals
Mechanical inertia-triggered penetration fuze
M904 Pyrotechnic delay M9 delay element Nose
FMU-81/B Pyrotechnic delay Nose/Tail Use with FZU-2/B
AV-1d/u Pyrotechnic delay Nose/Tail
AVPZ-M (AVP-Z Improved) Clockwork delay Nose/Tail
Electronic components
Smart
Void-sensing initiation
Layer-counting initiation
Delayed initiation with higher precision (Development of specialized penetration fuzes)
Exceptional anti-interference capability (Early forms of specialised fuzes for the penetration weapon)
Fourth-stage
Third-stage
Second-stage
First-stage
1930 s
1980 s
2000 s
2020 s
Years

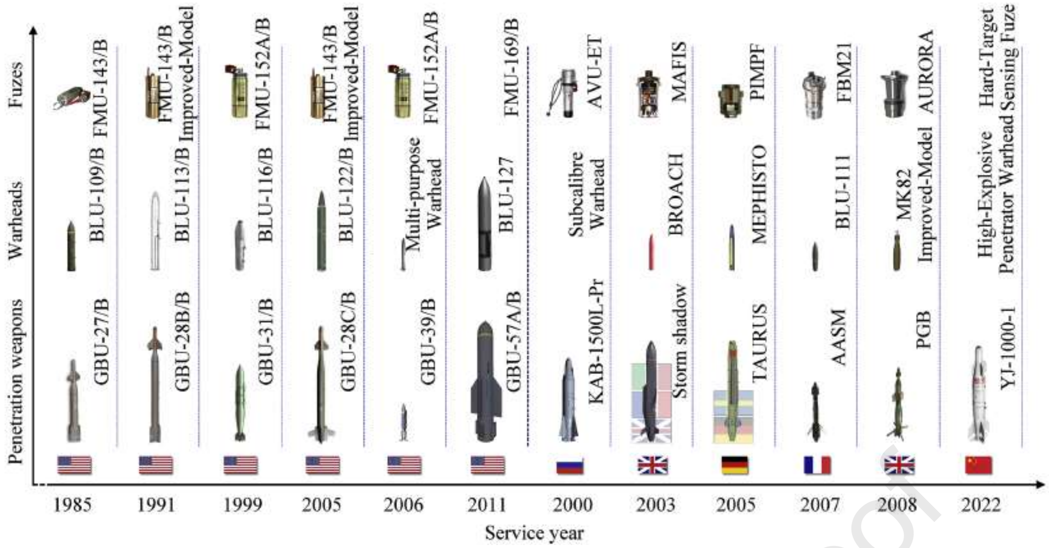
Fuzes
Warheads
Penetration weapons
FMU-143/B
BLU-109/B
GBU-27/B
FMU-143/B Improved-Model
BLU-113/B
GBU-28B/B
FMU-152A/B
BLU-116/B
GBU-31/B
FMU-143/B Improved-Model
BLU-122/B
GBU-28C/B
FMU-152A/B
Multi-purpose Warhead
GBU-39/B
FMU-169/B
BLU-127
GBU-57A/B
AVU-ET
Subcalibre Warhead
KAB-1500L-Pr
MAFIS
BROACH
Storm shadow
PIMPF
MEPHISTO
TAURUS
FBM21
BLU-111
AASM
AURORA
MK82 Improved-Model
PGB
Hard-Target Penetrator Warhead Sensing Fuze
High-Explosive
YJ-1000-1
1985
1991
1999
2005
2006
2011
2000
2003
2005
2007
2008
2022
Service year

(a) (b) (c) (d) (e) (f) (g) (h)

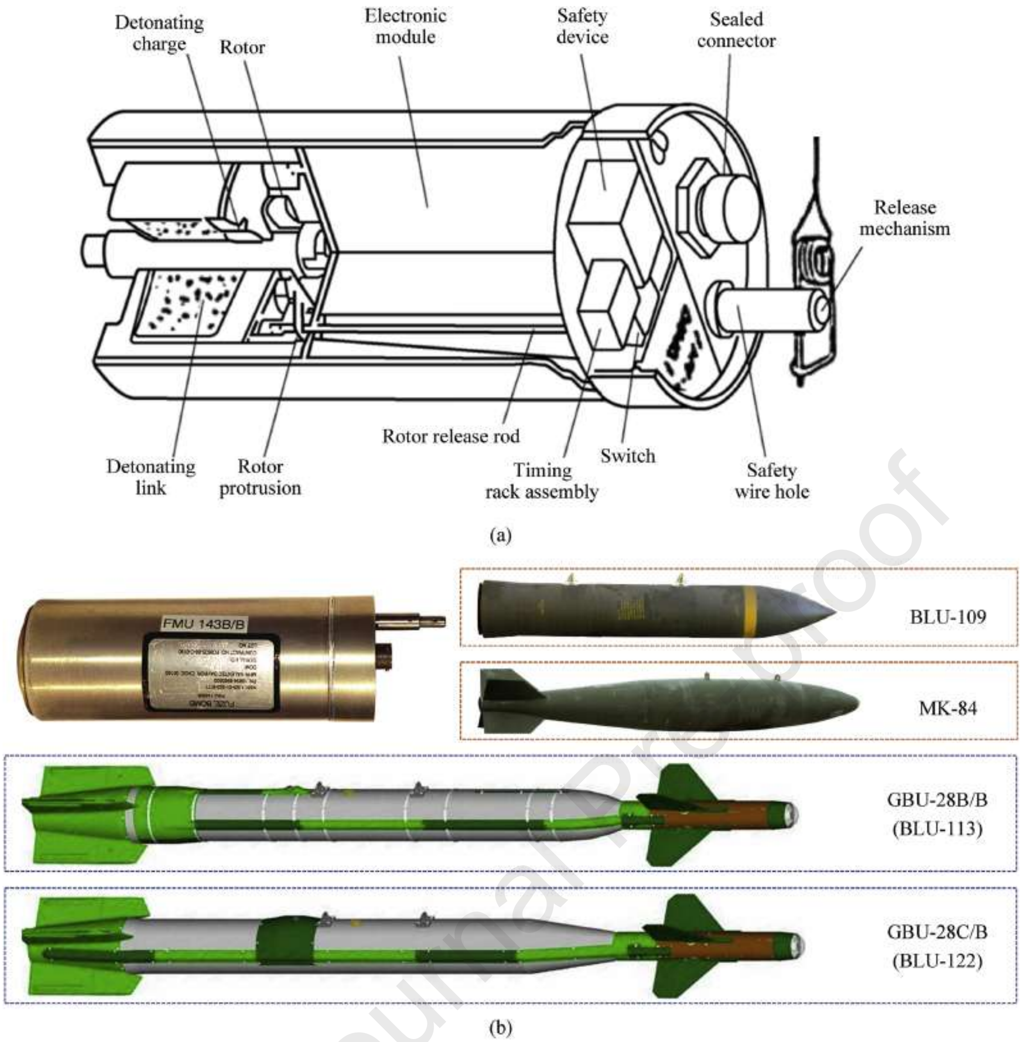
Detonating charge
Rotor
Electronic module
Safety device
Sealed connector
Release mechanism
Detonating link
Rotor protrusion
Rotor release rod
Timing rack assembly
Switch
Safety wire hole
(a)
FMU 143B/B
BLU-109
MK-84
GBU-28B/B (BLU-113)
GBU-28C/B (BLU-122)
(b)

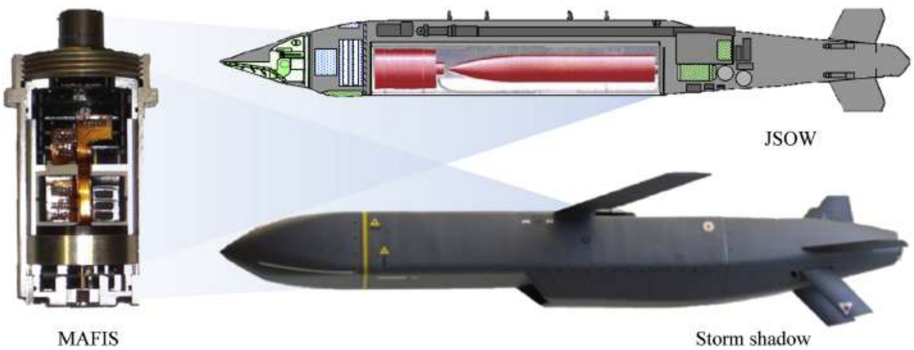
JSOW
MAFIS
Storm shadow


INERT
LD ARM
TIME SEC
DELAY TIME MSEC
24 HRS
4 HRS
15 MIN
HD ARM
TIME SEC
FMU-152
A(D-2)/B
HD LOCKOUT
FZU-55A/B
Power cable
Closure ring
FMU-152A/B
Safety pin assy

(a) (b)


FMU-159/B
Electronic, In-Line
Accelerometer-based fuze
Void sensing
Layer counting
Depth of burial
Back-up Timer
Compatible with existing fuze wells
Cockpit Programmable with JDAM interface
Fitted weapon systems:
GBU-24,-27,-28,-37,-31,AGM-130, etc.
FMU-167/B
Electronic, In-Line
Accelerometer-based fuze
Void sensing
Depth of burial
Back-up Timer
For use with the FZU-60/B initiator
With an independent electrically programmable backup time delay of 0 to 255 milliseconds
Potential weapon systems: GBU-72 , etc.

(a) (b)

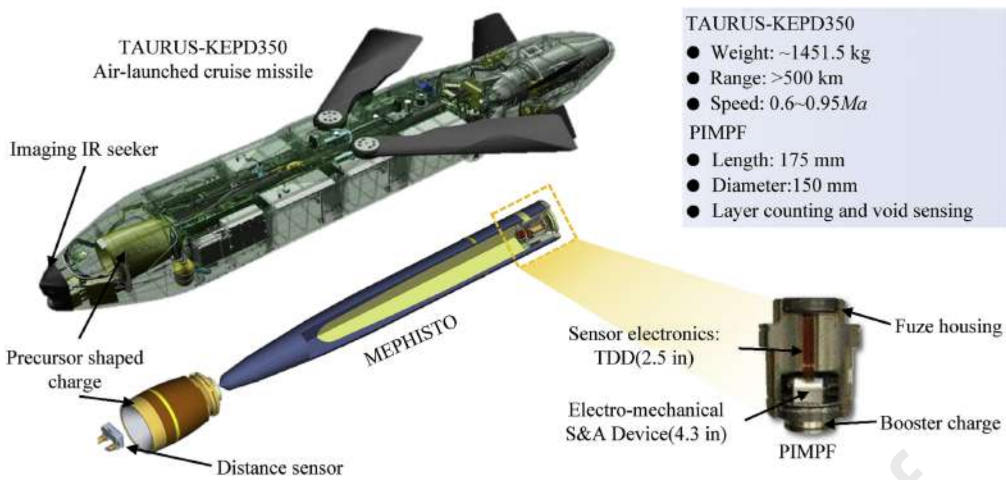
TAURUS-KEPD350
Air-launched cruise missile
Imaging IR seeker
Precursor shaped charge
Distance sensor
MEPHISTO
TAURUS-KEPD350
Weight: ~1451.5 kg
Range: >500 km
Speed: 0.6~0.95Ma
PIMPF
Length: 175 mm
Diameter:150 mm
Layer counting and void sensing
Sensor electronics: TDD(2.5 in)
Fuze housing
Electro-mechanical S&A Device(4.3 in)
Booster charge
PIMPF

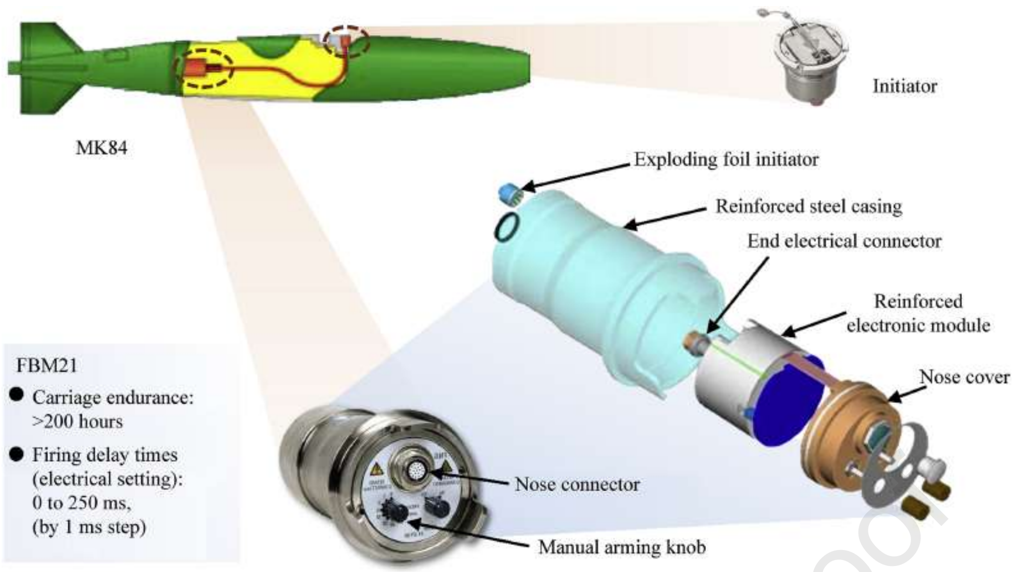

Initiator
MK84
Exploding foil initiator
Reinforced steel casing
End electrical connector
Reinforced electronic module
Nose cover
FBM21
Carriage endurance: >200 hours
Firing delay times (electrical setting): 0 to 250 ms, (by 1 ms step)
Nose connector
Manual arming knob

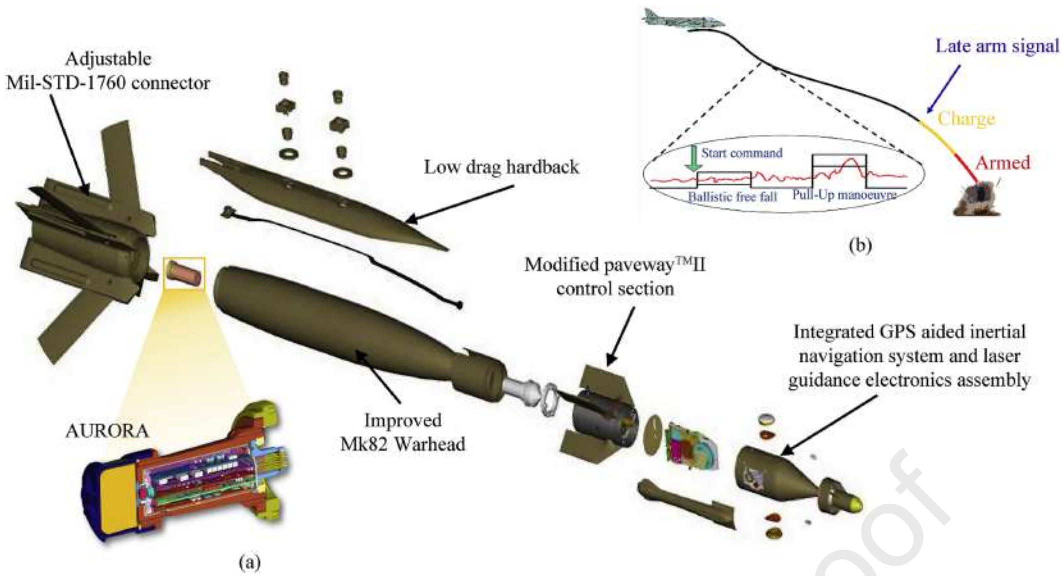
Adjustable
Mil-STD-1760 connector
Low drag hardback
Modified paveway™II
control section
Integrated GPS aided inertial
navigation system and laser
guidance electronics assembly
AURORA
Improved
Mk82 Warhead
(a)
Late arm signal
Charge
Armed
Start command
Ballistic free fall
Pull-Up manoeuvre
(b)

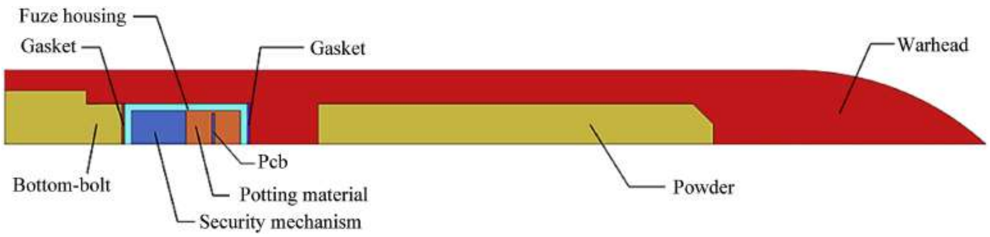
Fuze housing
Gasket
Gasket
Warhead
Pcb
Bottom-bolt
Potting material
Powder
Security mechanism

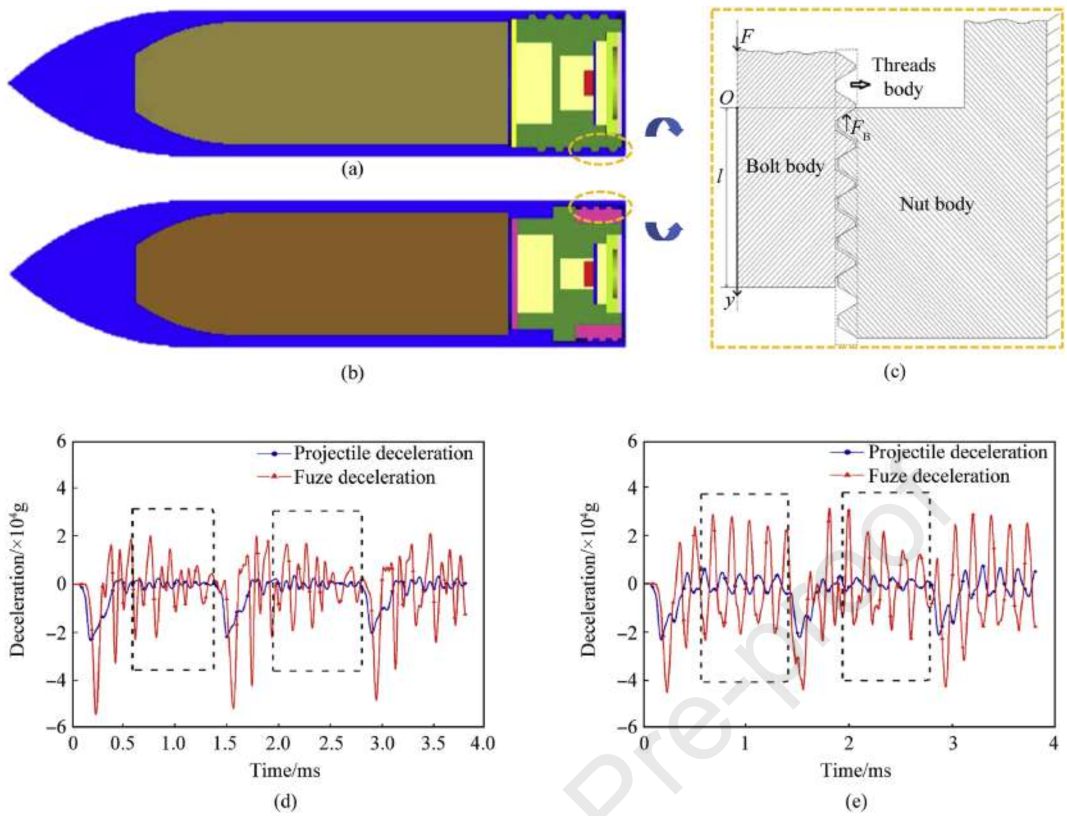

(a)
(b)
F
Threads
body
O
F_B
l
Bolt body
Nut body
y
(c)
Projectile deceleration
Fuze deceleration
Deceleration/×10⁴g
Time/ms
(d)
Projectile deceleration
Fuze deceleration
Deceleration/×10⁴g
Time/ms
(e)

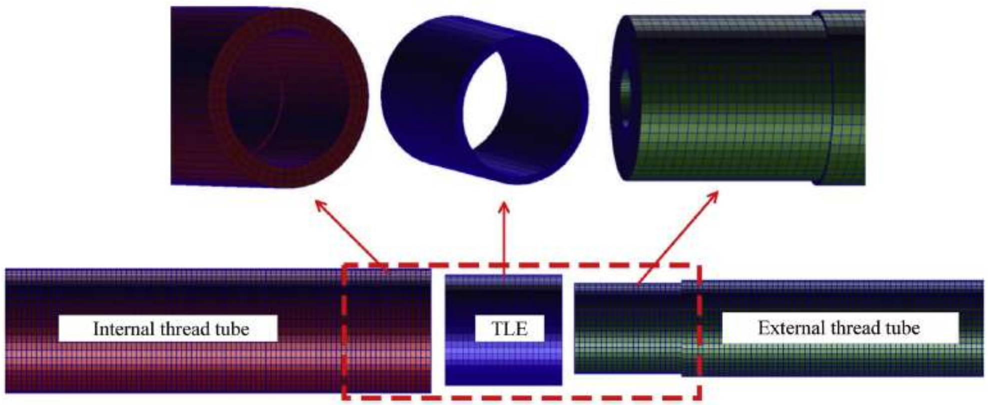
Internal thread tube
TLE
External thread tube

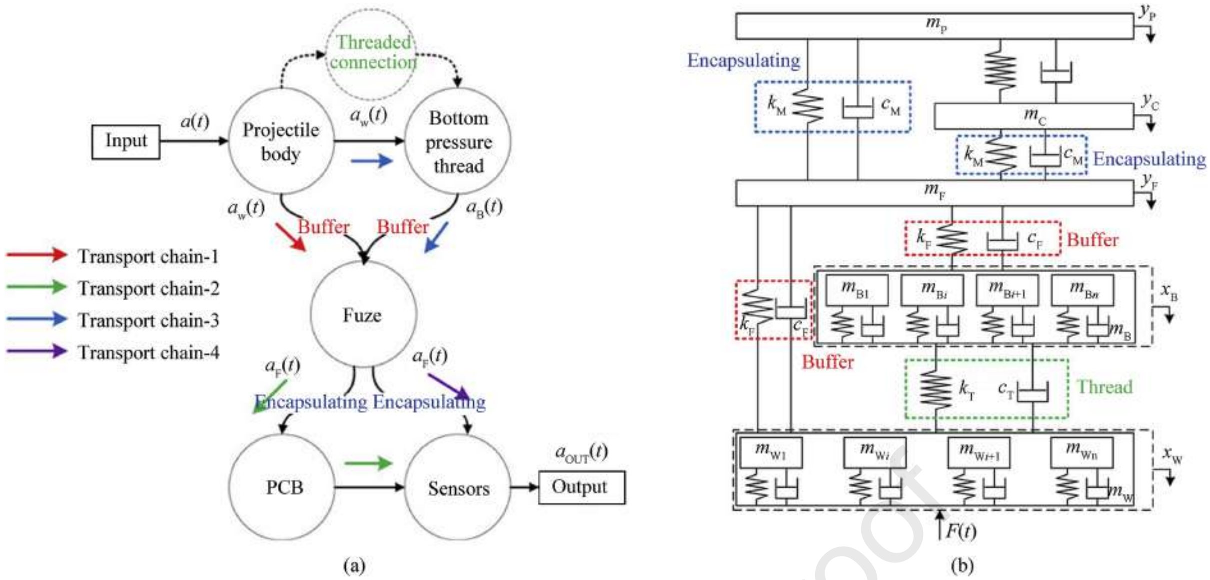
Threaded connection
Input
a(t)
Projectile body
a_w(t)
Bottom pressure thread
a_w(t)
a_B(t)
Buffer
Buffer
Transport chain-1
Transport chain-2
Transport chain-3
Transport chain-4
Fuze
a_F(t)
a_F(t)
Encapsulating
Encapsulating
PCB
Sensors
a_OUT(t)
Output
(a)
m_P
y_P
Encapsulating
k_M
c_M
m_C
y_C
k_M
c_M
Encapsulating
m_F
y_F
k_F
c_F
Buffer
m_B1
m_Bi
m_Bi+1
m_Bn
x_B
m_B
k_F
c_E
Buffer
k_T
c_T
Thread
m_W1
m_Wi
m_Wi+1
m_Wn
x_W
m_W
F(t)
(b)

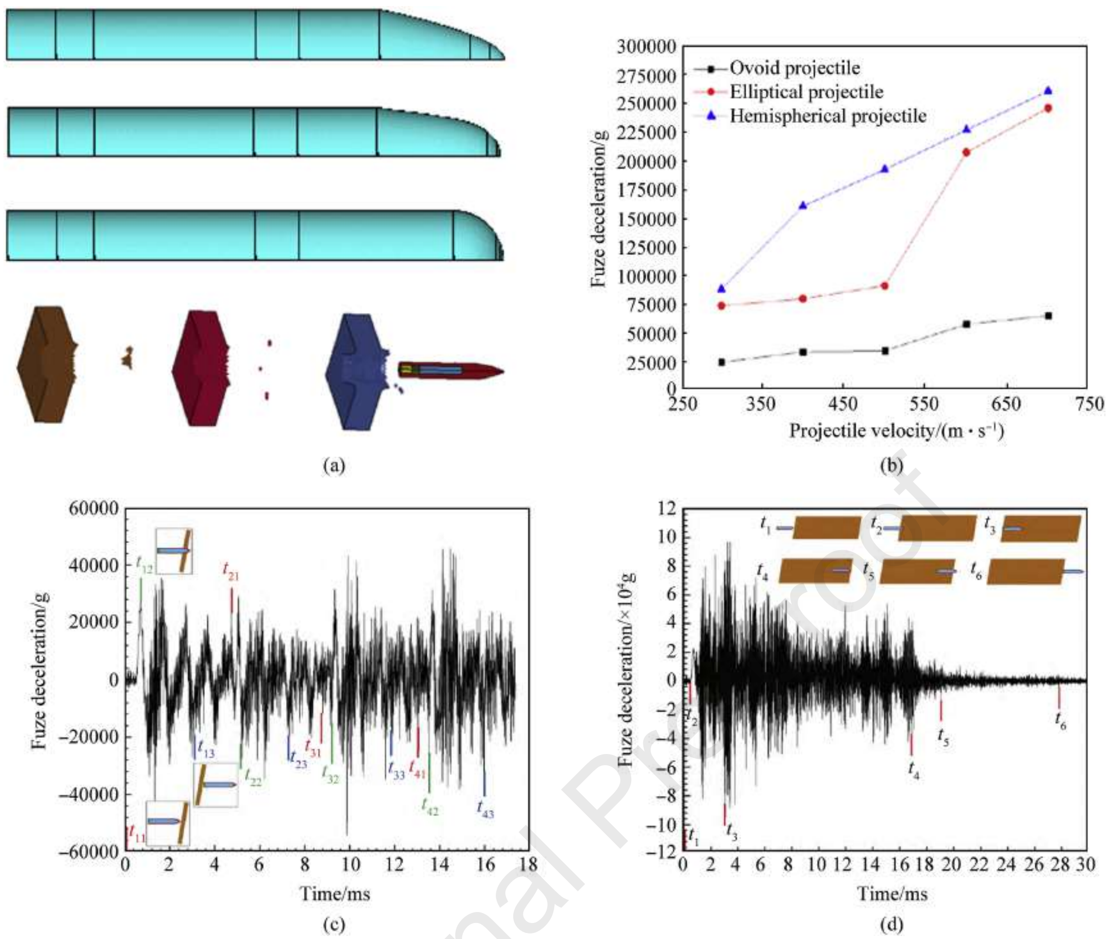

Ovoid projectile
Elliptical projectile
Hemispherical projectile
Fuze deceleration/g
Projectile velocity/(m · s⁻¹)
Fuze deceleration/g
Time/ms
Fuze deceleration/×10⁴g
Time/ms
(a)
(b)
(c)
(d)

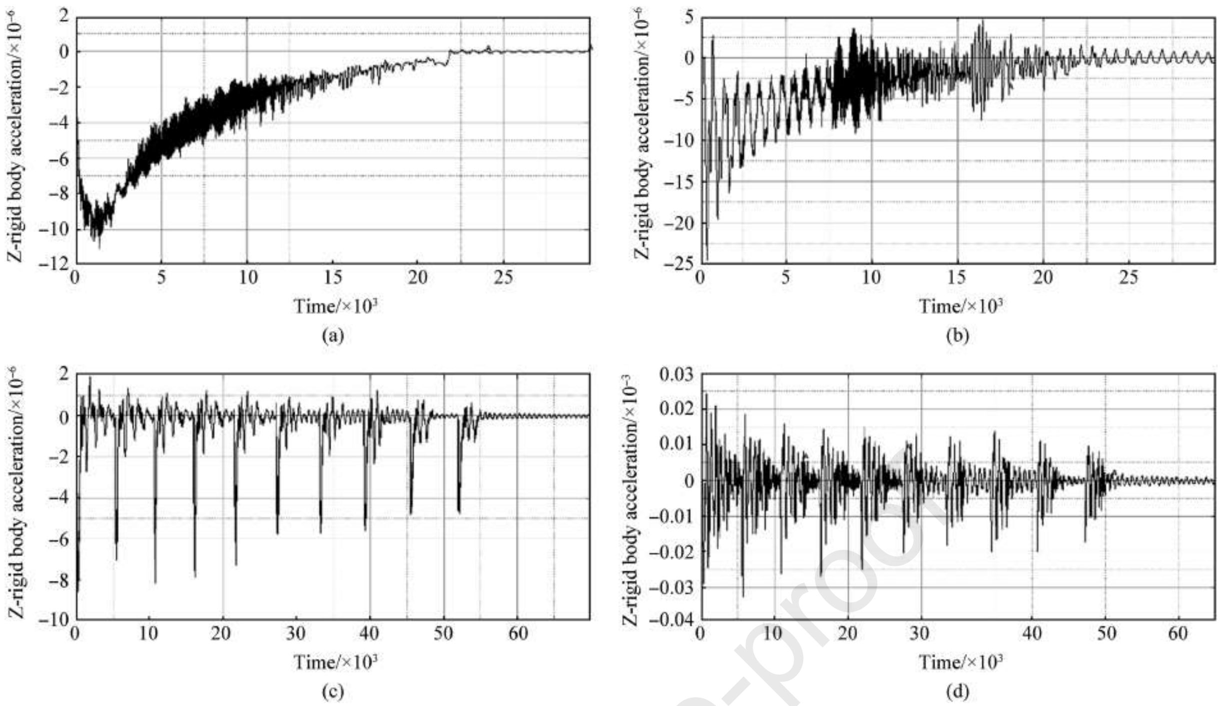
Z-rigid body acceleration/×10⁻⁶
Time/×10³
(a)
Z-rigid body acceleration/×10⁻⁶
Time/×10³
(b)
Z-rigid body acceleration/×10⁻⁶
Time/×10³
(c)
Z-rigid body acceleration/×10⁻³
Time/×10³
(d)

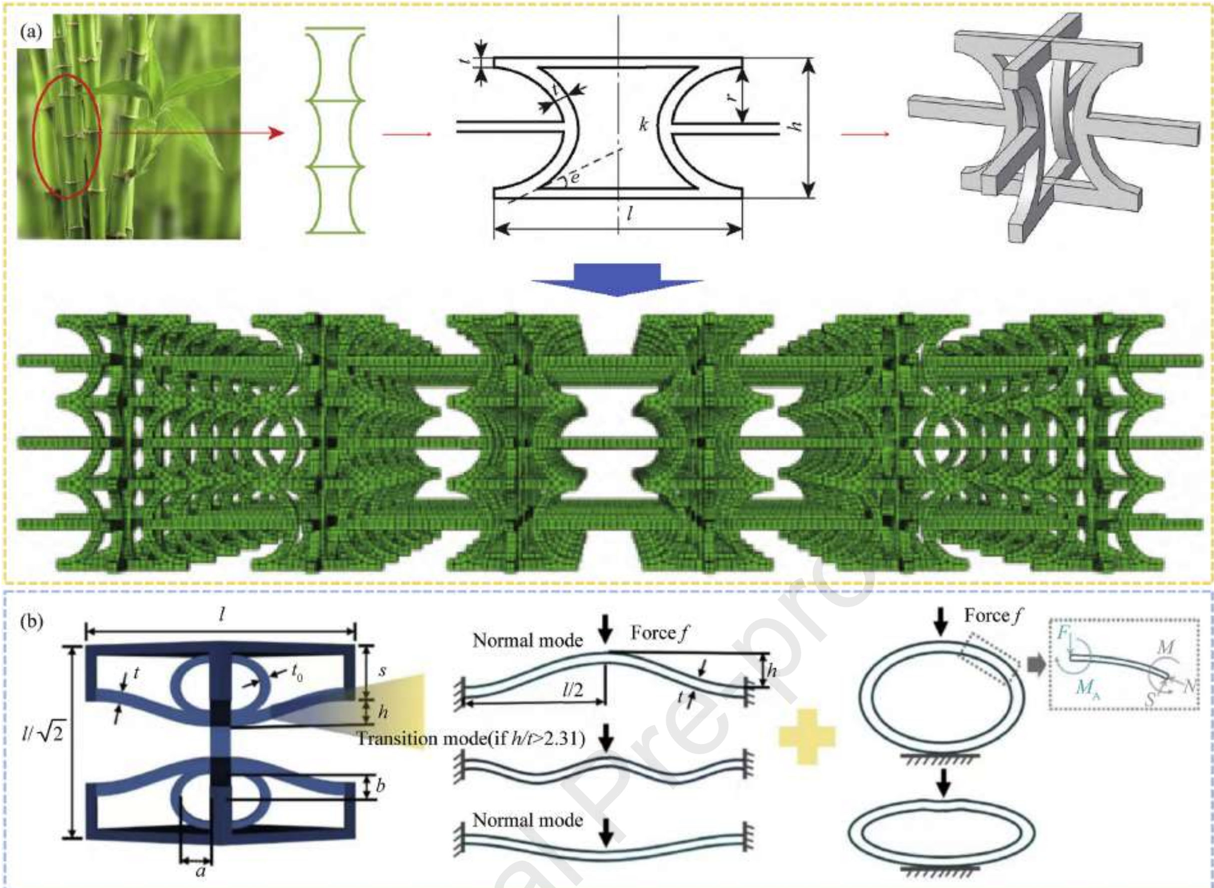
(a)
t
r
k
h
e
l
(b)
l
t
t0
s
h
l/√2
b
a
Normal mode
Force f
l/2
t
h
Transition mode(if h/t>2.31)
Normal mode
Force f
F
M
MA
S
N

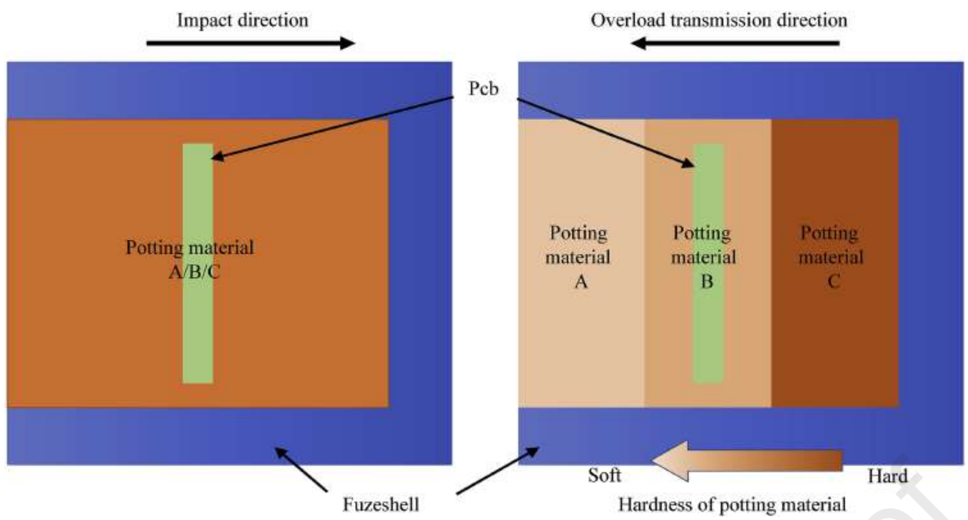
Impact direction
Overload transmission direction
Pcb
Potting material
A/B/C
Potting
material
A
Potting
material
B
Potting
material
C
Soft
Hard
Fuzeshell
Hardness of potting material

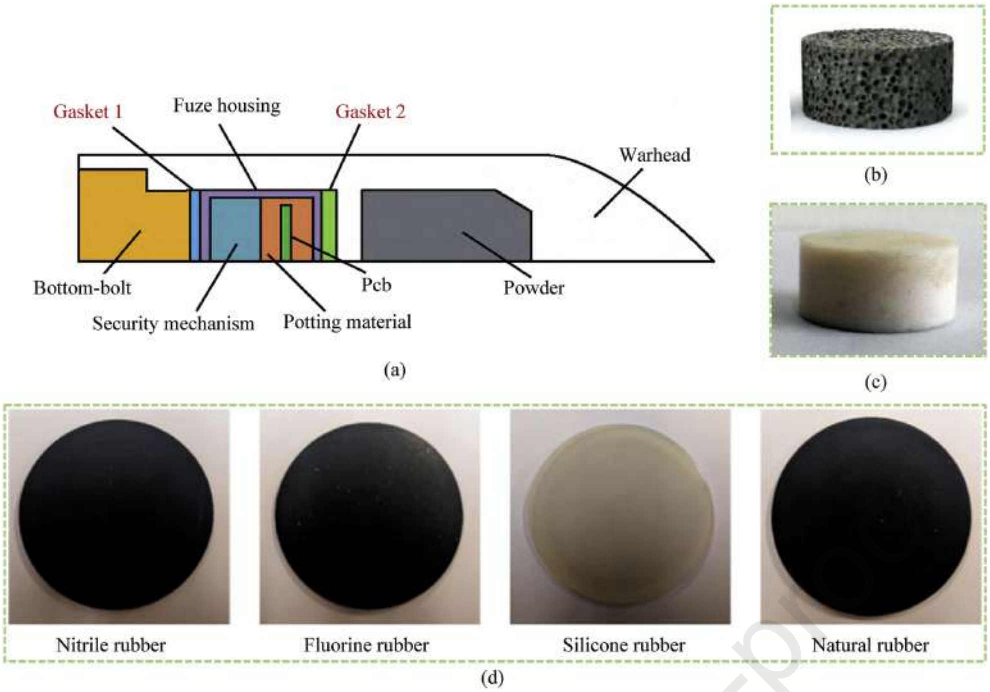
Gasket 1
Fuze housing
Gasket 2
Warhead
Bottom-bolt
Security mechanism
Potting material
Pcb
Powder
(a)
(b)
(c)
Nitrile rubber
Fluorine rubber
Silicone rubber
Natural rubber
(d)

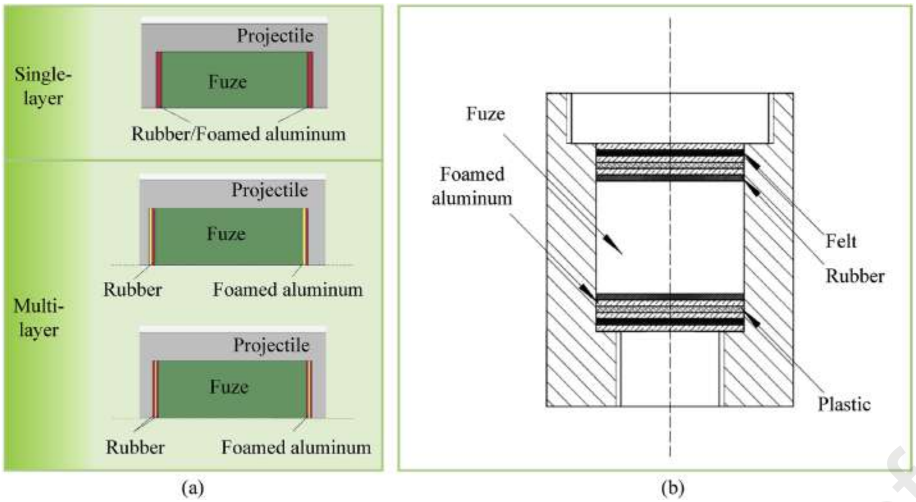
Single-layer
Projectile
Fuze
Rubber/Foamed aluminum
Multi-layer
Projectile
Fuze
Rubber
Foamed aluminum
Projectile
Fuze
Rubber
Foamed aluminum
(a)
Fuze
Foamed aluminum
Felt
Rubber
Plastic
(b)

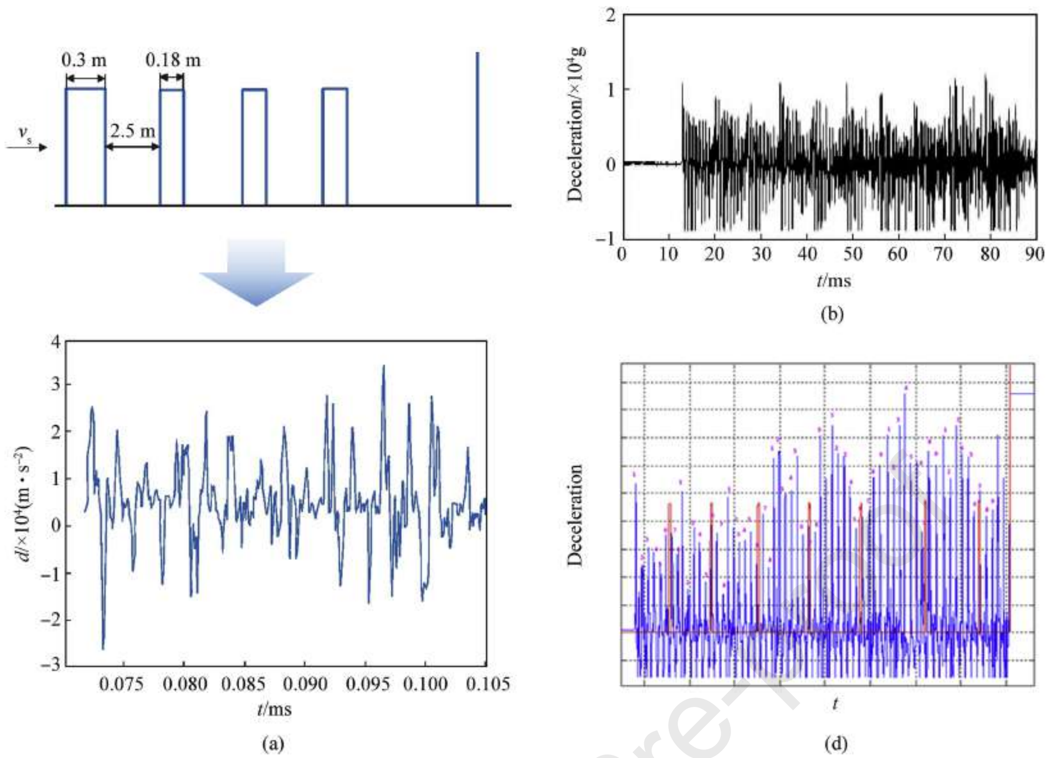
0.3 m
0.18 m
2.5 m
v_s
Deceleration/×10⁴g
t/ms
(b)
d/×10⁴(m · s⁻²)
t/ms
(a)
Deceleration
t
(d)

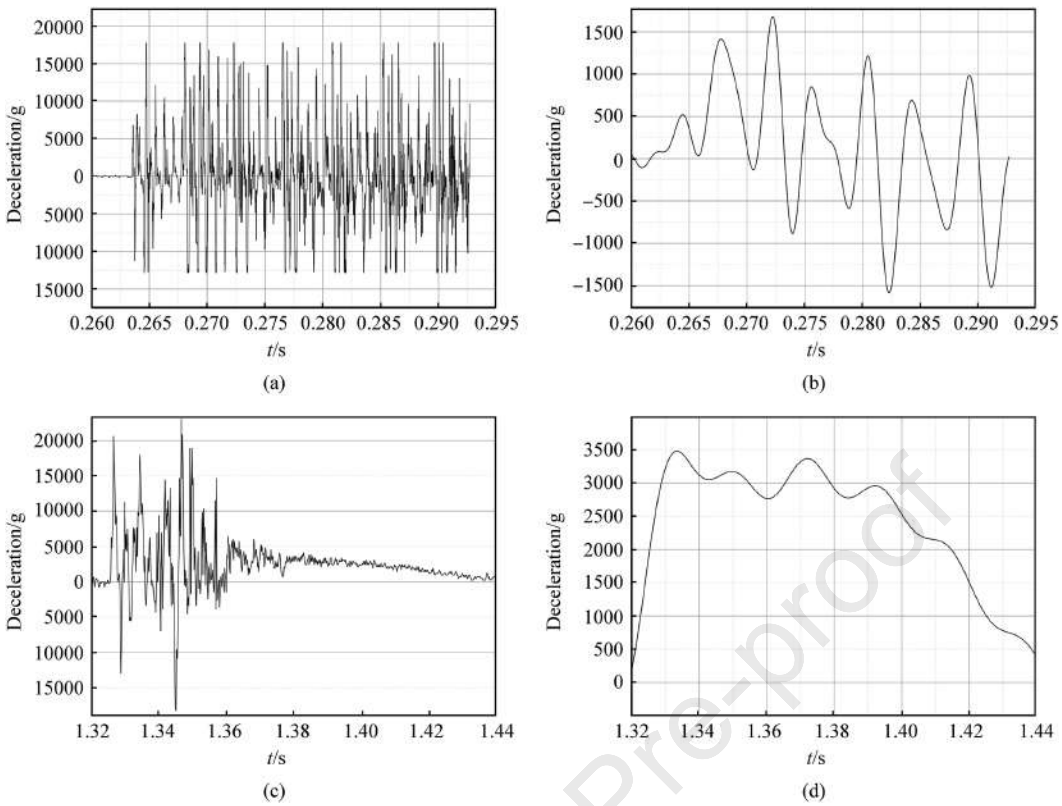
Deceleration/g
t/s
(a)
Deceleration/g
t/s
(b)
Deceleration/g
t/s
(c)
Deceleration/g
t/s
(d)

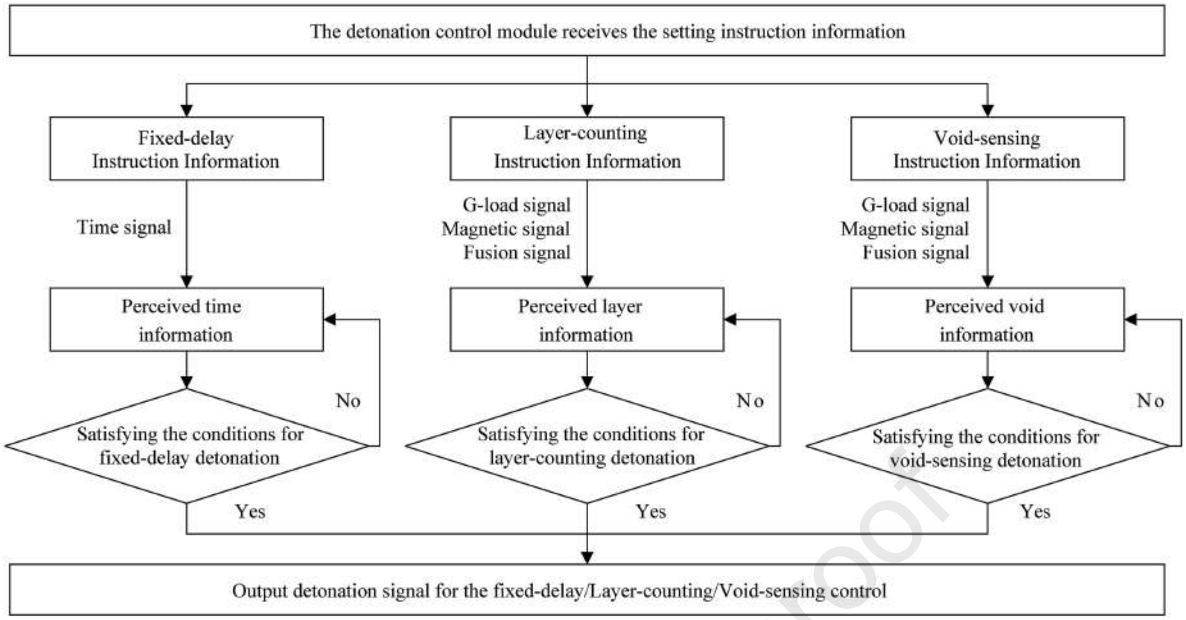
The detonation control module receives the setting instruction information
Fixed-delay Instruction Information
Layer-counting Instruction Information
Void-sensing Instruction Information
Time signal
G-load signal
Magnetic signal
Fusion signal
G-load signal
Magnetic signal
Fusion signal
Perceived time information
Perceived layer information
Perceived void information
No
No
No
Satisfying the conditions for fixed-delay detonation
Satisfying the conditions for layer-counting detonation
Satisfying the conditions for void-sensing detonation
Yes
Yes
Yes
Output detonation signal for the fixed-delay/Layer-counting/Void-sensing control

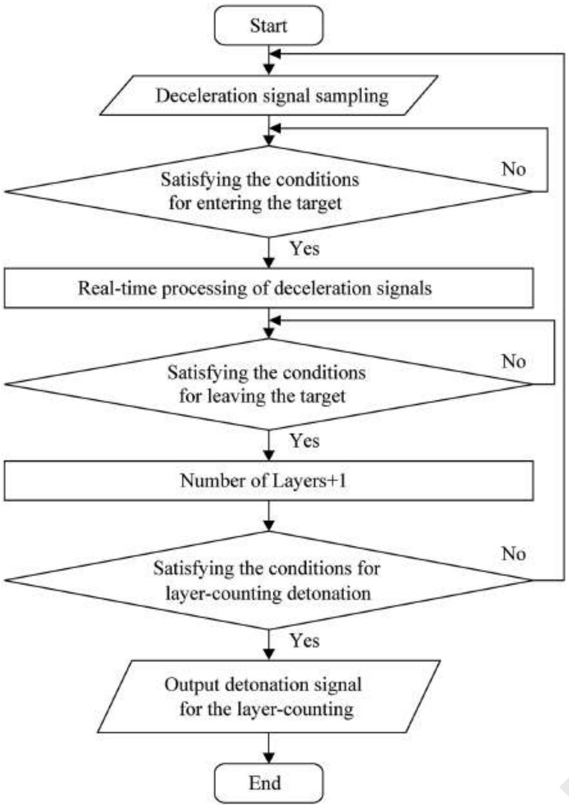
Start
Deceleration signal sampling
Satisfying the conditions for entering the target
No
Yes
Real-time processing of deceleration signals
Satisfying the conditions for leaving the target
No
Yes
Number of Layers+1
Satisfying the conditions for layer-counting detonation
No
Yes
Output detonation signal for the layer-counting
End

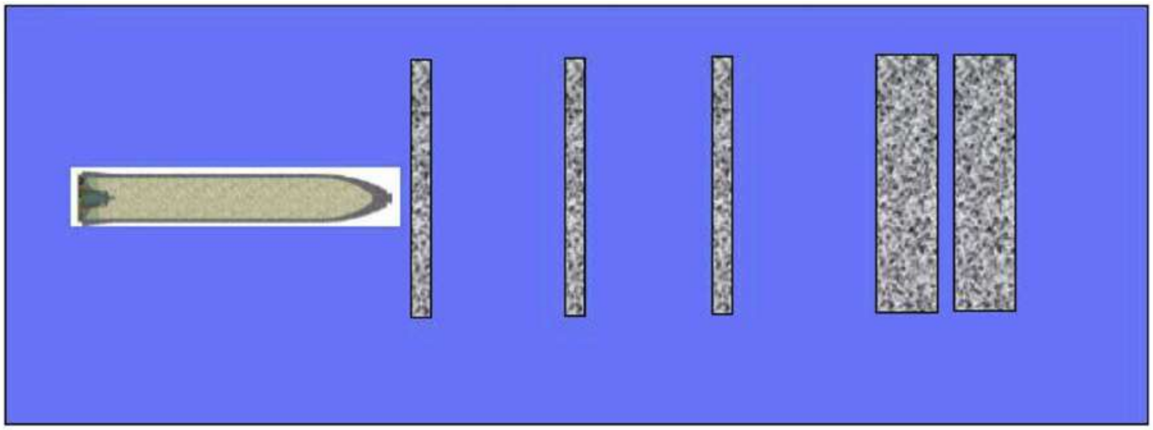

(a)

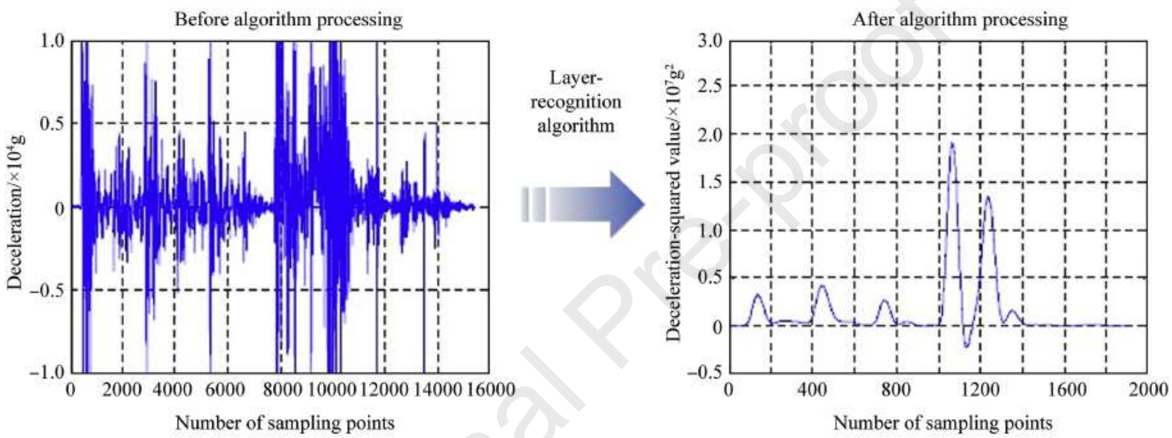
Before algorithm processing
Deceleration/×10⁴g
Number of sampling points
Layer-recognition algorithm
After algorithm processing
Deceleration-squared value/×10⁷g²
Number of sampling points

(b) (c)

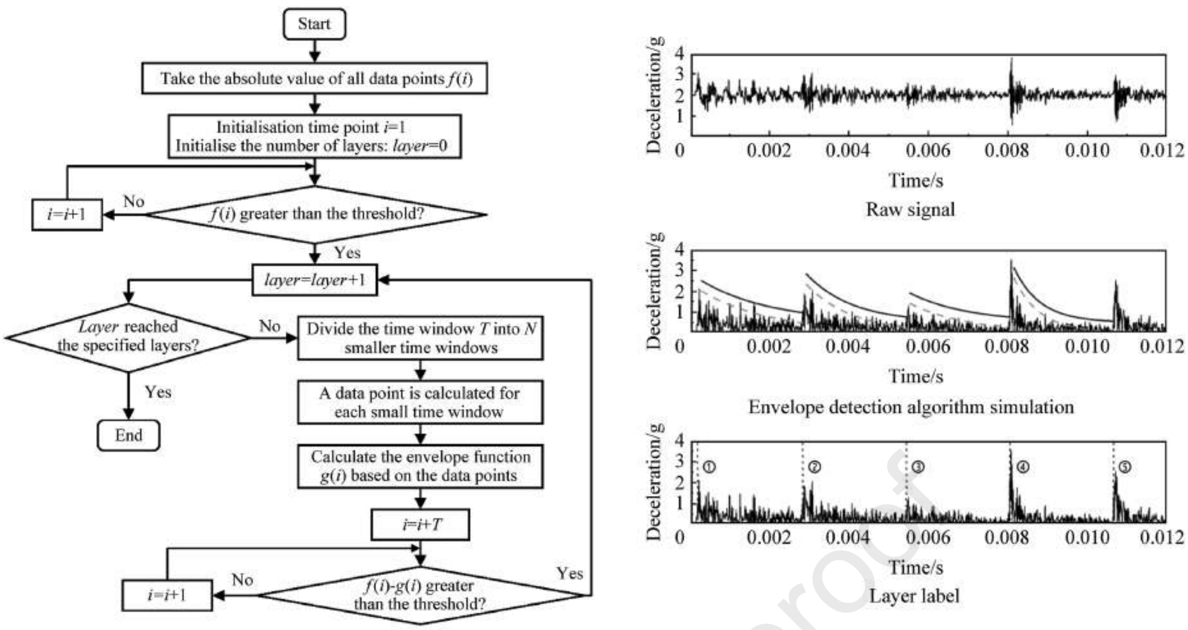
Start
Take the absolute value of all data points f(i)
Initialisation time point i=1
Initialise the number of layers: layer=0
No
i=i+1
f(i) greater than the threshold?
Yes
layer=layer+1
Layer reached
the specified layers?
No
Divide the time window T into N
smaller time windows
Yes
End
A data point is calculated for
each small time window
Calculate the envelope function
g(i) based on the data points
i=i+T
No
i=i+1
f(i)-g(i) greater
than the threshold?
Yes
Deceleration/g
Time/s
Raw signal
Envelope detection algorithm simulation
Layer label

(a) (b)

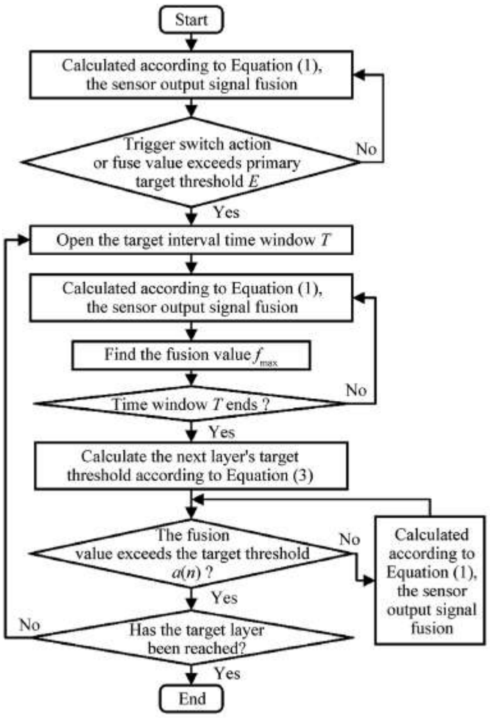
Start
Calculated according to Equation (1), the sensor output signal fusion
Trigger switch action or fuse value exceeds primary target threshold E
No
Yes
Open the target interval time window T
Calculated according to Equation (1), the sensor output signal fusion
Find the fusion value f_max
Time window T ends ?
No
Yes
Calculate the next layer's target threshold according to Equation (3)
The fusion value exceeds the target threshold a(n) ?
No
Yes
Calculated according to Equation (1), the sensor output signal fusion
Has the target layer been reached?
No
Yes
End

(a)

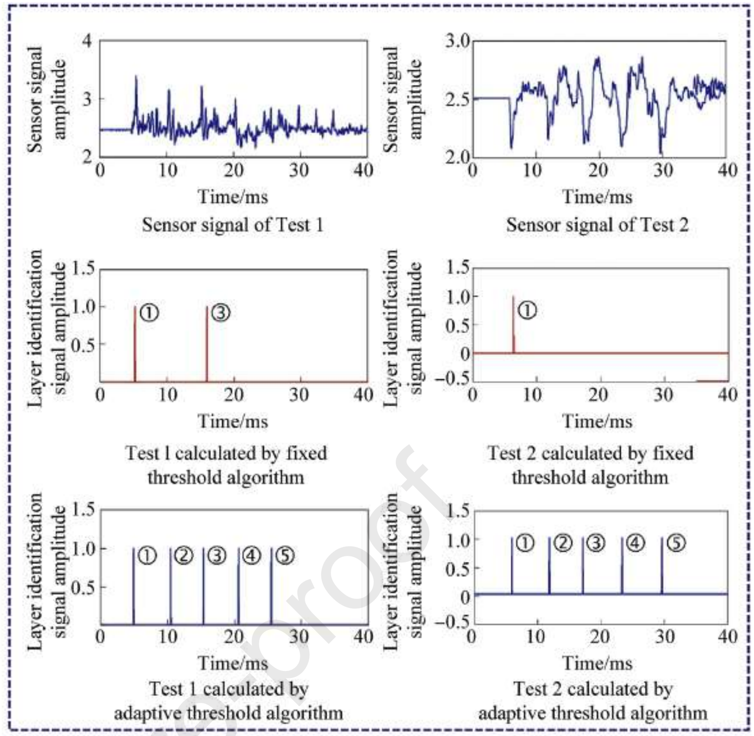
Sensor signal amplitude
Time/ms
Sensor signal of Test 1
Sensor signal of Test 2
Layer identification signal amplitude
Test l calculated by fixed threshold algorithm
Test 2 calculated by fixed threshold algorithm
Test 1 calculated by adaptive threshold algorithm
Test 2 calculated by adaptive threshold algorithm

(b)

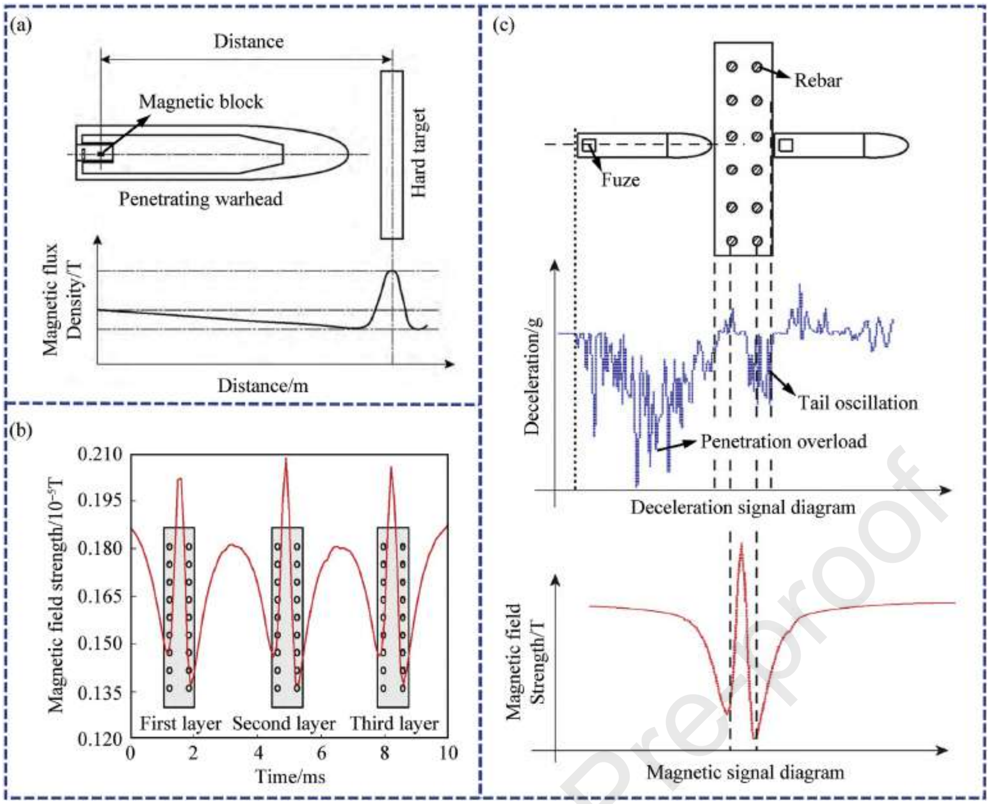
(a)
Distance
Magnetic block
Hard target
Penetrating warhead
Magnetic flux Density/T
Distance/m
(b)
Magnetic field strength/10⁻⁵T
0.210
0.195
0.180
0.165
0.150
0.135
0.120
First layer
Second layer
Third layer
0
2
4
6
8
10
Time/ms
(c)
Rebar
Fuze
Deceleration/g
Tail oscillation
Penetration overload
Deceleration signal diagram
Magnetic field Strength/T
Magnetic signal diagram

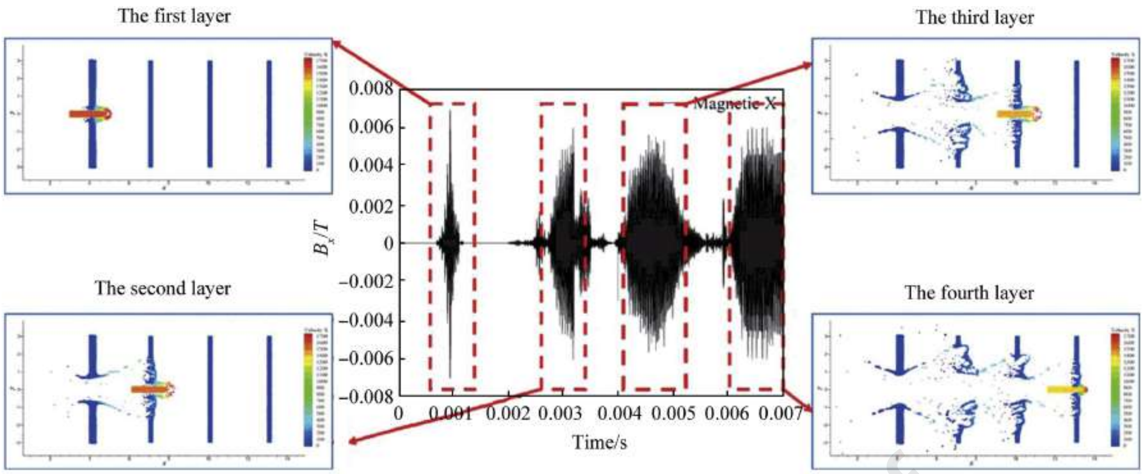
The first layer
The third layer
The second layer
The fourth layer
Magnetic-X
B_x/T
Time/s
0.008
0.006
0.004
0.002
0
−0.002
−0.004
−0.006
−0.008
0.001
0.002
0.003
0.004
0.005
0.006
0.007

(a)

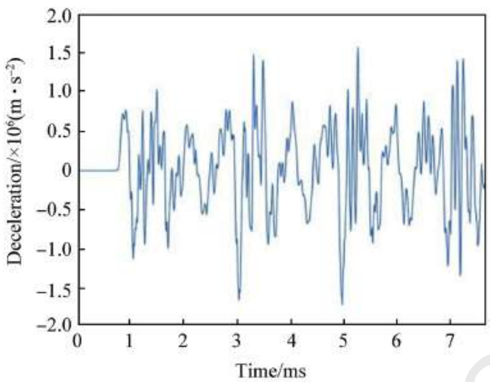
Deceleration/×10⁶(m · s⁻²)
Time/ms

(b)

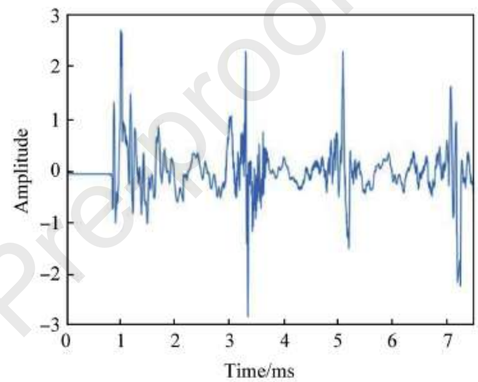
Amplitude
Time/ms

(c)

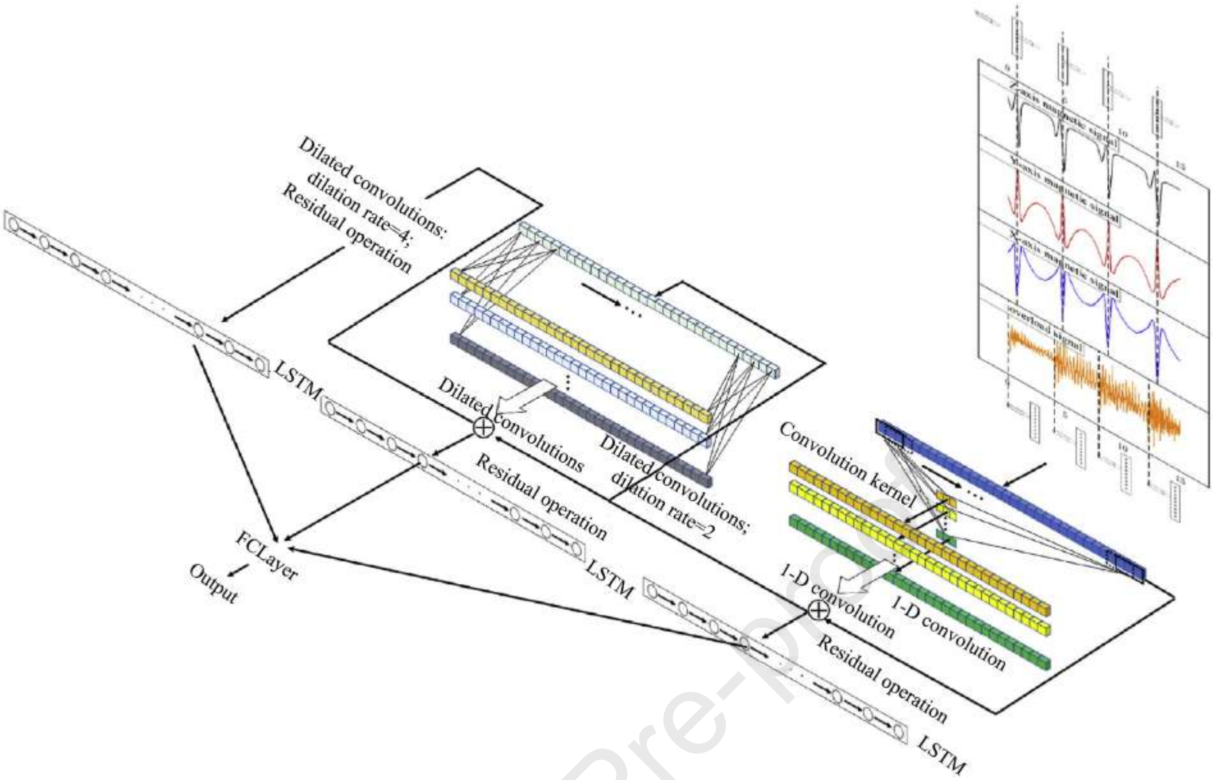
Dilated convolutions;
dilation rate=4;
Residual operation
LSTM
Dilated convolutions
Dilated convolutions;
dilation rate=2
Residual operation
LSTM
FCLayer
Output
Convolution kernel
1-D convolution
1-D convolution
Residual operation
LSTM
Z-axis magnetic signal
Y-axis magnetic signal
X-axis magnetic signal
overload signal

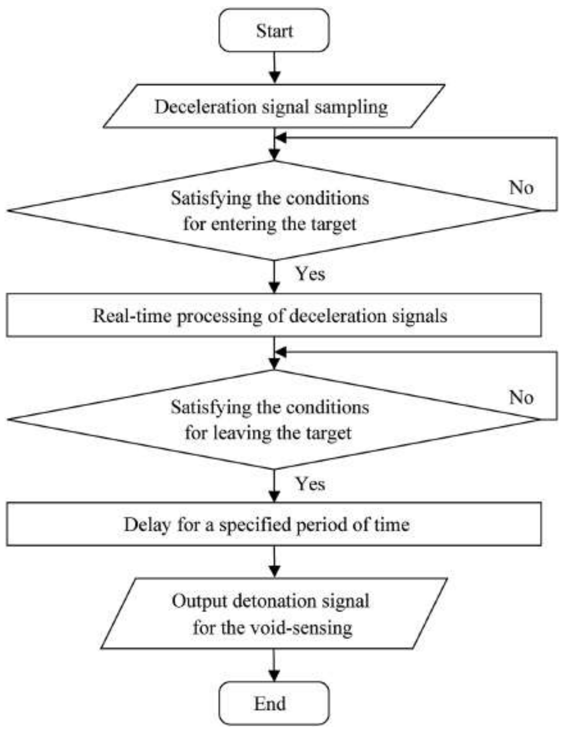
Start
Deceleration signal sampling
Satisfying the conditions for entering the target
No
Yes
Real-time processing of deceleration signals
Satisfying the conditions for leaving the target
No
Yes
Delay for a specified period of time
Output detonation signal for the void-sensing
End

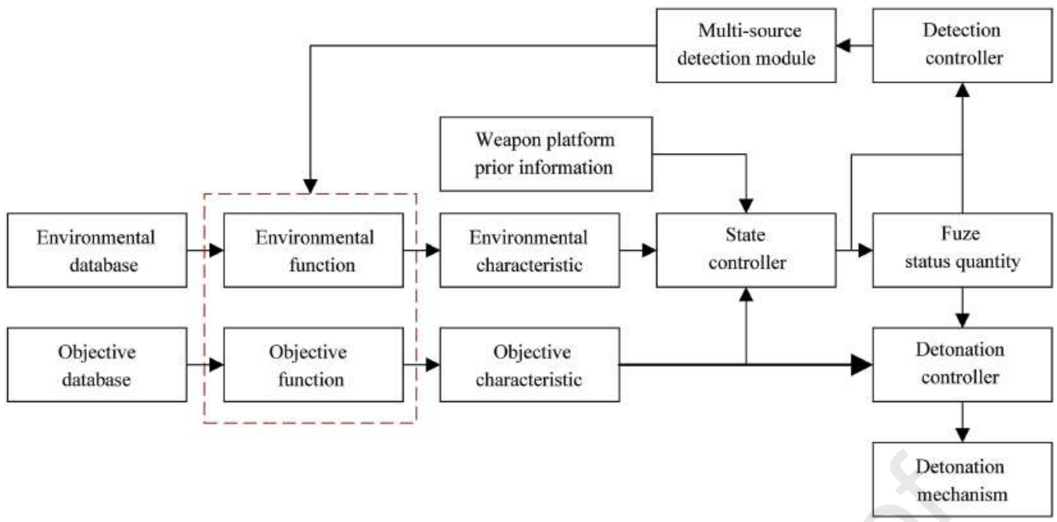
Multi-source detection module
Detection controller
Weapon platform prior information
Environmental database
Environmental function
Environmental characteristic
State controller
Fuze status quantity
Objective database
Objective function
Objective characteristic
Detonation controller
Detonation mechanism

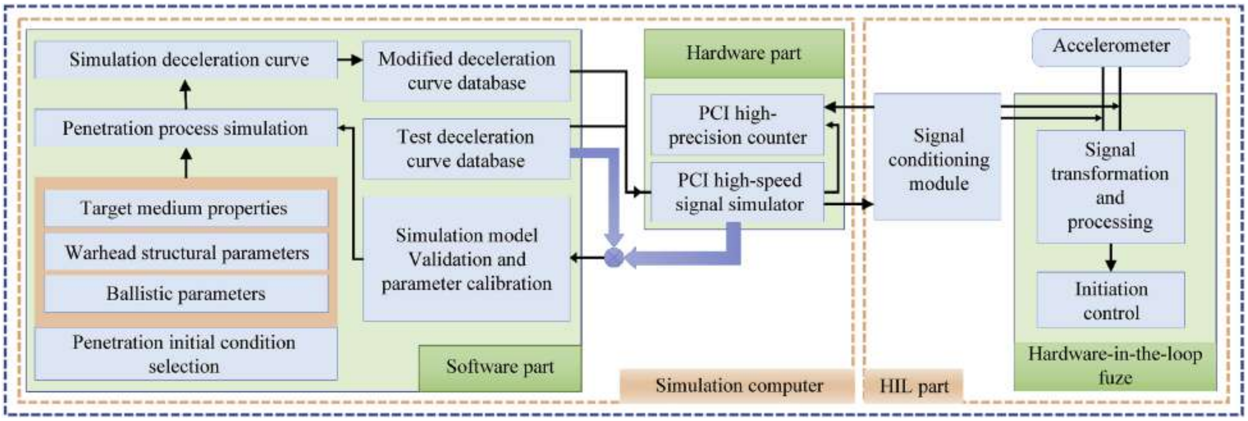
Simulation deceleration curve
Modified deceleration curve database
Hardware part
Accelerometer
Penetration process simulation
Test deceleration curve database
PCI high-precision counter
PCI high-speed signal simulator
Signal conditioning module
Signal transformation and processing
Target medium properties
Warhead structural parameters
Ballistic parameters
Simulation model Validation and parameter calibration
Initiation control
Penetration initial condition selection
Software part
Simulation computer
HIL part
Hardware-in-the-loop fuze

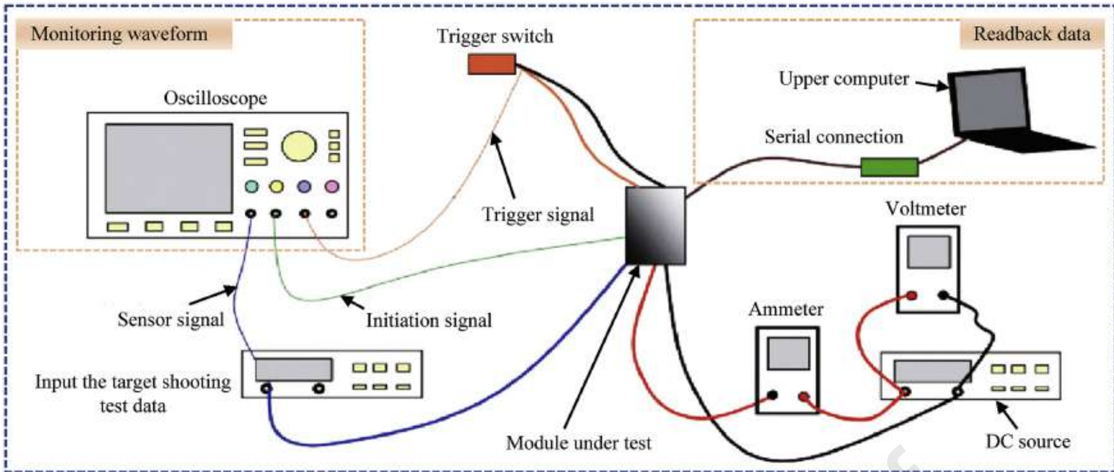
Monitoring waveform
Oscilloscope
Trigger switch
Readback data
Upper computer
Serial connection
Trigger signal
Voltmeter
Sensor signal
Initiation signal
Ammeter
Input the target shooting test data
Module under test
DC source

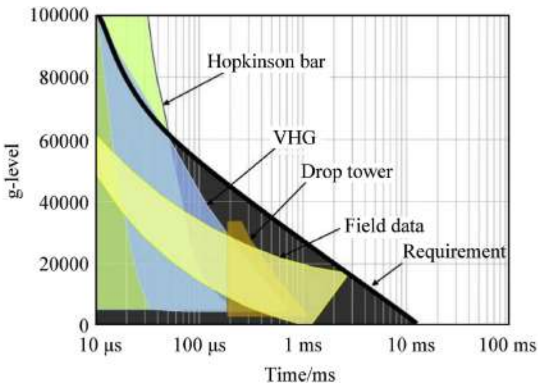
100000
80000
60000
40000
20000
0
g-level
Hopkinson bar
VHG
Drop tower
Field data
Requirement
10 μs
100 μs
1 ms
10 ms
100 ms
Time/ms

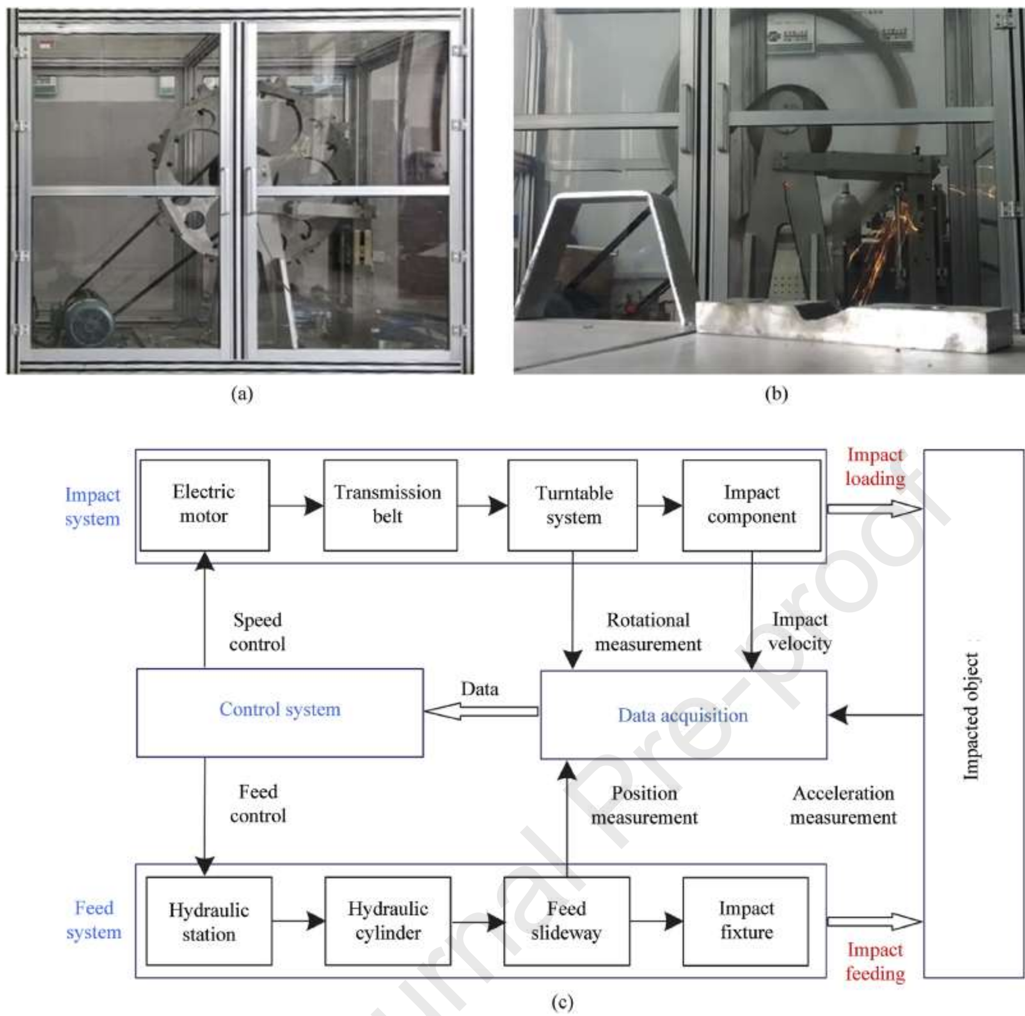
(a)
(b)
Impact system
Electric motor
Transmission belt
Turntable system
Impact component
Impact loading
Speed control
Rotational measurement
Impact velocity
Control system
Data
Data acquisition
Impacted object
Feed control
Position measurement
Acceleration measurement
Feed system
Hydraulic station
Hydraulic cylinder
Feed slideway
Impact fixture
Impact feeding
(c)

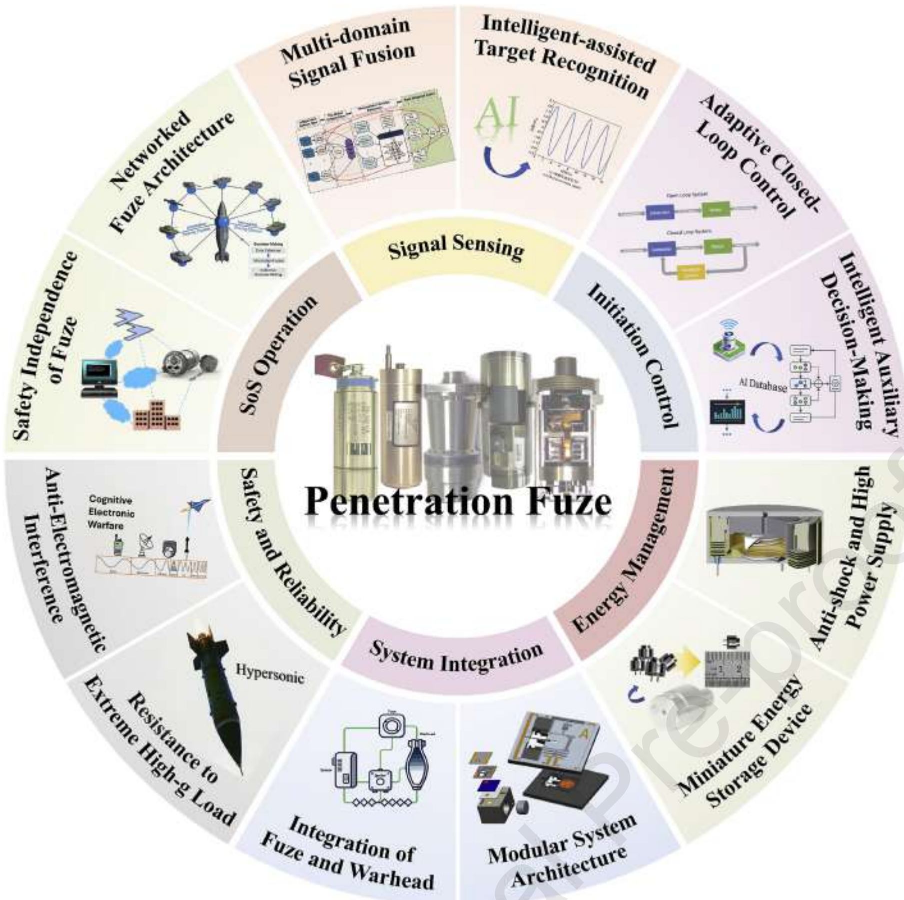
Penetration Fuze
Signal Sensing
Initiation Control
Energy Management
System Integration
Safety and Reliability
SoS Operation
Multi-domain Signal Fusion
Intelligent-assisted Target Recognition
AI
Adaptive Closed-Loop Control
Intelligent Auxiliary Decision-Making
AI Database
Anti-shock and High Power Supply
Miniature Energy Storage Device
Modular System Architecture
Integration of Fuze and Warhead
Resistance to Extreme High-g Load
Hypersonic
Anti-Electromagnetic Interference
Cognitive Electronic Warfare
Safety Independence of Fuze
Networked Fuze Architecture

Declaration of Competing Interest

The authors declare that they have no known competing financial interests or personal relationships that could have appeared to influence the work reported in this paper.